PROCEEDINGS OF THE ACADEMY OF SCIENCES OF THE USSR

Physical Chemistry Section

Volume 132, Numbers 1-6 May-June, 1960

CONTENTS

	PAGE	RUSS. ISSUE	RUSS. PAGE
Supplementary Data on the Equilibrium of Ethyl Alcohol Synthesis. Yu. M. Bakshi, A. I. Gel'bshtein, and M. I. Temkin	389	1	157
The Determination of the Electron Density Distribution in Crystals. N. N. Sirota, N. M. Olekhnovich, and A. U. Sheleg	393	1	160
The Mechanism of the Influence of Neutral Electrolytes on the Bond Between Particles in the Coagulation Structure. G. I. Fuks	397	1	164
An Investigation of the Gel-Forming Properties of Aluminum Oleates in Benzene. G. V. Benugina, V. V. Konstantinova, S. Kh. Zakieva, and P. A. Rebinder	401	2	380
Kinetics of the Vapor-Phase Hydration of Ethylene on a Phosphoric Acid Catalyst. A. I. Gel'bshtein, Yu. M. Bakshi, and M. I. Temkin	405	2	384
Automatic Oscillations During the Reduction of Perdisulphate Ions on Mercury. A. Ya. Gokhshtein and N. Frumkin	409	2	388
The Viscosity of Suspensions. E. F. Kurgaev	413	2	392
The Mechanism of Intermolecular Energy Exchange During the Dissociation of Diatomic Gases. E. E. Nikitin	417	2	395
The Influence of Certain Semiconducting Properties of the Surface on the Reaction Between Xanthate and Galenite. I. N. Plaksin and R. Sh. Shafeev	421	2	399
The Spontaneous Crystallization of Dissociated Salts. V. B. Ratinov and O. M. Todes	425	2	402
The Effects of High-Energy Electrons on Platinum Complexes. I. Spitsyn, G. N. Pirogova, A. K. Pikaev, and P. Ya. Glazunov	429	2	406
Anodic Processes Accompanying the Corrosion Cracking of Metals. N. D. Tomashov and N. I. Isaev	433	2	409
The Ionization Potentials of Organic Dyes and Several Complex Molecules in the Vapor Phase. F. I. Vilesov	437	3	632
Cathode Processes During the Electrodeposition of Titanium from Aqueous Solutions. N. T. Kudryavtsev, R. G. Golovchanskaya, and N. K. Baraboshkina	441	3	636
The Anodic Passivation of Zinc in Alkaline Solutions. T. I. Popova, V. S. Bagotskii, and B. N. Kabanov	445	3	639
The Effects of Radiation on the Solubility of Radioactive Solids. V. I. Spitsyn, E. A. Torchenkova, and I. N. Glazkova	449	3	643
Determination of the Rate Constant for the Reaction Between Atomic Oxygen and Molecular Hydrogen. V. V. Azatyan, V. V. Voevodskii, and A. B. Nalbandyan	453	4	864
The Structure of the Electrical Double Layer on Platinum. T. P. Birintseva and B. N. Kabanov	457	4	868
The Potential of a Platinum Electrode in an Irradiated Sulfuric Acid Solution. G. Z. Gochaliev, Ts. I. Zalkind, and V. I. Veselovskii	461	4	872
Statistical Thermodynamic Determination of the Adsorption Equilibrium of Argon on Graphite. A. V. Kiselev and D. P. Poshkus	465	4	876
The Effect of Irradiation on the Potential of a Platinum Electrode in a Solution of Sulfuric Acid. D. V. Kokoulina, P. I. Dolin, and A. N. Frumkin	469	4	880

CONTENTS (continued)

	PAGE	RUSS. ISSUE	RUSS. PAGE
The Effect Produced by the Interaction of Adsorbed Particles. V. I. Osherov	473	4	884
The Mechanism of the Protection of Magnesium from Oxidation. M. S. Beletskii and M. I. Erusalimskii	477	5	1122
Catalytic Oxidation of Propylene and Acrolein on Copper. V. M. Belousov, Ya. B. Gorokhovatskii, M. Ya. Rubanik, and A. V. Gershingorina	481	5	1125
Explosive Decomposition of Nitrous Oxide. B. B. Brandt and A. I. Rozlovskii	485	5	1129
The Effects of Benzene Vapor Adsorption on the Electrical Conductance of Transparent Platinum Films of Various Surface Densities. V. M. Gryaznov, V. I. Shimulis, and V. D. Yagodovskii	489	5	1132
The Transfer of Excitation Energy and the Sensitization of Chemical Reactions During the Radiolysis of Solutions of Organic Disulfides. V. A. Krongauz and Kh. S. Bagdasar'yan	493	5	1136
The Electrical Properties of Systems Composed of Polymers and Metals. S. D. Levina, K. P. Lobanova, and N. A. Platé	497	5	1140
Relation Between the Diffusion Coefficient and Amount of Adsorption on Active Carbons. D. P. Timofeev and I. T. Erashko	501	5	1144
The Kinetics of Distillation in Supercooled Systems. K. S. Shifrin and A. Ya. Perel'man	505	5	1148
The Thermodynamics of the Protonization of Isobutene. S. G. Entelis, K. S. Kazanskii, and N. M. Chirkov	511	5	1152
The Free Energy of Potassium Iodide in Ethanol and Acetone. V. V. Aleksandrov and Yu. A. Ershov	515	6	1327
The Effect of Solid Substances on the Decomposition of Carbon Tetrachloride in Aqueous Solution Under the Influence of Gamma Irradiation. A. S. Baberkin, N. P. Krushinskaya, and M. A. Proskurnin	517	6	1329
The Photonization of Vapors of Compounds Whose Molecules Contain Carbonyl Groups. F. I. Vilesov	521	6	1332
Determination of the Rate Constants for Elementary Reactions of Hydrogen Atoms with Hydrocarbons. H. I. Gorban' and A. B. Nalbandyan	525	6	1335
An Electromagnetic Method of Measuring the Velocity of Explosion Products. V. M. Zaitsev, P. F. Pokhil, and K. K. Shvedov	529	6	1339
The Effect of Pressure on the Rate of Laminar and Turbulent Combustion. V. P. Karpov and A. S. Sokolik	531	6	1341
The Mechanism of Heterogeneous Exchange between Acetone and Water in the Gas Phase. B. A. Kuznetsov and I. D. Elkina	535	6	1344
The Possibility of Increasing the Yield of Hydroperoxide in the Initation of the Oxidation of Cumol by Hydrogen Peroxide. R. V. Kuchev, S. D. Kaz'min and V. D. Enal'ev	539	6	1348
The Polarographic Catalytic Waves of Hydrogen and the Adsorption of a Catalyst. S. G. Mairanovskii	543	6	1352
Synthesis of Specific Silica Gels by Modification of Their Surface. I. E. Neimark, V. M. Chertov, R. Yu. Sheinfain, and N. S. Kruglikova	549	6	1356
The Part Played by Minority Current Carriers in the Anodic Dissolution of Electronic Germanium. Yu. V. Pleskov	553	6	1360
Some Features of the Crystallization of Alloys of the Eutectic Type at High Rates of Cooling. I. V. Salli and I. S. Miroshnichenko	557	6	1364
The Mechanism of the Change in Oxygen Overvoltage with Time at a Nickel Anode at Constant Current Density. Ya. I. Tur'yan	561	6	1368
The Nature of the Hydrogen Bond and its Influence on the Electronic Spectra of Molecules. D. N. Shigorin, N. A. Shcheglova, N. S. Dokunikhin, and V. A. Puchkov	565	6	1372
The Dipole Moments of Some Halopolynitroparaffins. A. N. Shidlovskii, Ya. K. Syrkin, S. S. Novikov, A. A. Fainzil'berg, V. V. Sevost'yanova, and V. I. Gulevskaya	571	6	1376

SUPPLEMENTARY DATA ON THE EQUILIBRIUM OF ETHYL ALCOHOL SYNTHESIS

Yu. M. Bakshi, A. I. Gel'bshtein, and M. I. Temkin

L. Ya. Karpova Physicochemical Institute

(Presented by Academician S. S. Medvedev, December 30, 1959)

Translated from Doklady Akademii Nauk SSSR, Vol. 132, No. 1, pp. 157-159, May, 1960

Original article submitted December 30, 1959

Previously [1] published data on the equilibrium

$$C_2H_4(g) + H_2O(g) = C_2H_5OH(g) \quad (1)$$

at pressures up to 81 atm show a linear dependence of log K_p upon the total pressure P. At a constant $N_{H_2O}/N_{C_2H_4}$ ratio, this dependence corresponds to the inclusion of a second virial coefficient in the equation of state for the gas mixture. The values of K_f obtained by linearly extrapolating log K_p to P = 0 were represented by the equation [1]

$$\log K_f = \frac{2093}{T} - 6.304. \quad (2)$$

Additional measurements, the results of which are reported here, make it possible to evaluate the relation between log K_γ / P and the composition of the mixture, and to obtain more exactly the dependence of this ratio

TABLE 1

Temperature, deg C	Pressure, atm	Space velocity based on C_2H_4, hr^{-1}	$N_{H_2O}/N_{C_2H_4}$	Composition of the mixture fed, mol. fractions			Composition of the mixture drawn off, mol. fractions			$K_p \cdot 10^3$, atm^{-1}	$K_p \cdot 10^3$ acc. to equation (2), atm^{-1}
				C_2H_4	H_2O	C_2H_5OH	C_2H_4	H_2O	C_2H_5OH		
286	36	3160 (40)	0,16	0,863	0,137	—	0,840	0,146	0,0102	2,32	2,34 for $N_{H_2O}/N_{C_2H_4}$ = 0,51
286	36	3160 (40)		0,848	0,139	0,0124	0,838	0,146	0,0104	2,36	
286	71	577 (40)	1,3	0,450	0,650	—	0,434	0,526	0,0345	2,13	2,08 for $N_{H_2O}/N_{C_2H_4}$ = 0,51
286	71	577 (40)		0,464	0,521	0,0154	0,463	0,496	0,0351	2,16	
332	41	1300 (12)	0,35	0,739	0,261	—	0,735	0,250	0,0110	1,46	1,43 for $N_{H_2O}/N_{C_2H_4} \cong 1,8$
332	41	2180 (40)		0,730	0,256	0,0149	0,728	0,258	0,0108	1,40	
332	51	1310 (12)	0,66	0,601	0,399	—	0,590	0,388	0,0164	1,41	
332	61	1270 (12)	0,96	0,511	0,489	—	0,497	0,477	0,0200	1,38	
332	71	1260 (12)	1,2	0,445	0,555	—	0,411	0,561	0,0224	1,37	
332	81	1200 (12)	1,5	0,400	0,600	—	0,363	0,606	0,0255	1,43	
332	81	466 (40)		0,373	0,593	0,0347	0,370	0,600	0,0255	1,42	

• In the parentheses is given the weight-percentage of H_3PO_4 in the catalyst.

TABLE 2

Temp. °C	Pressure, atm *	Experimental $K_p \cdot 10^3$, atm^{-1}	$K_p \cdot 10^3$ according to Eq. (5), atm^{-1}	Temp. °C	Pressure, atm *	Experimental $K_p \cdot 10^3$, atm^{-1}	$K_p \cdot 10^3$ according to Eq. (5), atm^{-1}
258	41	3,30	3,31	318	41	1,65	1,64
258	81	2,52	2,54	318	81	1,63	1,57
286	41	2,30	2,35	345	41	1,18	1,24
286	51	2,25	2,26	345	81	1,17	1,27
286	71	2,08	2,10	365	41	0,94	1,02
286	81	2,03	2,02				

* In the communication [1] the pressure unit was not clearly indicated. The pressures were measured in technical atmospheres (kg/cm^2).

TABLE 3

Equilibrium Degrees of Ethylene Conversion into Alcohol $\alpha \cdot 10^2$ at $N_{H_2O}/N_{C_2H_4} = 1$

Temp., °C	Pressure P, atm					
	1	20	40	60	80	100
250	0,253	4,14	6,85	8,64	9,78	10,5
270	0,184	3,10	5,40	7,11	8,40	9,35
290	0,130	2,36	4,28	5,85	7,15	8,24
310	0,0985	1,86	3,50	4,95	6,27	7,40
330	0,0746	1,45	2,83	4,15	5,40	6,74

TABLE 4

Equilibrium Degree of Ethylene Conversion into Alcohol $\alpha \cdot 10^2$ at 290°

$N_{H_2O}/N_{C_2H_4}$ in the mixture introduced	Pressure P, atm					
	1	20	40	60	80	100
0,4	0,0740	1,33	2,43	3,31	4,06	4,65
0,6	0,0972	1,75	3,20	4,37	5,34	6,25
0,8	0,115	2,09	3,79	5,20	6,36	7,29
1,0	0,130	2,36	4,28	5,85	7,15	8,24
2,0	0,173	3,14	5,68	7,78	9,51	10,9

upon the temperature ($K_\gamma = \gamma_{C_2H_5OH}/\gamma_{C_2H_4}\gamma_{H_2O}$, where $\gamma_{C_2H_5OH}$ is the activity coefficient of C_2H_5OH, etc.). The method of measuring did not differ from that described in [1]. The compositions of the mixtures were chosen in such a way that condensation did not occur. The results are given in Table 1, where also are shown the values of K_p calculated by means of Eq. (2) taking, in accordance with [1], $\log K_\gamma/P = 14.2 \cdot 10^{-4}$ at 286° and $K_\gamma = 1$ at 332°. As is obvious from Table 1, the value of K_p at a given P does not depend upon the composition of the mixture within the accuracy of the measurements. Moreover, it is obvious from the table that at 332° K_p does not depend upon P which means that this temperature is near to the "Guldberg-Waage temperature" [1]. At lower temperatures $K_\gamma > 1$*. Data on the ether content are not given in the table, because equilibrium is not attained with respect to the formation of ether.

As has been shown in [1],

$$\frac{\ln K_\gamma}{P} = \frac{2\sum_i \nu_i B_i - B\sum_i \nu_i}{RT}. \qquad (3)$$

The dependence of B_i and B upon T may be expressed by series of the form $a_0 + \frac{a_1}{T} + \frac{a_2}{T^2} + \ldots$. Assuming that two terms of the series are sufficient, we get the following formula for the dependence of $\log K_\gamma/P$ upon the temperature

$$\frac{\log K_\gamma}{P} = \frac{A_0}{T} + \frac{A_1}{T^2}. \qquad (4)$$

The experimental data correspond to values $A_0 = -10.47$; $A_1 = 6.37 \cdot 10^3$. Substituting $K_p = K_f/K$ in Eq. (2) gives

$$\log K_P = \frac{2093}{T} - 6{,}304 + \left(\frac{10{,}47}{T} - \frac{6{,}37 \cdot 10^3}{T^2}\right) P. \qquad (5)$$

* The corresponding formulation in [1] is in error.

Equation (5) describes the dependence of K_p upon T and P and expresses the independence of K_p from the composition of the mixture. In Table 2 the values of K_p, calculated from Eq. (5) are compared with the experimental values of K_p obtained previously [1]. Tables 3 and 4 contain the degrees of ethylene conversion α at equilibrium which have been calculated from Eq. (5), assuming that only reaction (1) takes place.

For the calculation of α it is convenient to use the series

$$\alpha = \frac{n}{1+n}\,\frac{K_N}{1+K_N} + \frac{n^2}{(1+n)^3}\left(\frac{K_N}{1+K_N}\right)^2 + 2\frac{n^3}{(1+n)^6}\left(\frac{K_N}{1+K_N}\right)^3 + \ldots, \tag{6}$$

where n represents the number of moles H_2O per mole C_2H_4 in the mixture introduced, $K_N = PK_p$. The equilibrium mixture at $N_{H_2O}/N_{C_2H_4} = 1$, 250° and 100 atm (perhaps also some others) is unstable with respect to condensation.

The data obtained make it possible to determine the heat of reaction (1). Because in the case considered, K_γ does not depend upon the composition of the gas mixture, it follows that

$$\left(\frac{\partial \ln K_\gamma}{\partial T}\right)_P = \frac{\Delta H^0 - \Delta H}{RT^2}. \tag{7}$$

From the relation

$$\frac{d \ln K_f}{dT} = \frac{\Delta H^0}{RT^2} \tag{8}$$

and the equality $K_p = K_f/K_\gamma$, we get

$$\left(\frac{\partial \ln K_p}{\partial T}\right)_P = \frac{\Delta H}{RT^2}. \tag{9}$$

Equation (5) gives

$$\Delta H = -9570 - \left(47{,}9 - \frac{5{,}83\cdot 10^4}{T}\right)P. \tag{10}$$

At 300° and 80 atm $\Delta H = -5263$ cal. This value differs considerably from $\Delta H^0 = -9570$ cal. Therefore, in technical calculations, the dependence of ΔH upon P must be taken into account.

LITERATURE CITED

1. Yu. M. Bakshi, A. I. Gel'bshtein, and M. I. Temkin, Doklady Akad. Nauk SSSR 126, 314 (1959).*

* Original Russian translation. See C. B. Translation

THE DETERMINATION OF THE ELECTRON DENSITY DISTRIBUTION IN CRYSTALS

Academician of the Byelorussian SSR Academy of Sciences
N. N. Sirota, N. M. Olekhnovich, and A. U. Sheleg

Solid and Semiconductor Physics Section, Academy of Sciences, Byelorussia

Translated from Doklady Akademii Nauk SSSR, Vol. 132, No. 1, pp. 160-163, May, 1960

Original article submitted January 5, 1960

Bragg [1] was the first to show the possibility of applying the Fourier series for the purposes of x-ray structural analysis. The subsequent development of this method [2, 3] has made it possible to approach the problem of determining the electron density distribution between the atoms in solids from the experimentally determined intensities of the diffraction maxima on the x-ray diagram. The problem of the electron density distribution in crystals, which determines the nature, anisotropy, and energy of the interaction between the atoms, is one of the most important general problems in the physics and chemistry of solids.

A large number of works [4-16] have been devoted to the determination of the electron density distribution in solids, and a list has been given in [16].

In order to determine the electron density distribution and to find the electron density $\rho(x,y,z)$ at any point with coordinates x, y, and z in a unit cell with volume v, it is necessary to carry out the summation of a three-dimensional Fourier series

$$\rho(x, y, z)=\frac{1}{v}\sum_{h}\sum_{k}^{+\infty}\sum_{-\infty}^{l}F(hkl)\exp\left[-2\pi i\left(\frac{hx}{a}+\frac{ky}{b}+\frac{lz}{c}\right)\right], \tag{1}$$

where F(hkl) is the structure factor. The number of terms in the series is limited by the number of the reflections which can be determined experimentally.

The uncertainty which arises as a result of the break in the series makes it impossible to obtain any clear idea of the actual distribution of electrons in a crystal lattice. A number of works have therefore suggested methods for eliminating the effect of the break in the series, by theoretical extrapolation of the f-curve to high values of the sum of the squares of the indices [4], or by the introduction of a temperature factor e^{-2M}, with considerable calculation temperatures of the order of 1000-10000°K [5, 6, 8, 9]. Both methods introduce considerable errors in the results of the calculation of the electron density distribution.

The use of a method suggested by Hosemann and Bagch [7] for the determination of the electron density using "convolution" operations and extrapolation of the f-curves provides a new approach. This method, however, is not free from certain defects.

As pointed out by Nowacki [18] Reijen has calculated the electron density by approximating the f-curve of the atomic scattering factor using a Gaussian function. The calculation of the electron density involved the calculation of the Fourier integral and summation of the series.

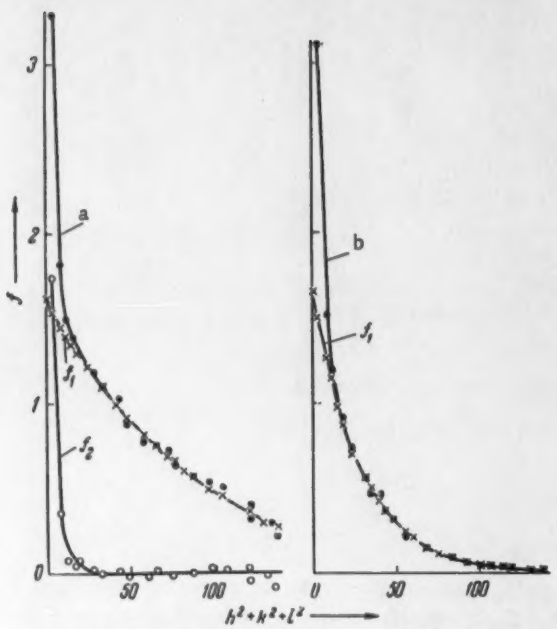

Fig. 1. Change in the atomic scattering factor f with change in the sum of the squares of the indices of the reflections of the diffraction maxima. a)Experimental f-curve for diamond [6]; f_1 is the calculated f-curve for electrons with the given density distribution; b) experimental f-curve with the introduction of a temperature factor for a calculation temperature of 7500°; f_2 is the difference between the experimentally determined scattering factor and that calculated for electrons with the given electron density distribution.

The present paper shows that it is possible to calculate the electron density by summation of three-dimensional Fourier series without introducing a temperature factor and without continuing the extrapolation of the f-curve, using instead the values of the atomic scattering factor, which can be obtained by using CuKα and softer radiation.

It is known [17] that the outer electrons of an atom introduce changes in the shape of the f-curve chiefly at low orders of reflection. At high orders of reflection, their contribution becomes extremely small. The value of the atomic scattering factor may therfore be divided into two fractions, produced by two groups of electrons with density distributions $\rho'_1(r)$ and $\rho_2(r)$, where $\rho'_1(r)$ is the principal fraction of the electron density, produced by the electrons situated for the most part close to each atom, and $\rho_2(r)$ is the remaining fraction of the electron density, produced by electrons situated for the most part in the outer region of the atoms. This separation of ρ'_1 and ρ_2 is not associated with any kind of electron layer. Both functions extend in all three dimensions.

The electron distribution in the first fraction can be described with sufficient accuracy by a Gaussian distribution function of the form

$$\rho'_1(r) = Ae^{-\alpha r^2}, \tag{2}$$

for which it is easy to calculate the curve giving the relationship between the scattering factor and the order of the reflection

$$f_1 = \int_0^\infty Ae^{-\alpha r^2} 4\pi r^2 \frac{\sin \mu r}{\mu r}\, dr = A\,\frac{\pi^{3/2}}{\alpha^{3/2}} \exp\left[-\frac{\mu^2}{4\alpha}\right], \tag{3}$$

where $\mu = 4\pi \sin\nu/\lambda$.

The values of α and A are determined from the two lines (h_1, k_1, l_1) and (h_2, k_2, l_2) with intensities I_1 and I_2 when $h^2 + k^2 + l^2 > 27$:

$$\alpha = \pi^2 \left(\frac{h_2^2 - h_1^2}{a^2} + \frac{k_2^2 - k_1^2}{b^2} + \frac{l_2^2 - l_1^2}{c^2}\right) \frac{1}{\ln \frac{I_1 C_1}{I_2 C_2}}, \tag{4}$$

$$A = \frac{\sqrt{C_1 I_1}}{(\pi/\alpha)^{3/2}} \exp\left[\frac{\pi^2}{\alpha}\left(\frac{h_1^2}{a^2} + \frac{k_1^2}{b^2} + \frac{l_1^2}{c^2}\right)\right], \tag{5}$$

where C_1 and C_2 are the products of factors which are taken into account experimentally.

As we have mentioned above, the f-curve of the first fraction of electrons $f_1(hkl)$, at high values of the indices, should coincide with the f-curve obtained experimentally. When $h^2 + k^2 + l^2 = 0$ ($\mu = 0$), the value of f_1 (0,0,0) is equal to the number of electrons in the first fraction.

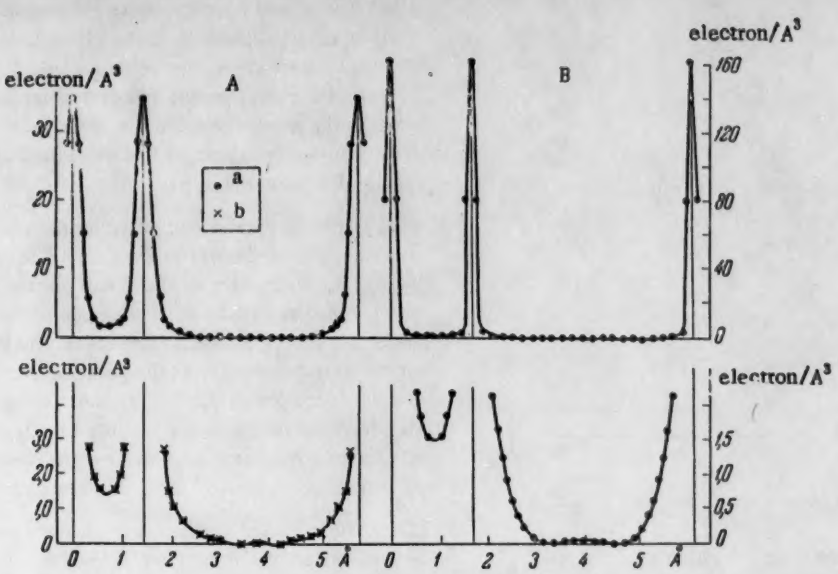

Fig. 2. Calculated values of the electron density in the diamond lattice in the [111] direction. A) At the calculation temperature (7500°K); a) by the usual method for summation of the series (1); b) by the proposed method; B) at 20°C, calculated by the new method without the introduction of a temperature factor.

Figure 1 shows that in the case of diamond the overlap of the f_1-curve for the first fraction of the electrons and the experimentally determined f-curve, starts, within the limits of experimental accuracy, when the sum of the squares $h^2 + k^2 + l^2 = 27$.

The curve f_2 in Fig. 1 gives the difference $f - f_1 = f_2$ produced by the electrons of the second fraction with unknown distribution ρ_2.

The electron density at any point in the crystal $\rho(\mathbf{r})$ may be represented as

$$\rho(\mathbf{r}) = \rho_1(\mathbf{r}) + \rho_2(\mathbf{r}) = \sum_j \rho_j \exp[-\alpha_j(\mathbf{r} - \mathbf{r}_{0j})^2] + \\ + \frac{1}{v}\sum_h \sum_k \sum_l F_2 \exp[-2\pi i \mathbf{r}\mathbf{H}]. \qquad (6)$$

$\rho_1(\mathbf{r})$ is the given density produced by summation of the density ρ'_1 over all the atoms of the lattice and ρ_2 is the unknown difference between the actual and given densities, which it is desired to find.

The actual calculation of the electron density distribution involves summation of the series

$$\frac{1}{v}\sum_h \sum_k \sum_l F_2 \exp(-2\pi i \mathbf{r}\mathbf{H}).$$

Figure 2 shows the calculated electron distribution in the [111] direction for diamond.

According to the data given, the radius of the carbon ion in diamond is 0.20-0.25 A, and the degree of ionization corresponds to C + 4.0.

In the spaces between the coordinates $^1/_2$, $^1/_2$, $^1/_2$, and $^3/_4$, $^3/_4$, $^3/_4$, the electron density is close to zero, within the limits of accuracy of the experimental data. In the space from 0,0,0 to $^1/_4$, $^1/_4$, $^1/_4$, the electron density minimum corresponds to 1.53 electron/A^3, this value being approximately 5 times that for silicon in the same position, which apparently results from the nature and energy of the interatomic bonds.

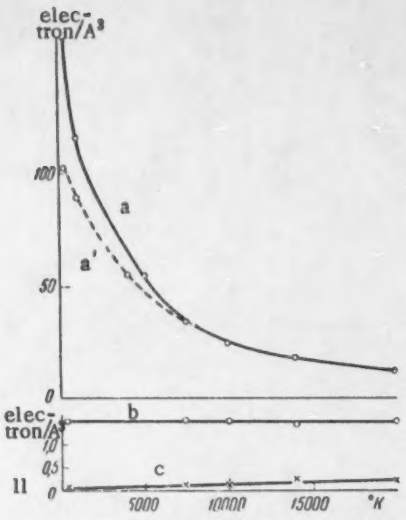

Fig. 3. Change in the calculated values of the electron density with change in the calculation temperature. a) At the point 0,0,0, calculated by the new method; b) at the point $^1/_8$, $^1/_8$, $^1/_8$; c) at the point $^1/_2$, $^1/_2$, $^1/_2$; a') at the point 0,0,0, calculated by the usual method.

The actual electron density distribution close to the nucleus differs slightly from the given distribution as a result of added terms which can be calculated from the difference between the experimental and given atomic scattering factors. In the spaces between the atoms, the value of the given density is negligibly small and the actual electron density is practically the same as ρ_2.

Figure 3 gives curves showing the change in the calculated electron density at the points 0,0,0, $^1/_8$, $^1/_8$, $^1/_8$ and $^1/_2$, $^1/_2$, $^1/_2$, with change in the calculation temperature. The graph shows that the introduction of the temperature factor has a very marked influence on the values obtained for the electron density at the point 0,0,0, and, to a lesser extent, at the points $^1/_8$, $^1/_8$, $^1/_8$, and $^1/_2$, $^1/_2$, $^1/_2$. It should also be noted that it is not possible to extrapolate to room temperature the curve obtained by introduction of the temperature factor.

The proposed method reveals new possibilities for the determination of electron density and for the solution of problems regarding the nature of the chemical bond in solids.

LITERATURE CITED

1. W. H. Bragg, Phil. Trans. Roy. Soc. 215, 253 (1915).
2. P. Epstein and P. S. Ehrenfest, Proc. Nat. Acad. Sci. 10, 133 (1924).
3. W. Duane, Proc. Nat. Acad. Sci. USA, 11, 489 (1925).
4. D. K. Froman, Phys. Rev. 36, 1339 (1930).
5. R. Brill, H. G. Grimm, et al., Naturwiss. 26, 479 (1938).
6. R. Brill, H. G. Grimm, et al., Ann. Phys. 34, 393 (1939).
7. R. Hosemann and S. N. Bagch, Nature 171, 785 (1953).
8. N. V. Ageev and D. L. Ageeva, Izvest. Akad. Nauk SSSR, Otd. Khim. Nauk 1, 17 (1948).
9. N. V. Ageev and I. N. Guseva, Izvest. Akad. Nauk SSSR, Otd. Khim. Nauk 5, 470 (1948).
10. A.J. Snow, Acta Cryst. 4, 481 (1951).
11. A. Wittl and E. Wölfel, Rev. Mod. Phys. 30, 51 (1958).
12. A. Kh. Breger and G. S. Zhdanov, Doklady Akad. Nauk SSSR 28, 1, 630 (1940).
13. Yu. N. Shuvalov, Zhur. Tekh. Fiz. 26, 9, 1870 (1956).
14. Yu. N. Shuvalov, Fiz. Tverd. Tela 1, 208 (1959).
15. W. Cochran, Rev. Mod. Phys. 30, 47 (1958).
16. N. N. Sirota, N. M. Olekhnovich, and A. U. Sheleg, Doklady Akad. Nauk Byelorussian SSR (1960).
17. R. James, Optical Principles of the Diffraction of X-Rays [Russian translation] (1950).
18 W. Nowackl, Fouriersynthese von Kristallen (1952).

THE MECHANISM OF THE INFLUENCE OF NEUTRAL ELECTROLYTES ON THE BOND BETWEEN PARTICLES IN THE COAGULATION STRUCTURE

G. I. Fuks

Scientific and Research Institute of the Timepiece Industry

(Presented by Academician P. A. Rebinder, December 8, 1959).

Translated from Doklady Akademii Nauk SSSR, Vol. 132, No. 1, pp. 164-167, May, 1960

Original article submitted December 1, 1959

The development of our knowledge of coagulation structure formation has enlarged our ideas of the coagulation interaction of the particles making up a disperse system. Although in the past this kind of interaction may have been thought to be characteristic only of dilute colloidal dispersions, it is known today that it also plays a

TABLE 1

Kinetic Bond between Plane-Parallel Quartz Discs (diameter 12 mm) in Electrolyte Solutions after Contact for 30 Minutes, under Pressure of 4 kg/cm^2 (tearing stress 0.08 kg/cm^2)

Electrolytes	Concentration of solution, meq/liter	Time of separation, sec	Electrolytes	Concentration of solution, meq/liter	Time of separation, sec
LiCl	10	2,9	$MgCl_2$	10	14,7
NaCl	1	3,7	$CaCl_2$	10	15,5
NaCl	10	4,3	$BaCl_2$	5	30,0
NaCl	1000	9,3	$BaCl_2$	10	34,0
KCl	10	13,0	$AlCl_3$	10	43,0
RbCl	10	14,1	$Th(NO_3)_4$	10	45,4

most important role in creating the properties of concentrated and polydisperse suspensions, pastes and deposits [1, 2]. Simultaneously with this expansion, there has also, naturally, been extended the problem of the influence of electrolytes on the coagulation bond between particles. In the present work, with the object of studying the elementary act of interaction between particles, dimensional models have been used [3]—the thickness and the resistance to thinning have been measured for the limiting layer of the electrolyte solution, in the space between the smooth-polished, plane-parallel, round quartz discs in these solutions, using the method described in [4]; and the friction of the spherical surfaces of negatively charged quartz and positively charged ruby in the same solution has been measured by the method described in [5]. In the disc apparatus the distance between the surfacescould be varied between the limits of 3-5 and 0.02 μ (within experimental error of $\pm 0.01\mu$); the contact pressure was from 0.04 to 10 kg/cm^2. In the tribometer, direct contact between pairs of surfaces was obtained with contact pressure from 50 to 550 kg/mm^2.

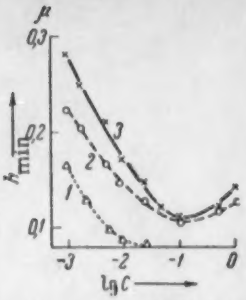

Fig. 1. Effect of concentration (in g-equiv/liter) on the thickness of the residual layer of solution in the space between quartz surfaces at a contact pressure of 0.2 kg/cm^2. 1) $BaCl_2$; 2) KCl; 3) NaCl.

TABLE 2

Thickness of the Residual Layer in 0.01 Solutions of Electrolytes, and Its Thinning Resistance in the Space between Quartz Discs

Electrolytes	h_{min} (μ) at stated contact pressure (kg/cm^2)			$\bar{E}$ (kg/cm^2) in the stated pressure intervals	
	0.2	2.0	4.0	0.2–2.0	2.0–4.0
LiCl	0,25	0,11	0,06	3,3	5,5
NaCl	0,14	0,09	0,05	5,0	6,7
KCl	0,12	0,08	0,04	7,7	10,6
RbCl	0,11	0,08	—	7,2	—
$CaCl_2$	0,08	0,06	0,04	4,1	9,6
$AlCl_3$	0,08	0,05	0,03	6,2	12,0
$Th(NO_3)_4$	0,07	0,03	0,03	6,0	18,0

It follows from the work reported in [3, 6] that the electrolytes increase the kinetic resistance of the thin water layers adjacent to the discs, and also give to these layers a static resistance (equilibrium and nonequilibrium), leading to the preservation in the space between the discs of a residual (nonremovable) layer of solution (whose thickness will be represented by h_{min}). The effect of electrolytes on the kinetic resistance of neighboring particles does not apparently reach large proportions, since the limiting viscosity in the peripheral part of the boundary layer is increased by ions by a factor of more than 5 [3], and the transition to the residual layer is sudden.

On the other hand, the kinetic bond between plane particles, expressed by the separation time [3], depends to a considerable extent on the composition of the solution which surrounds them (Table 1). It is known that the limiting viscosity exerts an influence on this effect, but a more important fact is that the composition of the solution determines the thickness of the residual layer (Table 2), and, therefore, also the space between the surfaces which can exist under any given pressure which is not too high. We may note that the kinetic bond depends not only on the distance between the surfaces, but also on the shape of the space, so that the effect of the electrolytes on the time of separation of convex particles ought to be considerably less than for planar ones.

The thickness of the residual layer is determined by the concentration of the solution (Fig. 1), the charge of the oppositely charged ions, and their radius (Table 2). With increase in contact pressure, and, correspondingly, reduction in the distance between the surfaces, the part played by the radius of the ions diminishes, and at high concentration of the solution the part played by the charge on the ions also diminishes. The curve of $h_{min} = f(C)$ is the reverse of the curve of the relationship between the coefficient of static friction and adhesion of microscopic particles, and the concentration of the solution of electrolytes [7]. The thinning resistance of the residual layer is primarily determined by its thickness, and therefore in a selected pressure range (from 6-8 kg/cm^2), in solutions which at this given pressure form the thinner residual layers, the index of this resistance is, in the majority of cases, higher. With increase in the concentration of the solution from 5-10 meq/liter, $\bar{E}$ is increased, but further increase causes little change.

A qualitative consideration of the data which have been obtained leads to the conclusion that the space between quartz surfaces in electrolyte solutions is linked with the thickness of the diffusion layer of the adsorbed ions and the interaction of these layers. Starting from the theories of the double layer proposed by Gouy and Chapman, B. V. Deryagin [8] and A. N. Frumkin [9], equations have been obtained describing the repulsion of plane diffusion layers. For the case in which the potential of the surface is considerably less than RT/F, these equations coincide. If we express χ (the index of the thickness of the ion atmosphere on the theory of Debye and Hückel) by means of $KZ\sqrt{C}$, where K is a constant, Z is the charge number on the ion in the diffusion layer, and C, the concentration of the solution, the equation may be rewritten in the following form, which is suitable for verification by a method of alignment: $F_r = KZ^2Ce^{-hKZ\sqrt{C}}$, where F is the force of repulsion between contiguous diffusion layers, and h is the distance between the surfaces.

Comparison of the experimental data (the points on Fig. 2) with the theoretical relationship shows that, in electrolyte solutions of concentrations up to 8-10 meq/liter, the ions impede the contact of the surfaces at a

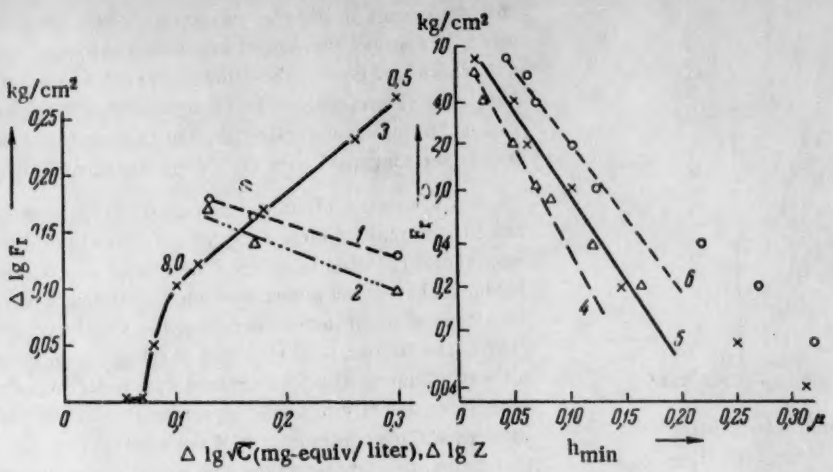

Fig. 2. Testing by the alignment method of the applicability of the equation for the forces of repulsive interaction between the diffuse layers of adsorbed ions. 1, 2) F_r = = f(z, C); 1) when $h_{min} = 0.06 \pm 0.01\ \mu$; 2) when $h_{min} = 0.04 \pm 0.01\ \mu$; 3) $F_r = f(C_{KCl})$ (the numbers on the curves denote the values of C in meq/liter); 4, 5, 6) F = f(h); 4) when χ = 1.5 meq in 1 lieter $CaCl_2$; 5) when χ = 2.5 meq in 1 liter KCl; 6) when χ = 1 meq in 1 liter NaCl.

TABLE 3

The Coefficient of Friction of Ruby and Quartz in 0.001 N Solutions of Neutral Electrolytes (contact pressure: ruby 530; quartz 108 kg/mm²; preliminary interaction between minerals and solution – one hour)

Electrolytes	Static friction		Kinetic friction		Electrolytes	Static friction		Kinetic friction	
	ruby	quartz	ruby	quartz		ruby	quartz	ruby	quartz
LiCl	0,105	0,440	0,150	0,320	K_2SO_4	0,110	0,490	0,170	0,370
KCl	0,097	0,465	0,160	0,330	$K_3Fe(CN)_6$	0,114	0,550	0,200	0,375
$AlCl_3$	0,112	0,420	0,220	0,330	$K_4Fe(CN)_6$	0,113	0,605	0,210	0,390
$Th(NO_3)_4$	0,114	0,350	0,225	0,350					

distance at which van der Waals forces are effective, owing to the electrostatic repulsion of the diffusion layers. In more concentrated solutions, and also when there are comparatively large distances between the surfaces of the order of thickness of the boundary layer, a nonelectrostatic factor should influence the interaction.* Since in these cases it is the radius of the ions which has the greatest significance (at least within the limits of uni- and bivalent cations [6]), it is most probable that this factor is the long-distance [10] or secondary [11] hydration of the ions.

The high contact pressure used in our tribometric experiments to determine the microhardness of the minerals under examination, was sufficient to overcome the repulsive forces of the adsorbed ions, but the effect of electrolytes on the interaction between the surfaces of these minerals was not disturbed. It can be seen from Table 3

*It is quite possible that a development of the theory of the interaction of diffusion layers on the basis of a more complete picture of their structure than was assumed by Gouy, would enlarge the region in which it was possible to apply an electrostatic repulstion mechanism, but there is no basis for the idea that such a mechanism could be universally applied.

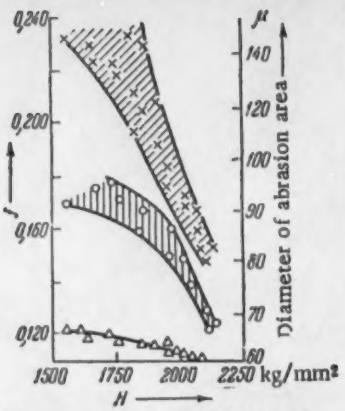

Fig. 3. Coefficient of friction (f) and abrasion of ruby in electrolyte solutions of various composition and concentration, in relation to the microhardness (H) of ruby in these solutions. 1) Static friction; 2) abrasion (duration of friction, 10 min); 3) kinetic friction.

that the change in friction, in relation to the composition of the solution, does not correspond to the expression derived for the repulsive forces between the diffusion layers, and the coefficient of friction is determined by the charge-number of the anions and cations, which demonstrates that the mechanism of the ionic effect is not concerned with the charge on the surface.

The specific effect of electrolytes at high contact pressure is linked with their influence on the surface of the minerals. It has been shown [12] that in solutions of neutral electrolytes the microhardness of ruby and quartz are reduced (which is one of the manifestations of adsorption-reduction of the solidity of solid bodies [13]). The friction (and abrasion) of ruby, and in special groups of solvents of quartz also, is increased with reduction of the microhardness, independently to a first approximation of the composition of the ions and the concentration of the solution (Fig. 3), which is explained by the increase in the true contact area with the "plastified" surface. If in such a case the specific strength of the molecular interaction is not reduced (which is very probable in the case under discussion), then the electrolytes must increase the total strength of molecular interaction.

The effective manifestation of the mechanism which has been considered, exerted by electrolytes on the bond between particles (and macrobodies) in solutions, is determined by the distance between the surfaces.

LITERATURE CITED

1. P. A. Rebinder, Proceedings of the Conference on the Viscosity of Liquids and Colloidal Solutions [in Russian] (Izd. AN SSSR, 1941) 1, p. 361; Koll. Zhur. 12, 228 (1950).
2. G. Freundlich, Tiksotropiya [Russian translation] (IL, 1939); G. I. Fuks, Koll. Zhur. 12, 228 (1950).
3. G. I. Fuks, Works Produced at the Third All-Union Conference on Colloid Chemistry [in Russian] (Izd. AN SSSR, 1956) p. 301; Koll. Zhur. 20, 748 (1958).
4. G. I. Fuks, Zavodskaya Lab. 21, 12, 1445 (1955).
5. G. I. Fuks, Zavodskaya Lab. 22, 5, 594 (1956).
6. G. I. Fuks and N. I. Kaverina, Doklady Akad. Nauk SSSR 121, 332 (1958).*
7. G. I. Fuks, V. M. Klychnikov, and E. V. Tsyganova, Doklady Akad. Nauk SSSR 65, 307 (1949).
8. B. V. Deryagin, Ser. Khim. (Izv. AN SSSR, 1937) 5, 1153.
9. A. N. Frumkin and A. V. Gorodetskaya, Acta Physicochimica, USSR 9, 327 (1938).
10. O. Ya. Samoilov, The Structure of Aqueous Solutions of Electrolytes and the Hydration of Ions [in Russian] (Izd. AN SSSR, 1957).
11. D. Bokris, Some Problems in Contemporary Electrochemistry [Russian translation] (IL, 1958).
12. G. I. Fuks, Koll. Zhur. 22, 2 (1960).*
13. P. A. Rebinder, Z. Phys. 72, 191 (1931); Physicochemical Mechanisms [in Russian] (Moscow, 1958).

* Original Russian pagination. See C. B. translation.

AN INVESTIGATION OF THE GEL-FORMING PROPERTIES OF ALUMINUM OLEATES IN BENZENE

G. V. Belugina, V. V. Konstantinova, S. Kh. Zakieva, and Academician P. A. Rebinder

Physical Chemistry Institute, Academy of Sciences of USSR

Translated from Doklady Akademii Nauk SSSR, Vol. 132, No. 2, pp. 380-383, May, 1960

Original article submitted February 6, 1960

Aluminum soaps of fatty acids, having the general formula $Al(OH)_n(OOCR)_m$, where n + m = 3, are well-known as solidifying agents for various liquid hydrocarbons. A great number of works has been devoted to the structure and properties of these soaps, and in the course of these it has been shown that the presence of hydroxyl groups in the molecules of aluminum soaps with any given hydrocarbon R has a determinative effect on their solidifying properties [1]. The greatest solidifying power is possessed by the doubly substituted soaps $Al(OH)(OOCR)_2$ (in which n = 1), a fact apparently connected with the association of the separate molecules into short chains through their hydroxyl groups, with the further formation by means of van der Waals forces and hydrogen bonds of irregular networks – so giving a gel structure. The unsatisfactory solidifying properties of the singly substituted soaps $Al(OH)_2(OOCR)$, where n = 2.0, may be explained by the emergence of intramolecular hydroxyl bonds. The possibility of the existence of the triply substituted soaps $Al(OOCR)_3$ can be regarded as small, for the ease of hydrolysis and instability, coupled with steric factors, which would impede the arranging of three organic radicals around a single aluminum atom, and other factors, all tell against it [1, 2].

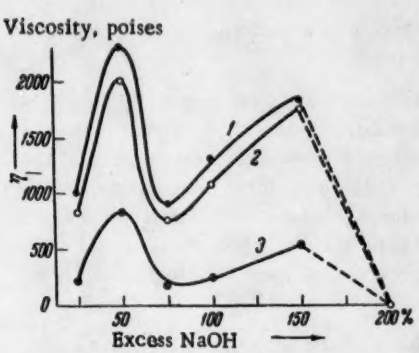

Fig. 1

The structure-forming properties of the aluminum soaps depend to a great extent on the molecular weight and nature of the radical [1, 3]. Thus, in the formation of the aluminum soap of naphthenic acids, whose hydrocarbon radicals have a complex cyclic structure, the optimum solidifying capacity is possessed by soaps precipitated with an excess of free alkali of 75% (in relation to the bound alkali), that is, with n = 1.17 [4]. This has been shown to be the case for naphthenic acids of various mean molecular weights from 214 to 250, in spite of the fact that the solidifying power of the soaps increases greatly with reduction of molecular weight in this range [5].

Insufficient attention has been given in the literature to the aluminum soaps of unsaturated fatty acids. It is a matter of interest to discover what influence the double bond in the radical of a fatty acid may exert on the structure-forming properties of aluminum soaps, and to establish the composition of the oleic acid soaps which correspond to maximum viscosity and stability of oleo gels.

Preparation of Aluminum Oleates and Their Benzene Gels. The aluminum soaps of oleic acid were prepared by the usual method of double decomposition [using a solution of $Al_2(SO_4)_3$ and an alkaline solution of the sodium

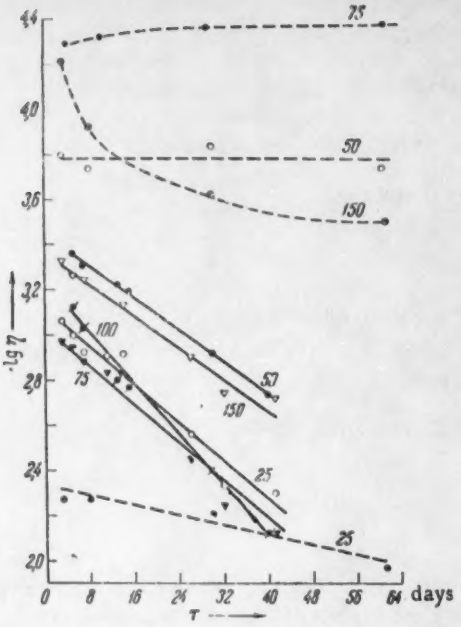

Fig. 2

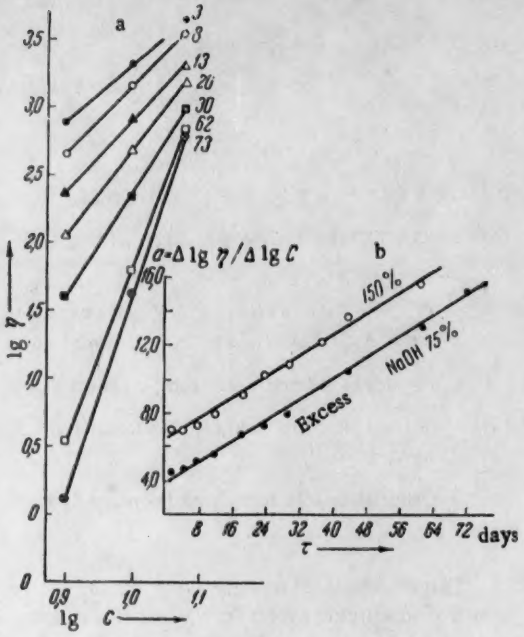

Fig. 3

soap of oleic acid, containing a definite quantity of free alkali]. Precipitation was performed at 70°, and the pH of the medium at the conclusion of precipitation was between 5.0 and 4.5.

Gels from these soaps were prepared by dissolving weight amounts of the soap in cryoscopically pure benzene with vigorous agitation at room temperature. The dissolution of the soap and the "maturing" of the gel takes place very slowly compared with the aluminum naphthenates, and therefore the first measurements of the viscosity are performed during a period of 3-5 days after the preparation of the gel. It has been found that gels of aluminum oleate possess considerably smaller solidifying power than those prepared from aluminum naphthenates under the same conditions and with the same compositions. Aluminum oleate gels possess elastic-solid properties, in contrast with those of aluminum naphthenates of the same concentrations, and have higher values of the limiting high elastic deformation [6].

Effect of the Composition of Aluminum Oleates on the Composition of Their Oleogels. Aluminum soaps of oleic acid have been precipitated in alkali excess of from 25 to 200%, and from them there have been prepared 8% gels with cryoscopically pure benzene.

The viscosity of the gels has been denoted, as in our earlier experiments, by the highest value of their viscosity (the limiting viscosity), η, corresponding to a practically undamaged structure. The invariance of this viscosity – that is, its independence of the order of events in the measurement (for low rates of sheer) – has been the subject of careful verification.

Figure 1 gives the relationship between the viscosity of 8% gels and the composition with respect to free alkali during the precipitation of the soap, for various keeping times of the gels. Curve 1 refers to 5 days, curve 2, to 7 days, curve 3, to 30-32 days. The viscosity reaches a maximum when the excess of alkali is 50% (n = 1.0), then falls, and then increases again to give a second, lower maximum at 150% excess alkali (n = 1.7). This is apparently due to the increased hydrophilic (oleophobic) character of the soap. Soaps precipitated in the presence of 200% excess alkali – that is, soaps of composition corresponding to the monosubstituted compound with n = 2 – are practically insoluble in benzene even after heating; upon standing, the individual particles of the soap swell and enclose gels, but there is no general formation of a gel structure throughout the mass of the benzene. It can be seen, therefore, that in the case of aluminum oleate, as in the cases of soaps of the saturated fatty acids, the optimum solidifying power is attained with the doubly substituted soap, where n = 1.0.

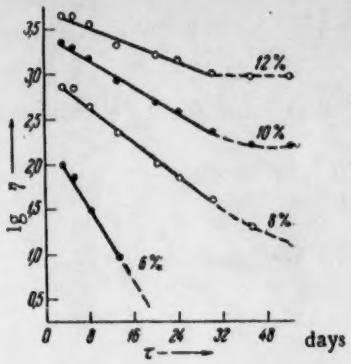

Fig. 4

Observations made on the aging of these oleogels (Fig. 2*) show that their stability is low. The viscosity decreases greatly with time. It is natural to connect this with chemical instability due to the presence of the double bond in the hydrocarbon radical, although this, on the other hand, helps the process of solution and subsequent solidification. However, addition of around 1.5% of such typical antioxidants as α-naphthol [7] to the soap does not, as we have shown, change the course of the automatic reduction in the viscosity of the gel – that is, does not affect its aging. The relationship between $\log\eta$ and τ is practically a straight line with almost constant slopes, except in the case where the excess of alkali is 100%. Thus, the composition of the soap exerts its influence basically on the viscosity of the gels, and is practically without effect on their stability. In contrast, the composition of the soap in the case of aluminum naphthenates influences strongly not only the viscosity level of the gels, but also their aging (see Fig. 2: 6% soap in benzene, dotted curve) [4].

Effect of Aluminum Oleate Concentration on the Properties of its Oleogels. Gels have been prepared with soap concentration from 6 to 12%. Figure 3,a** shows the increase of the viscosity of the oleogel with increase in the soap concentration. The soap was precipitated with an excess of alkali of 75%, or n = 1.17. It has been shown that within quite a wide range of soap concentrations a simple general relationship holds good:

$$\lg\eta = K + a\lg C, \tag{1}$$

where the constant $K(\tau) = \log\eta_{C=1}(\tau)$ and the constant $a(\tau)$ are found to depend on the time of aging of the gel:

$$a = a_0 + b\tau, \tag{2}$$

$$K = K_0 - \alpha\tau; \tag{3}$$

$K_0 = K_{\tau=0}$ and $a_0 = a_{\tau=0}$: these are constants dependent neither on C nor on τ. It follows from (1), (2), and (3) that:

$$\lg\eta = A - B\tau, \tag{4}$$

where

$$A = \lg\eta_{\tau=0} = K_0 + a_0\lg C, \tag{5}$$

$$B = \alpha - b\lg C, \tag{6}$$

$b = da/d\tau$, and is not only independent of the time [because of the linearity of $a(\tau)$ (2)], but also independent of the excess of alkali used in preparing the soap within the range 75-150% (Fig. 3,b). This linear relationship is well confirmed within the wide range of τ from 3-70 days, of η from $4.5\cdot10^3$ to 10, and of C from 6% and 8% to 12%. According to the nature of the decrease of η with time, so much the greater is the increase in concentration required to maintain the high level of viscosity required for structure formation.

Increase in concentration of soap (the numbers are given against the relevant curves in Fig. 4), when this has been precipitated with an alkali excess of 75%, diminishes the rate at which the aging process takes place in the gel, but even a 12% gel is not stable when preserved for more than 2 weeks, its viscosity decreasing appreciably during this period. In contrast with this, gels containing as little as 4% aluminum naphthenates and prepared under similar conditions remain stable over a protracted period of time [4, 8].

* The figures against the curves show the percentage excess of NaOH during the precipitation of the soap.

** The numbers by the curves denote the time of aging of the gel in days.

LITERATURE CITED

1. T. S. McRoberts and J. H. Schulman, Nature 162, 101 (1948); Proc. Roy. Soc. 200 A, 135 (1950); A. E. Alexander and V. R. Gray, J. Phys. Coll. Chem. 53, 9, 23 (1949); Proc. Roy. Soc. 200 A, 162 (1950).
2. C. G. McGee, J. Am. Chem. Soc. 71, 278 (1949).
3. G. A. Parry, et al., Proc. Roy. Soc. 200 A, 148 (1950); F. J. Licata, J. Am. Oil Chemists Soc. 31, 5, 204 (1954).
4. G. V. Belugina and A. A. Trapeznikov, Koll. Zhurn. 20, 1, 4 (1958).*
5. A. A. Trapeznikov, G. V. Belugina, and F. M. Rzhavskaya, Koll. Zhurn. 20, 2, 254 (1958).*
6. V. A. Fedotova and A. A. Trapeznikov, Doklady Akad. Nauk SSSR 120, 4, 841 (1958).*
7. W. H. Rueggeberg, J. Phys. Coll. Chem. 52, 9, 1444 (1948).
8. G. V. Belugina, S. Kh. Zakieva, P. A. Rebinder, and A. B. Taubman, Doklady Akad. Nauk SSSR 126, 2, 318 (1959). *

*See CB translation.

KINETICS OF THE VAPOR-PHASE HYDRATION OF ETHYLENE ON A PHOSPHORIC ACID CATALYST

A. I. Gel'bshtein, Yu. M. Bakshi, and M. I. Temkin

L. Ya. Karpova Physicochemical Institute

(Presented by Academician V. A. Kargin, December 30, 1959)

Translated from Doklady Akad. Nauk SSSR, Vol. 132, No. 2, pp. 384-387, May, 1960

Original article submitted December 21, 1959

The reaction

$$C_2H_4\,(g) + H_2O\,(g) = C_2H_5OH\,(g) \qquad (1)$$

is widely used in industry. The process is carried out at pressures of 60-80 atm and temperatures of 280-300° and phosphoric acid is used as a catalyst on a porous support consisting mainly of SiO_2. We investigated the kinetics of the reaction in a flow system using the phosphoric acid on silicagel catalyst in the form of 2.5 mm granules. Experiments in which the granule size and the H_3PO_4 content of the catalyst were varied showed that the reaction proceeded in the kinetic region.

It was obvious to assume that the mechanism of reaction (1) would be analogous to the mechanism of the vapor-phase hydration of C_2H_2 on a phosphoric acid catalyst previously investigated in our laboratory [1], that is, it would correspond to the olefin hydration mechanism proposed by Taft [2]. Then the kinetics of reaction (1) will differ from the hydration kinetics of C_2H_2 only insofar as it is necessary to take the reverse reaction into account. The mechanism, as adapted to reaction (1), may be given in the following form:

$$C_2H_4 \underset{-H^+}{\overset{+H^+}{\rightleftarrows}} H_2C\overset{H^+}{\uparrow}\!\!\!

TABLE 1

Total pressure, P, atm	Reaction time t sec	Partial pressures, atm			$\frac{a}{a_{co}}$	$k \cdot 10^3$	$P_{3}O_{4}$,%	h_0	$k_1 \cdot 10^3$	$k' \cdot 10$
		C_2H_4	H_2O	C_2H_5OH						
81	0,148	50,6	29,9	0,478	0,177	6,85	69,08	2,24	3,06	3,74
71	0,150	40,0	30,4	0,415	0,174	7,53	69,07	2,24	3,36	4,15
61	0,148	30,2	30,5	0,272	0,156	6,54	69,07	2,24	2,92	3,61
51	0,150	20,7	30,1	0,212	0,171	7,50	69,08	2,24	3,35	4,12
71	0,166	29,5	41,2	0,312	0,137	6,60	68,80	2,09	3,16	4,24
61	0,166	29,6	31,0	0,343	0,195	7,75	69,04	2,22	3,49	4,31
51	0,166	29,5	21,1	0,362	0,292	8,61	69,47	2,49	3,46	3,95
41	0,170	29,9	10,6	0,397	0,583	11,60	70,20	3,02	3,84	3,78
36	0,172	30,5	5,1	0,289	0,870	11,80	71,00	3,71	3,19	2,67
81	0,372	49,5	30,2	1,170	0,436	8,11	69,04	2,22	3,66	4,45
71	0,373	40,5	29,5	0,937	0,418	7,87	69,08	2,24	3,51	4,27
61	0,374	30,3	30,0	0,705	0,398	7,82	69,07	2,24	3,49	4,28
51	0,370	20,4	30,1	0,445	0,362	7,20	69,08	2,24	3,21	3,94
41	0,372	10,8	29,9	0,253	0,372	7,80	69,09	2,25	3,46	4,26
71	0,332	29,8	40,5	0,568	0,244	6,50	68,77	2,07	3,14	4,14
61	0,354	29,8	30,5	0,644	0,359	7,48	69,06	2,24	3,34	4,14
51	0,372	30,2	20,0	0,763	0,590	9,78	69,50	2,51	3,89	4,36
41	0,372	30,2	10,2	0,565	0,863	11,05	70,22	3,03	3,65	3,53
71	0,690	30,3	39,6	1,160	0,480	7,58	68,75	2,06	3,68	4,76
61	0,710	30,1	29,7	1,135	0,612	8,20	69,06	2,24	3,66	4,46
51	0,720	30,0	19,9	1,040	0,800	9,90	69,49	2,51	3,95	4,11
41	0,680	29,2	11,0	0,673	0,983	10,75	70,14	3,01	3,58	3,57

complex in the rate-determining step; h_0 – the acidity of phosphoric acid ($h_0 = a_{H^+} f_B / f_{BH^+}$, where B is a base); $P_{C_2H_4}$ – the partial pressure of C_2H_4.

Neglecting the change of $\underline{s}$ and of the ratio $f_\pi / f_{C_2H_4} f^{\neq}$ caused by the changing composition of the acid we get the equation

$$v_1 = k_1 h_0 P_{C_2H_4}. \tag{4}$$

In an analogous way we obtain for the reverse reaction

$$v_2 = k_2 h_0 \frac{P_{C_2H_5OH}}{P_{H_2O}}. \tag{5}$$

The constants k_1 and k_2 are connected with the equilibrium constant of reaction (1) by the relation

$$\frac{k_1}{k_2} = K_P. \tag{6}$$

Therefore, the observable reaction rate is given by the equation

$$v = k\left(P_{C_2H_4} - K_P^{-1} \frac{P_{C_2H_5OH}}{P_{H_2O}}\right); \tag{7}$$

where

$$k = k_1 h_0 \tag{8}$$

The value of $\underline{k}$ must be constant at constant P_{H_2O}. Because the degrees of conversion of C_2H_4 and H_2O are small, one may neglect the volume change caused by the reaction and take $v = dP_{C_2H_5OH}/dt$, where $\underline{t}$ represents the "reaction time" calculated as the ratio of the volume of the acid in the catalyst to the volume of the gas mixture charged [1].

TABLE 2

C°	270°	290°	310°	330°
$k_1 \cdot 10^2$	1.00	3.46	10.50	25.3
$k' \cdot 10$	2.46	4.24	7.21	9.43

Integrating Eq. (7) at constant $P_{C_2H_4}$ and P_{H_2O} one obtains

$$k = -\frac{1}{t} K_P P_{H_2O} \ln\left(1 - \frac{P_{C_2H_5OH}}{K_P P_{C_2H_4} P_{H_2O}}\right). \tag{9}$$

In Table 1 are given the experimental data and the values of k calculated by means of Eq. (9). The values of K_p have been determined from equilibrium data [3], since it has been found that K_p does not depend upon the $N_{H_2O}/N_{C_2H_4}$ ratio at given P and T [4]. The extent of approach to equilibrium is characterized by the ratio of the degree of ethylene conversion α to its equilibrium value α_∞.

It is obvious from the table that k is constant within the accuracy of the experiment, when $P_{C_2H_4}$ and even t are varied but P_{H_2O} is held constant. When P_{H_2O} is increased, the yield of alcohol not only does not increase, but even decreases slightly (provided that equilibrium is not attained) in qualitative agreement with Eq. (8).

To check Eq. (8) the composition of the acid was calculated from the H_2O partial pressure by means of the formula

$$\log \frac{P_{H_2O}}{P^0_{H_2O}} = \left(\frac{1075}{T} - 1{,}515\right)(72{,}4 - \%\ P_2O_5), \tag{10}$$

where $P^0_{H_2O}$ represents the H_2O partial pressure above H_3PO_4 (100%). Equation (10) has been derived from data previously published [5] as also from some additional data. The value of h_0 was determined from the composition of the acid assuming a linear dependence between $H_0 = -\log h_0$ and the temperature [6, 7]. In Table 1 are shown the values of $k_1 = k/h_0$ and they are approximately constant.

One should keep in mind that the value of h_0 are only approximations, since they have been obtained by extrapolation. In any case, the fact that the yield of alcohol changes only slightly when P_{H_2O} is varied considerably shows that the reaction is of zero order in H_2O and confirms the first assumption from which we started, namely, that H_2O does not take part in the rate-determining step.

For technical calculations it is convenient to give the reaction rate as an explicit function of P_{H_2O}. This may be done in the following way. Since the catalyst is equivalent to a solution of H_3PO_4 with a low H_2O content, one may in analogy of the result of Brand [8] for concentrated H_2SO_4 solutions suppose that

$$H_0 = \text{const} - \log \frac{X_{H_3PO_4}}{X_{H_3PO_4^-}}, \tag{11}$$

where $X_{H_3PO_4}$ represents the mol. fraction of H_3PO_4, etc. If we consider H_2O to be a base, we get

$$H_0 = pK - \log \frac{X_{H_3O^+}}{X_{H_2O}}. \tag{12}$$

Taking into account that $X_{H_3PO_4^-} = X_{H_3O^+}$ and assuming that X_{H_2O} is proportional to X_{H_2O} is proportional to P_{H_2O} and that $X_{H_3PO_4}$ is practically constant, we get the approximation

$$h_0 = \frac{C}{P^{1/2}_{H_2O}}, \tag{13}$$

where C is a factor which is dependent on the temperature.

Combining Eqs. (7), (8), and (13) one obtains

$$v = \frac{k'}{P_{H_2O}^{1/2}} \left(P_{C_2H_4} - K_P^{-1} \frac{P_{C_2H_5OH}}{P_{H_2O}} \right) \tag{14}$$

where $k' = k_1 C$. For the calculation of k' we used Eq. (9) and the relation

$$k' = k P_{H_2O}^{1/2}. \tag{15}$$

The values of k' given in Table 1 are approximately constant.

Data analogous to those given in Table 1 have been obtained in experiments at 270, 310, and 330° in the same range of $P_{C_2H_4}$, P_{H_2O} and t values.

Average values of k_1 and k' at various temperatures and $P_{H_2O} = 30$ atm are given in Table 2 (t in seconds).

The temperature dependence of k_1 and k' corresponds to the equations

$$\log k_1 = 12{,}18 - \frac{35\,150}{4{,}57T}, \tag{16}$$

$$\log k' = 5{,}39 - \frac{14\,860}{4{,}57T}. \tag{17}$$

The ethylene used in the experiments contained a small amount of $(C_2H_5)_2O$. The amount of ether in the reaction product differed but little from that in the original ethylene. Therefore, there was practically no ether formation under the conditions of the experiments. This has been confirmed by special experiments with ethylene which was nearly free of ether.

Upon investigating the absorption of C_2H_4 and C_3H_6 in sulfuric acid solutions [9] and the acidic hydration of C_2H_2, [1], it has been concluded that the conversion of the π-complex into the carbonium ion is the rate-determining step. The results of this paper enable the extension of the said conclusion to the acidic hydration of C_2H_4.

LITERATURE CITED

1. E. N. Tsybina, A. I. Gel'bshtein, et al., Zhur. Fiz. Khim. 32, 856 (1958).
2. R. W. Taft, J. Am. Soc. 74, 5372 (1952).
3. Yu. M. Bakshi, A. I. Gel'bshtein, and M. I. Temkin, Doklady Akad. Nauk SSSR 126, 314 (1959).*
4. Yu. M. Bakshi, A. I. Gel'bshtein, and M. I. Temkin, Doklady Akad. Nauk SSSR 132, 157 (1960).*
5. A. I. Gel'bshtein and M. I. Temkin, Zhur. Obshch. Khim. 23, 1278 (1953).*
6. A. I. Gel'bshtein, G. G. Shcheglova, and M. I. Temkin, Doklady Akad. Nauk SSSR 107, 108 (1956).*
7. A. I. Gel'bshtein, G. G. Shcheglova, and M. I. Temkin, Zhur. Neorg. Khim. 1, 282 (1956).
8. J. C. Brand, J. Chem. Soc. 997 (1950).
9. A. I. Gel'bshtein and M. I. Temkin, Zhur. Fiz. Khim. 31, 2697 (1957).

*See CB translation.

AUTOMATIC OSCILLATIONS DURING THE REDUCTION OF PERDISULFATE IONS ON MERCURY

A. Ya. Gokhshtein and Academician A. N. Frumkin

Electrochemical Institute of the Academy of Sciences, USSR

Translated from Doklady Akademii Nauk SSSR, Vol. 132, No. 2, pp. 388-391, May, 1960

Original article submitted February 11, 1960

Many cases are described in the literature in which oscillating currents and potentials arise in electrochemical systems in which the polarization characteristics are decreasing. Usually, however, these processes are complicated by passivation of the electrode or the separating out of a solid phase. It was therefore thought desirable to investigate the phenomenon of oscillation in systems free from complications of this kind.

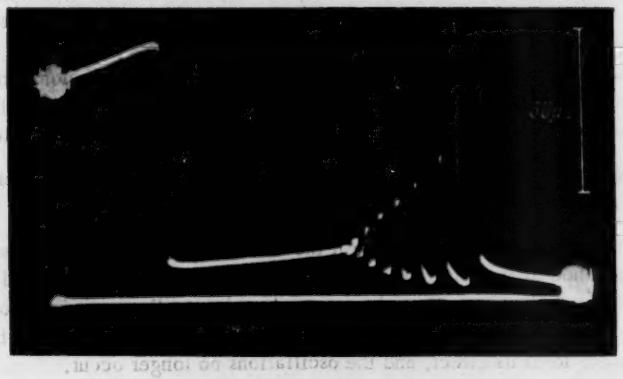

Fig. 1. Oscillogram of 10^{-2} M $K_2S_2O_8$. Rate of emf reduction 2.36 v/sec, amplitude of emf 0.61 v, initial emf: 1.0 v against the normal calomel electrode. Time from the moment of appearance of the drop to the appearance of the impulse = 3 sec.

For this purpose there was selected the reduction of the persulfate ion on a mercury cathode. The ion $S_2O_8^{2-}$ is one of these ions for which, within a certain potential range, a fall of current density takes place as the cathode polarization is increased [1]. In an electrical circuit, which includes this system, the authors have discovered that a self-induced oscillation of current and potential does arise. The circuit consisted of a stabilized emf source (the oscillographic polarograph GEOKhI, or a battery in conjunction with a sliding-wire bridge could be used), a cell with a capillary mercury cathode, a comparison electrode, and a series resistance which could be introduced into the circuit. Investigations were carried out both with constant emf across the ends of the circuit, and with potentials which varied with time at a constant rate. In the investigation of the process by means of the oscillographic polarograph, it was advantageous to vary the potential of the electrode in such a way that acceleration of the reaction occurred through the presence of excess of the reacting substance in the pre-electrode layer. Thus,

Fig. 2. Oscillogram of autooscillations in 10^{-2} M $K_2S_2O_8$, under a potential of 1.2 v relative to the mercury anode.

in the study of the reduction of the persulfate ion it is convenient to start in the region in which fall of current occurs, and the polarization characteristics are positive, and to carry out the study at emf's whose absolute values diminish with time (Fig. 1). The start of this oscillogram (the right-hand side) corresponds to a potential of −0.98 v (measured against the normal calomel electrode), and the oscillation occurs within the region shown. Reduction in the emf (moving from right to left) causing diminution of the polarization characteristics, causes current oscillations to arise. Further reduction of the emf results in reduction in the amplitude of the oscillations, though these do not vanish entirely; after this the trace descends slowly, corresponding to the diffusion current [2]. Further reduction of the emf to 0.2 v results in a rise of the positive current up to the polarographic maximum. Since the resistance of the electrolyte is high, the current oscillations are accompanied by appreciable oscillations of the electrode potential. The reduction of amplitude from right to left (Fig. 1) does not correspond in time to the dying out of the oscillations, since it depends essentially on the relationship between the amplitude on the emf at the ends of the circuit.

If it is desired to stop the change in potential, a sufficiently large series resistance in the circuit establishes the nondamping oscillations shown in Fig. 2. The time during which these oscillations may continue undamped is limited only by the life of the electrode. During work with slow-dripping electrodes a period of 90 sec was attained. The form of the oscillations for various amplitudes (Fig. 1, right to left) remained identical, consisting of a very steep forward face, a brief period of constancy at the maximum current value, which considerably exceeded the diffusion current obtained under conditions when diffusion was absent, after the lapse of the same time from the initiation of emf reduction; there follows a more gradual fall in the current, followed by a time lag in which the current rises slowly but remains smaller than the diffusion current. The frequency of the autooscillations depends on the conditions of the experiment. Under the conditions obtaining when Fig. 1 was obtained, the frequency of oscillation at the greatest amplitude was 57.5 cps, and at the least amplitude 175 cps.

Summing up the information obtained by the experimental investigation of the mercury–potassium persulfate system, we may note the following:

1. An essential condition for the development of the oscillations is a high series resistance (1-20 kohm). This is made up of the resistance of the solution itself, and of the resistance box included in series in the circuit. If a third electrode is introduced into the cell, and connected to the oscillographic polarograph through the grid of the value of the charging resistance compensator, then control of the emf is replaced by control of the electrode potential, the series resistance loses its effect, and the oscillations no longer occur.

2. In those cases where the remaining conditions do not favor the production of oscillations, these may be produced by increasing the rate of potential decrease. This has been studied within the range 0-75 v/ sec.

3. Oscillations may occur both on the growing drop of the dropping mercury electrode, and on the "stationary" mercury electrode (the amalgamated end of a gold wire sealed into glass).

4. If oscillations are to be produced, it is essential that the current value in the falling region shall be sufficiently low. The presence in the solution of substances accelerating the reaction in this region interferes with the development of oscillations. Thus, extraneous electrolytes, and mercury salts, in concentrations comparable with that of the persulfate, show this effect.

5. Prolonged electrolysis (1 hr) leads to the cessation of the oscillations. This is due to changes in the composition of the solution, and to the formation within it of mercury salts produced at the anode and the falling drops.

6. When the series resistance is large (5-20 kohm), oscillations may take place even at constant potential (Fig. 2). The amplitude of these does not change with time.

Fig. 3. Oscillogram of 10^{-2} M $K_2S_2O_8$. Rate of reduction of potential 8.60 v/sec. Remaining conditions the same as in Fig. 1.

7. The amplitude of the oscillations under constant potential is settled immediately as they begin, and does not depend on the rate at which the potential was falling up to this point.

8. Increase in drop diameter leads to reduction in amplitude, and for values of the diameter greater than some critical value, becomes zero. The extent of the change of amplitude with diameter, and the critical value, depend on the emf at the ends of the circuit.

9. During a short time after the moment of liberation of the drop, if artificial mixing is used or the series resistance is high, the behavior of the current with falling potential is as follows: at the beginning of the oscillation the current rises, is arrested for some milliseconds forming a zigzag, increases again, and then settles on to a sloping line corresponding to the positive polarographic maximum. This is confirmed by observation of the electrode under a microscope.

This behavior of the current is of interest because, under the conditions to which the foregoing points apply, the transition to the polarographic maximum is complete at 0.20-0.25 v to the positive side of the oscillation region. Intermediate conditions exist in which the polarographic maximum is attained either before the oscillations, or simultaneously. Two of these oscillograms are shown in Fig. 3, from which the origin of the zigzag appears: this is the top, and part of the rear "front" of the first oscillation.

10. Movement to the maximum at positive potentials of the oscillation region takes place without the intermediate arrest. The transition potential depends on the rate of decrease of potential: increase of the rate leads to retardation of the initiation of the rise. The retardation time for various rates of potential decrease is the same, but depends on the potential at which the decrease commences.

This retardation is not peculiar to the behavior of persulfate solutions: a solution of 10^{-2} M lead nitrate with normal polarization characteristics has been found by the authors to show the same phenomenon.

11. Introduction into the solution of 0.05% gelatin quenches the oscillations if the rate of change of emf is low (2.36 v/sec when the resistance box is not included in the circuit), and smooths them out when the rate is greater (4.17 and 8.60 v/sec).

12. With low series resistance, the initial potential exerts an influence on the development of the oscillations. If this starts at a value below that corresponding to the current fall, the result is the extinction of the oscillations.

13. Within any one set of conditions, the frequency of the oscillations is inversely proportional to the amplitude: $\nu = k/\gamma$. The length of the oscillation increases with its implitude. The coefficient of proportionality for the conditions outlined in Fig. 1 is $0.388 \cdot 10^{-2}$ amp/sec.

14. The amplitude of the oscillations depends greatly on the emf (Fig. 4). Interchange of the cations among K^+, Na^+, and NH_4^+ does not influence the phenomenon.

In the main experiments we used doubly recrystallized reagents and doubly distilled mercury and water and hydrogen was passed for 4 hr. A series of experiments were carried out on the first drop, which made it possible to apply the required potential to the electrode before the mercury came into contact with the persulfate solution.

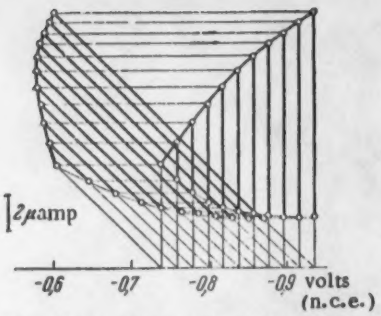

Fig. 4. Oscillations for the coordinates: current against emf (vertical lines), and current against potential (sloping lines). 10^{-2} M $K_2S_2O_8$; rate of mercury dropping $6.54 \cdot 10^{-3}$ mm^3/sec; time from the moment of dropping 6 sec. Series resistance 23 kohm ± 5%.

It is as yet impossible to formulate a complete theory for the oscillations described. Analysis of the results obtained shows that autooscillation on the mercury electrode is linked with the tangential movements of its surface. Observation of the particles suspended in solution under a microscope shows that the movement possesses an oscillatory character, directed from below to above at the forward front of the oscillation, with subsequent return. The displacements of the surface during the oscillations are most strongly expressed in the screened part of the electrodes, where they may amount to several microns. The direct and reverse displacements of the surface are identical, provided that the surface as a whole is not subject to disturbance. The part played by movement in the oscillation process is clear from the properties set out in paragraphs 6 and 7. The stability of the amplitude with time is difficult and its independence of the initial composition of the pre-electrode layer impossible to explain only on the basis of the substance being supplied to the electrode by diffusion. The invariable appearance of the zigzag in advance of the rise to the polarographic maximum (paragraph 9), during which the movement is known to occur from above downwards, confirms our assumption about the direction of movement of the surface during the first stage of oscillation: in order to change direction, the surface must first come to rest.

The mechanism whereby the movement arises may be explained in the following way. The nonuniform distribution of potential on the surface of the electrode when the surface is negatively charged leads to the formation in the screened part of the drop of a very high surface tension. This distribution of potential, which is usual for normal polarographic characteristics is apparently preserved for diminishing ones. Therefore, in the first stage of the oscillation, the movement is directed toward the capillary. But this movement is different from that at the negative polarographic maximum, in that it is not stationary, and produces short periodic impulses. The stopping and reversing of the direction of movement shortly after its initiation is connected, presumably, with the existence for reducing polarographic characteristics of the possibility of redistribution of the potential on the surface of the drop. The movement of the surface explains the large value of the current at the peak of the oscillation. At the advancing front of the oscillation, the substance is supplied to the electrode by means of convection. The cessation of movement corresponds to the fall in the current. The effect of surface-active substances confirms this position. In the presence of gelatin, the movement is less intense. The fact that gelatin, while completely repressing movements at the positive polarographic maximum, only smooths them out in the oscillation region, may possibly be explained by the different natures of the two movements (stationary and periodic).

Knowing the series resistance in the circuit, and the relationship between the amplitude and the constant emf (Fig. 4, heavy vertical lines), it is possible to construct the process of oscillation for the coordinates of current against potential. For a given emf the current and the potential oscillate along the heavy sloping lines of Fig. 4. This plan gives a simple explanation of some properties of the oscillations, in particular the relationship of the amplitude to the size of the electrode surface (paragraph 8); with increase in surface, the lower limit of the oscillations increases. It is interesting to note that the peaks of the oscillations for the coordinates of current against potential lie on points along a vertical curve, the abscissas of which are close to a value of −0.6 v (against the normal calomel electrode). This shows that the end of the first stage is associated with some condition assumed by the electrode in the neighborhood of this particular potential. Investigation of this discovery is to be continued.

LITERATURE CITED

1. A. N. Frumkin, V. S. Bagotskii, Z. A. Iofa, and B. N. Kabanov, The Kinetics of Electrode Processes [in Russian] (Moscow, 1952) p. 207.
2. Y. P. Gokhshtein and A. Y. Gokhshtein, Proc. Second Intern. Congress of Polarography (Cambridge, August, 1959).

THE VISCOSITY OF SUSPENSION

E. F. Kurgaev

All-Union Scientific and Research Institute for Railroad Transport

(Presented by Academician P. A. Rebinder, January 5, 1960)

Translated from Doklady Akademii Nauk SSSR, Vol. 132, No. 2, pp. 392-394, May, 1960

Original article submitted May 8, 1959

A disperse system, consisting of a suspension of solid particles in a liquid, possesses a higher viscosity than that of the liquid which constitutes the dispersion medium. This fact was first established on a theoretical basis by A. Einstein [1], who derived the following formula for the viscosity of low concentration dispersion on the basis of hydrodynamic equations:

$$\mu_c = \mu_0(1 + 2{,}5C), \tag{1}$$

where μ_0 is the viscosity of the pure dispersion medium, and C is the ratio of the volume of the particles of the disperse phase to that of the dispersed system.

In order to derive this formula the following assumptions were made: 1) that the particles were spherical in form; 2) that the mean distance between neighboring solid particles is very large compared with the dimensions of the particles themselves; 3) that the kinetic energies of the solid particles in the liquid are negligibly small.

The predicted increase in the viscosity for particles of the stipulated form is independent both of the dimensions of the particles, and of the molecular nature of both particles and medium.

Experimental determinations of the viscosities of suspensions [2-4] have shown that the Einstein formula is valid for values of C not greater than 0.03 to 0.05, a concentration range which satisfies the second of the above assumptions. The increase in the coefficient of C to 4.5 proposed by Hatschek [5] and to 4.75 [6], did not give satisfactory results, and only permitted the determination of the value of μ_c within a narrow range of C from 0.15 to 0.18.

The development of the formula for the viscosity of suspensions given below starts out with the following postulates. During flow of the solid particles, changes take place in the effective cross section of the liquid current, in consequence of which variations of velocity develop, and the local components of the stream take up a turbulent character. The reality of such variations has been confirmed experimentally [7, 8]. These variations produce an increase in the deformation resistance of the stream, equivalent to the rise in viscosity, and depending on the molar volume and the rate of flow in the liquid.

The increase of viscosity which is observed in turbulent currents, has been given the name "apparent" or "virtual." L. Prandtl, G. Taylor [9], and M. A. Velikanov [10] have derived semiempirical formulas for this viscosity. It is not possible, however, to apply these formulas to suspensions, since they relate only to free turbulence in the absence of obstacles to the stream in the form of solid surfaces, or at a considerable distance from such surfaces, while in suspension the stream is influenced by solid particles.

We believe that that the additional viscosity arising in the suspension due to the presence of solid particles in the liquid is proportional to the molecular viscosity of the liquid, and to the relative change in the displacement of unit mass of the liquid between that section where it is hendered by the solid particles, and the free section. The proportionality of the viscosity of the suspension to the molecular viscosity of the liquid is presumed in the Einstein formula and has been confirmed experimentally. The suggested change in the displacement, relative to the displacement with mean velocity, is given by:

$$\alpha \frac{\bar{v}_{max} - \bar{v}_{min}}{\bar{v}} = 2 \frac{\Delta \bar{v}}{\bar{v}} \alpha, \tag{2}$$

where $\bar{v}_{max}$ is the mean maximum velocity of the liquid in the minimum section between solid particles; $\bar{v}_{min}$ is the mean minimum velocity of the liquid in the section free from solid particles; $\bar{v}$ is the mean velocity of the liquid in the suspension; α is a coefficient of the rate of flow in the stream, representing the nonuniformity of the distribution of velocities across the section of the stream.

It follows, according to our hypothesis, that:

$$\frac{\mu_c}{\mu_0} = 1 + 2 \frac{\Delta \bar{v}}{\bar{v}} \alpha, \tag{3}$$

where μ_c is the viscosity of the suspension, and μ_0 is the viscosity of the pure liquid.

The mean velocity of the liquid in the suspension is given by:

$$\bar{v} = \frac{\bar{v}_{min}}{1 - C}, \tag{4}$$

where C is the volume concentration of the solid particles in the suspension.

Since $\Delta \bar{v} = \bar{v} - \bar{v}_{min}$, we obtain from Eq. (4):

$$\Delta \bar{v} / \bar{v} = C. \tag{5}$$

Hence,

$$\mu_c / \mu_0 = 1 + 2\alpha C. \tag{6}$$

The magnitude of the coefficient α is obtained from the equation:

$$\alpha = \frac{\int_{\omega} (\bar{v} + \Delta v)^2 \, d\omega}{\bar{v}^2 \omega}. \tag{7}$$

The evaluation of this integral requires a knowledge of the distribution of velocities across the section of the stream, which for the conditions under consideration does not appear to be possible. An approximate calculation of the coefficient α may be carried out from the following considerations. The magnitude of α is evidently proportional to the dissipation of energy in the turbulent stream, which in its turn depends on the square of the velocity of the liquid.

It should also be noted that in the Prandtl formula, the tangents of the strain in the turbulent stream are proportional to the square of the gradient of the velocity, and according to the hypothesis of T. Karman [9] they depend on the square of the velocity ratios.

This gives ground to believe that the magnitude of α is proportional to the square of the ratios of the mean velocities in the extreme sections taken by us in our consideration of the element of the liquid stream. That is, $\alpha \sim (\bar{v}_{max} / \bar{v}_{min})^2$, or,

	C=0.05	C=0.10	C=0.15	C=0.2	C=0.25	C=0.3
$\mu_c//\mu_0$ according to formula (11)	1.14	1.36	1.68	2.12	2.85	3.85
μ_c/μ_0 experimentally, according to Broughton	1.15	1.35	1.62	1.94	–	–
μ_c/μ_0 experimentally, according to Travinskii	1.17	1.35	1.67	2.10	2.8	4.10

$$\alpha = a\left(\frac{\bar{v}_{max}}{\bar{v}_{min}}\right)^2, \tag{8}$$

where a is some constant coefficient.

The square of the given velocity ratio is equal to the square of the ratio of the maximum and minimum effective cross-sectional areas of the stream, ω_{max} and ω_{min}. In the case under consideration these ratios depend on the volume concentration of the solid particles, and, together with the velocities in the extreme sections, determine the specific change of the velocities along the path of the stream.

If the magnitude ω_{max} is taken equal to 1, then ω_{min} is given by:

$$\omega_{min} = 1 - n^2\frac{\pi d^2}{4},$$

where d is the diameter of the solid particles, n is the number of particles in unit length of the volume occupied by the suspension.

The volume concentration of the solid particles in the suspension is given by:

$$C = n^3\frac{\pi d^3}{6},$$

so that

$$\omega_{min} = 1 - 1{,}2C^{2/3}, \tag{9}$$

and therefore

$$\left(\frac{\bar{v}_{max}}{\bar{v}_{min}}\right)^2 = \frac{1}{(1-1{,}2C^{2/3})^2}. \tag{10}$$

Comparison of these conclusions with the data obtained by experimental determination of the viscosities of suspensions has shown that formula (6), when the value of α from formulas (8) and (10) is substituted in it, gives completely satisfactory results when the calculations are made for a = 1.

Thus, the final formula for the viscosity of suspensions may be written in the following form:

$$\mu_c = \mu_0\left[1 + \frac{2C}{(1-1{,}2C^{2/3})^2}\right]. \tag{11}$$

The table gives the values of μ_c/μ_0, determined both experimentally and according to this formula.

It is not possible to obtain verification of formula (11) for concentrations higher than those given in the table. It is known that when C exceeds 0.25, strong mechanical interaction begins to be effective between the solid particles [3, 7], and no account is taken of this in our conclusions. Hence, formula (11) is only proposed for the determination of the viscosity of suspensionsbetween C = 0 and C = 0.25. This concentration range is the one most often met with in practice in the apparatus used in chemical technology, and is considerably wider than is provided for by the other existing formulas (due to Einstein, Hatschek, and Harrison), which may all thus be taken as partial cases of formula (11).

LITERATURE CITED

1. A. Einstein, Ann. Phys. 19, H. 2 (1906).
2. G. Broughton and C. S. Windebank, Ind. Eng. Chem. 4, 407 (1939).
3. H. Trawinski, Chem. Ing. Techn. No. 4 (1953).
4. S. Eirich, M. Bunzl, and H. Margaretha, Koll. Zs. 74, 276 (1936).
5. E. Hatschek, Koll. Zs. 7, 301 (1910).
6. F. Gan, Dispersion Analysis [in Russian] (1940).
7. E. F. Kurgaev, Izvest. Akad. Nauk SSSR, OTN, No. 5, 137 (1958).
8. E. F. Kurgaev, Inzh-fiz. Zhur. 1, 10, 120 (1958).
9. G. Shlikhting, The Theory of the Boundary Layer [in Russian] (IL, 1956).
10. M. A. Velikanov, Dynamics of Channeled Currents [in Russian] (1954).

THE MECHANISM OF INTERMOLECULAR ENERGY EXCHANGE DURING THE DISSOCIATION OF DIATOMIC GASES

E. E. Nikitin

Chemical Physics Institute, Academy of Sciences, USSR

(Presented by Academician V. N. Kondrat'ev, January 6, 1960)

Translated from Doklady Akademii Nauk SSSR, Vol. 132, No. 2, pp. 395-398, May, 1960

Original article submitted January 3, 1960

In recent years shock waves have been applied to the investigation of the thermal decomposition of diatomic molecules. The shock wave technique makes it possible to determine the true rates of the initial stages of the decomposition, since the experiment measures the concentration of still undissociated molecules. In this respect the shock wave method differs substantially from other determinations of decomposition rates (for example, the decomposition rate may be calculated from the recombination rate, as is discussed in [1]). The experimental results obtained in this work indicate that sometimes a pure diatomic gas will dissociate much more rapidly behind the shock wave front than under similar conditions in an atmosphere of an inert monoatomic gas. It will also be shown that this fact can find a ready explanation within the framework of previously developed theories for the mechanism of thermal dissociation [2, 13].

To be more specific, let us examine the following two reactions:

$$O_2 + A \rightarrow O + O + A, \quad \mu = m/2; \tag{1}$$

$$O_2 + O_2 \rightarrow O + O + O_2, \quad \mu = m/2, \tag{2}$$

the rates of which have already been determined [3] at temperatures between 3000 and 5000°K. It was found that k_2 exceeds k_1 by one order of magnitude. To the right of each equation we have placed the ratio of the reduced mass of the dissociating molecule (μ) to that of the colliding pair (m). Essentially, the nondissociating molecules in Eqs. (1) and (2) differ only in their internal structure since their respective reduced masses m_1 and m_2 can be assumed equal. The rate of Eq. (1) has been previously calculated [4] by the method used in [2], and was found to be in satisfactory agreement with the experimental data. In order to determine the relative rates (1) and (2), we will analyze the dissociation mechanism of a vibrationally excited molecule.

Let ϵ denote a vibrational quantum of the O_2 molecule, ϵ_0, its first vibrational quantum, then $0 \leq \epsilon \leq \epsilon_0$. Let then ΔE denote the average vibrational excitation energy transferred during each collision. When ϵ is large, which corresponds to low vibrational levels, the probability of vibrational excitation can be represented by the Landau–Teller equation; ΔE in such cases is very small and decreases exponentially with increasing ϵ. On the other hand, when ϵ is small, the quantization of vibrations becomes insignificant (nonadiabatic collisions), and consequently in accordance with classical mechanics, ΔE should be of the same order of magnitude as kT (this, of course, is only valid when the examined atoms all have masses of the same order of magnitude). The boundary line between these two regions, which is represented by the quantum ϵ^*, can be determined from the well-known equation:

$$\varepsilon^*/\hbar\bar{v}\alpha \simeq 1, \tag{3}$$

where $\bar{v}$ is the mean velocity of the colliding molecules, and α^{-1} is the effective radius of exchange forces. When $\epsilon > \epsilon^*$ we have mainly one-quantum transitions, while for $\epsilon < \epsilon^*$ many-quantum transitions predominate. When $\epsilon \simeq \epsilon^*$ the probability of a one-quantum transition is close to one so that $\Delta E \simeq (\epsilon^*) \simeq \epsilon$.

If the nondissociating molecule in Eq. (2) has a high probability for transferring during each collision a portion of its internal energy ϵ_1 to the vibrationally excited molecule, then the magnitude of quantum ϵ^* can be determined from the equation:

$$(\varepsilon^* - \varepsilon_1) / \hbar \bar{v} \alpha \simeq 1. \tag{4}$$

It has been previously shown (see [2]) that any disturbance in the Boltzmann distribution of the vibrational states of the dissociating molecule makes the dissociation rate depend on the vibrational excitation velocity, when the vibrational energy is in the range $E \simeq E^*$, the latter corresponding to a vibrational quantum ϵ^*. In fact, the dissociation energy in such cases comes out to be indeed E^*. It therefore follows that any increase in ϵ^*, resulting from the energy transfer ϵ_1 should decrease the value of E^* and, consequently, increase the decomposition rate. However, if the net dissociation energy E^* should become excessively reduced, there is a possibility that the vibrational excitation in the region of $E \simeq E^*$ will cease to control the decomposition rate, since a drop in the excitation energy E is accompanied by increased occupancy of the vibrational levels. In such cases the decomposition rate will be determined by the rate at which the vibrationally excited molecules pass from an energy state of the kT (in the vicinity of the dissociation limit) into the region of continuous spectrum. It is noteworthy that the probability of such a transition can even be determined by using the laws of classical mechanics. Such a dissociation mechanism has been proposed by Rice [5, 6] and more recently reexamined by Rice [7]* and Widom [8]. Thus, we have to conclude that any decrease in the net dissociation energy can not raise the frequency factor above a certain limiting value, which can be computed with the help of Rice's theory. It has already been shown [5, 8] that the maximum value of the frequency factor may exceed the collision number Z by about two orders of magnitude.

In case (1) $\epsilon_1 = 0$, and the value of E^* can be computed by using any one of the several relationships for $E = E(\epsilon)$. For the particular case where ϵ is a linear function of the vibrational quantum number $\underline{v}$ (Morse's oscillator) the following expression is readily derived:

$$D - E(\varepsilon) = D\varepsilon^2/\varepsilon_0^2. \tag{5}$$

The value of α in Eq. (3) is approximately constant for all the molecules and can be determined from the known Morse potentials for diatomic molecules. If the relationship $\omega \simeq \sqrt{2D/\mu}$ is used to represent α in terms of the fundamental vibrational frequency and the dissociation energy of diatomic molecules, then from Eqs. (3) and (5) we get:

$$D - E(\varepsilon^*) = \frac{D(\varepsilon^*)^2}{\varepsilon_0^2} = \gamma^2 \frac{\mu}{2m} kT. \tag{6}$$

Here the number 1 on the right side of Eq. (3) is replaced by a dimensionless number γ, making it possible to represent expression (6) as an exact equation. Using Eq. (6) one can readily verify the fact that the net dissociation energy in case (1) is reduced by $\sim kT/4$, which makes an entirely insignificant contribution to the decomposition rate constant.

In case (2), $\epsilon_1 \neq 0$, so that one has to analyze all the possible contributions to the constant k_2 from the internal energy of the nondissociating molecule. The vibrational degree of freedom of an unexcited O_2 molecule can not contribute anything since the difference between ϵ^* and ϵ_0 is very great. The probability of electronic exitation energy transfer is not very large either, since the spectra reveal no strong combinations between the excited electronic states, all of which converge to a single dissociation limit. The rotation of nondissociating O_2 molecules constitutes the only degree of freedom capable of contributing substantially to constant k_2 (relative to k_1); the rotation of dissociating molecules was taken into account in the equations derived before in [2]. One can readily verify the fact that the energy ϵ_1, which corresponds to two average rotational quanta of O_2, can be easily transferred to a vibrationally excited oxygen molecule. The experimental rotational relaxation time τ of O_2, which was measured in shock waves and represented the conversion of translational energy into rotational, was of the order of $1/10Z$ (see, for example [9]). The multistage relaxation time (a gradual excitation of rotational

* The author of this work takes this opportunity to thank Prof. Rice for a preprint of paper [7].

states) is related to the probability of a two-quantum transition P and to the energy ϵ_1 through the following relationship: $\tau \simeq (ZP\frac{\epsilon_1}{kT})^{-1}$. Substituting into this equation $\epsilon_1 \simeq 4\sqrt{BkT}$ (B is the rotation constant of O_2 equal to 1.4 cm^{-1}) T = 2000°K, and equating to the experimentally determined τ we get $P \simeq 1$. On the other hand, strongly rotationally excited molecules have vibrational amplitudes of the same order of magnitude as the parameter which represents the assymetry of intermolecular interactions and is responsible for the excitation of rotational states. Consequently, the probability of transferring a part of the rotational energy ϵ_1 to the vibrations of the dissociating molecule should be of the same magnitude as the probability for the exchange between the rotational and translational energies. Let us note that according to the Schwartz–Herzfelder theory [10] the possibility that rotational energy may be converted into vibrational has to be considered in calculating the vibrational relaxation time of lower vibrational levels of diatomic molecules. By means of the Landau–Teller equation it can be readily shown that the transfer of the rotational energy ϵ_1 will increase the probability of vibrational excitation by a factor of $\exp(2\chi\epsilon_1/\epsilon_0)$, which corresponds to a coefficient of 3-5, if the usual value of $\chi \simeq 10$ [10] is used. At the same time one should remember that the energy ϵ_1 depends on the velocity of the colliding molecules and consequently on χ, so that under ordinary conditions where the collisions are strongly nonadiabatic with respect to the rotational excitation ϵ_1 may greatly exceed twice the energy of the average rotational quantum. It is obvious that neglecting the rotation should render the agreement between the experimental and calculated values poorest when χ is large. Looking at Table 1 in [10] one can see that this is indeed the case.

Equation (4) can now be transformed into the form:

$$\varepsilon^* = \gamma[\hbar\bar{\nu}\alpha + 4\sqrt{BkT}] = \gamma\hbar\sqrt{\frac{kT}{m}}[\alpha + 4/r_e], \tag{7}$$

where r_e is the equilibrium interatomic distance in O_2. Taking r_e = 1.2 A and α^{-1} = 0.5 A, and using Eq. (5) we get

$$E(\varepsilon^*) = D - {}^9/_4\gamma^2 kT. \tag{8}$$

Thus, the net dissociation energy is reduced by $\sim {}^9/_4$kT, while the vibrational quantum, which controls the decomposition rate, increases by a factor of ~ 3 when we change from case (1) to (2). The combined effect of these two factors, according to Eq. (7) of paper [2], increases the relative rate of reaction (2) by about $3\gamma\exp(2\gamma^2) \simeq$ $\simeq$20 times. This coefficient, of course, will have no effect on the temperature dependence of k_2.

A different relationship between k_1 and k_2 arises in cases where the inert gas and the dissociating molecule have different molecular weights. As an example, we can use the decomposition of bromine which was studied by Palmer and Hornig [11],

$$Br_2 + A \rightarrow Br + Br + A, \quad \mu = m; \tag{9}$$

$$Br_2 + Br_2 \rightarrow Br + Br + Br_2, \quad \mu = m/2. \tag{10}$$

The rate constant for reaction (9) has already been computed [2]. The experimentally determined frequency factor in reaction (9) is 4Z at T = 2000°K, whereas Widom's calculations [8] based on Rice's mechanism yield $\sim$50Z. Using Eqs. (6) and (7), we get $E_9^* = D - \gamma^2/2$kT and $E_{10}^* = D - \gamma^2$kT [$r_e(Br_2)$ = 2.28 A]. The vibrational quantum Σ^* of reaction (10) exceeds that of reaction (9) by a factor of $\sqrt{2}$, so that the relative rate of reaction (10) is $\simeq \sqrt{2e}$. The experimental ratio k_{10}/k_9 varies between 1.5 and 2.4 in temperature range from 1600 to 1200°K [11].

In closing, let us recall the following facts. Equations (3) and (4), on which our estimates were based, were given as only approximate expressions. Consequently, the final expression includes a dimensionless constant $\gamma \simeq 1$. It was therefore interesting to get an independent check for the value of γ and verify Eqs. (3) and (4). This can to a certain degree be accomplished by studying the forced infrared absorption of molecules which depends on the formation of the molecular electron cloud during collisions. Equations similar to Eqs. (3) and (4) can be written to represent the half-widths of various spectral bands, and it turns out that γ is very close to one [12]. Moreover, the band shapes of $k = k(\omega)$ (where $\underline{k}$ is the absorption coefficient) qualitatively correspond to those for the above-described function $\Delta E = \Delta E(\epsilon)$. As far as the linear relationship between ϵ and $\underline{\nu}$ (proposed in [5]) is concerned, the more rapid decline in ϵ frequently observed near the dissociation limit does not alter our qualitative

arguments. In the case of oxygen dissociation, for example, when this effect is considered the calculated value of the ratio k_2/k_1 comes out somewhat larger.

I wish to thank Prof. N. D. Sokolov for appraising this work.

LITERATURE CITED

1. E. E. Nikitin and N. D. Sokolov, Doklady Akad. Nauk SSSR 124, 336 (1959).*
2. E. E. Nikitin, Doklady Akad. Nauk SSSR 119, 526 (1958).*
3. M. Camac, J. Camm, et al., Chem. Relaxation in Air, Oxygen and Nitrogen, Preprint No. 802, Inst. Aeronaut Sci. (1958).
4. E. E. Nikitin, Dissertation, Chemical Physics Institute, Acad. Sci. USSR (1958).
5. O. K. Rice, J. Chem. Phys. 9, 258 (1941).
6. O. K. Rice, J. Chem. Phys. 21, 750 (1953).
7. O. K. Rice, Monatsh. Chem. 90, 330 (1959).
8. B. Widom, J. Chem. Phys. 31, 1027 (1959).
9. J. C. McCoubrey and M. D. McGrath, Quart. Rev. 11, 87 (1957).
10. R. N. Schwartz and K. F. Herzfeld, J. Chem. Phys. 22, 767 (1954).
11. H. B. Palmer and D. F. Hornig, J. Chem. Phys. 26, 98 (1957).
12. E. E. Nikitin, Optika i Spektroskopiya 7, 6 (1959); E. E. Nikitin and N. D. Sokolov, J. Chem. Phys. 31, 1369 (1959).

* See CB translation.

THE INFLUENCE OF CERTAIN SEMICONDUCTING PROPERTIES OF THE SURFACE ON THE REACTION BETWEEN XANTHATE AND GALENITE

Corresponding Member, Acad. Sci. USSR I. N. Plaksin and R. Sh. Shafeev

Mining Institute, Academy of Sciences, USSR

Translated from Doklady Akademii Nauk SSSR, Vol 132, No. 2, pp. 399-401, May, 1960

Original article submitted January 23, 1960

Galenite, like many sulfide minerals, is a typical impurity semiconductor of the mixed type, so that the sign of the electric charge carriers is determined by the nature of the impurity in the mineral lattice. Lead atoms present in excess of the stoichiometric quantity may act as donor impurity, and excess sulfur atoms, or oxygen adsorbed on the mineral surface, may act as acceptor impurities.

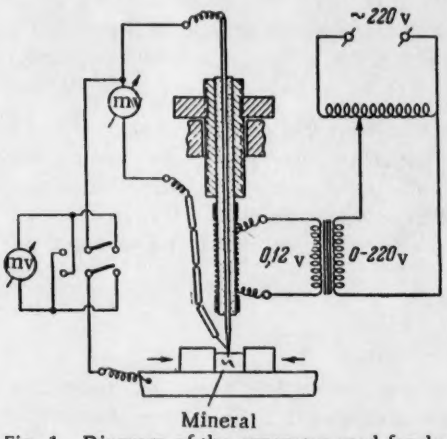

Fig. 1. Diagram of the apparatus used for determining the thermo-emf of sulfide minerals.

The behavior of the surface of "electronic" galenite toward xanthate is not the same as that of "hole" galenite, since in the first case there is an increased concentration of electrons at the mineral surface, while in the second case there is an increased concentration of holes, which by recombining with the electrons of xanthate anions are able to form stable chemical bonds with the mineral surface.

It should be noted that on the surface of galenite, and also of many other sulfides, we can expect areas of hole and electronic conductivity existing together, and this, as a result of the necessary condition that the chemical potentials be equal, creates an electrical field with nonuniform potential on the surface of the sulfide mineral. Our earlier work [1] on the cathodic polarization of sulfide mineral surfaces in dilute solutions of copper or silver ions established experimentally the existence of electrochemically nonuniform regions on the surface of sulfide minerals.

Regions with different electrochemical potentials were detected in these experiments from depositions of cathodic metal on the surface of the mineral, observed under the microscope. In addition, in the study of the changes in the outline of the deposits of cathodic copper with change in the negative voltage applied to the sulfide mineral surface, it was established that on galenite, regions exist where the negative potential is such that the copper starts to be deposited at the electrocapillary zero, together with regions where the copper is not deposited, even at very high negative voltages (−1.4 v).

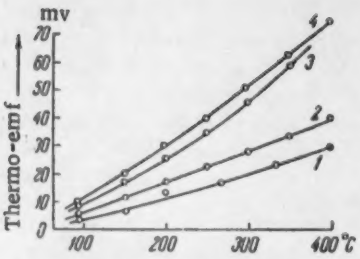

Fig. 2. Relationship between the thermo-emf and temperature: 1) MoS_2; 2) FeS_2; 3) $CuFeS_2$; 4) PbS.

It is probable that xanthate attaches itself only with great difficulty to a sulfide surface exhibiting electronic conductivity. This assumption is confirmed by the fact that sulfide minerals do not react with xanthate if the surface has not been treated beforehand with oxygen [2]. Moreover, it is known that xanthate attaches itself to a much smaller extent to the surface of sphalerite (a typical electronic semiconductor).

An apparatus with an electrical thermal probe, illustrated in Fig. 1, has been constructed to determine the nature of the electric charge carriers and the thermal coefficient of the thermoelectromotive force (thermo-emf) of sulfide minerals. The electric thermal probe was constructed from a piece of pointed steel, heated by the passage of an electric current through a nichrome spiral wound above the probe. The temperature in the contact zone between the thermal probe point and the sulfide mineral surface was followed by means of the thermocouple formed by the point of the thermal probe and a nickel wire welded to the probe close to the point of the latter. The thermo-emf measurements were made at different temperatures between room temperature and 400°, on galenite, chalcopyrite, molybdenite and pyrites. The results of the thermo-emf measurements are given in Fig. 2. The thermal coefficient amounted to 200 μv/deg for galenite, 160 μv/deg for chalcopyrite, 110 μv/deg for pyrites, and 70 μv/deg for molybdenite. The high values of the thermo-emf indicate that the sulfide minerals are of the impurity type. In addition, the change in the sign of the thermo-emf showed that our specimens of galenite and chalcopyrite, exhibited electronic conducticity, while the molybdenite and pyrites exhibited hole conductivity. For the electronic semiconductors, the chemical potential level increases towards the lower boundary of the free zone with increase in donor impurity concentration, while for the hole semiconductors this level approaches the upper boundary of the valence zone, as a result of which the electron concentration in the free zone decreases.

A simplified energy diagram for the process of attachment of xanthate to galenite in the presence of oxygen is shown in Fig. 3. In this scheme the energy of the boundary of the filled zone is denoted by E_1, and the energy of the boundaries of the free zone by E_2. The donor level of the impurity lead atoms is denoted by E_d, and the acceptor level of the adsorbed oxygen by E_a. In addition, the forbidden zone contains the chemical potential level corresponding to the change of the mineral from the electronic type to the hole type, φ, and the energy level of the xanthate anion.

In galenite of the electronic type, the concentration of electrons in the free zone (above E_2), and also the position of the chemical potential level, depend on the concentration of interstitial impurity lead atoms, and can be calculated, for any specific case, from the relationship between the Fermi level and the free electron concentration. At small concentrations of impurity lead atoms, in the absence of electron degeneracy, which is quite probable for sulfide minerals, the Fermi-Dirac statistics can be replaced by Maxwell-Boltzmann statistics. In this case the relationship becomes

$$n = N_{Pb} \exp -(E_2 - \varphi)/kT,$$

where n is the concentration of electron formed by the ionization of the impurity lead atoms, N_{Pb} is the concentration of impurity lead atoms in the galenite, k is the Boltzmann constant, and T is the absolute temperature. As a result of the presence of free electrons on the galenite surface, a charge is produced, whose magnitude can be calculated using the Poisson equation. The increase in the magnitude of the surface potential produced by the free electrons creates a potential barrier which must be overcome by the xanthate anions if they are to attach themselves to the mineral surface. The attachment of xanthate to the galenite surface starts when the mineral changes from the electronic type to the hole type as a result of the production of acceptor levels of oxygen in the forbidden zone.

The oxygen adsorbed on the galenite surface takes up electrons from the free zone in the ionization process, and in this way decreases the height of the potential barrier at the mineral surface

$$^1/_2O_2 \rightarrow O^{2-}_{ads} - 2e.$$

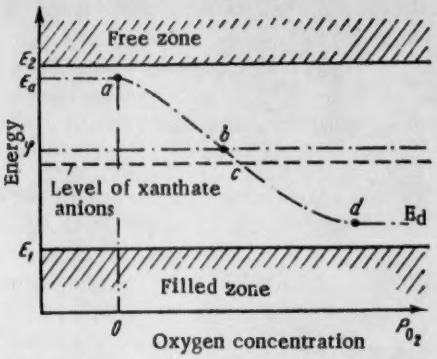

Fig. 3. Diagram illustrating the galenite energy levels.

The decrease in the electron concentration depending on the oxygen concentration in the pulp is probably parabolic [3]. The height of the potential barrier, and hence the chemical potential level of the electrons, decreases gradually with increase in the concentration of dissolved oxygen in the pulp, and at the same time the probability that the xanthate anions will overcome the energy barrier gradually increases.

At the point of intersection with the chemical potential level corresponding to equal numbers of electrons and holes in the galenite, the potential barrier disappears and is replaced by a potential trough, whose depth increases with increase in the number of holes in the filled zone (section bcd in Fig. 3) At this moment the attachment of xanthate to the galenite surface begins, with the formation of a chemical bond with the cation of the lattice. With further increase in the oxygen concentration, the concentration of holes increases so much that the electrons of the xanthate begin to be absorbed in extremely large quantities, and create conditions for the oxidation of xanthate to dixanthate.

It should be noted that as a result of the nonuniformity of the galenite surface, the change from the electronic type of mineral to the hole type takes place in nonequilibrium fashion, so that we can expect that regions with hole conductivity and regions with electronic conductivity may exist together on the surface, leading to an irregular, patchy distribution of xanthate on the surface of the galenite particles.

LITERATURE CITED

1. I. N. Plaksin and R. Sh. Shafeev, Doklady Akad. Nauk SSSR 121, 145 (1958). *
2. I. N. Plaksin and S. V. Bessonov, Proceedings of the Second International Congress of Surface Activity (London, (1957) 3, p. 361.
3. S. R. Morrison, Advances Catal. and Related Subjects 7, 259 (1955).

* See CB translation.

THE SPONTANEOUS CRYSTALLIZATION OF DISSOCIATED SALTS

V. B. Ratinov and O. M. Todes

(Presented by Academician P. A. Rebinder, January 6, 1960)

Translated from Doklady Akademii Nauk SSSR, Vol. 132, No. 2, pp. 402-405, May, 1960

Original article submitted January 6, 1960

The probability α of formation of a nucleus of a new phase in unit volume in unit time is exponentially dependent on the height of the energy barrier associated with the formation of an interphase boundary possessing a surface free energy σ. If γ is the coefficient of the shape of the nucleus, v_k the molar volume of the new phase, μ_1 the molar chemical potential of the dissolved substance, and μ_2 the molar chemical potential of the crystal produced, we have [1-3],

$$\alpha = A \exp\left\{-\frac{4\gamma\sigma^3 v_k^2}{RT(\mu_1-\mu_2)^2}\right\}. \quad (1)$$

For nondissociated substances in dilute solution

$$\mu_1 = RT \ln \frac{c}{\varphi(p,T)}, \quad \mu_2 = RT \ln \frac{c_{equil}}{\varphi(p,T)}, \quad (2)$$

where c is the concentration of dissolved substance and c_{equil} is the equilibrium concentration of the saturated solution. We then have

$$\mu_1 - \mu_2 = RT \ln \frac{c}{c_{equil}}, \quad (3)$$

$$\ln \alpha = \ln A - \frac{4\gamma\sigma^3 v_k^2}{(RT)^3} \frac{1}{\ln^2 \frac{c}{c_{equil}}}. \quad (4)$$

By measuring the concentration of the supersaturated solution c and the probability of formation of nuclei α, it is possible to determine the free surface energy σ from the slope of the straight line (4) with coordinates $\ln \alpha = 1/\ln^2(c/c_{equil})$.

For dissociated salts, the initial expression (2) for the chemical potentials should contain not the total concentration of dissolved salt c but only the concentration of undissociated molecules in solution $c^* < c$. This concentration can in turn be determined from the law of mass action and the dissolved ion balance.

We shall carry out the calculation for the specific case where the component C, which is crystallizing, is dissociated in solution into two ions A and B according to the equation

$$C = A + B \quad (5)$$

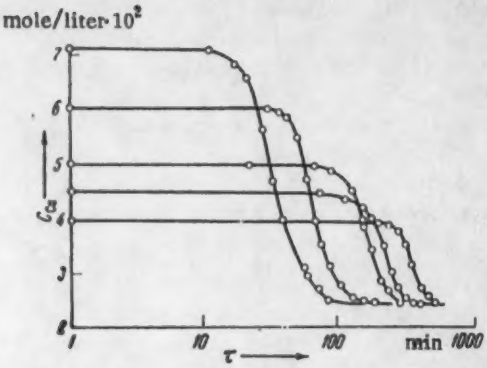

Fig. 1. Kinetics of the crystallization of gypsum at different degrees of supersaturation $C_{Ca} = C_{SO_4}$; t = 24°.

From the law of mass action

$$c^* = Ka^*b^*, \tag{6}$$

it is possible to represent the motive force of the crystallization process in two equivalent forms

$$\mu_1 - \mu_2 = RT \ln \frac{c^*}{c_{\text{equil}}} \tag{7^1}$$

or

$$\mu_1 - \mu_2 = RT \ln \frac{Ka^*b^*}{c_{\text{equil}}} = RT \ln \frac{a^*b^*}{L}, \tag{7^2}$$

where

$$L = c_{\text{equil}}/K \tag{8}$$

is the product of the concentrations of the dissociated ions in equilibrium with the solid phase.

Since the dissociation equilibrium is established almost instantaneously, the true concentrations of ions in solution a* and b* differ from their total concentrations a and b and are related by the following balance equations

$$c^* + a^* = a, \quad c^* + b^* = b. \tag{9}$$

By solving Eqs. (6) and (9) simultaneously, it is possible to find the values of a*, b*, and c*, and to substitute these in (7^1) or (7^2). We then have

$$\mu_1 - \mu_2 = RT \ln \frac{1 + Ka + Kb - \sqrt{(1 + Ka + Kb)^2 - 4K^2ab}}{2Kc_{\text{equil}}}. \tag{10}$$

For the stoichiometric relationship a = b = c for the ions, formula (10) is much simpler and becomes

$$\mu_1 - \mu_2 = RT \ln \frac{1 + 2Kc - \sqrt{1 + 4Kc}}{2Kc_{\text{equil}}}. \tag{11}$$

For sparingly dissociated salts Kc ≫ 1, c* ≈ c, and in the limit expression (11) becomes the same as formula (3) for nondissociated salts. In the opposite limiting case Kc ≪ 1, the dissociation is practically complete, a* ≈ a, b* ≈ b, and

$$\mu_1 - \mu_2 \approx RT \ln \frac{ab}{L}. \tag{12}$$

It should be noted that for strong electrolytes the concentrations a and b should be replaced by the activities of the corresponding ions. It is possible to proceed in another way – by assuming on the basis of Eq. (12) that the equilibrium product of the concentrations L is itself a function of the concentrations of the dissolved ions and the ionic strength of the solution. This method has been used in our previous work [4], in which the method for calculating the value of L was developed.

By substituting expression (12) in (1), we bring the latter to the form

$$\ln \alpha = \ln A - \frac{4\gamma\sigma^3 v_k^2}{(RT)^3} \frac{1}{\ln^2 \frac{ab}{L}}. \tag{13}$$

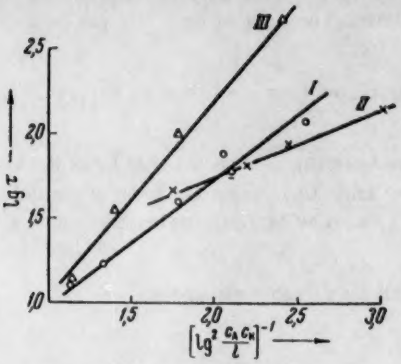

Fig. 2. The relationship between the probability of formation of crystallites of calcium hydrosilicate and the degree of supersaturation at 24°. Series I) C_{SiO_2} = const, $C_{Ca} \neq$ const, $\sigma_1 = 24$ erg/cm²; Series II) $C_{SiO_2} \neq$ const; C_{Ca} = const; $\sigma_2 = 19$ erg/cm²; Series III) $C_{Ca}/C_{SiO_2} = 6$ = const, C_{SiO_2} and $C_{Ca} \neq$ const, $\sigma_3 = 28$ erg/cm².

This relationship has been studied experimentally for spontaneous crystallization from supersaturated solutions of calcium sulfate dihydrate (gypsum) and monocalcium hydrosilicate. The supersaturation was achieved chemically by mixing appropriate solutions, with vigorous stirring. The gypsum was prepared using solutions of calcium chloride and potassium sulfate, and the monocalcium hydrosilicate, using solutions of calcium hydroxide and silicic acid. The initial concentrations of cation and anion, and their relative concentrations, were varied in different series of experiments.

The decrease in supersaturation with time was measured by removing 2-3 ml samples at intervals by suction through a No. 4 filter from 500 ml of the solution undergoing crystallization. The filtrate was analyzed for calcium ions by complexometric titration with Trilon B, and for silicic acid by a colorimetric method using the colored complex formed with ammonium molybdate in sulfuric acid. In the crystallization of the calcium hydrosilicate, carbonization was avoided by preparing the solutions in boiled-out water, and by carrying out the experiments and the removal and storage of samples in an atmosphere of nitrogen.

Figure 1 shows the decrease in supersaturation with time for the crystallization of gypsum. The kinetic curves for the crystallization of monocalcium hydrosilicate have the same S-shaped form with a clearly-defined induction period τ.

In a previous work [3] it was shown that as a result of the very sharp decrease in α with decrease in the supersaturation, nuclei of the new phase are formed practically only at the start of the induction period, and afterwards grow with linear velocity $\lambda = dl/d\tau$, which changes comparatively little with change in supersaturation. The number of nuclei in unit volume is equal to

$$N_0 = k\left(\frac{\alpha}{\lambda}\right)^{3/4}, \tag{14}$$

where the proportionality coefficient k is also only very slightly dependent on the supersaturation.

The decrease in the supersaturation towards the end of the induction period τ is equal to

$$\Delta c = \frac{\rho}{M}\gamma N_0 l^3 = \frac{\rho}{M}\gamma k \lambda^{3/4}(\alpha\tau^4)^{3/4}, \tag{15}$$

where ρ is the density and M the molecular weight of the substance crystallizing.

In the experiments the induction periods were compared for identical, comparatively small, but accurately measurable reduction in the supersaturation. For gypsum, Δc was taken as $6 \cdot 10^{-4}$ mole/liter, and for monocalcium hydrosilicate Δc was taken as $5 \cdot 10^{-5}$ mole/liter. Thus, from (15) we obtain a relationship between α and τ of the form

$$\alpha\tau^4 = \left(\frac{M}{\rho}\frac{\Delta c}{\gamma k \lambda^{3/4}}\right)^{4/3} \approx \text{const}. \tag{16}$$

From (13) and (16) we obtain the relationship between τ and the supersaturation

$$\lg\tau = \text{const} + \frac{\gamma\sigma^3 v_k^2}{(2{,}3\ RT)^3}\frac{1}{\lg^2\frac{c_A c_C}{L}}, \tag{17}$$

in other words, $\log\tau$ should be a linear function of $1/\log^2(c_A c_C/L)$.

Figure 2 shows this relationship for the kinetics of crystallization of monocalcium hydrosilicate. This figure shows that the experimental points for different series lie on straight lines. The slope of these straight lines can be used to find the angular coefficient, which is equal to $\gamma\sigma^3 v_k^3/(2.3\,RT)^3$.

By assuming $\gamma = \frac{4}{3}\pi r$ (sphere) and substituting the values of v_k calculated from the literature data, we can calculate the effective value of σ for the crystal/solution interface.

The average value of σ calculated in this way for monocalcium hydrosilicate was found to be of the order of 24 erg/cm^2. The average value of σ for gypsum, determined in the same way, was found to be of the order of 12 erg/cm^2, which is close to the value of σ previously obtained for gypsum by M. L. Chepelevetskii using a different method.

The authors wish to express their gratitude to M. L.Chepelevetskii for valuable discussion.

LITERATURE CITED

1. J. W. Gibbs, Thermodynamic Works [Russian translation] (Moscow–Leningrad, 1950).
2. I. Stranskii and R. Kaishev, Uspekhi Fiz. Nauk 21, 408 (1939).
3. O. M. Todes, Problemy Kinetiki i Kataliza 7, 91 (1949).
4. T. I. Rozenberg and V. B. Ratinov, Sbornik Trud. Nauch–Issled. Inst. Zhelezobeton 1, 36 and 49 (1957).

THE EFFECTS OF HIGH-ENERGY ELECTRONS ON PLATINUM COMPLEXES

Academician Vic. I. Spitsyn, G. N. Pirogova, A. K. Pikaev, and P. Ya. Glazunov

Physical Chemistry Institute, Academy of Sciences, USSR

Translated from Doklady Akademii Nauk SSSR, Vol. 132, No. 2, pp. 406-408, May, 1960

Original article submitted February 9, 1960

Some time ago one of the authors [1] prepared platinum possessing a high catalytic activity by bombarding aqueous solutions of platinum salts with a beam of fast electrons. The effects of ionizing radiation on solid complexes of platinum of various compositions and structures are examined in the present work. The only known work in this field is that of Halder [2], who studied the radiochemical effects of thermal neutrons on platinum complexes.

TABLE 1

The Preparation and Composition of the Investigated Platinum Salts.

Compound	Synthesis	Percent Pt	
		found	calculated
Potassium chloroplatinate $K_2[PtCl_6]$	$H_2[PtCl_6] + KCl$	40.02	40.16
Ammonium chloroplatinate $(NH_4)_2[PtCl_6]$	$H_2[PtCl_6] + NH_4Cl$	44.07	43.97
Potassium chloroplatinite $K_2[PtCl_4]$	See [3]	46.81	47.04
Ammonium chloroplatinite, $(NH_4)_2[PtCl_4]$	See [4]	52.01	52.32
Dichlorotetrammine platinum (II),* $[Pt(NH_3)_4]Cl_2 \cdot H_2O$	See [5]	55.28	55.42
Cis-dichlorodiammine platinum (II) $[Pt(NH_3)_2Cl_2]$	See [6]	65.50	65.03
Trans-dichlorodiammine platinum (II), $[Pt(NH_3)_2Cl_2]$	See [5]	64.86	65.03

* The sample was prepared in anhydrous state.

In Table 1, we have tabulated the compositions of the investigated compounds and the methods used to prepare them. We dried our samples for several hours at 120° in a desiccator, passed them through a sieve with 0.15 mm diameter holes, then dried them again under a reduced pressure (4 mm of Hg) at 56°C in a drying pistol.

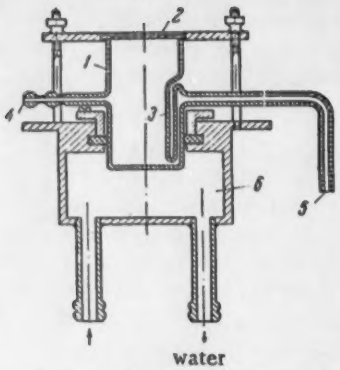

Fig. 1. Schematic diagram of the reaction cell: 1) glass cell; 2) mica window; 3) thermocouple pocket; 4) gas inlet; 5) gas outlet; 6) condenser.

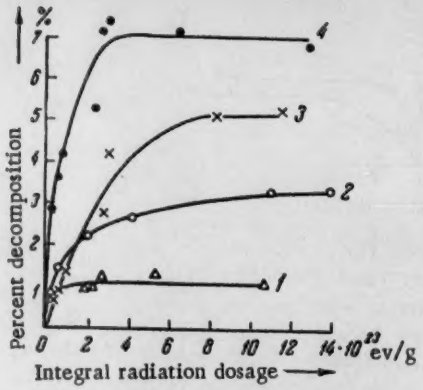

Fig. 2. The decomposition of salts under the impact of high-energy electrons as a function of integral dosage: 1) $(NH_3)_2[PtCl_6]$; 2) $[Pt(NH_3)_4]Cl_2$; 3) cis-$[Pt(NH_3)_2Cl_2]$; 4) trans-$[Pt(NH_3)_2]Cl_2$. Experimental temperature 145-150°.

TABLE 2

Initial Yield of Platinum Metal from Irradiated Complexes

Compound	Initial yield of Pt, atoms/ / 100 ev
$(NH_4)_2[PtCl_6]$	0.090
$(NH_4)_2[PtCl_4]$	0.143
$K_2[PtCl_4]$	0.018
$[Pt(NH_3)_4]Cl_2$	0.047
Cis-$[Pt(NH_3)_2Cl_2]$	0.036
Trans-$[Pt(NH_3)_2Cl_2]$	0.338

A 1.0 Mev linear accelerator served as a radiation source [7]. A weighed sample of the compound (an approximately 2 mm thick layer weighing about 0.2 g) was placed in a thermally regulated glass cell (20 mm in diameter) which had a side pocket for the thermocouple and two outlets for the circulating gas. The cell was covered with a 8-10 μ thick mica window (Fig. 1).

A 0.8 Mev electron beam was totally absorbed by the investigated salts. The electron current intensity in the reaction cell was measured by means of a Faraday commutator, which had an inlet of the same size as the cell window. The measured integral dosage was in the range from 10^{22}- 10^{24} ev/g. The dose intensity was $5 \cdot 10^{19}$-10^{20} ev/g·sec.

The experiments were carried out at constant temperature in a stream of dry argon. The irradiation temperature was 90-95° for the potassium and ammonium chloroplatinites, and 145-150° for the remaining salts. The energy lost by the absorbed electrons raised the temperature of the irradiated samples. Preliminary experiments showed that the investigated salts were stable at the indicated temperatures when not exposed to the radiation.

After irradiation the samples were dissolved in water. Slightly soluble salts were treated with hot water. The freed platinum metal was filtered out and determined gravimetrically. The experimental results are shown in Figs. 2 and 3. The initial yields are given in Table 2.

Under the impact of fast electrons the investigated platinum salts were readily reduced to platinum metal. Potassium chloroplatinate constitutes an exception since no detectable changes were observed under our experimental conditions and dosage. The reduction of ammonium chloroplatinate is not very extensive either. Salts of divalent platinum are much more readily decomposed than are those of tetravalent platinum. In the range of dosage from 10^{22}-$5 \cdot 10^{23}$ ev/g the extent of decomposition of Pt^{++} complexes increases with the dosage. When the integral dosage is further increased the extent of decomposition remains constant. As can be seen in Figs. 2 and 3, the percent decomposition depends on the type of salt. Ammonium salts decompose much more readily than do potassium salts. Complexes having dissimilar ligands in the inner sphere decompose faster than do salts with one type of ligand. For example, we observed 5% decomposition in cis-$[Pt(NH_3)_2Cl_2]$ and 7% in trans-$[Pt(NH_3)_2Cl_2]$ under our experimental conditions, but only 3% decomposition in $[Pt(NH_3)_4]Cl_2$ under identical conditions. Thus, stereoisomerism also affects the radiochemical stability of complexes.

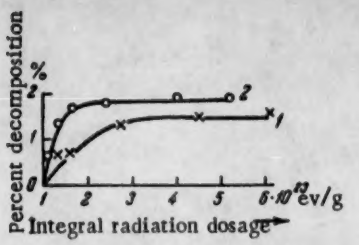

Fig. 3. The decomposition of potassium (1) and ammonium (2) chloroplatinites under the impact of high energy electrons. Experimental temperature 90-95°C.

It is noteworthy that the decomposition practically ceases after a certain integral radiation dosage has been absorbed. In one set of experiments irradiated $K_2[PtCl_4]$ and $(NH_4)_2[PtCl_4]$ samples were thoroughly reground and again exposed to radiation. Yet the salts still failed to show any increase in the extent of reduction.

One could assume that at high integral radiation dosages a reverse reaction comes into play – the newly formed platinum metal is oxidized by the atomic chlorine which is liberated from the irradiated compound. The fact that complexes containing reducing agents (NH_3 or the cation NH_4^+) in their inner sphere decompose much more readily then do complexes containing only chlorides in their inner sphere would tend to support this assumption. We also found qualitative evidence for the presence of NH_4Cl and free chlorine in the gas which was passed through the cell containing the irradiated samples.

Aqueous solutions of platinum complexes begin to undergo decomposition at radiation dosages considerably below those required for the solid salts. A solution of $[Pt(NH_3)_4]Cl_2$ undergoes 8.7% decomposition at a dosage of $1.5 \cdot 10^{21}$ ev/ml and 17.4% at a dosage of $3 \cdot 10^{21}$ ev/ml. Salts dried at room temperature also decompose more readily than do salts dried in vacuo at higher temperatures. Thus, K_2PtCl_4 dried at room temperature undergoes 17% reduction at a dosage of $7 \cdot 10^{23}$ ev/g. In most samples the reduction is probably induced by the products of water radiolysis.

LITERATURE CITED

1. A. A. Balandin, Vic. I. Spitysn, et al., Zhur. Fiz. Khim. 33, 3, 736 (1959).
2. B. C. Halder, J. Am. Chem. Soc. 76, 4229 (1954).
3. I. I. Chernyaev, Izvest. Sekt. Plat. Institute Obshchei i Neorg. Khim. Akad. Nauk SSSR 8, 167 (1931).
4. L. F. Nilson, J. Prakt. Chem. 16, 241 (1877).
5. Kh. I. Gil'dengershel', Zhur. Neorg. Khim. 1, 400 (1950).
6. V. V. Lebedinskii and V. A. Golovnya, Izvest. Sekt. Plat. Instituta Obshchei i Neorg. Khim. Akad. Nauk SSSR 20, 95 (1947).
7. P. Ya. Glazunov and G. B. Radzievskii, Coll. Effects of Radiation on Organic and Inorganic Systems [in Russian](Izd. AN SSSR, 1958) p. 395.

ANODIC PROCESSES ACCOMPANYING THE CORROSION CRACKING OF METALS

N. D. Tomashov and N. I. Isaev

Physical Chemistry Institute, Academy of Sciences USSR

(Presented by Academician A. N. Frumkin, January 22, 1960)

Translated from Doklady Akademii Nauk SSSR, Vol. 132, No. 2, pp. 409-412, May, 1960

Original article submitted January 14, 1960

The tensile stresses which accompany the corrosive action of solutions on metals are clearly manifested in the corrosion cracking, which is a form of destructive corrosion of metals.

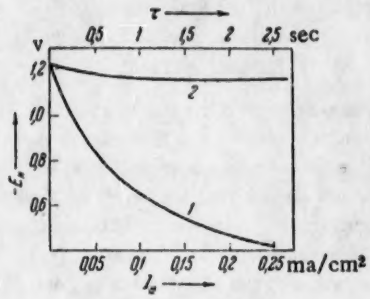

Fig. 1. Anodic polarization of a MA2-1 alloy under conditions where the current is constantly increased at the rate of 0.1 ma/ cm^2 · sec. 1) Without stress; 2) during the development of a corrosion crack.

Of the numerous mechanisms proposed to explain corrosion cracking, the most universally accepted one is based on the electrochemical theory; the process is attributed to a highly increased anodic solubility inside the crack of a metal under mechanical stress. A detailed treatment of this theory was presented in foreign chemical literature (Mears, Brown, and Dix [1], and Harwood [2]) and in some Soviet papers (A. V. Ryabchenkov and co-workers [3, 4]). The reduction of metallic strength caused by adsorption, which was discovered by P. A. Rebinder and co-workers [5, 6], is also very important in the corrosion cracking of metals.

Thus, the mechanical strains, the electrochemical anodic solution of metals, and the effects of adsorption on the metal strength constitute the principal factors in the corrosion cracking of metals.

In the present work we have examined the electrochemical factors in the corrosion cracking of metals. According to the electrochemical theory the corrosion crack spreads as a result of a greatly enhanced anodic reaction inside the crack. This hypothesis is based on the observed oxidation potential drop when a stress is applied to the metal and the crack expands. However, there are no quantitative data on the extent to which the anodic reaction is enhanced during the expansion of a corrosion crack. Since the crack usually develops in a very short period of time, it was impossible to investigate the polarizability at various stages of crack propagation by recording the polarization curves in the usual manner, whereby a steady potential is established at fixed current densities.

In the present work, by using automatic recording devices and a square-wave current, we recorded the potential and the pulse polarization and determined the exact electrode potential at the apex of the expanding crack; the resulting data enabled us to calculate precisely to what extent the anodic reaction was enhanced at any given instant from the time that the crack arose until the metal had completely disintegrated.

We used in our work an MA2-1 type of alloy of the following composition: Al 4.5%; Zn 1.1%; Mn 0.6%; Mg the balance. Its tensile strength was 28.1 kg/ mm^2, proportionality limit 17.2 kg/ mm^2. Though this alloy is

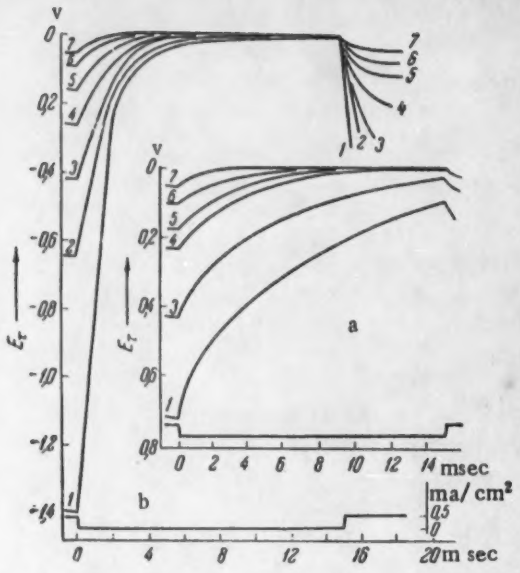

Fig. 2. The decline in the potential (discharge) of a MA2-1 alloy with time after the outside anodic current is disconnected: a) air-oxidized surface; b) anodized surface. 1) Before the application of stress; 2, 3, 4, 5, 6, 7) correspond to 10, 20, 40, 60, 80, and 100 sec, respectively, after the crack develops. The broken line below gives the shape of the polarization current.

fairly resistant to corrosion it shows a very strong tendency to undergo corrosion cracking in many media. Experiments were carried out on flat samples, which were cut out from a sheet along the lines of rolling. The working portion of the sample had a cross section of 5 × 1 mm^2. The tensile stress remained constant during the experiment and had the value of 15 kg/ / mm^2 of the original cross section. Before each test the samples were subjected to the following treatment. After a mechanical polishing with No. 14 emery cloth the samples were dipped for 30 sec in 20% NaOH at 90°, then washed thoroughly with distilled water, and left for 48 hours in a desiccator. Another batch of samples was subjected to anodic passivation for 30 min at I_a = 1 amp/dm^2 and 80°C in a 240 g/liter solution of NaOH after the mechanical polishing. These samples were subsequently washed with distilled water and left in a desiccator for 48 hours. The potential was automatically recorded on the photocell of a C.R. oscilloscope which had an electronic amplifier and an input resistance of 10^{10} ohms [7]. The potential inside the crack was measured by means of a glass capillary with an internal diameter of 3-5 μ. The tip of the capillary was placed directly above the apex of the crack (not higher than 1-2 μ) with the help of a micromanipulator and was constantly moved to accompany the expanding crack.

Data on the extent of polarization in an alloy during the expansion of a crack yield the polarization curves which were recorded at a direct and rapidly increasing polarization current (0.1 ma/cm^2 · sec); the potential was recorded automatically with the help of a photocell on an oscillograph. The results obtained on an air-oxidized MA2-1 alloy in a solution containing 20 g/liter K_2CrO_4 + 35 g/liter NaCl are shown in Fig. 1. The figure shows that in the absence of mechanical stresses (curve 1) the polarization of the alloy at current densities below 0.1 ma/cm^2 is relatively light, 5800 v · cm^2/amp on the average. The anodic curve recorded during the expansion of the crack (curve 2) shows that inside the crack the polarizability was strongly reduced and did not exceed 450-500 v · cm^2/amp in the same range of current densities. Thus, even this method makes it quite obvious that the expansion of the corrosion crack is accompanied by a decline in anodic polarization inside the crack to one tenth of the initial value. More precise quantitative data on the decreased anodic polarization resistance at any time after the corrosion cracking sets in and before a complete disintegration of the sample takes place yielded pulse polarization values.

Since each electrochemical cell constitutes a system composed of a condenser with the capacitance C and a total resistance R in parallel, the discharge (or charge) rate will depend on the magnitude of C and R. The potential drop accompanying the discharge is connected with the electrochemical reaction taking place and at a fixed C and will be determined by the resistance R, which consists of a sum of the polarization (P) and ohmic (R_{ohm}) resistances : $R = P + R_{ohm}$. In strongly conducting solutions $R_{ohm} \ll R$, and, consequently, we can assume that $R \approx P$. Thus, during the anodic polarization the total resistance R essentially involves only the polarization resistance of the anodic process which in this case is denoted by P_a.

The potential drop $\Delta E_\tau(v)$ within the time interval (sec) after the external polarization current i_0 (ma/cm^2) is turned on can be determined [8] from the equation:

$$\Delta E_\tau = b \cdot \ln\left(\frac{i_0 \tau}{bC} + 1\right),$$

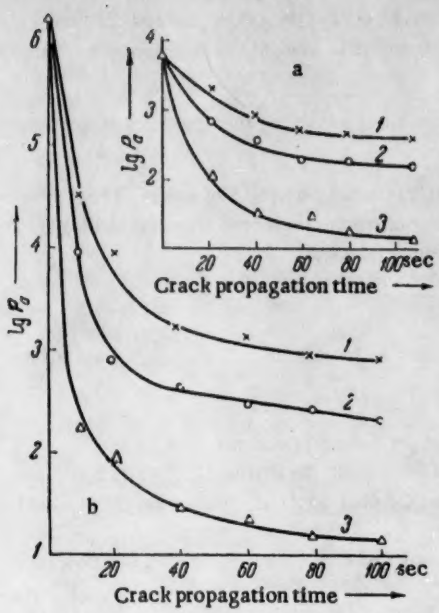

Fig. 3. The anodic polarization of the MA2-1 alloy as a function of time during the expansion of the corrosion crack: a) air-oxidized surface; b) anodized surface. 1, 2, 3) Corresponding to samples with working surfaces of 0.5, 0.05, and 0.005 cm^2, respectively.

where C is the electrode capacitance (f) and b is the coefficient of the Tafel's equation for an anodic reaction. If we know i_0 and ΔE_τ (from the experimental discharge curves) we can use the equation to determine the electrode capacitance at any stage in the development of the corrosion crack.

In Fig. 2 we have plotted a series of discharge curves (for an MA2-1 alloy in a solution of 20 g/liter K_2CrO_4 + 35 g/liter NaCl) obtained when a square-wave current was used to produce anodic pulse polarization; the current was varied from 0-0.5 ma/cm^2. The curves correspond to different times in the development of the crack. Curves 1,a and 1,b represent samples before the application of stress; curves 7,a and 7,b were recorded at 1-2 sec before the disintegration of the sample. An analysis of the curves in Fig. 2 indicates that they can be fairly well represented by the discharge equation for a condenser C in parallel with a resistance R:

$$E_\tau = E_0 \cdot e^{-\frac{\tau}{RC}},$$

where E_τ is the potential (v) at time τ (sec) after the current is turned off; E_0 is the potential before the current is turned off. In our case the resistance R represents the anodic polarization resistance P_a.

One can readily show that when $\tau = P_aC$ then $E_\tau = 0.63 E_0$, or in other words the potential declines to 63% of E_0. Next, after determining the potential drop during a full discharge from the curve in Fig. 2 we can evaluate the product P_aC, as the time during which the system undergoes 63% discharge. Hence, if we know the value of P_aC and C at each stage, we can determine P_a.

Figure 3 shows the anodic polarization at various stages in the development of a corrosion crack in the investigated alloy MA2-1, in a solution of 20 g/liter K_2CrO_4 + 35 g/liter NaCl. The curves indicate that the crack expansion is accompanied by a considerable decline in the anodic polarizability at the apex of the crack. When the intial surfaces are very small (0.005 cm^2) and the inside area of the crack is comparable in magnitude to the total working surface, the anodic polarization changes from $6 \cdot 10^3$ v·cm^2/amp to 15-20 v·cm^2/amp on air-oxidized samples and from 10^6 v·cm^2/amp to 20-25 v·cm^2/amp on anodized surfaces.

On the basis of these results one may presume that the extremely sharp decline in the anodic polarization (by six orders of magnitude) in the zone of cracking is chiefly responsible for the propagation of corrosion cracks. If all other conditions are maintained similar while the initial working surface is reduced the anodic polarization will undergo an even greater decline during the crack expansion. As the initial working surface is reduced the anodic zone, though its average area remains constant, will constitute a larger fraction of the total working surface and consequently, the decline in anodic polarizability (computed for the entire working surface) becomes more pronounced.

One can visually (with the help of a microscope) detect a very vigorous evolution of hydrogen 10-20 μ ahead of the visible peak of the crack. The hydrogen in these zones is evolved in the form of staggered "spouts" from underneath the oxide film on the metal surface. The amount of hydrogen evolved along both sides of the visible peak of the crack is insignificant. Practically no hydrogen is evolved along the crack walls at distances beyond 40-50 μ from the apex.

The experimental data lead to some definite conclusions with regards to the kinetics of the corrosion crack propagation. The appearance of a crack is accompanied by a strong (and abrupt) decline of the anodic polarizability. Subsequently, the anodic polarizability decreases much slower. This indicates that not the entire crack

constitutes an effective anode during the corrosion cracking, but only a relatively small segment concentrated around its peak. The slow decline in the anodic polarizability, observed during the crack propagation, indicates that as the crack expands, the anodic effectiveness of its side surface gradually declines at a distance from the apex.

Visual observation shows that segments of metal outside the crack but adjoining the apex of a steadily expanding corrosion crack constitute the most efficient cathodes.

Thus, the large experimentally demonstrated decline in anodic polarizability (by 5-6 orders of magnitude) and the concentration of the effective anodic zone at the apex of the corrosion crack constitute the two fundamental electrochemical factors on which the corrosion cracking of metals depends.

LITERATURE CITED

1. R. Mears, R. Brown, and E. Dix, Symp. on Stress-Corrosion Cracking of Metals (Am. Soc. Testing Material, 1944).
2. J. Harwood, Corrosion 6, 8, 249 (1950); 9, 290 (1950).
3. A. V. Ryabchenkov, The Resistance of Steel to Corrosion-Fatigue [in Russian] (Moscow, 1953).
4. A. V. Ryabchenkov and V. M. Nikiforova, Metallurgy and Metal Processing [in Russian] (1954) 8, 2.
5. P. A. Rebinder, Anniv. Coll. for the Thirtieth Anniv. of the Great October Socialist Revolution [in Russian] (Izd. AN SSSR, 1947) 1, p. 533.
6. V. I. Likhtman, P. A. Rebinder, and G. V. Karpenko, The Effects of Surface-Active Agents on the Deformation of Metals [in Russian] (Izd. AN SSSR, 1954).
7. N. D. Tomashov, L. A. Andreev, and N. I. Isaev, Zavodskaya Lab. 25, 10 (1959).
8. A. N. Frumkin, V. S. Bagotskii, et al., The Kinetics of Electrode Processes [in Russian] (Moscow, 1952).

THE IONIZATION POTENTIALS OF ORGANIC DYES AND SEVERAL COMPLEX MOLECULES IN THE VAPOR PHASE

F. I. Vilesov

Physical Institute of the Leningrad State University

(Presented by Academician A. N. Terenin, January 25, 1960)

Translated from Doklady Akademii Nauk SSSR, Vol. 132, No. 3, pp. 632-635, May, 1960

Original article submitted January 10, 1960

The majority of complex organic compounds, particularly dyes, have very low vapor pressures at ordinary temperatures. This explains why there is no data on the first ionization potentials of many important classes of compounds in the vapor phase. We previously determined the first adiabatic ionization potential of several volatile compounds by using the photoionization technique [1]. In the present work we obtained the ionization potentials of nonvolatile compounds by using the same technique, with the exception that the ionization cell (40 mm in diameter, 50 mm long) was dismountable and made of metal. All the leads had teflon seals and insulating jackets. The cell was constructed in such a way that the investigated samples could be heated to 250°C.

TABLE 1

Absorption Bands and First Ionization Potentials of Certain Dyes in the Vapor Phase

Dye	λ_1	λ_2	I_p	$I_p-\lambda_1$	$I_p-\lambda_2$
Rhodanine 6-G	5300 2,55	—	7,26	4,9	—
Indigo red	5390 2,3	4975 2,5	7,32	5,0	4,8
Indigo blue	6048 2,07	—	7,17	5,1	—
Meracyanin			7,35*		
Quinoline blue(ethyl cyanin)	5526 2,3	5146 2,45	7,35*	5,05	4,9
Pinacyanol	6100 2,05	—	7,25**	5,2	—

* On the red side there is a region of low ionization yield below 7.2 ev.

** The low ionization yield region extends to 7.1 ev.

The ionization potentials I_p previously reported and the new data are compiled in Tables 1 and 2*. Due to the fact that in the present work we did not measure the amount of absorbed radiation and used greater slit-widths in the monochromator (the resolution was about 5 A) to improve the sensitivity, we failed to detect any inflection points on the ionization curves of most of the measured compounds, and consequently, I_p in Tables 1 and 2 corresponds to the photoionization threshold. Previous work would indicate [1] that these values may be several hundredths of an electron volt below the adiabatic ionization potentials. The errors in the determination of the red photoionization boundary did not exceed 0.03 ev. In Tables 1 and 2 we have also listed the positions of λ_1, λ_2, and λ_3 for the first absorption bands of the compounds in neutral hydrocarbon solvents; these were copied from the literature (see, for example, [2]) and are expressed in angstroms and electron volts. We know that these bands are not displaced when the compounds are examined in the vapor phase. In the last three columns we have listed the differences between the ionization potentials and the positions of the corresponding absorption bands, in electron volts.

* V. I. Kleimenov, a candidate for an advanced degree, took part in these determinations.

Tables 1 and 2 show that within each series of compounds the regular decrease of ionization potential is accompanied by a simultaneous displacement of the first absorption band in the direction of longer wave-lengths. Acetophenone constitutes an exception since its I_p is somewhat higher than that of benzaldehyde. For each class of compounds the differences between the ionization potentials and the corresponding absorption bands remain constant with an accuracy of 0.1-0.2 ev. This empirical rule may be used, with certain reservations, to estimate the ionization potentials from the location of the first absorption bands of the higher members within each series if the ionization potentials of the lower members have been accurately determined. However, our data show that values of $I_p - \lambda_1$ have a considerable variance among compounds of different classes, by as much as 2 ev. Thus, for the linear polycyclic hydrocarbons from benzene to naphthalene the difference is 4.1-4.3 ev, whereas for quinone and anthraquinone it is 6.1-6.3 ev. It is noteworthy that the ionization potentials of various dyes listed in Table 2 differ very little from each other and yield a red photoionization boundary slightly over 7 ev. Similar observations have been reported before [3]; it has been shown that the photoemission of various dyes increases sharply in the vicinity of 2000 A, which corresponds to a photon energy of 6 ev.

It is interesting to compare our results with the indirectly determined ionization potentials of polymethine dyes recently reported by Scheibe and co-workers [4]. These workers found that the absorption bands in the spectra of polymethine dyes form a series which is in good agreement with Rydberg's equation. They assumed that the first excited level in the dye molecule is 3.4 ev below the ionization boundary, just as in the case of a hydrogen atom. In their opinion a conjugated electronic π-system can only exist in the ground state. Excitation of the electron to the first excited level of the molecule results in a complete uncoupling of the conjugated system, and the electron finds itself in the field of a positive molecular frame thus resembling an electron in the hydrogen system. Consequently, a very simple equation is proposed for calculating the ionization potential: $I_p = E + 3.4$ ev, where E is the energy difference between the ground and the first excited level.

Hydrogen-like series of absorption bands were discovered in the spectra of many classes of organic compounds but only in the vacuum ultraviolet region, i.e., at excitation energies above 6 ev. This serial dependence was successfully used for the determination of the first adiabatic ionization potentials of several classes of compounds. Spectroscopically determined ionization potentials conform to the molecular structure and are in good agreement with the values of I_p obtained by direct photoionization measurements. However, Price's and Wood's work [5] shows that even in the spectra of such simple compounds as aliphatic hydrocarbons and alkyl derivatives of benzene the first terms of the Rydberg's series are displaced to such an extent that it is difficult to identify them; hence, it seems that the hydrogen-like treatment is only valid for the higher members of each series. It has also been shown [6] that when the ground state of these same molecules is lowered all the terms decrease and the decrease becomes more pronounced for the higher terms, bringing them closer to the normal ionic level, or in other words, the bands of the higher members of each homologous series should converge much more rapidly to the continuum than the bands of the lower members. We in turn showed [1] that the above-mentioned rule can be extended to other benzene derivatives, such as aromatic amines, phenols, etc. Finally, Price and Walsh [7] have very clearly demonstrated that within the series: ethylene, butadiene, and hexatriene the displacement of the $N - V_1$ band towards longer wave-lengths proceeds 1.2 times as fast as the accompanying decrease of ionization potential.

It still remains an open question whether the regular property changes established by Scheibe pertain to the vapor phase or to molecules located in a medium with a high dielectric constant, which is known to decrease the ionization energy. Hence, considering the above-established relationship between I_p and E we cannot regard the ionization potentials given by Scheibe as very reliable. We measured the photoemission of electrons from compact layers of various dyes and found that the work functions of these molecular systems were all at least 6 ev in magnitude.

The ionization potentials of several dyes and other complex molecules listed in this work indicate that the ionization potentials calculated from Scheibe's equation are usually too low and have to be used with certain reservations.

The author is deeply indebted to Academician A. N. Terenin for his constant interest and valuable advice during the work.

TABLE 2

Absorption Bands and the First Ionization Potential of Complex Organic Molecules

Compound	λ_1	λ_2	λ_3	I_p	$I_p-\lambda_1$	$I_p-\lambda_2$	$I_p-\lambda_3$
Benzene	2550 4,9	1980 6,25	1800 6,9	9—24	4,3	3,0	2,3
Naphthalene	3140 4,0	2750 4,5	2200 5,65	8,14	4,15	3,65	2,5
Anthracene	3800 3,26	—	2500 5,0	7,38	4,1	—	2,4
Naphthalene	4800	—	—	6,88	4,3	—	—
Pyridine	2500 5,0	1900 6,4	—	9,40	4,4	3,0	—
Quinoline	3110 4,0	2750 4,5	—	8,30	4,3	3,8	—
Acridine 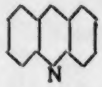	3470 3,55	2520 4,9	—	7,78	4,23	2,9	—
Quinone	4200 3,35	3000 4,7	2500 5,65	9,68	6,3	5,0	4,0
Anthraquinone 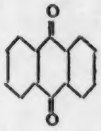	4400 3,2	3230 4,4	—	9,34	6,1	5,0	—
α-Naphthylamine 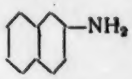	3200 3,9	2400 5,2	—	7,30	3,4	2,1	—
β-Naphthylamine 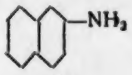	3400 3,7	2800 4,4	2200 5,7	7,25	3,55	2,85	1,55
Benzaldehyde 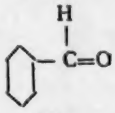	3280 3,8	2800 4,45	2440 5,1	9,60	5,8	5,15	4,5
Acetophenone 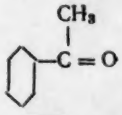	3190 3,9	2780 4,45	2440 5,1	9,65	5,75	5,2	4,55
Benzophenone 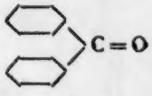	3300 3,75	—	2520 4,9	9,45	5,7	—	4,55

LITERATURE CITED

1. F. I. Vilesov and A. N. Terenin, Doklady Akad. Nauk SSSR 115, 744 (1957)*; F. I. Vilesov, Experimental Techniques and Instruments [in Russian] (1958) 4, 89; F. I. Vilesov, Doctoral Dissertation [in Russian] (LGU, 1958).
2. A. Gillam and E. Stern, Electron Absorption Spectra of Organic Compounds [Russian translation] (IL, 1957).
3. Hlucka, Zs. Phys. 81, 66, 521 (1933); Zs. Phys. 95, 486 (1935).
4. G. Scheibe, D. Brück, and F. Dörr, Chem. Ber. No. 9-10, 867 (1952).
5. W. C. Price and R. W. Wood, J. Chem. Phys. 3, 339 (1935); A. D. Walsh, Trans. Farad. Soc. 42,62 (1946); W. C. Price and A. D. Walsh, Proc. Roy. Soc. A191, 22 (1947).
6. W. C. Price, Chem. Rev. 41, 257 (1947); Pap. Confer. Molecular. Spectrosc. (London, Feb. 1958).
7. W. C. Price and A. D. Walsh, Proc. Roy. Soc. A 185, 182 (1946).

* See CB translation.

CATHODE PROCESSES DURING ELECTRODEPOSITION OF TITANIUM FROM AQUEOUS SOLUTIONS

N. T. Kudryavtsev, R. G. Golovchanskaya, and N. K. Baraboshkina

D. I. Mendeleev Moscow Chemicotechnical Institute

(Presented by Academician A. N. Frumkin, December 12, 1959)

Translated from Doklady Akademii Nauk SSSR, Vol. 132, No. 3, pp. 636-638, May, 1960

Original article submitted December 12, 1959

The first attempt to electroplate titanium from aqueous and nonaqueous solutions of its salts was made in 1901. However, the chemical and electrochemical properties of titanium and the practical uses of the metal had not been adequately investigated prior to 1948. Until very recently the research was concentrated primarily on the investigation of the corrosion properties of Ti, with very little work devoted to the surface treatment.

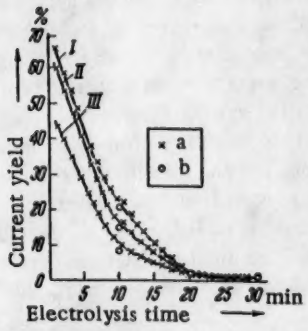

Fig. 1. The current yield as a function of the electrolysis time, in alkaline electrolytes at 20° and d_c = 20 amp/dm². I) Lead cathode; II) copper cathode; III) platinum cathode; a) the yield of metal with reference to a gasometrically determined current; b) the yield of metal based on the current as determined from the titanium weight.

The metal is prepared by the reduction of titanium oxides with aluminum or carbides, the decomposition of TiI_4 at high temperatures, the reduction of $TiCl_4$ with magnesium, and the electrolysis of fused titanium fluoborate or chlorides mixed with alkali metals. According to the literature data [1], the last method is currently the most widely used one. The industrial preparation of titanium by the electrolysis of fused salts involves great difficulties. However, the electrolysis of aqueous solutions of titanium salts would be the most convenient and cheapest method of preparing titanium plates. Since this problem has not been adequately explored, the chemical literature is of very little help.

Before deciding whether titanium can be plated on the cathode, one has to know the following important electrochemical properties: the standard electrode potential (the position of the metal in the oxidation potential scale) and the overvoltage of hydrogen. The standard oxidation potential of titanium, E_0, calculated by Botts and Krauskopf [2] from the measured potentials in 0.25 M $Ti_2(SO_4)_3$ and in $TiCl_3$, is −0.168 and −0.218 v, respectively. The standard oxidation potential of the Ti^{+++}/Ti^0 system was also calculated from other experimental data [3]. The value was −0.355 v. The potential was measured in unpolarized electrodes in 0.0215 M $Ti_2(SO_4)_3$, at 19° under argon. According to Latimer [4] the standard oxidation potential for the Ti^{+++}/Ti^0 system can be calculated thermodynamically from the following set of reactions:

$$Ti^{3+} + 3e \rightarrow Ti^0 = \varepsilon_0^1,$$
$$Ti^{3+} + e \rightarrow Ti^{2+} = -0{,}37\text{v}\ (\varepsilon_0^2),$$

$$Ti^{2+} + 2e \rightarrow Ti^0 = \varepsilon_0^3 = -1{,}63 \text{ v},$$
$$\varepsilon_0^1 = \frac{-0{,}37 + 2\cdot(-1{,}63)}{3} = -1{,}21 \text{ v}.$$

The thermodynamically calculated potential of the Ti^{+++}/T^0 system is −1.3 v [5]. According to the calculations titanium should lie between aluminum and magnesium in the electronegativity series, whereas the experimentally determined oxidation potentials place it between cadmium and cobalt. The discrepancy between the experimental and the theoretical values of E_0 is attributed to the irreversibility of the titanium electrode. It seems that the position between aluminum and manganese in the electronegativity series is more correct.

During the study of titanium corrosion it was established [5-9] that the formation of a passive film on the electrode surface reduces the oxidation potential of titanium considerably below the value obtained when the film is destroyed by the electrolyte. A kinetic study of the evolution of hydrogen on titanium was also of some interest. As is well known [10], one mole of titanium can absorb 2 moles of hydrogen at 20°, but at higher temperatures the absorption is reduced and only 0.2 moles are taken up at 1100°C [11]. It is usually assumed that metals capable of absorbing large quantities of hydrogen have low hydrogen overvoltages. It has been established that in 0.01N H_2SO_4 the minimum hydrogen overvoltage on Ti is 0.236 v [12]. The data of Tajima and others [13, 14] indicate that the hydrogen overvoltage on titanium is much higher in alkaline solutions than in acidic (−1.3 v).

Thus, judging by the position of Ti in the electronegativity series (between aluminum and manganese) it should be possible to plate Ti out of nonaqueous organic or aqueous solutions of its salts (as is done with aluminum) under conditions of high hydrogen overvoltage. It is quite obvious that alkaline solutions are more suitable for this since the overvoltage of hydrogen on titanium can then be made very large.

EXPERIMENTAL

Alkaline Electrolytes. We tried to prepare the alkaline solutions of the following salts: sodium, manganous, chromic, and ferric metatitanates. As it turned out all the metatitanates were poorly soluble in sodium hydroxide (up to 6-8 g/liter of Ti) and were readily hydrolyzed. We investigated the solubility of sodium metatitanate and the stability of the solution as a function of the base concentration, leaching time, temperature, stirring velocity, and amount of organic additives. These experiments revealed that the solubility of metatitanates increases considerably (to 15-20 g/liter) when certain organic compounds are added to the alkaline solution, probably due to the formation of more soluble Ti compounds. At higher temperatures (above 50°C) the solubility of metatitanates declines, which is probably due to the decomposition of the organotitanium compounds. The maximum Ti solubility (15-20 g of metal per liter of solution) was obtained by leaching sodium metatitanate at 50°C with stirring (mechanical stirrer) in a 20-30% NaOH solution to which some organic compounds were added. After the leaching the resulting solution was filtered to remove any undissolved sodium metatitanate. Chemical analysis indicates that in alkaline solutions the Ti is present in the form of tetravalent ions. We used copper, brass, platinum, and lead cathodes, and stainless steel and platinum anodes.

The current yields were determined in two ways: gasometrically, from the amount of hydrogen evolved (measured at minute intervals), and gravimetrically. In the gravimetric method the amount of Ti was determined by analyzing the solution resulting after the deposit was removed from the cathode. It turned out that regardless of the metal used for the cathode, the current yield declines during the electrolysis from about 60-0.5% within 20-30 min. Only the starting point of the electrolysis shows slight dependence on the cathode materials. After the cathode becomes entirely covered with titanium only hydrogen is evolved, which seems to be due to a very low hydrogen overvoltage on Ti. The current yield decreases with increasing current density and temperature.

The resulting coat of pure titanium metal is 3-4 μ thick. When a stainless steel anode is used, traces of iron and chromium appear in the deposit and the coat becomes 15 μ thick.

Acidic Electrolytes. In acidic solutions of fluorides the Ti exists in the form of trivalent and tetravalent ions. There are some indications in the literature [14] that the electrolysis of such solutions first reduces the Ti to the divalent state. In order to find out which titanium ion is reduced to the metal, in one case we electrolyzed a solution containing trivalent titanium exclusively and in another a solution of just the tetravalent ions. It turned out that no metal was deposited on the cathode of the solutions containing the tetravalent ion. The entire current

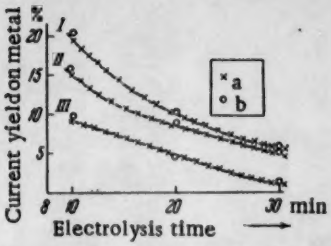

Fig. 2. The current yield of titanium as a function of electrolysis time in acidic electrolytes at 20°C and $d_c = 10$ amp/dm^2. I) Lead cathode; II) copper cathode; III) platinum cathode; the letters are defined in Fig. 1.

was consumed in the production of hydrogen and a partial reduction of tetravalent titanium to trivalent; only after the ionic concentrations attained the ratio Ti^{++++}: Ti^{+++} = 1 : 1 did some Ti metal begin to deposit on the cathode. We failed to detect the formation of any divalent titanium in solution.

We also proved that the titanium deposited on the cathode does not redissolve during the electrolysis. Just as in the case of the alkaline solutions only the initial current yield depends slightly on the cathode material. After the entire cathode surface becomes coated with Ti, the yield of metal for a given amount of current declines, though to a smaller extent than in alkaline electrolytes; it seems that this difference can be accounted for by the fact that the deposits obtained in acidic electrolytes are more porous. The current yields of metal were determined in a H-shaped vessel in an atmosphere of argon and with the cathode compartment separated from the anode by a glass diaphragm. The vessel was made completely gas-tight. The anode compartment was filled with a solution of potassium fluoride, slightly acidified with fluoboric acid.

To study the distribution of the current consumed in the reactions: $Ti^{4+} \rightarrow Ti^{3+}$; $Ti^{3+} \rightarrow Ti^0$; $2H^+ \rightarrow H_2\uparrow$, we filled the cathode compartment with a solution containing trivalent and tetravalent Ti ions in the ratio 7 : 1. This ratio corresponds to the equilibrium which is normally established in solutions of trivalent titanium when the work is done in air.

Surface-active agents: gelatin, glue, and glycol have no apparent effect on the current yield of metal. The pure titanium deposit was 3-4 μ thick.

LITERATURE CITED

1. Coll. Translations, Special State Planning Institute [in Russian] (Tekhnicheskii Otdel., Moscow, 1958).
2. E. D. Botts and F. S. Krauskopf, J. Phys. Chem. 31, 1404 (1927).
3. By Shunichi Satoh and Koshin Jamane, J. Scient. Res. Inst. 50, 134(1956).
4. K. E. Powell and W. M. Latimer, J. Chem. Phys. 19, 1139 (1951).
5. G. E. Huthinson, and P. A. Permer, Corrosion 6, 10 (1949).
6. G. M. Parker, Corrosion 5, 303 (1949).
7. Werkstoffe und Korrosion 11, 442 (1951).
8. S. Tajima, N. Fujiwara, and T. Mori, J. Elektrochem. Soc. Japan 24, 5, 212 (1956).
9. H. Böhm, Metalloberfläche 2, 6, 197 (1957).
10. M. E. Straumais, S. T. Shin, and A. W. Schlechten, J. Phys. Chem. 59, 317 (1955).
11. R. W. G. Wycktoff, Crystal Structure, Interscience (1948).
12. B. Diethelm and F. Foerster, Z. phys. Chem. 62, 122 (1948).
13. S. Tajima, J. Seki, and T. Mori, J. Electrochem. Soc. Japan 24, 10, 461 (1956).
14. Japanese Patents No. 2357, April 11, 1955 and July 27, 1955.
15. Coll. Translations: Communications, Kenkya 8, 1, 12 (1957).

THE ANODIC PASSIVATION OF ZINC IN ALKALINE SOLUTIONS

T. I. Popova, V. S. Bagotskii, and B. N. Kabanov

Electrochemical Institute, Academy of Sciences, USSR

(Presented by Academician A. N. Frumkin, January 25, 1960)

Translated from Doklady Akademii Nauk SSSR, Vol. 132, No. 3, pp. 639-642, May, 1960

Original article submitted January 11, 1960

Several workers [1-3] have proposed that the passivation of zinc may be caused by the formation of a solid film of zinc oxide or hydroxide; the initiation of passivation has also been occasionally connected with electrode processes in the solution layer adjoining the electrode. Yet the formation mechanism and the nature of the passivating film are still unknown. To be more specific, there are no papers covering any quantitative aspects of the diffusion phenomena connected with passivation.

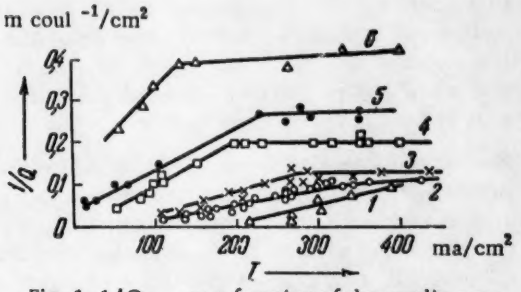

Fig. 1. $1/Q_{pass}$ as a function of the anodic current density i in KOH solutions: 1) 1.5 N; 2) 1 N; 3) 0.75 N; 4) 0.5 N; 5) 0.25 N; 6) 0.1 N.

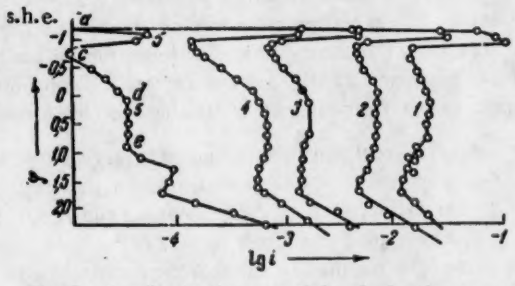

Fig. 2. Anodic static potential polarization curves in KOH solutions: 1) 1 N; 2) 0.5 N; 3) 0.25 N; 4) 0.1 N; 5) 0.03 N.

In the present work we hoped to find out what effects the composition of the solution layer next to the electrode might have on the passivation of zinc and also establish the nature of the passivating layer covering the zinc in order to determine the effects of adsorbed oxygen and of the oxide layer on the passivation of zinc. In investigating the anodic behavior of zinc in KOH solutions we recorded the curves of voltage against time ($\varphi - t$) on an oscillograph at constant current densities using a rotating disc electrode. The amount of current required to achieve passivation $Q_{pass} = it_p$ (where i is current density and t_p passivation time) was determined as a function of current density, base concentration, and stirring velocity. In addition to this, we measured the electrostatic polarizations, which could be used to determine the solution rates of active and passive zinc as a function of voltage and help define the range of potentials at which passivation takes place. We also recorded some activation curves of a passive zinc cathode which enabled us to determine the point at which the reduction of the solid film begins.

In Fig. 1, we have plotted $1/Q_{pass}$ as a function of i; the points were obtained from oscillographic measurements at constant current densities*. At moderate current densities a linear relationship between $1/Q_{pass}$ and i

* Q_{pass} is the average (of 10-12 measurements) quantity of charge in mcoul/cm^2.

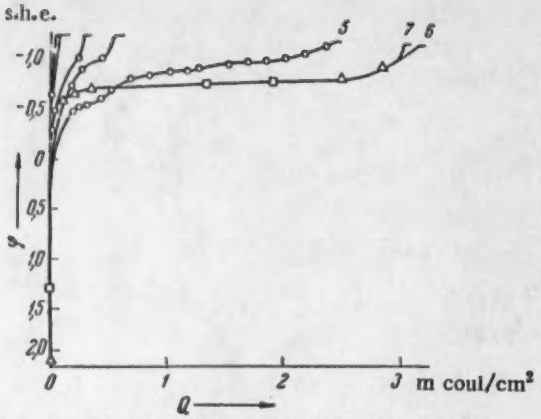

Fig. 3. The increase in voltage after 60 min of passivation at a 0.017 mamp/ cm^2 cathodic current density and at various constant potentials: 1) − 1.1 v and −0.9 v; 2) −0.7 v; 3) −0.3 v; 4) + 0.1 v; 5) + 0.5 v; 6) + 1.3 v; 7) + 2.1 v.

is observed, similar to that previously reported by other workers [2, 3]. Our experiments indicate that Q_{pass} is independent of the stirring velocity in the range from 60 to 5000 rpm when the polarization is carried out at moderate and high current densities. At lower current densities the indicated linearity disappears and a large Q_{pass} (40-200 mcoul/ cm^2) is required to achieve passivation. In this case Q_{pass} increases with increasing stirring velocity. At low current densities, particularly when the stirring is vigorous (3000-5000 rpm), no passivation is observed in concentrated solution of 0.5-2.5 N KOH. Calculations revealed that at moderate and high current densities the passivation time is shorter than the time required to attain steady diffusion. This would explain why Q_{pass} is independent of stirring velocity, since initially stirring has very little effect on the velocity of nonstationary diffusion. The Q_{pass} is found to increase rapidly with the stirring velocity when the current density and the stirring rate are such that the passivation time is either greater or comparable in magnitude to the time required to attain steady diffusion.

At high current densities (see Fig. 1) Q_{pass} is practically independent of the polarization current density.

Experimental data indicate that certain changes in the concentrations of alkali and zincate have to take place in the vicinity of the electrode before the passivation can set in. At low current densities and rapid stirring the required concentration changes do not occur, and even after steady diffusion is achieved no passivation of zinc is observed. The experimental results can be readily explained if we assume that at moderate current densities a portion (Q_1) of the current which is needed for the passivation is used to dissolve the zinc and produce the accompanying changes in OH^- ion and zincate ion concentrations, while another portion (Q_2) (probably independent of current density) is consumed in altering the zinc electrode surface so as to produce the passivation.

At high current densities Q_1 becomes very small and the measured amount of current (required for that passivation) Q_{pass} approaches Q_2. Experiments show that at high current densities Q_{pass} is directly proportional to the alkali concentration. In very dilute solutions (0.01; 0.03 N KOH as well as 0.1 N KOH saturated with the zincate) Q_{pass} is approximately equal to 1 mcoul/ cm^2. If we take a roughness coefficient of 2.5-3 and assume that about 0.5 mcoul/ cm^2 is required to adsorb a monomolecular layer of oxygen then our data would indicate that, in dilute solutions at least, the passivation sets in when a monolayer of oxygen is adsorbed or even when the zinc surface is incompletely covered.

In Fig. 2., we have plotted some anodic polarization curves which were recorded under conditions of static potential in various KOH solutions. The curve shapes are typical of many passivating metals [4, 5].*

During the anodic polarization one at first observes a region of active zinc dissolution (for example, Fig. 2, curve 5, section ab). When the voltage is rendered more positive the zinc passivation is reflected in the declining solution rate (section bc), which is reduced by about two orders of magnitude from the solution rate of a smooth electroplated and active zinc surface, and in a slower increase of the solubility rate when the voltage is further raised (section cd). At sufficiently high positive potentials the solution rate of zinc becomes practically independent of the voltage (section de). The curve shape and the calculations indicate that this "limiting" current observed during passivation is not an ordinary limiting diffusion current. One may assume that the magnitude of the "limiting" current depends on the chemical solution rate of the solid film, the thickness of which remains unchanged [4]. When the anodic current is switched on after the passivation has set in and the potential has strongly shifted in the positive direction, and also when the cathodic polarization is weak, the potential is at first rapidly reversed in the negative direction and then becomes constant at −0.7 to −0.9 v (see Fig. 3). This

* Very recently similar anodic curves were also obtained on zinc [6].

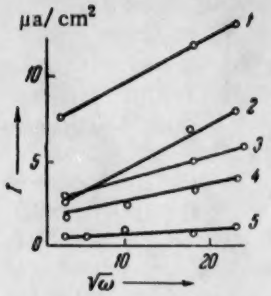

Fig. 4. The solubility rate of a passive zinc electrode as a function of the angular velocity of the stirrer (ω). In 0.5 N KOH: 1) + 0.6 v; 2) −1.1 v; in 0.5 N KOH saturated with zincate; 3) + 0.6 v; in 0.25 N KOH: 4) + 0.6 v; 5) −1.1 v.

plateau results from a partial reduction of the thin solid film which had formed during the anodic polarization. The voltage at which the reduction of the solid film begins would indicate that besides zinc oxide the film also contains a compound at a higher oxidation state than ZnO, possibly, zinc peroxide.

When the "limiting" current is attained, the solubility rate of zinc is apparently determined by the rate of chemical solution of zinc oxide (and peroxide):

$$ZnO + 2OH^- \rightarrow ZnO_2^{2-} + H_2O.$$

This would explain why the "limiting" current was found to depend so strongly on the concentration of the alkali (Fig. 2). The relationship we found between the "limiting" current and the zincate ion concentration in the vicinity of the electrode* is attributed to the hindering effects of zincate ions on the film solution rate. This would also explain why the solubility rate of zinc depends on the stirring velocity (Fig. 4).

The formation of a solid film and the zinc peroxide within are not essential to the passivation of the zinc electrode. This is apparent from the fact that the passivation already begins at −1.1 or −1.0 v (Fig. 2), at voltages more negative than the reduction potential of the zinc peroxide inside the solif film. Besides, as has already been demonstrated, the amount of current Q_2 consumed for the passivation is less than the amount required to form a solid film on the electrode surface under similar conditions. The formation of zinc peroxide inside the solid layer is a consequence and not a cause of the electrode passivation; unless a zinc electrode has been rendered passive beforehand its potential cannot be raised to the value at which this compound begins to form.

The experiments discussed above indicate that the passivation of zinc electrodes which accompanies anodic polarization depends on concentration changes (in the vicinity of the electrode surface) which affect the physical state of the surface in such a way as to reduce the solubility rate of zinc. In alkaline solutions zinc becomes even when the amounts of adsorbed oxygen or hydroxyl ion are inadequate to cover the entire surface with a mono molecular layer; iron exhibits similar passivation behavior in alkaline solutions [7]. The formation of solid phase films containing zinc peroxide constitutes a secondary process.

LITERATURE CITED

1. Z. A. Iofa, S. Ya. Mirlina, and N. B. Moiseeva, Zhur. Priklad. Khim. 22, 9, 983 (1949).
2. Z. Ya. Nikitina, Zhur. Priklad. Khim. 31, 213 (1958).* *
3. R. Landsberg, Z. phys. Chem. 206, 291 (1957); R. Landsberg and R. Bartelt, Z. Elektrochem. 61, 9, 1162 (1957).
4. K. F. Bonhoeffer, Z. Elektrochem. 59, 594 (1955); U. F. Franck and K. Weil, Z. Elektrochem. 56, 314 (1952); K. Weil and K. F. Bonhoeffer, Z. phys. Chem. 4, 175 (1955).
5. Ya. M. Kolotyrkin and Z. M. Knyazheva, Zhur. Fiz. Khim. 30, 1990 (1956).
6. J. Sanghi and M. Fleischman, Proc. Indian Acad. Sci. A-49, 6 (1959).
7. B. N. Kabanov and D. I. Leikis, Doklady Akad. Nauk SSSR 58, 1685 (1947).

* For example, in $1.7 \cdot 10^{-2}$ N zincate the solubility rate is 2-2.5 times greater than in a $3.5 \cdot 10^{-2}$ N solution.
* * See CB translation.

THE EFFECTS OF RADIATION ON THE SOLUBILITY OF RADIOACTIVE SOLIDS

Academician Vic. I. Spitsyn, E. A. Torchenkova, and I. N. Glazkova

Physical Chemistry Institute, Academy of Sciences, USSR

Translated from Doklady Akademii Nauk SSSR, Vol. 132, No. 3, pp. 643-645, May, 1960

Original article submitted February 24, 1960

We know of only relatively few papers dealing with the effects of radioactivity on the surface charge of solids [1] and other physicochemical properties [2], such as the isotopic exchange rate in heterogeneous systems [3], catalytic activity [4], and adsorptivity [5].

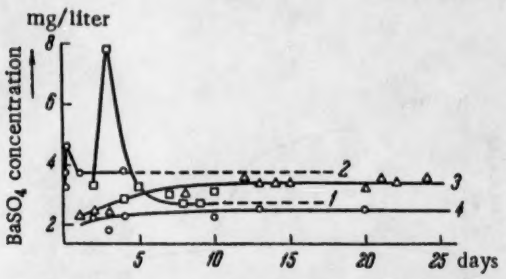

Fig. 1. Solubility kinetics of various $BaSO_4$ samples in water at 20°C. Sample activity: 1) 0.7 mC/g; 2) 1.0 mC/g; 3) 9.0 mC/g; 4) 19.0 mC/g; The samples were prepared by mixing equivalent amounts of 0.1 N $BaCl_2$ and Na_2SO_4 solutions.

In the present communication we describe the effects of radioactivity on the solubility and the solution rate of barium sulfate, labeled with S^{35}. The solubility of barium sulfate has been previously determined by various methods and the accepted value is 2.3 mg/liter at 18°C [6]. Unusual solubility properties of $BaSO_4$ have been noted by several workers; for example, solutions twice as concentrated as the normal saturated solutions may be formed for brief periods of time (not over 24 hours) [7]. It has also been pointed out [8] that the solubility of $BaSO_4$ remains approximately constant if the crystal size does not exceed 1-2 μ.

Sulfur-35 was introduced into barium sulfate during the precipitation step. The $BaSO_4$ samples were prepared by following the method given in [9]. Hot 0.1 N solutions of $BaCl_2$ and Na_2SO_4 (in some cases we used 0.1 N H_2SO_4), which contained a fixed amount of S^{35}, were poured at an equal rate into a stirred reaction vessel. The mixture was heated with stirring for one hour at 70-80°. Subsequently, the precipitate was allowed to settle from the mother liquor over a period of 20 hours. The $BaSO_4$ precipitate was first washed with water, then with ethyl alcohol, and dried at 80-85°C to a constant weight. The specific surface of $BaSO_4$ samples was determined with the help of an optical microscope (1200×) and an electron microscope (12000 ×). The $BaSO_4$ particle size ranged from 2.7-8.1 μ. These results were in agreement with the literature data [9].

To study the solubility we mixed 0.5 g of radioactive $BaSO_4$ and 50 ml of twice-distilled water in a test tube. The mixture was stirred at 20±0.5°C. At fixed time intervals we removed fixed aliquots of the solution, centrifuged them three times at 5000 rpm, and measured their activity. From the activity of the aliquot and the activity of the $BaSO_4$ precipitate we calculated the salt concentration in solution [10]. In Fig. 1 we have plotted the results obtained from our study of the solubility kinetics of various $BaSO_4$ samples, which were prepared by mixing 0.1 N solutions of $BaCl_2$ and Na_2SO_4.

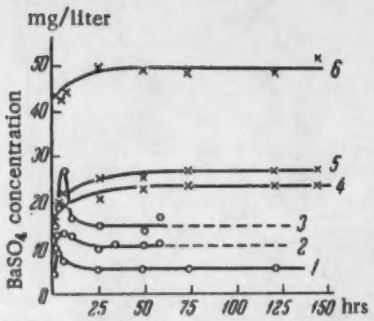

Fig. 2. The solubility kinetics in water (at 20°C) of $BaSO_4$ samples with activities of 0.6-0.7 mC/g (1, 2, 3) and 8-9 mC/g (4, 5, 6). Samples 1 and 4 were prepared by mixing equivalent amounts of 0.1 N $BaCl_2$ and Na_2SO_4 solutions; samples 2 and 5 contained 20% excess of Na_2SO_4; samples 3 and 6 contained a 20% excess of $BaCl_2$.

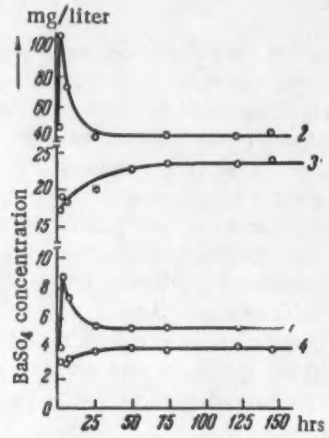

Fig. 3. The solubility kinetics in water (at 20°C) of various $BaSO_4$ samples. The activities were: 1) 0.13 mC/g; 2) 1.47 mC/g; 3) 8.2 mC/g; 4) 98.1 mC/g. The salt was prepared by mixing equivalent amounts of 0.1 N $BaCl_2$ and H_2SO_4 solutions.

One can not fail to notice that when the specific radioactivities of samples are about 0.7-1.0 mC/g there appears at first a considerable degree of supersaturation which subsequently disappears when the precipitate and the solution are stirred for 25 hours. Samples with activities of 9-20 mC/g do not exhibit any such behavior – the $BaSO_4$ concentration increases with time.

A comparison of the final concentrations of our solutions reveals that the barium sulfate prepared in the above-described manner exhibits maximum solubility at about 2 mC/g; when the specific radioactivity is either increased or decreased, the solubility declines (Fig. 4, curve 1). One of us previously observed a simflar behavior while studying the effects of radioactivity on the isotopic sulfur exchange in the $K_2SO_4-SO_3$ system [3, 11] and oxygen exchange in the $Na_2SO_4-O_2$ system at high temperature [2]. It should be noted, however, that in all of our experiments the solubility of radioactive $BaSO_4$ still exceeded the solubility given in the chemical literature.

The solubility of $BaSO_4$ increases even more if one of the reagents used in the preparation of the compound is in excess. The highest solubility was observed when $BaCl_2$ was used in excess (Fig. 2).

Samples of varying specific radioactivities (0.6-0.7 and 8-9 mC/g) all equilibrate with the saturated solution in the manner described before (Fig. 1).

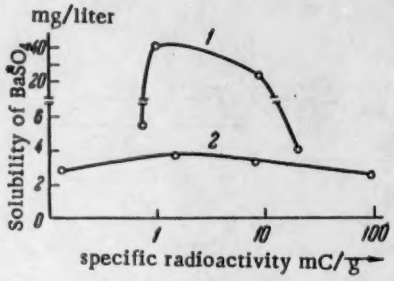

Fig. 4. The effects of specific radioactivity of $BaSO_4$ on its solubility in water at 20°C. The samples were prepared from: 1) $BaCl_2 + Na_2SO_4$; 2) $BaCl_2 + H_2SO_4$.

The solubility of $BaSO_4$ was much smaller when the salt was prepared in the same manner [9] but 0.1N H_2SO_4 was used instead of Na_2SO_4 (Fig. 3). Still the solubility kinetics curves had the same shape as those in Fig. 1. Samples with a specific radioactivity of 0.1 and 1.5 mC/g exhibited a strong tendency to supersaturation. When the activities were 8.2 and 98.1 mC/g this tendency was not observed. All the investigated radioactive $BaSO_4$ samples were more soluble in water than is normal nonradioactive barium sulfate. When the concentration of saturated solutions are plotted against the specific radioactivity of the $BaSO_4$ thus prepared, the curve shows a maximum (Fig. 4, curve 2) similar to the one observed on the curves of samples prepared from $BaCl_2$ and Na_2SO_4 (Fig. 4, curve 1). However, the maximum is much less pronounced on curve 2.

The above-described phenomena apparently have to be attributed to the steady emission of β-particles from the radioactive $BaSO_4$ samples. The charges which arise at the phase boundary influence the double layer structure and promote additional adsorption of ions on the precipitate. It seems that the electric fields which arise have the same effect on the solubility as the ionic strength. It is a well-known fact that the solubility of sparsely soluble compounds depends very much on the ionic strength [12-14]. The maximum on the curves of $BaSO_4$ solubility versus its specific radioactivity can be explained by assuming that the interaction between the solid and the β-particles changes when the number of the latter is greatly increased [11]. One would expect the effects of the specific radioactivity on the solubility of the precipitates to be most pronounced when the compounds are sparsely soluble and emit high-energy radiation.

LITERATURE CITED

1. P. Curie and M. Curie, Compt. Rend. 130, 647 (1900).
2. Vic. I. Spitsyn, Izvest. Akad. Nauk SSSR, Otdel. Khim. Nauk 11, 1296 (1958).*
3. Vic. I. Spitsyn and I. E. Mikhailenko, Doklady Akad. Nauk SSSR 121, 319 (1958).*
4. A. A. Balandin, Vic. I. Spitsyn, et al., Doklady Akad. Nauk SSSR 121, 495 (1958).*
5. Vic. I. Spitsyn and V. V. Gromov, Doklady Akad. Nauk, SSSR 123, 722 (1958)*; Radiokhimiya 1, 181 (1959).
6. F. Kohlrausch, Z. phys. Chem. 64, 129 (1908).
7. G. A. Hulett, Z. phys. Chem. 37, 385 (1901).
8. B. Fischer, Anal. Chem. 23, 1667 (1951).
9. A. M. Rutgers and W. van den Heuvel, Experientia 11, Fasc. 12, 481 (1955).
10. Vic. I. Spitsyn, P. N. Kodochigov, et al., The Use of Radioactive Tracer Techniques [in Russian] (Izd. AN SSSR, 1955) p. 234.
11. I. E. Mikhailenko and Vic. I. Spitsyn, Doklady Akad. Nauk SSSR 131, 129 (1960).*
12. G. N. Lewis and M. Randall, Chemical Thermodynamics [Russian translation] (Moscow, 1936) p. 287.
13. E. B. Shternina, Izvest. Sektora Fiz. Khim. Anal. IONKh Akad. Nauk SSSR 19, 345 (1949).
14. Vic. I. Spitsyn and I. A. Savich, Zhur. Neorg. Khim. 3, 1979 (1958).

* Original Russian pagination. See C.B. translation.

DETERMINATION OF THE RATE CONSTANT FOR THE REACTION BETWEEN ATOMIC OXYGEN AND MOLECULAR HYDROGEN

V. V. Azatyan, Corresponding Member of the Academy of Sciences USSR V. V. Voevodskii and A. B. Nalbandyan

Chemical Physics Institute of Academy of Sciences of USSR

Translated from Doklady Akademii Nauk SSSR, Vol. 132, No. 4, pp. 864-867, June, 1960

Original article submitted February 9, 1960

The reaction of atomic oxygen with molecular hydrogen, forming the hydroxyl radical and atomic hydrogen,

$$O + H_2 = OH + H \qquad \text{(III)}$$

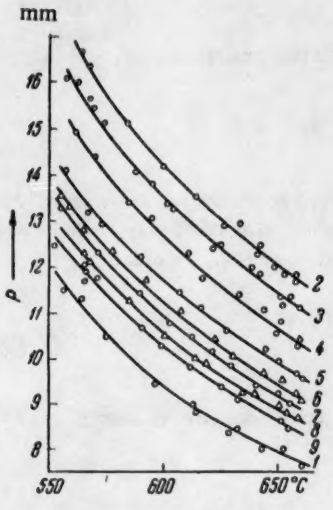

Fig. 1. First ignition limits of 1) a mixture of 1.9 $H_2 + O_2$; and mixtures of $2CO + O_2 + xH_2$ where x in percent is: 2) 0.76; 3) 1.02; 4) 1.47; 5) 2.34; 6) 3.30; 7) 3.95; 8) 5.34; 9) 8.04.

plays an essential part in the mechanism of many oxidation processes. This reaction, however, has been quite inadequately investigated, and there is no reliable information in the literature on the magnitude of its velocity constant. The value of the activation energy of this reaction has been determined from the temperature dependence of the rate of the reaction between atomic oxygen and molecular hydrogen in one work only [1], and in this paper the rate of formation of water was taken as a measure of the rate of the reaction in issue. Moreover, it is impossible to verify that the value of E, given as 6±1 kcal/mole, can really be referred to the elementary reaction (III). In addition to this, the authors determined E by the use of data referring to only two of the three temperatures at which measurements had been made. The values of the preexponential factor calculated by different authors [2-4] differ very widely, varying from 10^{-14} to 10^{-11} $cm^3 \cdot mol^{-1} \cdot sec^{-1}$.

The method used by us for determining the magnitude of the rate constant of reaction (III) is based on the measurement of the first ignition limit of mixtures of carbon monoxide and oxygen in the presence of small added amounts of hydrogen, determining the variation in the limit with the quantity of hydrogen.

The ignition limits of mixtures of carbon monoxide and oxygen containing hydrogen, and the kinetic behavior within the ignition peninsula, may be explained by means of the following reaction scheme, which was used as the basis for the mechanism proposed by Buckler and Norrish [5], Kondrat'ev [6] and Enikolopyan and Nalbandyan [7]:

$H_2 + O_2 = 2OH$	(0)	$O + H_2 = OH + H$	(III)
$OH + CO = CO_2 + H$	(I)	H + wall = destruction	(IV)
$H + O_2 = OH + O$	(II)	O + wall = destruction	(V)

$H + O_2 + M = H_2O + M$	(VI)	$O_3 + M = O_2 + O + M$	(X)
$OH + H_2 = H_2O + H$	(VII)	$O_3 + CO = CO_2 + O_2$	(XI)
$O + O_2 + M = O_3 + M$	(VIII)	$O + O_3 = 2O_2$	(XII)
$O + CO + M = CO_2 + M$	(IX)		

From the critical condition for ignition [8], we may obtain the equation for the ignition limit:

$$(O_2) = \frac{k_{IV}}{2k_{II}}\left[1 + \frac{k_{VI}(O_2)(M)}{k_{IV}}\right] \times \left[1 + \frac{k_V + k_{VIII}(O_2)(M) + k_{IX}(CO)(M) + k_{XII}(O_2)}{k_{III}(H_2)}\right], \tag{1}$$

where k_i, etc., are rate constants for reactions numbered (1) etc.

It is easy to show that, at the first ignition limit, the quantity $k_{VI}(O_2)(M)/k_{IV}$ is equal to the ratio of the first ignition limit of the mixture of carbon monoxide and oxygen to the second ignition limit of the mixture of hydrogen and oxygen. This implies that at temperatures appreciably higher than the temperature at the peak of the ignition peninsula, $k_{VI}(O_2)(M)/k_{IV} \ll 1$.

At pressures close to the first ignition limit, it is known that, of the possible chain breaking mechanism, a decisive part is played by surface chain breaking. Hence, the quantities $k_{VIII}(O_2)(M)$, $k_{IX}(CO)(M)$, $k_{XII}(O_2)$ at this point become negligible compared with k_V. This is confirmed by comparing the values of these quantities at the point corresponding to the first ignition limit. Equation (1) can then be rewritten in the form:

$$(O_2) = \frac{k_{IV}}{2k_{II}}\left[1 + \frac{k_V}{k_{III}(H_2)}\right]. \tag{2}$$

When reactions (IV) and (V) take place in the diffusion region (for cylindrical vessel) [3],

$$k_{IV} = \frac{23,2}{d^2} D_H, \quad k_V = \frac{23,2}{d^2} D_O$$

where D_H and D_O are the diffusion coefficients for atoms of hydrogen and oxygen respectively. If we insert these values of k_{IV} and k_V into Eq. (2), and take into account the dependence of the diffusion coefficients on the temperature and the pressure, substituting partial pressures for the concentrations (O_2) and (H_2), we obtain:

$$Pp_{O_2} = \frac{k_{IV}^0 T^{2,5}}{2k_{II} \cdot 0,97 \cdot 10^{19}}\left(1 + \frac{k_V^0 T^{2,5}}{k_{III} \cdot 0,97 \cdot 10^{19}} \frac{1}{Pp_{H_2}}\right). \tag{3}$$

In this equation P, Pp_{O_2} and P_{pH_2} are the total pressure of the mixture and the partial pressures of oxygen and hydrogen, respectively, at the first ignition limit,

$$k_{IV}^0 = \frac{23,2}{d^2}(D_H)^{CO} \frac{760}{(273)^{1,5}}, \tag{4}$$

$$k_V^0 = \frac{23,2}{d^2}(D_O)^{CO} \frac{760}{(273)^{1,5}}, \tag{5}$$

where $(D_H)^{CO}$ and $(D_O)^{CO}$ are the diffusion coefficients of atoms of hydrogen and oxygen under normal conditions.

According to (3), in the diffusion region of heterogeneous chain destruction, the value of P_{pO_2} for the first limit at constant temperature should be related linearly to $1/P_{pH_2}$. That is, if we measure the first ignition limit

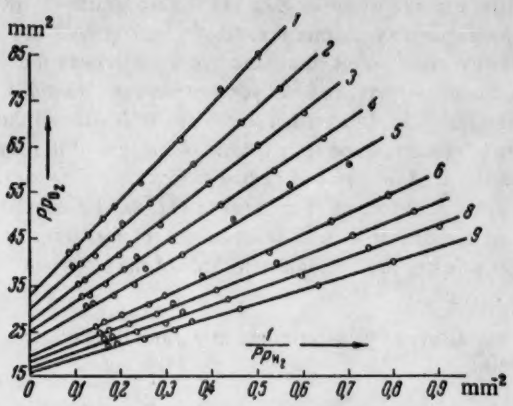

Fig. 2. Relationship between $P_{p_{O_2}}$ and $1/P_{p_{H_2}}$ for mixtures of $2CO + O_2 + xH_2$ at temperatures: 1) 570°; 2) 580°; 3) 590°; 4) 600°; 5) 610°; 6) 630°; 7) 640°; 8) 650°; 9) 660°.

of mixtures of carbon monoxide and oxygen in the presence of various quantities of hydrogen, we shall find from the curve relating $P_{p_{O_2}}$ to $1/P_{p_{H_2}}$ that

$$b = \frac{k_{IV}^0 T^{2.5}}{2k_{II} \cdot 0{,}97 \cdot 10^{19}} \qquad (6)$$

is the magnitude of the intercept of the straight line on the axis of ordinates, and

$$\operatorname{tg}\alpha = \frac{k_{VI}^0 T^{2.5}}{2k_{II} \cdot 0{,}97 \cdot 10^{19}} \frac{k_V^0 T^{2.5}}{k_{III} \cdot 0{,}97 \cdot 10^{19}}, \qquad (7)$$

where α is the angle of slope towards the axis of abscissas.

It follows from (6) and (7) that:

$$\frac{\operatorname{tg}\alpha}{b} = \frac{k_V^0 T^{2.5}}{k_{III} \cdot 0{,}97 \cdot 10^{19}} = \frac{k_V^0 T^{2.5}}{k_{III}^0 \cdot 0{,}97 \cdot 10^{19} \exp(-E_{III}/RT)}$$

or,

$$\lg \frac{\operatorname{tg}\alpha}{bT^{2.5}} = \lg \frac{k_V^0}{k_{III}^0 \cdot 0{,}97 \cdot 10^{19}} + \frac{E_{III}}{3RT}, \qquad (8)$$

where E_{III} is the activation energy of reaction (III).

Thus, if we obtain values of tan α and b for various temperatures, we may calculate the value of E_{III} from (8), and, obtaining k_V^0 from (5), we may determine the value of k_{III}^0. Hence, by measuring the first ignition limit of mixtures of carbon monoxide and oxygen containing various added amounts of hydrogen, in the diffusion region of heterogeneous chain destruction, we may determine both the magnitude of the activation energy and the value of the preexponential term of the reaction rate constant for reaction (III).

The experiments were carried out in a standard vacuum static apparatus. To determine the ignition limit, the reaction mixture from the reservoir was collected into a by-pass vessel, and then immersed in an evacuated quartz vessel of diameter 34mm, heated to the desired temperature. Treatment of the surface of the vessel with magnesium oxide greatly accelerated the destruction of active centers on the surface [9-11], and this ensured the continuation of heterogeneous chain destruction in the diffusion region. This ensured the high value of the limits, good reproducibility for their values, and reduction of the limit by the dilution of the mixture with inert gases.

Figure 1 shows the relationship between the first ignition limit and the temperature for mixtures of $2CO + O_2$, containing various amounts of added hydrogen. From the observed values of the limit, P, the values of $P_{p_{O_2}}$ and $1/P_{p_{H_2}}$ have been calculated, the relationship between which at various temperatures is shown in Fig. 2. It can be seen from this figure that the relationship is linear, as was anticipated from Eq. (3). Taking into account that, for the mixture of hydrogen and oxygen, $k_{IV}/2k_{II} = (O_2)^{(H_2)}$, where $(O_2)^{(H_2)}$ is the concentration of oxygen at the first ignition limit of the hydrogen–oxygen mixture, Eq. (6) may be presented in the form:

$$b = P^{H_2}_{p_{O_2}} \frac{(D_H)^{CO}}{(D_H)^{H_2}}, \qquad (9)$$

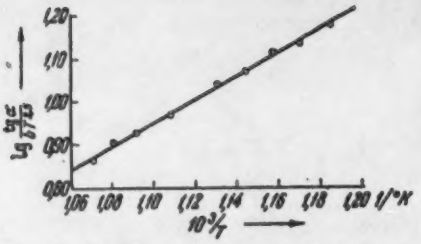

Fig. 3. Relationship between $\log(\tan\alpha/bT^{2.5})$ and $1/T$.

where p^{H_2} and $p_{O_2}^{H_2}$ are the total pressure of the mixture and the partial pressure of the oxygen at the first ignition limit of the hydrogen–oxygen mixture; $(D_H)^{CO}$ and $(D_H)^{H_2}$ are the diffusion coefficients of atomic hydrogen through the carbon monoxide–oxygen and hydrogen–oxygen mixtures, respectively. Thus, in addition to the determination of the quantity b by the method stated, from the values of the first ignition limits of mixtures of carbon monoxide and oxygen with varying additions of oxygen (as in Fig. 2), this quantity should be determinable in an independent manner from Eq. (9) from the value of the first ignition limit of the hydrogen–oxygen mixture.

The values of b, determined at various temperatures by these two independent methods, differ by not more than 10%.

Thus, the correctness of the method is confirmed both by the linear relationship between $P_{p_{O_2}}$ and $1/P_{p_{H_2}}$, and by the agreement (within the accuracy of determination of the coefficients of diffusion of atomic hydrogen) of the values of b obtained by the two independent methods.

Figure 3 gives the relationship between $\log(\tan\alpha/bT^{2.5})$ and $1/T$, where the values of $\tan\alpha$ and b are determined graphically from Fig. 2. From the slope of the straight line in Fig. 3, E_{III} was calculated by means of Eq. (8), and found to be 12.3±0.2 kcal/mole; while from the intercept of the same line with the axis of ordinates, the value of k^0_{III} was found to be equal to $1.55\cdot10^{-10}$ cm³·mol⁻¹·sec⁻¹. For mixtures of the composition 3CO + O_2 with various additions of hydrogen, the values obtained were: E_{III} = 12.0±0.2 kcal/mole, and $k^0_{III} = 1.45\cdot10^{-10}$ cm³·mol⁻¹·sec⁻¹.

Thus,

$$k_{III} = 1{,}5\cdot10^{-10}\exp\left(-\frac{12100\pm400}{RT}\right)\text{cm}^3\cdot\text{mole}^{-1}\cdot\text{sec}^{-1}.$$

LITERATURE CITED

1. P. Harteck and U. Kopsch, Zhur. Fiz. Khim. 12, 5, 327 (1931).
2. B. L'yuis* and G. El'be*, Combustion, Flame, and Explosion in Gases [in Russian] (Moscow, 1948).
3. A. B. Nalbandyan and V. V. Voevodskii, Mechanism of Oxidation and Combustion of Hydrogen [in Russian] (Moscow, 1949).
4. V. N. Kondratiev, Seventh Symposium (International) on Combustion (London, 1958).
5. E. I. Buckler and R. G. W. Norrish, Proc. Roy. Soc. London A167, 930, 292 (1938).
6. V. N. Kondrat'ev, Spectroscopic Investigation of Chemical Gas Reactions [in Russian] (Moscow, 1944).
7. N. S. Enikolopyan and A. B. Nalbandyan, The Kinetics of Chain Oxidation Reactions [in Russian] (Moscow, 1950).
8. N. N. Semenov, Chain Reactions [in Russian] (Leningrad, 1934).
9. G. K. Lavrovskaya and V. V. Voevodskii, Zhur. Fiz. Khim. 25, 9, 1050 (1951).
10. D. R. Warren, Trans. Faraday Soc. 53, 199, 206 (1957).
11. I. C. Greaves and I. W. Linnet, Trans. Faraday Soc. 55, 8, 1346 (1959).

* Transliteration of the original Russian.

THE STRUCTURE OF THE ELECTRICAL DOUBLE LAYER ON PLATINUM

T. P. Birintseva and B. N. Kabanov

Electrochemistry Institute, Academy of Sciences, USSR

(Presented by Academician A. N. Frumkin, February 3, 1960)

Translated from Doklady Akademii Nauk SSSR, Vol. 132, No. 4, pp. 868-871, June, 1960

Original article submitted January 29, 1960

In order to examine the structure of the double layer, it is necessary to know the electrocapillary zero. It has been shown by adsorption methods that on reduced Pt the electrocapillary zero φ_0 in Na_2SO_4 solution is approximately 0.11-0.15 v [1, 2], in NaCl solution 0.05 v, and in NaBr solution 0.02 v [1], relative to the normal hydrogen electrode. A less accurate method involving measurement of the contact angle of gas bubbles has given for H_2SO_4 solution the value $\varphi_0 = 0.27$ v [3]. Recently a new crossed filament method has given the value $\varphi_0 = 0.2$ v [4].

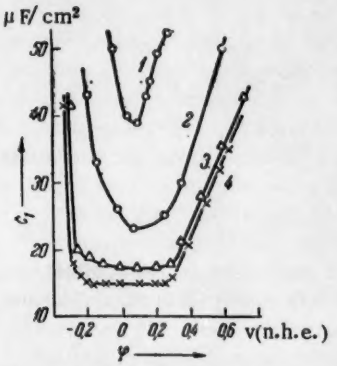

Fig. 1. Curves showing the relationship between the capacity and the potential in 0.01 N H_2SO_4 solution at different frequencies: 1) 0.2 cps; 2) 1 cps; 3) 5 cps; 4) 10 cps.

The method involving measurement of the capacity with alternating current has in a number of cases given more positive values for φ_0, equal to 0.6-1.1 v [5, 6]. These values have been found to depend markedly on the pH of the solution: φ_0 changes from +0.5 to −0.35 v when the pH changes from 1 to 12 [7]. Calculation from the work of electron removal gives the value $\varphi_0 = 0.6$-0.7 v [6]. It should be noted that adsorption methods indicate that on oxidized platinum, $\varphi_0 = 0.7$ to 0.9 v [1, 2]. In view of the contradictory data for the value of the electrocapillary zero on platinum, we have considered it necessary to make a more detailed study of the capacity of the double layer on platinum.

In the present work we have measured the capacity of a smooth platinum electrode in sulfuric acid solutions of different concentrations at different alternating current frequencies. The method of measuring the capacity has been described in an earlier paper [8]. The electrode is regarded as equivalent to a capacity C_1 and R_2 connected in series.

The relationship between the capacity of a platinum electrode measured in this way and the potential at different frequencies in 0.1 N H_2SO_4 and 1 N Na_2SO_4 + 0.01 N H_2SO_4 solutions is given in Figs. 1 and 2, which show that, irrespective of the solution concentration, the capacity curves at low frequencies pass through a fairly sharp minimum at a potential close to 0.5 v. With increase in the alternating current frequency, however, the shape of the capacity curve changes, and at a frequency of 200 cps, the left-hand ascending section of the capacity curve disappears completely.* The fact that the value of the

* In the first of these solutions, the measurements cannot be carried out at such high frequencies as in the second case, because of the large specific resistance of the first solution.

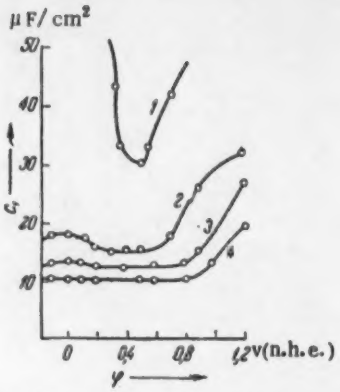

Fig. 2. Curves showing the relationship between the capacity and the potential in 1 N Na_2SO_4 + + 0.01 N H_2SO_4 solution at different frequencies: 1) 1 cps; 2) 20 cps; 3) 100 cps; 4) 200 cps.

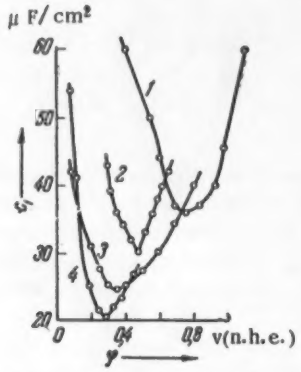

Fig. 3. Curves showing the relationship between the capacity and the potential (ν = =1 cps) in dilute solutions: 1) 1 N H_2SO_4; 2) 0.01 N H_2SO_4; 3) 0.01 N Na_2SO_4 + + 0.0001 N H_2SO_4; 4) 0.01 N Na_2SO_4 + 0.00002 N H_2SO_4.

capacity and the shape of the curve are so markedly dependent on the frequency, together with the magnitude of the phase shift, indicate that at low frequencies the measurements record the pseudocapacity [9], which disappears completely only at high frequencies. On smooth platinum, as a result of the presence of adsorbed atoms even in the "double-layer" region, a small pseudocapacity is observed at low frequencies [10, 8], and the capacity curve passes through a minimum, which apparently corresponds to the potential of the least degree of adsorption of atoms on Pt. Thus, the minimum on the capacity curve for the platinum electrode at low frequencies results from the intersection of two adsorption capacity curves corresponding to two processes: the process of discharge of ions and ionization of adsorbed atoms of hydrogen on the one hand [9, 8] and the process of deposition and removal of adsorbed oxygen on the other [11-13]. The capacity minimum at a potential of 1.07 v observed by Robertson [5] on Pt in 1 N HCl appears to have a similar explanation. As a result of the displacement of the platinum oxidation potential [14] and the region of hydrogen adsorption to more negative potential values, the minimum on the capacity curves, which we have observed at low frequencies (Fig. 3) is also displaced. Comparison of Fig. 3 with the data given in [7] show that the potential corresponding to the capacity minimum coincides with the values of the electrocapillary zero obtained at the same pH values by V. L. Kheifets and B. S. Krasikov. These authors measured the capacity at low frequency (50 cps) but did not study the change in the shape of the capacity curve with change in the alternating current frequency, and they concluded that the minimum corresponded to the point of maximum diffuseness of the double layer, i.e., to the electrocapillary zero, which is obviously incorrect.

In order to measure with sufficient accuracy the capacity of the double layer on reduced platinum in the region of the electrocapillary zero in dilute solutions, it is necessary to exclude the adsorption capacity relative to hydrogen. By increasing the alternating current frequency, it is possible to reach a limit when the measurements will record only the capacity of the double layer [at pH 2 this apparently is the case at a frequency of 200 cps (Fig. 2)]. At the same time, in dilute solutions, the high resistance of the solution at these frequencies means that the sensitivity of the bridge to the capacity is small, so that in the case of 0.01 N solutions we have restricted ourselves to carrying out measurements at 10 cps and subsequently decreasing the hydrogen ion concentration in the solution in order to shift the region of hydrogen adsorption from the electrocapillary zero towards more negative potentials [9]. Figure 4 gives curves showing the change in the capacity with change in potential at a frequency of 10 cps in 0.01 N Na_2SO_4 solutions with different hydrogen ion concentrations. In the solution with pH 5 at this frequency and at potentials more positive than 0.05 v, the pseudocapacity is almost absent (Fig. 4, 3) and the measurements record the capacity of the double layer (the angle of the phase shift here is equal to 90°). Figure 4 shows, however, that there is no capacity minimum at the electrocapillary zero.

In order to try to explain this, we must examine the peculiar features of the double layer on platinum and other similar metals. On many solid metals there is considerable dispersion of the capacity with change in frequency, and, what is particularly important, the magnitude of the capacity at sufficiently high frequencies is small, even when the solution concentration is high [15-17, 5, 6, 8]. For example, according to our data, the capacity in acidified 1 N Na_2SO_4 solution is 16 μ per cm^2 visible surface at 20 cps, and 11 μ per cm^2 visible surface

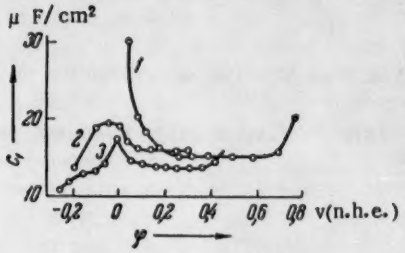

Fig. 4. Curves showing the change in potential (ν = 10 cps) in 0.01 N Na_2SO_4 solutions of different pH: 1) pH 2; 2) pH 3; 3) pH 5.

at 200 cps, while in the region of the electrocapillary zero, the increase which in the case of the mercury and lead electrodes characterizes anion deformation is absent (Fig. 2). If it is assumed that at a frequency of 200 cps the measurable surface is practically equal to the visible surface, then the capacity in the near cathodic region proves to be lower than that in the case of mercury by a factor of one and a half, while the capacity in the anodic region (i.e., more positive than the electrocapillary zero) is lower than that in the case of mercury by a factor of 3-4. The dispersion which is not associated with the adsorption pseudocapacity can be explained by the geometrical nonuniformity of the solid surface (microcracks and pores). The reason for the low total value of the capacity over a wide range of potentials at all frequencies at which the adsorption pseudocapacity has no effect, is not clear, however. It may be due to a decrease in the electron density in the metal at the surface, associated with the chemisorption of atoms of oxygen and hydrogen *, or to the separation of the faces of the electrical double layer with the formation of the atomic adsorbed layer even though this takes place only on part of the surface [18]. Slight chemisorption takes place even in the "double-layer" potential region. In contrast to the case of the decrease in the electron density observed in the case of germanium [19], the effect of reduced electron density in the case of metals should not be closely related to the electrocapillary zero, but should be observed throughout the whole potential range in which adsorption of atoms, and hence decrease in the density of the charges of the double layer, takes place.

The decrease in the surface charge as a result of the diffuse nature of the electron face of the double layer should lead, at the same potential, to an increase in the diffuseness of the ionic face, i.e., to an additional decrease in the capacity and to a broadening of the potential range in which the electrocapillary zero has an effect on the capacity (the width of the minimum). Further "broadening" of the minimum can take place as a result of physical and chemical nonuniformity of the polycrystalline surface, since different crystal faces probably have electrocapillary zero values differing by several tens or hundred millivolts, while regions differing chemically (as a result of adsorption of atoms) may have electrocapillary zero values differing by several hundred millivolts. As a result of the diffuse nature of the electron face, there should also be a sharp decrease in the effect resulting from anion deformation. Nevertheless, even when all these factors are taken into account, we should still expect small changes in capacity with change in potential, outside the limits of experimental error: such changes are not in fact observed experimentally.

The capacity, measured at high frequencies, increases only at very high positive potentials (Fig. 2). McMullen and Hackerman [6] assume that this increase is associated with the deformation of anions on the pure platinum surface, and from this they obtain $\varphi_0 = 0.8 \pm 0.2$ v. Judging from the decreased phase shift, however, this increase in the capacity is associated with the pseudocapacity, which is determined by the rate of deposition and removal of oxygen at the platinum surface [12, 13]. The increase in the capacity with potential can only be partly related to distortion of the anions on the platinum, and this evidently applies to platinum covered with adsorbed oxygen [1, 2], since it is extremely probable that the value given is the electrocapillary zero for oxidized platinum, and not pure platinum.

From all that has been said above, it follows that the method involving measurement of the double layer using alternating current in dilute and concentrated solutions cannot be used to determine the position of the electrocapillary zero for the case of a platinum electrode. Values of the electrocapillary zero for platinum obtained by this method [5-7] are inaccurate. The accuracy of the results of the calculation of φ_0 from the work of electron removal is doubtful [6], since it is not clear how far the surfaces of such different metals as Pt and Hg can be brought to the same state. Examination of the available literature data on the experimental determination of the electrocapillary zero for platinum leads to the conclusion that the most accurate results are those obtained by adsorption methods (in particular the value 0.15 v in 1 N Na_2SO_4 solution).

We wish to thank Academician A. N. Frumkin for taking part in the discussion of the results.

* An analogous suggestion has been made in [17].

LITERATURE CITED

1. A. I. Shlygin, A. N. Frumkin, and V. I. Medvedovskii, Acta Phys. Chim. USSR 4, 911 (1936).
2. N. A. Balashova and A. N. Frumkin, Doklady Akad. Nauk SSSR 20, 449 (1938); N. A. Balashova, Doklady Akad. Nauk SSSR 103, 639 (1955).
3. A. V. Gorodetskaya and B. N. Kabanov, Zhur. Fiz. Khim. 4, 529 (1933).
4. T. N. Voropaeva, B. V. Deryagin, and B. N. Kabanov, Doklady Akad. Nauk SSSR 128, 981 (1959).*
5. W. D. Robertson, J. Electrochem. Soc. 100, 194 (1953).
6. J. J. McMullen and N. Hackerman, J. Electrochem. Soc. 106, 341 (1959); P. V. Popat and N. Hackerman, J. Phys. Chim. 62, 1198 (1958).
7. V. L. Kheifets and B. S. Krasikov, Doklady Akad. Nauk SSSR 109, 586 (1956).*
8. T. P. Birintseva and B. N. Kabanov, Zhur. Fiz. Khim. 33, 844 (1959).
9. P. I. Dolin and B. V. Érshler, Zhur. Fiz. Khim. 14, 886 (1940).
10. B. V. Érshler, Acta Phys. Chim. USSR 7, 397 (1937).
11. A. I. Shlygin and A. N. Frumkin, Acta Phys. Chim. USSR 3, 791 (1936).
12. A. D. Obrucheva, Zhur. Fiz. Khim. 24, 1448 (1952).
13. M. Becker and M. Breiter, Z. Elektrochem. 60, 1080 (1956).
14. K. J. Vetter and D. Berndt, Z. Elektrochem. 62, 378 (1958).
15. K. I. Rozental', P. I. Dolin, and B. V. Érshler, Zhur. Fiz. Khim. 19, 601 (1945).
16. V. V. Losev, Doklady Akad. Nauk SSSR 88, 499 (1953).
17. A. A. Rakov, T. I. Borisova, and B. V. Érshler, Zhur. Fiz. Khim. 22, 1390 (1948).
18. L. V. Vanyukova and B. N. Kabanov, Zhur. Fiz. Khim. 28, 1025 (1954).
19. K. Bohnenkamp and H. Engel, Z. Elektrochem. 61, 1184 (1957); E. A. Efimov and I. G. Erusalimchik, Zhur. Fiz. Khim. 33, 441 (1959).

* Original Russian pagination. See C.B. translation.

THE POTENTIAL OF A PLATINUM ELECTRODE IN AN IRRADIATED SULFURIC ACID SOLUTION

G. Z. Gochaliev, Ts. I. Zalkind, and V. I. Veselovskii

L. Ya. Karpov Physicochemical Institute

(Presented by Academician A. N. Frumkin, February 26, 1960)

Translated from Doklady Akademii Nauk SSSR, Vol. 132, No. 4, pp. 872-875, June, 1960

Original article submitted February 25, 1960

We have already shown [1-4] that the potential of a platinum electrode in an irradiated solution of 0.8 N sulfuric acid (dose power of irradiation $2 \cdot 10^{15}$ ev/ $cm^3 \cdot sec$) has a value close to that of the potential of a hydrogen electrode in the same solution. This has subsequently been confirmed in papers by other workers [5, 6].

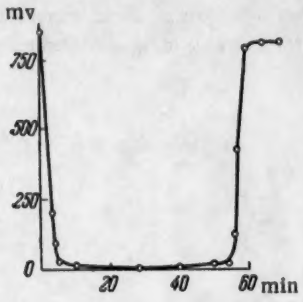

Fig. 1. Relationship between the potential of the platinum electrode and the duration of the irradiation (0. 8 N sulfuric acid, surface area of electrode 6 cm^2, solution volume 10 cm^3, volume of gaseous phase 50 cm^3).

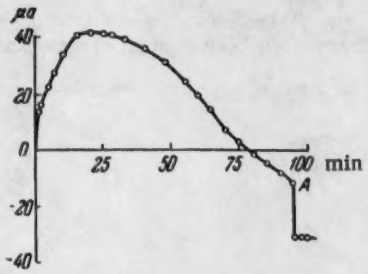

Fig. 2. Relationship between the value of the polarization current and the duration of the irradiation at a platinum electrode potential of 0.4 v (0.8 N sulfuric acid, surface area of electrode 6 cm^2, solution volume 10 cm^3, volume of gaseous phase 50 cm^3).

The present communication gives some results obtained in a study of the effect of radiation of much greater dose power on the platinum/ sulfuric acid solution system. The experiments were carried out on the Co^{60} source of the L. Ya. Karpov Physicochemical Institute [7], and the dose power of the radiation amounted to $6.1 \cdot 10^{16}$ ev $\cdot$ $cm^3 \cdot$ $\cdot$sec. The method of preparing and carrying out the experiment has been described in earlier papers [2, 3].

Figure 1 gives a curve showing the relationship between the potential of a platinum electrode in a deoxygenated solution of 0.8 N sulfuric acid and the duration of the irradiation. The figure shows that at this dose power, as in the previous experiments, the platinum electrode is selective towards the reducing products of the radiolysis of water, and a potential of 10-20 mv is established. This value of the potential is retained up to doses of $2 \cdot 10^{20}$ ev/ cm^3, after which it increases to 0.85 v.

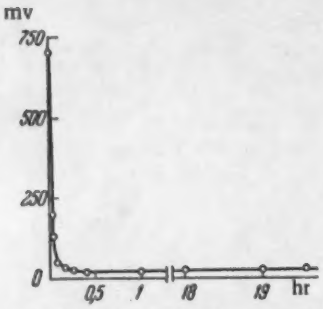

Fig. 3. Relationship between the potential of the platinum electrode and the duration of the irradiation (0.8 N sulfuric acid, surface area of electrode 120 cm^2, solution volume 9 cm^3, no gaseous phase).

A necessary condition for the establishment of a stationary potential in the irradiated solution is that the rates of the processes involving oxidation of the reducing radiolysis products and reduction of the oxidizing products should be equal. The rates of these processes for the stationary potential may be written in the form

$$I_R = k_R [\text{Red}] \exp\left(\frac{\alpha_R F \varphi_{st}}{RT}\right), \quad (1)$$

$$I_{Ox} = k_{Ox} [\text{Ox}] \exp\left(-\frac{\alpha_{Ox} F \varphi_{st}}{RT}\right). \quad (2)$$

It would be more accurate to write

$$I_R = \sum_i k_{R_i} [\text{Red}]_i \exp\left(\frac{\alpha_{R_i} F \varphi_{st}}{RT}\right)$$

with a corresponding expression for I_{Ox}, but this complicates the calculation without effecting any significant improvement in the final results.

Equations (1) and (2) can be written as follows:

$$I_R = k'_R [\text{Red}] \exp\left(\frac{\alpha_R F \Delta\varphi_R}{RT}\right), \quad (1')$$

$$I_{Ox} = k'_{Ox} [\text{Ox}] \exp\left(\frac{\alpha_{Ox} F \Delta\varphi_{Ox}}{RT}\right), \quad (2')$$

where [Red] and [Ox] are the concentrations of reducing and oxidizing radiolysis products, respectively; $\Delta\varphi_R = \varphi_{st} - \varphi^0_R$, $\Delta\varphi_{Ox} = \varphi^0_{Ox} - \varphi_{st}$ ($\varphi^0_R < \varphi_{st} < \varphi^0_{Ox}$); φ^0_R and φ^0_{Ox} are the corresponding equilibrium potentials, and the other symbols have their usual significance.

Using the steady-state condition $I_R = I_{Ox}$, we obtain

$$\frac{k'_R [\text{Red}]}{k'_{Ox} [\text{Ox}]} = \frac{\exp\left(\frac{\alpha_{Ox} F \Delta\varphi_{Ox}}{RT}\right)}{\exp\left(\frac{\alpha_R F \Delta\varphi_R}{RT}\right)}, \quad (3)$$

which gives, on taking logarithms,

$$\ln \frac{k'_R [\text{Red}]}{k'_{Ox} [\text{Ox}]} = \frac{F}{RT}(\alpha_{Ox}\Delta\varphi_{Ox} - \alpha_R \Delta\varphi_R). \quad (4)$$

Under conditions when no current flows through the system and all the radiolysis products remain in the solution, [Red] = [Ox] and

$$\ln \frac{k'_R}{k'_{Ox}} = \frac{F}{RT}(\alpha_{Ox}\Delta\varphi_{Ox} - \alpha_R \Delta\varphi_R). \quad (5)$$

If $k'_R \gg k'_{Ox}$, which is a measure of the selectivity of one process relative to the other, the term in brackets on the right-hand side of the equation should be greater than 1, and $\Delta\varphi_{Ox} > \Delta\varphi_R$. Consequently, in this case the stationary potential of the electrode should be closer to the equilibrium potential of the reducing radiolysis products, which is in fact the case for a platinum electrode, as a result of its selectivity towards the process of hydrogen ionization. From Eq. (4), taking $\alpha_R = \alpha_{Ox} = \alpha$, we can obtain the following expression for the value

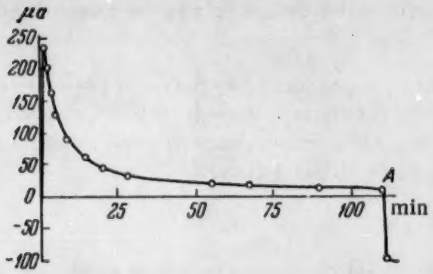

Fig. 4. Relationship between the value of the polarization current and the duration of the irradiation at a platinum electrode potential of 0.4 v (0.8 N sulfuric acid, surface area of electrode 120 cm^2, solution volume 9 cm^3, no gaseous phase).

of the stationary potential φ_{st}:

$$\varphi_{st} = \frac{\varphi^0_{Ox} + \varphi^0_R}{2} + \frac{RT}{2\alpha F} \ln \frac{k'_{Ox}[Ox]}{k'_R[Red]}. \qquad (6)$$

If [Red] ≠ [Ox], i.e., if the stoichiometry between the oxidizing and reducing products of the radiolysis of water is broken down, then the stationary potential of the eletrode will have a different value. It is then necessary to remember that the shift of the stationary potential associated with the fact that the concentrations are not equal may be greater than expected from Eq. (6), since the rates of the processes determining the value of the stationary potential may at certain potential values be determined by the diffusion of the substances to the electrode.

The results given in Fig. 1 were obtained under conditions where the volume of the gas phase was approximately 5 times the volume of the solution. The hydrogen formed in the radiolysis was distributed between the gaseous phase and the solution, and in the solution the stoichiometry between the oxidizing and reducing radiolysis products was broken down, i.e., [Red]< [Ox]. According to Eq. (6), this should lead to a shift of potential in a positive direction, which is in fact observed at doses greater than $2 \cdot 10^{20}$ ev / cm^3. Measurement of the relationship between the values of the depolarization current and the duration of the irradiation confirm this.

Figure 2 gives a curve showing the relationship between the depolarization currents at a potential of 0.4 v and the duration of the irradiation, and characterizes the accumulation of the radiolysis products. The current increases sharply at first, after which it increases more slowly, reaches a limiting value, and then decreases with time. The point A corresponds to the removal of the source. The complex shape of the curve is associated with the fact that at a potential of 0.4 v, both oxidation of hydrogen and reduction of hydrogen peroxide may take place. As a result of the selectivity of platinum towards the ionization of hydrogen, the process of hydrogen oxidation predominates in the initial period. As the hydrogen peroxide accumulates in the solution (in one hour the hydrogen peroxide concentration in the solution is $1 \cdot 10^{-3}$ N) and the hydrogen passes into the gaseous phase, the rate of reduction of the hydrogen peroxide increases, the total current, equal to $I_{H_2} - I_{H_2O_2}$, starts to decrease, and at doses greater than $2 \cdot 10^{20}$ ev/ cm^3 it becomes negative. We have studied the relationship between the potential of a platinum electrode and the duration of the irradiation under conditions which prevented the condition [Red] = [Ox] from being broken down. The compartment in the apparatus containing the test electrode was filled completely with solution, i.e., no gaseous phase was present above the solution. This part of the apparatus was connected by means of fine capillaries to the sections of the apparatus containing the reference electrode and the auxiliary polarization electrode, which were separated from the main electrode by means of taps. The test electrode consisted of platinum foil wound to form a loose cyclinder. Its surface area amounted to ~120 cm^2, and the solution volume was equal to 9 cm^3.

Figure 3 gives a curve showing the relationship between the potential of the platinum electrode in this system and the duration of the irradiation. It can be seen that the potential rapidly acquires the value + 20 mv, which remains unchanged for the total experiment time of ~20 hr (the total dose amounted to $3 \cdot 10^{21}$ ev/ cm^3).

In the system described above, the ratio of electrode surface to solution volume is such that when a positive current is passing, i.e., during the ionization of hydrogen, the concentrations of oxidizing and reducing radiolysis products rapidly become unequal, since there is practically no "reservoir" from which the hydrogen used up at the electrode can be replaced. It can be seen from the curve in Fig. 4 that these concentrations become unequal during the recording of the current–time curve at a potential of 0.4 v. The accumulation of oxidizing radiolysis products in large concentration which then takes place leads to a rapid decrease in the current during the irradiation, and to the production of a negative current when the irradiation is stopped, in spite of the selectivity of the platinum towards the process of hydrogen ionization.

If the irradiation solution contains a second electrode, at which a process involving the reduction of the oxidizing radiolysis products may take place selectively, for example, a gold electrode [3, 4], then the condition

[Ox]=[Red] would be preserved even when a current of definite magnitude passed, throughout the entire duration of the irradiation. The potentials of the electrodes in this case would be determined only by the selectivity of the latter towards the products of the radiolysis of water.

Consequently, the ionization, at a platinum electrode, of the hydrogen formed by the radiolysis of water may only take place at a stationary potential if the reduction of oxidizing radiolysis products takes place at equal velocity at the same electrode (total current equal to zero), or at another electrode, selective towards the oxidizing products, in which case a corresponding current will flow through the external circuit.

LITERATURE CITED

1. V. I. Veselovskii, Report of the Soviet Delegation to the International Conference on the Peaceful Uses of Atomic Energy, Studies in the Field of Geology, Chemistry and Metallurgy [in Russian] (Izd. AN SSSR, 1955) p. 320.
2. Ts. I. Zalkind and V. I. Veselovskii, Collection of Works on Radiation Chemistry [in Russian] (Izd. AN SSSR, 1955) p. 66.
3. Ts. I. Zalkind and V. I. Veselovskii, Collection: The Action of Ionizing Radiation on Inorganic and Organic Systems [in Russian] (Izd. AN SSSR, 1958) p. 66.
4. Ts. I. Zalkind, V. I. Veselovskii, and G. Z. Gochaliev, Proceedings of the First All-Union Conference on Radiation Chemistry [in Russian] (Izd. AN SSSR, 1958) p. 123.
5. Ya. M. Kolotyrkin, N. Ya. Buné, and G. S. Tyurikov, Proceedings of the First All-Union Conference on Radiation Chemistry [in Russian] (Izd. AN SSSR, 1958) p. 143; M. A. Proskurnin and Ya. M. Kolotyrkin, Proceedings of the Second International Conference on the Peaceful Uses of Atomic Energy, Geneva, 1958 [in Russian] (Izd. Glavn. Upr. po Ispol'zov. Atomn. Energii, Moscow, 1959) 4, p. 211.
6. W. E. Clark, J. Electrochem. Soc. 105, 483 (1958).
7. A. Kh. Breger, V. A. Belynskii, V. L. Karpov, S. D. Prokudin, and V. B. Osipov, All-Union Conference on the Applications of Isotopes and Nuclear Radiation, The Preparation of Isotopes, etc. [in Russian] (Izd. AN SSSR, 1958) p. 183.

STATISTICAL THERMODYNAMIC DETERMINATION OF THE ADSORPTION EQUILIBRIUM OF ARGON ON GRAPHITE

A. V. Kiselev and D. P. Poshkus

Physical Chemistry Institute, Academy of Sciences, USSR
and the Chemistry and Chemical Technology Institute, Academy of Sciences Lithuanian SSSR

(Presented by Academician M. M. Dubinin, January 23, 1960)

Translated from Doklady Akademii Nauk SSSR, Vol. 132, No. 4, pp. 876-879, June, 1960

Original article submitted January 21, 1960

Calculation of the adsorption equilibrium strictly on the basis of the physical properties of the adsorbent and the adsorbate constitutes one of the most important problems in the theory of adsorption [1, 2]. The first and most important step in the solution of this problem is the theoretical calculation of the potential energies of adsorbed molecules. Earlier success achieved in calculating the adsorption energies of simple and complex nonpolar molecules on graphite and on ionic crystals [2-6] now lead to a complete solution of the problem for the enumerated cases, i.e., the change in the partial free energy of the adsorbate, $\Delta\mu$, can now be computed.

Hill and Drenan [7, 8] both used statistical methods to calculate the "kinetic" factor A in the constant of the BET equation, $C = A \exp[(E_1 - L)/RT]$, where E_1 is the heat of adsorption for the first layer and L, the heat of vaporization (or condensation). However, their calculations were for an "imaginary" adsorbent and were based on potential energy functions (for the adsorbed molecules) derived from the integrated instead of the summed interactions between atoms in the adsorbed molecules and atoms in the adsorbent lattice. We calculated the constant C for benzene on graphite and on MgO by using the equation $C = \exp(\Delta S^0/R) \times \exp(-\Delta U^0/RT)$, where S^0 and ΔU^0 were the changes in the standard partial entropy and total adsorption energy, respectively [9]. However, though we calculated very accurately the adsorption energy we used in [9] the value of ΔS^0 which was based on a simplified model for the state of a benzene molecule on the adsorbent surface [10].

In the present work we calculated the approximate value of $\Delta\mu$ for the adsorption of argon on the basal face of graphite under conditions where the fraction of surface covered θ is small. The potential energy of an argon molecule adsorbed on the basal face of graphite has already been calculated by several workers [2, 3, 11, 12].

When the value of θ is fairly small the partition function for the adsorbed molecules F_a, for both a localized and nonlocalized adsorption, can be written in the form [13]:

$$F_a = \frac{1}{N_a!} f_a^{N_a}, \tag{1}$$

where N_a is the number of adsorbed molecules, f_a – the partition functions for a single adsorbed molecule over the entire adsorbent surface. In such a case when the adsorbate is transferred from the gaseous standard state (p^0 = 760 mm Hg) onto a surface covered to the extent θ, then:

$$\Delta\mu = -RT \ln \left(\frac{h^2}{2\pi mkT}\right)^{3/2} \frac{f_a' \omega_m}{kT j_i} \frac{p^0}{\theta}, \tag{2}$$

where k and h are the Boltzmann and Planck constants, respectively, m—the molecular weight of the adsorbate, ω_m the area occupied by the molecule in a dense monomolecular layer, j_i— the partition functions for the internal degrees of freedom of the adsorbate in the vapor phase; moreover $\theta = N_a\omega_m/s$ and $f'_a = f_a/s$, where s is the surface area.

In calculating f_a we followed the example of [7, 8] and used the approximation [14]:

$$f = f_{class}\,\nu^{**}, \tag{3}$$

where f_{class} is a purely classical partition function:

$$f_{class} = \frac{1}{h^n}\int \dots \int e^{-H/kT}\,dp_1 \dots dp_n\,dq_1 \dots dq_n \tag{4}$$

(n being the number of molecular degrees of freedom, and H, the classical Hamiltonian for the adsorbate molecule), and:

$$\nu^{**} = f_{quant.\ harm.\ osc.}/f_{class.\ harm.\ osc.} \tag{5}$$

where $f_{quant.\ harm.\ osc.}$ and $f_{class.\ harm.\ osc.}$ are the quantum-mechanical and classical forms, respectively, for the partition function of a harmonic oscillator; these were calculated from the potential energy contour surface for the adsorbed molecule near the minimum.

The Hamiltonian for an adsorbed argon atom is:

$$H = \frac{p_x^2 + p_y^2 + p_z^2}{2m} + \Phi(x, y, z), \tag{6}$$

where p_x, p_y, and p_z are the linear momentum components, m is the atomic weight, and (x, y, z) the potential energy of the adsorbate over the basal face of the graphite (x, y). According to [2, 6],

$$\Phi(x, y, z) = -C_1\sum_j^{\infty} r_{ij}^{-6} - C_2\sum_j^{\infty} r_{ij}^{-8} + B\sum_j^{\infty} e^{-r_{ij}/0.28}, \tag{7}$$

where C_1 and C_2 are the coefficients for van der Waals attraction, $r_{i,j}$ is the distance from the center of the ith argon atom to the center of the jth carbon atom in graphite, B is the repulsion coefficient. The values of the constants C_1 and C_2 and of the summations $\sum_j^{\infty} r_{ij}^{-6}$, $\sum_j^{\infty} r_{ij}^{-8}$, $\sum_j^{\infty} e^{-r_{ij}/0.28}$ are given in [3]. The power summation for the given distance z from the argon atom to the outer plane xy formed by carbon atoms of graphite as well as the slopes of semilogarithmic plots of the exponential sums as a function of z show little dependence on the precise position of the examined point over the crystal face (i.e., they depend very little on the coordinates x and y). In order to facilitate the calculations in working with the sums $\sum_j^{\infty} r_{ij}^{-6}$, $\sum_j^{\infty} r_{ij}^{-8}$ at fixed values of z and and with slopes of the function $\log\sum_j^{\infty} e^{-r_{ij}/0.28}$ vs. z we selected three mean positions: c over the carbon atom, b over the midpoint of the line joining two nearest atoms, and h over the center of the hexagonal plane formed by these atoms. The averaged (as well as unaveraged [3]) values of the power and exponential sums can be expressed with a fair degree of accuracy by the power functions $p_1 z^{-q_1}$ and $p_2 z^{-q_2}$ and the exponential function $ke^{-z/l}$, respectively, where $q_1 = 3.82$, $p_1 = 5.18 \cdot 10^{16.44}$, $p_2 = 3.80 \cdot 10^{15.48}$, $q_2 = 5.94$, and $l = 0.303 \cdot 10^{-8}$ *.

With the help of these approximations we can transform Eq. (7) into the form:

$$\Phi(x, y, \alpha) = u_{o1}(x, y)\,\alpha^{-q_1} + u_{o2}(x, y)\,\alpha^{-q_2} + u_{op}(x, y)\exp\left(-\frac{(\alpha - 1)\,z_0(x, y)}{l}\right), \tag{8}$$

* In [3] some of the letters b and h are erroneously transposed in the first column of Table 7.

Position		z_0	$I(x, y)$	Position		z_0	$I(x, y)$
x	y			x	y		
0	0	3,32	0,262	$a/8$	$a\sqrt{3}/8$	3,45	0,0300
0	$a\sqrt{3}/8$	3,42	0,0462	$a/4$	$a\sqrt{3}/4$	3,54	0,0081
0	$a\sqrt{3}/4$	3,49	0,0175	$3a/8$	$a\cdot 3\sqrt{3}/8$	3,59	0,0043
0	$a\cdot 3\sqrt{3}/8$	3,53	0,0095	$a/2$	$a\sqrt{3}/2$	3,61	0,0036
0	$a\sqrt{3}/2$	3,54	0,0081	$a/4$	$a\sqrt{3}/2$	3,59	0,0043

where

$$u_{01}(x, y) = -C_1 p_1 z_0^{-q_1}, \quad u_{02}(x, y) = -C_2 p_2 z_0^{-q_2},$$
$$u_{0\rho}(x, y) = Bke^{-z_0/l} = -\frac{l}{z_0}[u_{01}q_1 + u_{02}q_2], \quad \alpha = \frac{z}{z_0}. \tag{9}$$

The equilibrium distance from the center of the argon atom to the first lattice plane formed by the centers of the carbon atom is:

$$z_0 = \sqrt{r_e^2 - (x_C - x)^2 - (y_C - y)^2}, \tag{10}$$

where x, y are the argon atom coordinates, x_C, y_C, the coordinates of the carbon atom nearest to the argon, r_e – the equilibrium distance from the center of the argon atom to the center of the nearest carbon atom; we obtained r_e [3] by adding the Van der Waals radius of argon (1.91 A) to that of carbon in graphite (1.70 A).

Substituting Eqs. (8) and (6) into Eq. (4) and integrating over the momentum components [7] we get:

$$f_{\text{class}} = \left(\frac{2\pi mkT}{h^2}\right)^{3/2} \frac{2s}{3a^2\sqrt{3}} \iiint \exp\left(-\frac{\Phi(x, y, \alpha)}{kT}\right) \operatorname{erf}\left(-\frac{\Phi}{kT}\right)^{1/2} z_0\, dx\, dy\, d\alpha, \tag{11}$$

where $3a^2\sqrt{3}/2$ is the area of the hexagon formed by the carbon atoms in the basal face (the graphite lattice parameter a = 1.418 A); $\operatorname{erf}(-\Phi/kT)^{1/2}$ is a probability integral. Equation (11) is integrated graphically with respect to x and y within the limits of a single hexagon. In the table we have compiled the values of $I(x, y)$, obtained by integration with respect to α for various positions over the hexagon at T = 77.8°K (the origin coincides with the hexagon center, while the x-axis passes through the center of a carbon atom). Integration was limited to those values of α for which the potential energy of the adsorbed atom $\Phi(x, y, \alpha) \leq 0$ [7]. The value of $\exp[-\Phi(x, y, \alpha)/kT]$ declines sharply when α deviates from one. We disregarded the factor $\operatorname{erf}(-\Phi/kT)^{1/2}$, since it is practically equal to one in the range of α values covered by our integration. Integration over x and y within the limits of one hexagon yielded $J = 0.034a^2$ (T = 77.8°K).

The quantum mechanical factor ν^{**} (Eq. 5) for the case of an argon atom over graphite surface is:

$$\nu^{**} = \left(\frac{h\nu_x}{kT}\right)\left[1 - \exp\left(\frac{h\nu_x}{kT}\right)\right]^{-1} \times \frac{h\nu_y}{kT}\left[1 - \exp\left(-\frac{h\nu_y}{kT}\right)\right]^{-1} \frac{h\nu_z}{kT}\left[1 - \exp\left(-\frac{h\nu_z}{kT}\right)\right]^{-1}, \tag{12}$$

where ν_x, ν_y, and ν_z are the vibrational frequencies of the adsorbed argon atom along the respective axes near the potential minimum (over the hexagon center when $z = z_0$). To calculate the vibrational frequencies:

$$\nu_x = \frac{1}{2\pi}\sqrt{\frac{K_x}{m}}, \quad \nu_y = \frac{1}{2\pi}\sqrt{\frac{K_y}{m}}, \quad \nu_z = \frac{1}{2\pi}\sqrt{\frac{K_z}{m}}, \tag{13}$$

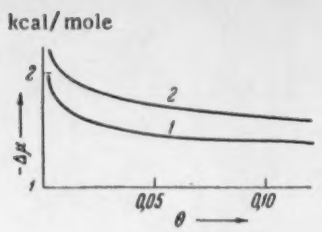

Fig. 1

we determined the constants K_x, K_y, and K_z analytically,

$$K_x = \left(\frac{\partial^2\Phi}{\partial x^2}\right)_{x=0,\ y=0,\ z=z_0}, \quad K_y = \left(\frac{\partial^2\Phi}{\partial y^2}\right)_{x=0,\ y=0,\ z=z_0},$$
$$K_z = \left(\frac{\partial^2\Phi}{\partial z^2}\right)_{x=0,\ y=0,\ z=z_0} \qquad (14)$$

with the help of Eqs. (8) and (9) and an appropriate approximation to Eq. (10). Moreover, $\nu_x \approx \nu_y = 5 \cdot 10^{11} - 11 \cdot 10^{11}\ \text{sec}^{-1}$ and $\nu_z = 1.5 \cdot 10^{12}\ \text{sec}^{-1}$,* whence $v^{**} \approx 2$.

The value of ω_m depends on the packing of argon atoms over the surface. We used for ω_m the values: 12.8 and 14.7 A^2, listed in [16] for hexagonal and square packing, respectively. We assumed that the partition functions j_i for the internal degrees of freedom were identical for argon in the gaseous state and in the adsorbed state.

Substituting the appropriate expressions and values into Eq. (2), we obtain the following expression for $\Delta\mu$ as a function of θ when argon is transferred from the gaseous state at $p^0 = 760$ mm to the basal plane of graphite, at T = 77.8°K:

$$\Delta\mu = -1{,}2_5 + 0{,}355 \lg\theta \text{ kcal/mole} \qquad (\omega_m = 12{,}8\ \text{Å}^2); \qquad (15)$$

$$\Delta\mu = -1{,}3_0 + 0{,}355 \lg\theta \text{ kcal/mole} \qquad (\omega_m = 14{,}7\ \text{Å}^2). \qquad (16)$$

Thus, the $\Delta\mu$ of argon is relatively independent of ω_m. In Fig. 1 we have compared the initial segments of the experimental and calculated curves of $-\Delta\mu = f(\theta)$. The experimental curve 1 was calculated from the adsorption isotherm (which was determined in [16]) using the thermodynamic equation $-\Delta\mu = RT\ln 760/p(\theta)$. The calculated curve 2 seems close to the experimental**. Thus, by using statistical methods one can derive from the theoretically calculated adsorption energy a satisfactory approximation to the partial free energy change accompanying the transfer of an argon atom from the gas phase to the adsorbed state, provided the graphite surface is still sparsely covered with argon.

LITERATURE CITED

1. A. V. Kiselev, Vestnik Akad. Nauk SSSR No. 10, 43 (1957).
2. N. N. Avgul', A. V. Kiselev, et al., Izvest. Akad. Nauk SSSR, Otdel Khim. Nauk, 1314 (1957).***
3. N. N. Avgul', A. V. Kiselev, et al., Izvest. Akad. Nauk SSSR, Otdel Khim. Nauk, 1196 (1959).***
4. W. Orr, Proc. Roy. Soc. A 173, 349 (1939).
5. T. Hayakawa, Bull. Chem. Soc. Japan 30, 236 (1957).
6. A. V. Kiselev and D. P. Poshkus, Zhur. Fiz. Khim. 32, 2824 (1958).
7. T. L. Hill, J. Chem. Phys. 16, 181 (1948).
8. J. W. Drenan and T. L. Hill, J. Chem. Phys. 17, 775 (1949).
9. A. V. Kiselev and D. P. Poshkus, Proc. Second Internat. Congress on Surface Activity (London, 1957) 2, p. 202.
10. G. Shreiner and C. Kemball, Trans. Farad. Soc. 49, 292 (1953).
11. R. M. Barrer, Proc. Roy. Soc. A161, 476 (1937).
12. E. L. Pace, J. Chem. Phys. 27, 1339 (1957).
13. T. L. Hill, J. Chem. Phys. 14, 441 (1946).
14. K. S. Pitzer and W. D. Gwinn, J. Chem. Phys. 10, 428 (1942).
15. A. D. Crowell, J. Chem. Phys. 26, 1407 (1957).
16. S. Ross and W. J. Winkler, J. Coll. Sci. 10, 319 (1955); S. Ross, W. W. Pultz, J. Coll. Sci. 13, 397 (1958).

* In [15] an approximate value of $\nu_z = 1.19 \cdot 10^{12}\ \text{sec}^{-1}$ was computed.

** When θ becomes larger interactions between the adsorbed molecules are reflected in the experimental curve; we have not yet considered these effects in our calculated curve (the energy of this interaction, though, has been calculated [12]).

*** See CB translation.

THE EFFECT OF IRRADIATION ON THE POTENTIAL OF A PLATINUM ELECTRODE IN A SOLUTION OF SULFURIC ACID

D. V. Kokoulina, P. I. Dolin, and Academician A. N. Frumkin

Institute of Electrochemistry of Academy of Sciences of USSR

Translated from Doklady Akademii Nauk SSSR, Vol. 132, No. 4, pp. 880-883, June, 1960

Original article submitted February 26, 1960

The appearance of the products of radiolysis of water during the treatment of the solution with ionizing radiation should be attributed to a change in the oxidation-reduction properties of the medium, and gives evidence of the electrochemical behavior and corrosion properties of metals contained in the irradiated solution. When the solution does not contain substances which would enter into oxidizing or reducing reactions with the radiolysis products of water, the radiolysis products may exert a direct effect on the electrode, and so produce a definite potential. V. I. Veselovskii and Ts. I. Zalkind were the first to discover that the irradiation of a solution of sulfuric acid caused the establishment at a platinum electrode of a potential close to the reversible hydrogen potential, while on gold the potential was ~0.95 v. Thus, in the system Pt/ H_2SO_4 solution saturated with N/ Au, the difference of potential obtained was ~0.9 v. These effects were explained by the authors by the selective interaction of the platinum with the reducing (principally hydrogen atoms) and of the gold with the oxidizing (principally hydroxyl radicals)components of the radiolysis of water [1]. According to data provided by Clark [2] a smooth platinum electrode is specially sensitive to the effect of irradiation compared with a platinized electrode, although in their behavior the two electrodes are basically similar.

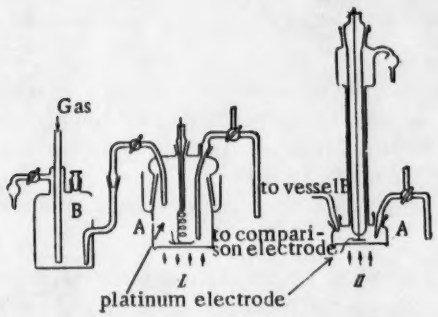

Fig. 1. Schematic representation of measuring cells. A) Measuring vessel containing the solution under investigation; B) auxiliary vessel for preliminary saturation of the solution with the required gas. The diagram does not show the leads into the measuring cell for the entry and removal of gases, nor the lead for the removal of solution from the cell, which is a fine tube attached to the base and bearing a tap.

Developing the idea of Allen concerning the approach to equilibrium concentration conditions of the oxidized and reduced forms of a substance under prolonged irradiation of the solution, Dainton and Collinson suggested that the state in which the rates of the oxidation and reduction processes are equal is characterized by the oxidation-reduction potential equivalent to that of irradiated water [3]. Henderson and his colleagues [4] found that, in the presence of an oxidation-reduction indicator (usually KI), the constant potential of a platinum electrode in an irradiated solution attained the value of 0.85 v in relation to a hydrogen electrode in the same solution. This value does not depend on the nature of the oxidation-reduction indicator, the magnitude of the

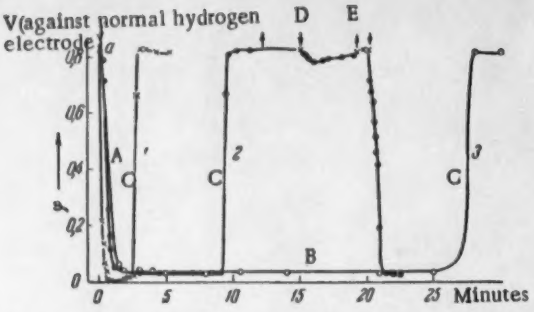

Fig. 2. Relationship between the potential of the platinum electrode and the time of irradiation for various dose-intensities (in ev/ cm^3 sec). 1) $2 \cdot 10^{17}$; 2) $5 \cdot 10^{16}$; 3) $2 \cdot 10^{16}$. Solution I was saturated with nitrogen, ↓) irradiation commenced, ↑) irradiation discontinued. Measurements carried out in cell I.

radiation dose or the value of the pH, and is taken by the authors to be the same as the oxidation-reduction potential of irradiated water.

We have devoted our work to the problem of discovering the conditions under which, using a platinum electrode, the hydrogen potential is attained, and those under which the value close to 0.85 v is attained, as well as that of determining the part played by the products of irradiation (whether molecular or radicals) in the setting up of the potential. We have studied the behavior of a smooth platinum electrode in sulfuric acid solution over a wide range of radiation dosage and of dose-intensity. Irradiation was carried out with Röntgen rays (potential 80 kv, maximum current strength 200 ma), in glass cells of two designs (Fig. 1, I and II), in which the maximum attainable dose-intensity was, respectively, $\sim 3 \cdot 10^{17}$ and $\sim 7 \cdot 10^{16}$ ev/ $cm^3 \cdot$ sec). In cell I, owing to the large liquid meniscus and the small thickness of the solution layer (2-3 mm), the hydrogen formed by radiolysis can separate from the solution in the course of the experiment; in cell II the liquid meniscus is very small, and so the removal of the hydrogen into the gas phase is more difficult. In both cells the possibility was envisaged of changing the solution in the course of the experiment by transferring it from the reserve vessel B, where it could be saturated beforehand with the corresponding gas. In some of the experiments the cell took the form of a vertical, thin walled tube of diameter 7 mm, though which the solution flowed; irradiation by a horizontal beam was applied to a part of the cell, of height 3 mm, in which the electrode was situated. A solution of 0.8 N H_2SO_4 was prepared from doubly distilled sulfuric acid. The hydrogen and nitrogen for saturating the solution were purified of traces of oxygen and other impurities. Measurement of potential was performed by means of a cathodic voltmeter, and the comparison electrode was either a hydrogen electrode or a mercury-sulfate electrode. The platinum electrode was prepared by extracting in hot aqua regia and washing in hot, doubly distilled water; before use in the experiments, the electrode was submitted to cathodic-anodic polarization in turn, either in the same or in a different apparatus.

Figure 2 shows the relationship between the potential of the platinum electrode and the time of irradiation for various dose intensities. It can be seen from this figure that the potential of the platinum in a solution saturated with nitrogen, under the influence of radiation, is displaced initially in a negative direction (section A), and reaches a value close to that of the reversible hydrogen electrode (section B). However, the hydrogen potential on platinum is not constant, since as the irradiation is continued, the potential is again displaced, this time in a positive direction (section C) reaching the value of ~ 0.85 v.

The potential under irradiation reaches the reversible hydrogen value after the absorption of $3-5 \cdot 10^{18}$ ev/ cm^3, independently of the dose intensity.* If we suppose that the yield of molecular hydrogen in the solution of 0.8 N H_2SO_4 is equal to 1.0 molecule per 100 ev [5]. The concentration of molecular hydrogen in the solution for a dose of $4 \cdot 10^{18}$ ev/ cm^3 would be $1.0 \cdot 4 \cdot 10^{18} \cdot 10^3 / (100 \cdot 6 \cdot 10^{23}) = 6.6 \cdot 10^{-5}$ mole/ liter. The concentration of hydrogen in the sulfuric acid solution, when this is saturated with hydrogen at atmospheric pressure and room temperature, is $\sim 6 \cdot 10^{-4}$ mole/ liter. Since, in our experiments, the potential of the platinum during irradiation is some 10-40 mv less than the equilibrium hydrogen electrode, and the temperature of the solution during the irradiation period rises to 40°, we calculate that the observed value of the potential corresponds to the concentration of molecular hydrogen formed by radiolysis. This conclusion is confirmed by the following observations.

1. If the irradiation is interrupted before the greatest negative value of the potential has been attained, the potential continues to be displaced in the negative direction; a similar phenomenon has been observed earlier in

* Approximately the same dose is required, according to the data of Ts. I. Zalkind and V. I. Veselovskii, using gamma radiation from Co^{60}, in experiments where the dose intensity was $2 \cdot 10^{15}$ ev/ $cm^3 \cdot$ sec.

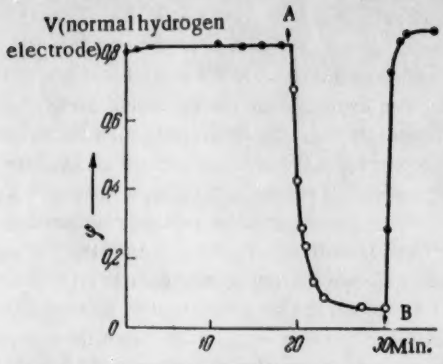

Fig. 3. Relationship between the potential of platinum and the time for a flowing solution under irradiation. Rate of flow equals 0.2 cm^3/ sec; linear rate equals 0.42 cm/ sec. The solution is saturated with nitrogen. At point A the flow is interrupted, and at point B, resumed.

our laboratory with nitrate solutions [6]. In cell I the displacement of potential continues to a value of 0.85 v, while in cell II the potential remains for a considerable time close to that of the hydrogen electrode. This shows that the potential is dependent on the concentration of the molecular hydrogen product, and that the stationary state at the electrode is not set up instantaneously.

2. Addition to a solution of sulfuric or perchloric acids of active acceptor radicals ($4 \cdot 10^{-3}$ mole/ liter KBr), although reducing the hydrogen atom concentration by a factor of 10^3, does not alter the relationship between the potential and the dose as compared with a pure solution of the acid.

3. When the solution is caused to flow through the cell—that is, under conditions when the stationary concentration of the molecular products of radiolysis is appreciably reduced, and the stationary concentration of radicals is changed only slightly in comparison with that in a nonflowing solution, irradiation does not cause any shift of potential in the negative direction. When flow is discontinued, the potential on irradiation changes according to the same law as in cell II (Fig. 3).

4. In cell II, the rise of the potential to a value of 0.85 v takes place at a larger dose than in cell I, in which the stoichiometric relation between the concentrations of H_2O_2 and H_2 in the solution is disturbed in the direction of increased H_2O_2.

All this shows that atomic hydrogen does not play a significant part in establishing the hydrogen potential under irradiation. S. D. Levina and T. V. Kalish came to the same conclusion in their work on the behavior of nickel electrodes during irradiation [7].

The potential of 0.85 v appears to be the stable state of the platinum electrode in an irradiated solution of sulfuric acid, though the dose at which this value of the potential is reached depends to some extent on the composition of the electrode surface, and on the rapidity with which exchange takes place between solution and gas phase of the gaseous reaction products. The value of 0.85 v in apparatus I is arrived at after the absorption of $3 \cdot 10^{19}$ ev/ cm^3, and in apparatus II after $2-5 \cdot 10^{20}$ ev/ cm^3, independent of the dose intensity.* After this value has been reached, further irradiation for an hour or more (dose intensity $1 \cdot 10^{17}$ ev/ $cm^3 \cdot$ sec) does not change it further. Interruption of irradiation at this point also leaves the value of the potential practically unaffected. Repeating of the irradiation after this stable value has been attained, using the same electrode in the same solution, produces a negative shift of potential of 20-50 mv, after which the value again rises to the stable value (Fig. 2, curve 2, commencement of irradiation, point D). If the solution is replaced by a fresh one, the potential on irradiation is again shifted to the equilibrium hydrogen value (Fig. 2, curve 2, replaced solution — point E), and afterward to 0.85 v. These phenomena are repeated over and over again at the same electrode, whenever change of solution takes place.

A shift of potential from the hydrogen value toward the positive is associated with the accumulation of hydrogen peroxide in the solution during the course of irradiation. Figure 4 gives for comparison curves showing the relationship between the potential of platinum in the sulfuric acid solution and the concentration of H_2O_2. Curve 1 shows the change in the potential of the platinum on addition of a solution of H_2O_2 saturated with nitrogen to the solution of H_2SO_4 saturated with hydrogen. Initially the change in the potential is very small, but at a concentration of H_2O_2 around $2.4 \cdot 10^{-3}$ mole/ liter, there is a sudden shift in a positive direction, up to a value of ~0.8 v. Curve 2 shows the relationship between the potential and the dose when the dose intensity is $7 \cdot 10^{16}$ ev/ $cm^3 \cdot$ sec, determined in cell II and recalculated to give the relationship between the potential and the

* According to the data of Ts. Zalkind and V. I. Veselovskii, approximately the same dose of ^{60}Co γ-radiation was required in experiments where the dose strength was $2 : 10^{15}$ ev/cc.sec.

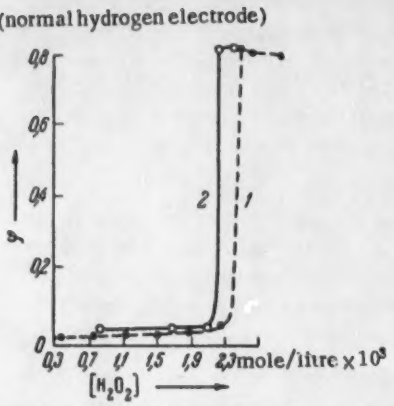

Fig. 4. Relationship between the potential of a platinum electrode in 0.8 N sulfuric acid and the concentration of H_2O_2: 1) a solution of H_2O_2 saturated with nitrogen is added to the H_2SO_4 solution saturated with hydrogen; 2) the H_2O_2 is formed in situe on the irradiation of the H_2SO_4 solution saturated with nitrogen.

concentration of the H_2O_2 formed (taking the yield of H_2O_2 as 0.8 molecule per 100 ev). It is seen from Fig. 4 that the H_2O_2, independently of the manner in which it is introduced into the solution, produces a shift of potential to a value of ~0.8 v. The following results are also explained by the accumulation of H_2O_2 up to a stationary concentration. The hydrogen potential at atmospheric pressure of hydrogen is not changed by prolonged irradiation. But the potential of platinum in H_2SO_4 solution, at a hydrogen pressure of 0.1 atmosphere under prolonged irradiation (dose $\sim 3 \cdot 10^{20}$ ev/cm^3) is shifted to 0.85 v. In the first case, because of the large exchange current of the reaction of formation or ionization of hydrogen, the accumulation of H_2O_2 up to the stationary concentration is not able to shift the potential in a positive direction. When the concentration of hydrogen is reduced by a factor of 10, and a corresponding reduction takes place in the exchange current of the hydrogen, the reduction of H_2O_2 which takes place in the solution at the stationary concentration causes the potential to shift in the negative direction.

Thus, the potential of the platinum electrode in 0.8 N sulfuric acid solution under the influence of irradiation is determined by the accumulation in the solution of the molecular products of the radiolysis of water: that is, by hydrogen and hydrogen peroxide. The radicals produced do not play a significant role in establishing the potential of the platinum: the major part of these, evidently, is recombined in the volume of the solution and on the electrode surface.

LITERATURE CITED

1. V. I. Veselovskii, Proceedings of the Soviet Delegation to the International Conference on the Peaceful Use of Atomic Energy: The Investigations in the Realms of Geological Chemistry and Metallurgy [in Russian] (Izc. AN SSSR, 1955) p. 320; Ts. I. Zalkind and V. I. Veselovskii, Collected Works on Radiation Chemistry [in Russian] (Izd. AN SSSR, 1955) p. 66; Ts. I. Zalkind, V. I. Veselovskii, and G. Z. Gochaliev, Transactions of the First All-Union Congress on Radiation Chemistry [in Russian] (Izd. AN SSSR, 1958) p. 123; Ts. I. Zalkind and V. I. Veselovskii, Collected Works on the Effect of Ionizing Radiation on Inorganic and Organic Systems [in Russian] (Izd. AN SSSR, 1958) p. 66.
2. W. E. Clark, J. Electrochem. Soc. 105, 483 (1958).
3. F. S. Dainton and E. Collinson, Ann. Rev. Phys. Chem. 2, 99 (1951).
4. J. H. S. Henderson, E. G. Lovering, et al., Canad. J. Chem. 37, 164 (1959).
5. P. I. Dolin, Collected Works on Radiation Chemistry [in Russian] (Izd. AN SSSR, 1955) p. 20.
6. N. A. Bach and V. D. Bityukov, Izvest. Akad. Nauk SSSR, Organic Chemistry [in press].
7. S. D. Levina and T. V. Kalish, Dokl. Akad. Nauk SSSR 130, 573 (1960). *

* See CB translation.

THE EFFECT PRODUCED BY THE INTERACTION OF ADSORBED PARTICLES

V. I. Osherov

L. Ya. Karpov Physicochemical Institute

(Presented by Academician A. N. Frumkin, January 22, 1960)

Translated from Doklady Akademii Nauk SSSR, Vol. 132, No. 4, pp. 884-887, June, 1960

Original article submitted January 18, 1960

The effect of the mutual interaction of chemisorbed particles (atoms or molecules) [1] is basically bound up with the delocalized pertubation functions of the electrons in the crystal adsorbent, which should lead to the development of repulsions between the particles which will diminish with the distance Δ considerably more slowly than exp $(-\Delta / a_0)$, where a_0 is the Bohr radius.

In order to consider the relationship between the differential heat of adsorption and the extent to which the surface is covered – which is one of the evidences that mutual interaction is occurring – we make use of the method of localized states in the molecules and the crystals [2, 3], in its application to adsorption [4]. The results constitute a development of those obtained earlier by another method [5].

We introduce the following relationships:

$$H_1 = H_0 + V_1 \tag{1}$$

the Hamiltonian of an electron in a crystal in a one-electron approximation (where H_0 is the kinetic energy, and V_1, the mean potential in the crystal);

$$H_2 = H_0 + V_2 \tag{2}$$

the Hamiltonian of an electron in the layer of chemisorbed atoms, taking no account of the interaction between them and the adsorbent (where V_2 is the potential of the atomic skeleton);

$$H = H_0 + V_1 + V_2 \tag{3}$$

the Hamiltonian of an electron in the adsorbate-adsorbent system. The corresponding eigenvalues and eigenfunctions are: $\epsilon_{\mathbf{k}}^{j}$, ϵ_0 [neglecting the interaction exp $(-\Delta/a_0)$], ε; $|\mathbf{k}, j\rangle$, $\sum_{\mathbf{m}} d_{\mathbf{m}} |a_{2\mathbf{m}}\rangle$, $|I\rangle$ (where $\mathbf{k}$ is the quasi-impulse in the zone j; $\mathbf{m}$ is the position of the adsorbed atom on the surface).

Let

$$|I\rangle = \sum_{\mathbf{k},j} c_{1\mathbf{k}}^{I} |\mathbf{k}, j\rangle + \sum_{\mathbf{m}} c_{2\mathbf{m}} |a_{2\mathbf{m}}\rangle. \tag{4}$$

Then putting $\langle k, j \mid a_{2m} \rangle = 0$, we obtain,

$$c^j_{1k} = \sum_{k',j'} c^{j'}_{1k'} \frac{\langle k, j \mid V_2 \mid k', j' \rangle}{\varepsilon - \varepsilon^j_k} + \sum_m c_{2m} \frac{\langle k, j \mid V_1 \mid a_{2m} \rangle}{\varepsilon - \varepsilon^j_k},$$

$$c_{2m} = \sum_{m'} c_{2m'} \frac{\langle a_{2m} \mid V_1 \mid a_{2m'} \rangle}{\varepsilon - \varepsilon_0} + \sum_{k,j} c^j_{1k} \frac{\langle a_{2m} \mid V_2 \mid k, j \rangle}{\varepsilon - \varepsilon_0}. \tag{5}$$

The Fourier transformation for the quasi-impulse k of each zone j, corresponding to the transfer to the crystal under discussion by means of the Vanier function [4], gives:

$$c^j_{1n} = \sum_{n',n'',j'} c^{j'}_{1n'} \langle a^j_{1n''} \, V_2 \, a^{j'}_{1n'} \rangle I^j_{n''-n} + \sum_{m,n'} c_{2m} \langle a^j_{1n'} \mid V_1 \mid a_{2m} \rangle I^j_{n'-n},$$

$$c_{2m} = \sum_{m'} c_{2m'} \langle a_{2m} \mid V_1 \mid a_{2m'} \rangle \frac{1}{\varepsilon - \varepsilon_0} + \sum_{n,j} c^j_{1n} \langle a_{2m} \; V_2 \mid a^j_{1n} \rangle \frac{1}{\varepsilon - \varepsilon_0}, \tag{6}$$

where c^j_{1n} and $a^j_{1n}>$ are the Fourier forms c^j_{1k} and $|k, j>$,

$$I^j_{n'-n} = \frac{1}{N} \sum_k \frac{e^{ik(n'-n)}}{\varepsilon - \varepsilon^j_k}, \tag{7}$$

N being the fundamental region of the crystal.

We suppose, now, that $V_1 \sim$ constant (as in the case of metals), and that $< a^j_{1n} \mid V_2 \mid a^{j'}_{1n} > = 0; j \neq j'$. Under these conditions (6) can be converted to the form:

$$c^j_{1n} = \sum_{n'} c^j_{1n'} \langle a^j_{1n'} \mid V_2 \mid a^j_{1n} \rangle I^j_{n'-n} + \sum_{m,n'} c_{2m} \langle a^j_{1n'} \mid V_1 \mid a_{2m} \rangle I^j_{n'-n},$$

$$c_{2m} (\varepsilon - \varepsilon_0 - \langle a_{2m} \mid V_1 \mid a_{2m} \rangle) = \sum_j c^j_{1m} \langle a_{2m} \mid V_2 \mid a^j_{1m} \rangle + O(e^{-\Delta'/a_0}). \tag{8}$$

Limiting the equation to the nearest neighbors of atom number m, we obtain:

$$c^j_{1m} (1 - \alpha^j_2 I^j_0) = c_{2m} \beta^j_1 I^j_0 + \sum_{\vec{\Delta}} c^j_{1m+\vec{\Delta}} \alpha^j_2 I^j_{\vec{\Delta}} + \sum_{\vec{\Delta}} c_{2m+\vec{\Delta}} \beta^j_1 I^j_{\vec{\Delta}} + A e^{-a/a_0},$$

$$c_{2m} (\varepsilon - \varepsilon_0 - \alpha_1) = \sum_j c^j_{1m} \beta^j_2. \tag{9}$$

At this point we use the relationships:

$$\alpha_1 = \langle a_{2m} \mid V_1 \mid a_{2m} \rangle, \quad \beta^j_1 = \langle a^j_{1m} \mid V_1 \mid a_{2m} \rangle, \quad \beta^j_2 = \langle a_{2m} \mid V_2 \mid a^j_{1m} \rangle. \tag{10}$$

For α^j_2 may be obtained limiting values on both sides:

$$\langle a^j_{1m} \mid V_2 \mid a^j_{1m} \rangle < \alpha^j_2 < \frac{1}{N} \sum_k \langle k, j \mid V_2 \mid k, j \rangle. \tag{11}$$

The function $A \exp(-a/a_0)$ may be discarded if a limit is imposed on the degree of covering of the surface, of the form $\theta > (a_0/a)^2$ (where a is a lattice constant).

On the assumption of a sufficiently correct arrangement of the adsorbed atoms, the solution of (9) for the state localized on the surface of the adsorbent may be expressed in the form:

$$c^l_{1m} = C^l_1 e^{i\vec{\varkappa}\vec{m}}, \quad c_{2m} = C_2 e^{i\vec{\varkappa}\vec{m}}, \tag{12}$$

The corresponding eigenvalues are found from the equations:

$$\varepsilon - \varepsilon'_0 = \sum_l z_l \frac{I^l_0 + 4I^l_\Delta \cos \varkappa_1 \cos \varkappa_2}{1 - \alpha^l_2 (I^l_0 + 4I^l_\Delta \cos \varkappa_1 \cos \varkappa_2)}; \tag{13}$$

$$I^l_0 = \frac{1}{(2\pi)^3} \int \frac{d\mathbf{k}}{\varepsilon - \varepsilon^l_{\mathbf{k}}}, \quad I^l_\Delta = \frac{1}{(2\pi)^3} \int \frac{e^{i\mathbf{k}\vec{\Delta}}}{\varepsilon - \varepsilon^l_{\mathbf{k}}} d\mathbf{k}; \tag{14}$$

$$\varepsilon'_0 = \varepsilon_0 + \alpha_1, \quad z_l = \beta^l_1 \beta^l_2. \tag{15}$$

In (12) and (13) $\varkappa_1$ and $\varkappa_2$ may vary within the limits of $-\pi$ and π.

The solution of equation (13) may be written in the form

$$\varepsilon = \varepsilon_{\text{loc}} + f_1(\Delta, \vec{\varkappa}), \tag{16}$$

where ϵ_{loc} to a first approximation is the solution of (13) for $I^l_\Delta = 0$. The effective asymmetry of the zone of Eq. (16) produces, for the linking states of the last named, of the order of a chemical bond, part of the interaction effect.

The other part of the effect is associated with the relationship between the level of the volume state of the adsorbent and the degree of covering of the surface. It may be shown that the solution of (9) in this case can be adequately expressed in the form:

$$c^l_{1m} = C^l_{1\mathbf{k}} e^{i\mathbf{k}\mathbf{m}}, \quad c_{2m} = C_{2\mathbf{k}} e^{i\mathbf{k}\mathbf{m}}. \tag{17}$$

Then [5],

$$\varepsilon = \varepsilon^l_{\mathbf{k}} + \frac{M}{N} f^l_2(\Delta, \mathbf{k}); \tag{18}$$

where M is the number of atoms adsorbed on the fundamental region of the crystal:

$$f^l_2(\Delta, \mathbf{k}) = \nabla \varepsilon^l_{\mathbf{k}} \vec{\delta}^l(\Delta, \mathbf{k}). \tag{19}$$

In the case where $\epsilon^l_{\mathbf{k}} = \epsilon^l_{\mathbf{k}}\ \delta^l(\Delta, \mathbf{k})$ is found from the equation

$$\varepsilon^l_k - \varepsilon_0 = \sum_{l'} z_{l'} \frac{I^{l'}_0 + 4I^{l'}_\Delta \cos k_1\Delta \cos k_2\Delta}{1 - \alpha^{l'}_2 (I^{l'}_0 + 4I^{l'}_\Delta \cos k_1\Delta \cos k_2\Delta)}, \tag{20}$$

in which,

$$\begin{aligned} I^l_0 &= \frac{1}{(2\pi)^3} \text{v. p.} \int \frac{d\mathbf{k}'}{\varepsilon^l_k - \varepsilon^l_{k'}} + \pi \frac{dk}{d\varepsilon^l_k} \operatorname{ctg} \pi\delta^l(\Delta, k), \\ I^l_\Delta &= \frac{1}{(2\pi)^3} \text{v. p.} \int \frac{e^{i\mathbf{k}'\vec{\Delta}}}{\varepsilon^l_k - \varepsilon^l_{k'}} d\mathbf{k}' + e^{i\mathbf{k}\vec{\Delta}} \frac{dk}{d\varepsilon^l_k} \operatorname{ctg} \pi\delta^l(\Delta, k), \\ I^{l'}_0 &= \frac{1}{(2\pi)^3} \int \frac{d\mathbf{k}'}{\varepsilon^l_k - \varepsilon^{l'}_{k'}}, \quad I^{l'}_\Delta = \frac{1}{(2\pi)^3} \int \frac{e^{i\mathbf{k}'\vec{\Delta}}}{\varepsilon^l_k - \varepsilon^{l'}_{k'}} d\mathbf{k}'. \end{aligned} \tag{21}$$

If the zones j and j' are crossed at some part of the k area, the corresponding $\delta^j(\Delta, k)$ as before, is found from Eq. (20) in which $I_0^{j'} = \infty$, $I_\Delta^{j'} = \infty$. Therefore,

$$\varepsilon_k^j - \varepsilon_0' = z_j \frac{I_0^j + 4I_\Delta^j \cos k_1\Delta \cos k_2\Delta}{1 - \alpha_2^j (I_0^j + 4I_\Delta^j \cos k_1\Delta \cos k_2\Delta)} - \sum_{j' \neq j} \frac{z_{j'}}{\alpha_2^{j'}}. \tag{22}$$

We suppose now that the density of the levels in the volume zone (18) is considerably greater than in the surface zone (16). We then obtain for the differential heat of adsorption,

$$Q = Q_0 - \frac{2}{(2\pi)^2} \int f_1(\Delta, \vec{x})\, d\vec{x} - \frac{2}{(2\pi)^3} \sum_j \int f_2^j(\Delta, k)\, dk, \tag{23}$$

where

$$Q_0 = \Phi + \varepsilon_{k_F} + \varepsilon_0 - 2\varepsilon_{loc}, \tag{24}$$

and Φ is the energy of interaction of the atomic skeleton with the lattice skeleton. In (23) the first integral is performed over the entire zone of (16), and the second to the Fermi impulse k_F of the crystal; when the former appears as $\exp(-\Delta/a)$, and the second as $(\sin k_F \Delta)/\Delta$. Both these terms decrease much more slowly than the usual repulsion $\exp(-\Delta/a_0)$.

After neutralizing by Δ, (23) gives:

$$Q = Q_0 + F_1(A_{int}, \lambda)\theta + F_2(k_F)\theta. \tag{25}$$

Here A_{int} is a combination of α_1, α_2, and z; $\lambda = |(\varepsilon_0 - \alpha)/2\beta|$ may be called the degree of localization of the bond; α and β are the effective Coulomb and resonance integrals of the crystal; θ is the degree of covering of the surface; $F_1 < 0$, $F_2 < 0$, $|F_1(\lambda)| \sim \exp(-\lambda)$, $|F_2(k_F)|$ have maximum value in the mean part of the valency zone.

Even at this stage it is possible to derive definite confirmation of the theory by experiment. Thus, according to the magnitude of $dQ/d\theta$ the metals should be arranged in the following order:

$$Pt > W > Ta > Pd > Ni > Co > Fe.$$

For the gases there is a corresponding sequence, decided on the basis of the degree of dipolar character of the bond, thus

$$N_2 > H_2 > CO > O_2.$$

The author wishes to express his thanks to Professor M. I. Temkin for his comments on the results.

LITERATURE CITED

1. M. I. Temkin, Collected Works on the Problem of Chemical Kinetics, Catalysis and Reactivity [in Russian](AN SSSR, 1955) p. 484.
2. G. F. Koster, Phys. Rev. 89, 67 (1953).
3. G. F. Koster and J. C. Slater, Phys. Rev. 95, 1167 (1954).
4. J. Koutecky, Trans. Farad. Soc. 54, 1038 (1958).
5. V. I. Osherov, Doklady Akad. Nau, SSSR 130, 1, 117 (1960).*
6. I. M. Lifshits, Zhur. Éksp. i Teoret. Fiz. 17, 1076 (1947).

* See CB translation.

THE MECHANISM OF THE PROTECTION OF MAGNESIUM FROM OXIDATION

M. S. Beletskii and M. I. Erusalimskii

All-Union Aluminum–Magnesium Scientific Research Institute

(Presented by Academician G. V. Kudryumov, February 13, 1960)

Translated from Doklady Akademii Nauk SSSR, Vol. 132, No. 5, pp. 1122-1124, June, 1960

Original article submitted February 6, 1960

Pure magnesium, when stored for a prolonged period in air at room temperature, becomes covered with an oxide film which prevents the penetration of oxygen to the interior of the metal. The thickness of the oxide layer increases with increase in temperature. When a certain limiting temperature is reached, the Mg ignites and continues to burn.

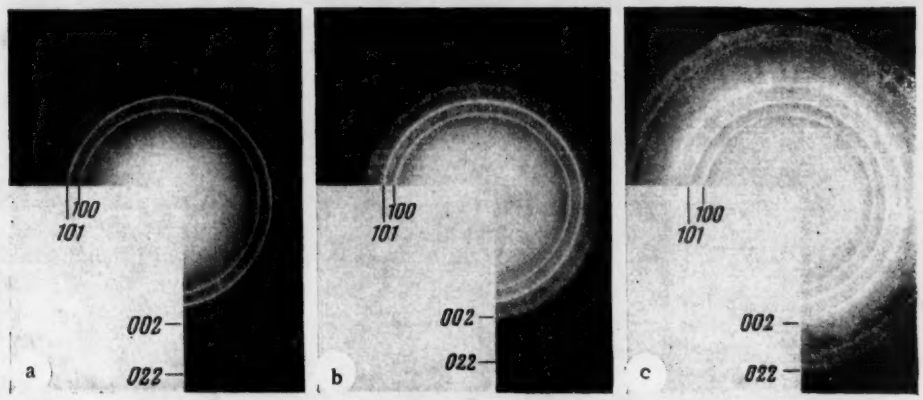

Fig. 1. Electron diffraction diagram for magnesium immediately after transfer from the pulverization chamber (a), and after storage in air for 24 hr (b), and 72 hr (c).

The reason for this behavior of magnesium and for its interaction with oxygen is explained by the specific structure of its electron shell. In the magnesium atom, the two valence electrons, with spins in opposite direction, occupy the 3s subgroup in the free state. In the crystal, the two valence electrons from each atom are arranged in 3s3p hybrid orbitals, and their spins are in the same direction. In magnesium atoms, situated on the surface of the solid metal, some of the bonds are not compensated and the potential field created by the surrounding atoms is weaker in this case. It can, therefore, be assumed that the properties of these surface atoms are closer to those of free atoms, than atoms in the interior of the metal. Thus, the valence electrons of the surface layer of magnesium atoms, being for the most part in the 3s-state, should readily form an exchange with the p-electrons of oxygen.

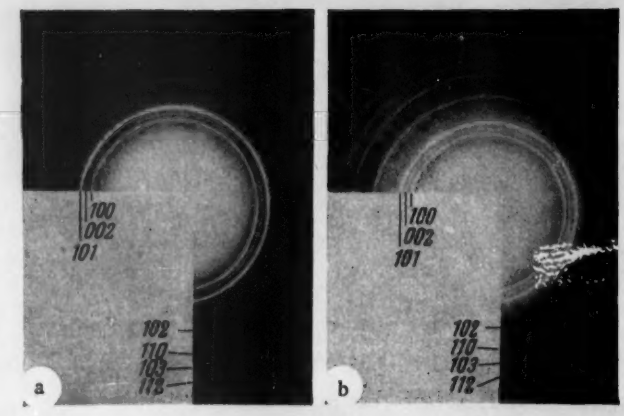

Fig. 2. Electron diffraction diagram of magnesium containing a small quantity of Nd, immediately after pulverization (a) and after storage in air for one month (b).

These views regarding the mechanism of the oxidation of magnesium have been confirmed experimentally by introducing into the surface layer of the magnesium atoms of neodymium, which apparently raise the valence 3s electrons of the magnesium atom to the higher 3p level, preventing them, in accordance with the "selection rule," from forming an exchange bond with the valence electrons of the oxygen. Examination of the structure of the electron shells of the atoms has established that certain other elements can also be used, in addition to neodymium, for this purpose.

The ease of oxidation of the magnesium was estimated from the change in the character of the electron diffraction patterns obtained from appropriate specimens.

The specimens for the electron diffraction studies were prepared in a vacuum pulverization chamber, in which pressures of the order of $5-7\cdot10^{-6}$ mm could be achieved, and which made it possible to avoid oxidation of the metal. The supports for the pulverized metals consisted of very fine collodion films deposited on brass washers. The materials pulverized consisted of 98% neodymium and magnesium–neodymium alloy containing 45% neodymium. Magnesium of 99.98% purity was also oxidized.

The conditions under which the metals were pulverized were kept identical as far as possible. The distance from the collodion film to the molybdenum spiral was equal to 95-97 mm. In order to pulverize the magnesium and the magnesium–neodymium alloy, the heating current of the spiral containing the metal specimen was slowly raised to 5 amp, then raised rapidly to 7-8 amp, and kept at this value for 3-5 sec. The neodymium was pulverized at a higher temperature. In this case the current in the spiral was slowly increased to 10 amp, then raised rapidly to 18-20 amp and kept at this value for 10-15 sec.

The metallic films obtained under these conditions were cooled in vacuo, removed from the pulverization chamber, and quickly placed in the electron diffraction apparatus, which had previously been made ready for operation. After the first electron diffraction diagrams had been recorded, the films were stored in air for different intervals of time at room temperature and the electron diffraction studies repeated, at a voltage of 40 kv.

Figure 1,a,b, and c, shows electron diffraction diagrams for pulverized magnesium films after storage in air for different intervals of time. It was found that the rate of oxidation of pure magnesium is very high. Magnesium oxide is formed in the very short time interval (1-2 min) during which the film is transferred from the pulverization chamber to the electron diffraction apparatus.

Figure 1,a, shows the electron diffraction diagrams for one of these specimens. It shows, in addition to the interference rings with indices (100) and (101) characteristic of magnesium, weak (002) and (022) rings belonging to magnesium oxide.

In the electron diffraction diagram for the same film after storage in air for 24 hr (Fig. 1,b), the interference rings of the magnesium oxide are much more intense, while the magnesium rings are less intense.

Increase in the time of storage of the magnesium film in air leads to more complete oxidation. The electron diffraction diagram (Fig. 1,c) shows that the quantity of magnesium in the specimen is much smaller than before. The quantity of magnesium oxide, on the other hand, has increased.

The oxidation of neodymium takes place in quite different fashion. The electron diffraction diagram for neodymium, which has not been exposed to the action of air, shows distinct interference lines with indices (100), (102), (103), (106), etc. After the neodymium has been stored in air at room temperature for 1 hr, certain changes take place, as a result of which some of the interference rings on the electron diffraction diagram disappear, while others become blurred. These changes in the diffraction pattern may indicate the start of the oxidation of neodymium and a decrease in the degree of long-range order in the arrangement of the atoms in the crystal lattice.

Similar studies were carried out with films of magnesium which had reacted with neodymium. In this case it was necessary to pulverize, on to the magnesium surface, a quantity of neodymium which would not produce the intermetallic compound Mg_9Nd, whose properties differ considerably from those of magnesium. This was achieved successfully by choosing suitable pulverization conditions.

Figure 2,a, shows the electron diffraction diagram obtained immediately after the pulverization of magnesium and an extremely small quantity of neodymium. Examination of the electron diffraction diagram showed that all the intense interference rings belong to magnesium. Only one weak ring belongs to magnesium oxide. The formation of oxide in this case results from the small quantity of oxygen remaining in the pulverization chamber in spite of the high vacuum (10^{-5} mm).

Fig. 2,b, shows the electron diffraction diagram obtained for the film of magnesium and neodymium after storage in air for one month at room temperature. The diagram shows that the magnesium interference rings have not changed, in spite of the prolonged exposure to atmospheric oxygen. This indicates the marked influence of the neodymium in retarding the oxidation of the magnesium. This effect, shown by the neodymium is undoubtedly related to the particular features of the structure of the electron shells of its atom and of the magnesium atom. In the neodymium atom, one valence electron is situated in the 5d shell and two in the 6s shell. According to the selection rule, however, the 5d shell can hold 10 electrons.

The fact that only the magnesium interference rings are present in the last electron diffraction diagrams indicates that the quantity of neodymium present is extremely small. It can therefore be assumed, in accordance with semiconductor structure theory [2], that the energy zones in the neodymium atoms of the test specimens do not overlap, and that the distribution of electrons in these zones is the same as in the free atoms.

LITERATURE CITED

1. W. Hume-Rothery, Atomic Theory for Students of Metallurgy [Russian translation] (Moscow, 1954).
2. A. F. Ioffe, Semiconducor Theory [in Russian] (Izd. AN SSSR, 1957).

CATALYTIC OXIDATION OF PROPYLENE AND ACROLEIN IN COPPER*

V. M. Belousev, Ya. B. Gorokhovatskii, M. Ya. Rubanik and A. V. Gershingorina

L. V. Pisarzhevskii Physical Chemistry Institute, Academy of Sciences, USSR

(Presented by Academician A. A. Balandin, February 15, 1960).

Translated from Doklady Akademii Nauk SSSR, Vol. 132, No. 5, pp. 1125-1128, June, 1960

Original article submitted February 11, 1960

Under mild catalytic conditions the oxidation of hydrocarbons produces some carbon dioxide and water (complete combustion) besides the desired oxygenated hydrocarbons. In certain selective oxidations such as ethylene to ethylene oxide [1, 2], naphthalene to phthalic anhydride [3], and several other cases the CO_2 does not result from the oxidation of the end product but is formed by an independent concurrent route. The amount of work on the oxidation of propylene to acrolein is rather limited [4, 5], and hence, it is impossible to make any definite statements with regards to the mechanism by which carbon dioxide is formed in this reaction.

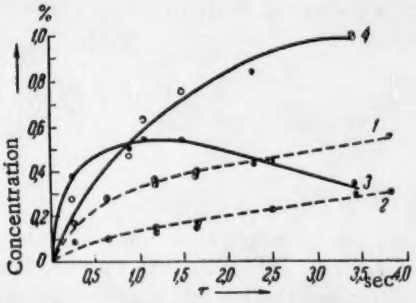

Fig. 1. The concentrations of acrolein and carbon dioxide as a function of contact time. 1) C_3H_4O, 320°; 2) $CO_2/3$, 320°; 3) C_3H_4O, 380°; 4) $CO_2/3$, 380°.

To clarify this problem we investigated the concentration of the products formed in the oxidation of C_3H_6 as a function of contact time, and studied the oxidation of acrolein and propylene on the same catalyst under similar conditions. The catalyst was prepared by depositing $Cu(NO_3)_2$ (from solution) on pieces of carborundum (2-3 mm grain size) and firing the deposits at 400-450° in a stream of air. The study was carried out by means of a flow method and the absence of diffusion hindrance was checked in specially designed experiments. The starting mixture in the oxidation of propylene contained 4.8-5.1% O_2, 20-21% C_3H_6, and 74-75% N_2, while τ = 0.4-0.8 sec; the gases which had passed the contact area contained up to 0.4-0.6% acrolein while the oxygen content was reduced by 1-3%. In the oxidation of acrolein the starting mixtures contained 1.4-1.6% C_3H_4O, 3.2-3.6% O_2, and 95% N_2. We determined the acrolein content by the bromide–bromate method; small amounts of carbon dioxide were determined by absorption in standardized $Ba(OH)_2$ solutions, while large amounts by direct gas analysis; C_3H_6, O_2, and CO were also determined in a VTI-2 gas analyzer.

The data presented in Table 1 show that neither propylene nor acrolein undergo any significant oxidation in either the empty reactor or on the carrier of temperatures between 300 and 400°C, though acrolein turned out to be less stable than propylene.

* The paper was presented at the All-Union Conference on Organic Catalysis, November 19, 1959.

TABLE 1

The Oxidation of Propylene and Acrolein in an Empty Glass Reactor and on a Carbon Carrier. The Reactor Diameter was 16 mm, the Heated Zone 80 mm High, the Flow Rate of the Mixture 121-133 cm^3/min

Experimental conditions	Propylene oxidation				Percent O_2 consumed	Acrolein oxidation			Percent C_3H_4O consumed
	temp. °C.	gases beyond the reactor				temp. °C	gases beyond the reactor		
		C_3H_4O	CO_2	O_2			C_3H_4O	CO_2	
Empty reactor	380	traces	—	5,0	0	300	1,61	0,00	0
						350	1,53	0,05	1
						400	1,55		7*
						430	1,24	0,54	17
On a carborundum carrier	381	traces	—	4,8	0	349	1,50	0,03	1
	419	0,04	—	5,0	0	400	1,50		8*
						431	1,20	0,48	19

* Calculated values.

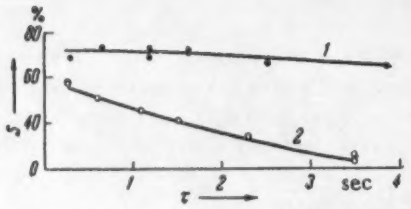

Fig. 2. Selectivity in the oxidation of propylene to acrolein as a function of contact time: 1) at 320°; 2) at 380°C.

The Effect of Contact Time. The contact time τ was varied by changing the flow rate of the reaction mixture and altering the amount of catalyst. When large contact surfaces were used, the first 2 cm^3 of gas would diffuse into the carrier, and consequently the temperature variations throughout the catalytic layer did not exceed 3-4° even at large percent conversions. The data presented in Fig. 1 show that at lower temperatures (320°C) the amounts of C_3H_4O and CO_2 increase steadily with increasing τ. At the same time the selectivity varies very little (Fig. 2) over a wide range of τ (0.28-3.87 sec). This indicates that the predominant reaction at 320° is the formation of acrolein and carbon dioxide by two concurrent and independent routes:

$$C_3H_6 + O_2 \begin{cases} \nearrow C_3H_4O \\ \searrow CO_2 + H_2O \end{cases}$$

At 380° the acrolein concentration curve exhibits a maximum at τ = 1.2 sec; meanwhile the amount of carbon dioxide steadily increases while the selectivity decreases; all of this provides clear evidence that the acrolein which is being formed undergoes oxidation. The formation of carbon dioxide follows at this temperature a concurrent – consecutive reaction scheme:

$$C_3H_6 + O_2 \begin{cases} \nearrow C_3H_4O \xrightarrow{+O_2} CO_2 + H_2O \\ \searrow CO_2 + H_2O \end{cases}$$

Acrolein Oxidation. We investigated the catalytic oxidation of acrolein by varying the amounts of copper per unit volume of the catalyst; oxidation of propylene was studied in a similar manner. As a rule the reaction would ensue even at temperatures below 300° when samples containing large amounts (9 g Cu per liter of catalyst) of copper were used; at 310-320°C and τ = 0.8 sec the reaction products contained 0.3-0.4% CO_2 (Fig. 3). On contacts containing less copper (2.5 g Cu per liter) the oxidation of acrolein would not proceed below 310-320°C

TABLE 2

The Oxidation of Acrolein on Oxidized and Reduced Copper Catalysts

Expr No.	Catalyst treatment conditions	Expti. temp., °C	% composition of outflowing gases			%C_3H_4O consumed
			C_3H_4O	CO_2	O_2	
1	O_2; 345°; 2 hr	347	1,27	0,71	2,12	16
2	H_2; 345°; 2½ hr	345	1,31	0,30	2,45	7
3	H_2; 345°; 2 hr	344	1,45	0,20	2,70	5
5	O_2; 345°; 2½ hr	345	1,29	0,48	2,30	11
6	O_2; 345°; 5 hr	346	1,19	0,64	2,10	14
7	H_2; 346°; 3½ hr	346	1,35	0,38	2,70	9
9	Decompn. of $Cu(NO_3)_2$ at 420°					
	420° $Cu(NO_3)_2$	377	1,10	1,17	1,6	26
10	H_2; 380°; 4 hr	380	1,25	0,69	2,0	15
11	O_2; 375°; 3 hr	380	1,16	1,15	1,35	25
12	H_2; 375°; 5 hr	377	1,35	0,68	2,10	15

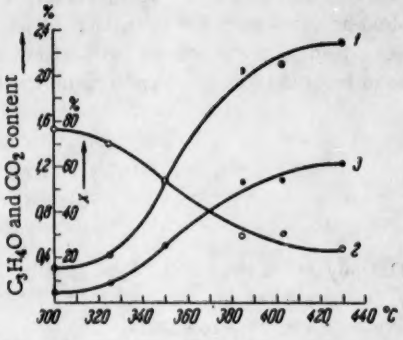

Fig. 3. The temperature dependence of acrolein oxidation on a catalyst containing 9 g of Cu per liter. 1) CO_2; 2)C_3H_4O; 3) percent C_3H_4O consumed (X).

(Fig. 4). The reaction rate decreases considerably when the contact time is reduced. Thus, when τ = 0.8 sec 30% of the acrolein is oxidized at 360°C on a catalyst containing 9 g of Cu per liter, and above 380° half the initial acrolein is oxidized (Fig. 3). But when τ = 0.4 sec and a similar contact is used (10 g per liter) only 10% of acrolein is oxidized at 355° and 30% at 385°C.

Thus, the product can undergo partial oxidation at the temperatures normally used in the catalytic synthesis of acrolein (330-370°). However, our experiments have shown that when the same type of a contact surface is used, the oxidation of propylene was accompanied by appreciable evolution of carbon dioxide even at temperatures well below those required for the oxidation of acrolein. Curve 1, in Fig. 4 shows the amount of CO_2 formed when C_3H_6 is oxidized under conditions identical to those used in the oxidation of C_3H_4O. It is quite obvious that at any one temperature propylene yields much more CO_2 upon oxidation than does C_3H_4O. No explanation is possible for this observation if we assume that all of the carbon dioxide is produced by the oxidation of acrolein.

The propylene and acrolein oxidation data support the above-presented hypothesis that at lower temperatures (300-325°) C_3H_4O and CO_2 are formed in two concurrent reactions, while at higher temperatures simultaneous concurrent and consecutive reactions take place.

In a recently published paper [6] it has been proposed that the oxidation of propylene on copper contacts follows a concurrent consecutive scheme and that the consecutive reaction predominates. The authors of the work cited above carried out the reaction at high temperature (396°C) and used a long contact time (τ = 1.2 sec), under which conditions the reaction is not selective. Our data indicate that at these temperatures and contact times CO_2 is indeed formed in a reaction concurrent with the formation of acrolein as well as through the oxidation of the latter, the oxidation of C_3H_4O being very extensive. When propylene is oxidized under selective conditions, the concurrent formation of C_3H_4O and CO_2 constitutes the principal reaction. The reaction temperature constitutes the decisive factor in determining whether the concurrent or the consecutive reaction should predominate. It is rather difficult to determine the precise temperature threshold at which the oxidation of acrolein begins since it depends on the amount of copper on the contact surface and the contact time.

As has already been shown [7, 8], the original cupric oxide is partially reduced during the catalytic reaction to cuprous oxide on which the oxidation of propylene to acrolein subsequently proceeds. It was interesting to determine the activity of various phases with respect to the oxidation of acrolein. To do this we either reduced the

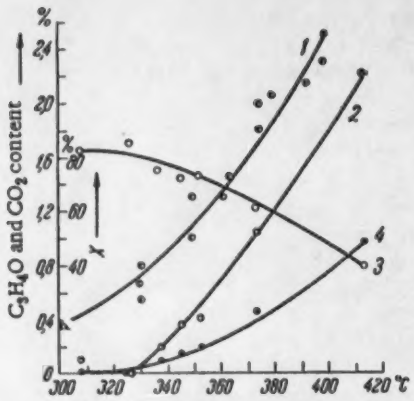

Fig. 4. The temperature dependence of acrolein oxidation and CO_2 evolution during the oxidation of propylene on a catalyst containing 2.5 g of Cu per liter. 1) CO_2 evolved in the oxidation of C_3H_6; 2) CO_2 evolved in the oxidation of C_3H_4O; 3) oxidation and decline in the concentration of C_3H_4O; 4) percent C_3H_4O oxidized (X).

catalyst with hydrogen before using it, or oxidized it with oxygen to CuO and tested its activity. We were unable to make any quantitative deductions with regard to the course of reaction on any of the individual phases (CuO, Cu_2O, or Cu) since as soon as the gaseous mixture is introduced into the system some of the mixture components alter the chemical composition of the catalytic surface. However, Table 2 shows that in all the cases where the contact was first reduced, the oxidation of acroleinhad less extent than in cases where the catalyst was heated in an atmosphere of O_2, or in other words, the catalytic activity of the contact with regards to acrolein oxidation is directly proportional to the oxidation state of the catalyst.

In the light of these data it becomes clear why the contact selectivity was found to increase (with respect to the initial preference) with time during the oxidation of propylene. Initially, when the catalyst contains large amounts of cupric oxide, the oxidation of acrolein proceeds more rapidly. As the catalyst is gradually reduced, the amount of CuO decreases, the oxidation of acrolein becomes more difficult, and the selectivity increases. In this manner the contact composition regulates itself so as to favor the formation and greater stability of acrolein.

LITERATURE CITED

1. M. Ya. Rubanik, Yu. A. Snigurovs'ka, and M. A. Pointkovs'ka, Doklady Akad. Nauk USSR 2, 37 (1949).
2. Ya. B. Gorokhovatskii, M. Ya. Rubanik, and K. M. Kholyavenko, Doklady Akad. Nauk SSSR 125, 83 (1959).*
3. V. P. Ushakova, G. P. Korneichuk, and V. A. Roiter, Ukrainskii Khim. Zhur. 23, 910 (1957).
4. N. I. Popova, V. I. Belyaev, and R. N. Stukova, Izvest. Vostochnogo Filiala Akad. Nauk SSSR 7, 40 (1957).
5. O. V. Isaev, L. Ya. Margolis, and S. Z. Roginskii, Zhur. Obshchei Khim. 29, 1522 (1959).*
6. O. V. Isaev, L. Ya. Margolis, and I. S. Sazonova, Doklady Akad. Nauk SSSR 129, 141 (1959).*
7. N. I. Popova and E. E. Vermel', Doklady Akad. Nauk SSSR 124, 842 (1959).*
8. O. V. Isaev and M. Ya. Kushnerov, Doklady Akad. Nauk SSSR 124, 858 (1959).*

* See CB translation.

EXPLOSIVE DECOMPOSITION OF NITROUS OXIDE

B. B. Brandt and A. I. Rozlovskii

Industrial Institute of Nitrogen and Synthetic Organic Products

(Presented by Academician Ya. B. Zel'dovich, February 18, 1960)

Translated from Doklady Akademii Nauk SSSR, Vol. 132, No. 5, pp. 1129-1131, June, 1960

Original article submitted February 1, 1960

While studying the critical parameters in the inflammation of cyclohexane–nitrous oxide mixtures we were struck by the unusually low threshold fuel concentration in dilute mixtures: 0.33% C_6H_{12}. The heat of combustion of cyclohexane can barely heat such a mixture adiabatically to 400°C. Since combustion could not be sustained under these conditions, it is obvious that the combustion temperature T_b must be raised by the exothermic decomposition of nitrous oxide. We have therefore proposed the possible existence of a stationary flame in the decomposition of nitrous oxide. Let us recall that the self-inflammation of N_2O was predicted by D. A. Frank-Kamenetskii [1] and subsequently experimentally confirmed by Ya. B. Zel'dovich and V. I. Yakovlev [2]. Later on N_2O was found to ignite spontaneously when compressed in shock tube [3] ($T \approx 1400°K$).

We examined the propagation of flame through cold nitrous oxide ignited by point-impact from the standpoint of the "theory of the limit of slow flame propagation" [4]. As the heat is conducted from the reaction zone to adjoining layers of combustion products and lost, the reaction will slow down and the flame become extinguished. In fairly wide tubes, $d > d_{cr}$ (normally $d_{cr} \approx 5$ cm at 1 atm), heat transfer to the walls is insignificant and most of the heat is dissipated through radiation.

Heat losses increase in relative importance when the normal flame velocity u_n is reduced. At a certain minimum $u_n = u_{cr}$, we attain the critical conditions which set the concentration limits of flame propagation. For air–carbon monoxide mixtures the calculations of Ya.B. Zeldovich yielded $u_{cr} = 2$-3 cm/sec; subsequent exact measurements [5] on several mixtures of CO and hydrocarbons containing air yielded $u_{cr} = 3.1$-4.2 cm/sec. These data can essentially provide an answer to the basic problems involving the inflammability of N_2O.

One may assume that the product of intensity and the adsorption band width in unburned gas is very small in comparison with the total radiant energy produced in the combustion of N_2O. At the same time the heat transferred from a unit weight of combustion products by radiation is independent of the pressure. Therefore, under variable pressure the flame propagation limit does not depend on u_{cr} but on the combustion mass velocity $u\rho$ (ρ being the density), the magnitude of which determines the velocity of heat transfer. Since $u\rho \sim \sqrt{\Phi}$ [6], where Φ is the reaction rate in the flame, the heat losses from the reaction zone of any exothermic reaction of an order higher than zero decrease with increasing pressure p; when $p = p_{cr}$ stationary combustion becomes possible.

A rough estimate of p_{cr} can be made by assuming that $u_{cr} = 3$ cm/sec in any burning mixture at $p = 1$ atm. When applied to the decomposition of N_2O, this assumption should make the calculated p_{cr} slightly higher since the emission from O_2 and N_2 is much weaker than from CO_2 and H_2O and u_{cr} is expected to be greater in hydrocarbon mixtures than in N_2O. It seems that even very small amounts of NO (one of the products of N_2O combustion) substantially affect the radiation intensity. Let us also note that u_{cr} does not depend exclusively on the radiation intensity–other conditions being similar higher activation energies will also tend to increase it.

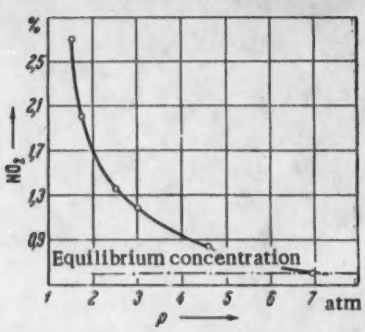

Fig. 1

At higher pressures the decomposition of nitrous oxide is known to be a monomolecular process, the raction follows first-order kinetics and the asymptotic (at $p = \infty$) rate constant $k_\infty = 4.2 \cdot 10^9 \cdot e^{-55000/RT}\,sec^{-1}$ [7]. Thermodynamically calculated $T_b = 1860°K$, while the equilibrium NO concentration in the reaction products is 0.61% (T_b is also independent of pressure). We calculated the thermal conductivity λ of the reaction products at $T = T_b$ by using the method and the collision parameters given by Hirschfelder [8]: $\lambda = 2.90 \cdot 10^{-4}$ cal/cm·sec·deg. The normal combustion theory [6] yields:

$$u_n = \sqrt{2\lambda(T_b)\,\theta^2(T_b)\,k_\infty(T_b)\,RT_0^2/pQ(T_b - T_0)\,T_b},$$

where $\theta = RT^2/A$, A being the activation energy, $T_0 = 290°K$, the temperature of the ignition gas, $Q = 1.95 \cdot 10^4$ cal/mole, the molar heat of reaction. In the absence of any heat losses $u_n = 1.7$ and 0.54 cm/sec, respectively, at 1 and 10 atm. Taking $u_{cr}p_{cr} = 3$ cm·atm/sec we get $p_{cr} = 3.1$ atm. Interpolating some more recent data [9] we get for our experimental conditions $k = 1.2 \cdot 10^{11} \cdot e^{-60900/RT}$, whence $p_{cr} = 1.2$ atm.

The critical inflammation conditions were experimentally determined in a stainless steel cylindrical bomb 61 mm in diameter and 545 mm long. To permit visual observation 5 window holes were punched at equal intervals along the resulting bomb. The charge was ignited by short-circuiting a current from a 220·12 v transformer across a copper wire 0.2-0.3 mm in diameter; the wire was attached to the electrode plugs at one end of the bomb.

It was thus experimentally demonstrated that the inflammation of cold N_2O is indeed possible. When the lower end of the vertically placed bomb is ignited $p_{cr} = 1.60 \pm 0.08$ atm. This value was fully reproducible. In several experiments, where a current from a 10-times-as-powerful transformer was used, the value of p_{cr} remained unchanged. The same value of p_{cr} was obtained in isobaric combustion; to achieve isobaric conditions a 40 liter shock-absorber bulb was filled with nitrogen at the same pressure and attached to the bomb prior to ignition.

To determine the effects of T_b on the critical inflammation pressure we added various amounts of nitrogen gas to the oxide. Experiments where the lower end of the bomb was ignited revealed that even small amounts of an inert gas could increase p_{cr} substantially: N_2(%) 4.5, 10.0; ΔT_b^0 61, 137; p_{cr} (atm) 2.15; 4.5.

Such an effect is equivalent to the well-known extension of concentration limits of inflammation caused by any increase in pressure. It is interesting to compare these results with the (obviously erroneous) proposal put forth by Spalding [10] that the concentration inflammation limits become wider with increasing pressures only in cases where the reaction inside the flame is of an order higher than one (actually any order in excess of zero will do).

When we ignited the tube at the upper end instead of at the lower, p_{cr} increased to 10 atm. It is known that in the two extreme cases of ignition from above or below the ratio between the critical concentrations of the deficient component π_{cr} may become as high as 1.20 [11], if the diffusion coefficient and the thermal conductivity remain the same. It is obvious that the corresponding change in Φ observed in our experiments at constant π and T_b results from a change in pressure. Due to the low order of reaction any pressure changes should in this case have relatively small effects. When ignition takes place at the top instead of at the bottom, the corresponding increase in p_{cr} (by a factor of 6.25) resembles the change produced by diluting the mixture with nitrogen. Extrapolating the relationship given above we find that $p_{cr} = 10$ atm when $N_2 = 13$-19% ($\Delta T_b = 179$-264°), or, in other words, the equivalent $\Delta\pi_{cr}$ is entirely reasonable.

The critical inflammation pressure calculated above should be compared with the one observed when the bomb is ignited from above, since we have analyzed the flame propagation without considering a very important external factor, namely, convection. Moreover, it is not very clear why the calculated p_{cr} is too low, instead of being too high, as one would have expected, although it is at least of the right order of magnitude.

One should also look into the practical aspects of the results obtained above. Nitrous oxide is a by-product in several industries, it is prepared in a pure form for medicinal purposes, compressed and usually burned without

the necessary precautions. In principle one can not exclude the possibility that it might become accidentally ignited by electrostatic discharge (a spark) when compressed adiabatically, and in a shock wave.

Let us note that we observed some very powerful explosions in our preliminary experiments where N_2O was ignited at p = 50 atm in a special apparatus [12] with a 70 cm^3 detonation chamber. Combustion in a dead space inside a stainless steel (Kh18N9T) connecting pipe 4 mm in diameter, 1.2 mm thick resulted (in one experiment at least) in rupture along the generatrix line and destruction of a 600 atm manometer. This indicates that the maximum pressure must have been somewhere between 1000 and 4000 atm.

The explosive decomposition of N_2O yields, among other products, appreciable amounts of NO_2, which seems to be formed from the combustion product NO. To determine the yield of NO a small amount of reaction products (determined from the bomb volume and the pressure drop) is slowly bubbled through a standardized solution of sodium hydroxide. The excess base is titrated potentiometrically on a glass electrode (without oxidizing the nitrite). The titration results were checked and confirmed in all cases by determining the NO_2 spectrophotometrically. Figure 1 shows how the NO_2 concentration depends on the initial pressure. The yield of NO increases with decreasing pressure which fact at first glance seems to be unusual. At the inflammation threshold the NO yield is 2.7%, while at high pressures NO approaches asymptotically the equilibrium concentration.

The combustion of mixtures containing $N_2 + O_2$ is always known to produce some NO. The concentration of this product does not depend on the type of fuel nor on the nature of combustion, but it is always below the equilibrium value for $T = T_b$ [13]. In our experiments the concentration of NO exceeds the equilibrium value. A similar effect was also noted in the slow decomposition of N_2O.

Further research will be needed to explain the formation of NO in excess of the equilibrium concentration.

LITERATURE CITED

1. D. A. Frank-Kamenetskii, Zhur. Fiz. Khim. 13, 738 (1939).
2. Ya. B. Zel'dovich and V. I. Yakovlev, Doklady Akad. Nauk SSSR 19, 699 (1938).
3. R. A. Strehlow and A. Cohen, J. Chem. Phys. 30, 257 (1959).
4. Ya. B. Zel'dovich, Zhur. Éksp. i Teoret. Khim. 11, 159 (1941)
5. G. K. Badami and A. C. Egerton, Proc. Roy. Soc. A 228, 297 (1955).
6. Ya. B. Zel'dovich and D. A. Frank-Kamenetskii, Zhur. Fiz. Khim. 12, 100 (1938); Ya. B. Zel'dovich, Zhur. Fiz. Khim. 22, 27 (1948).
7. L. S. Cassell, The Kinetics of Homogeneous Gas Reactions [Russian translation] (Moscow, 1937).
8. J. O. Hirschfelder, C. F. Curtiss, and R. B. Bird, Molecular Theory of Gases and Liquids (1954).
9. H. S. Johnston, J. Chem. Phys. 19, 663 (1951).
10. D. Spalding, Proc. Roy. Soc. A 240, 83 (1957).
11. N. P. Drozdov and Ya. B. Zel'dovich, Zhur. Fiz. Khim. 17, 134 (1943).
12. C. M. Cooper and P. J. Wiezevich, Ind. and Eng. Chem. 21, 1210 (1929).
13. Ya. B. Zel'dovich, P. Ya. Sadovnikov, and D. A. Frank-Kamenetskii, The Oxidation of Nitrogen During Combustion [in Russian] (Izd. AN SSSR, 1947).

THE EFFECTS OF BENZENE VAPOR ADSORPTION ON THE ELECTRICAL CONDUCTANCE OF TRANSPARENT PLATINUM FILMS OF VARIOUS SURFACE DENSITIES*

V. M. Gryaznov, V. I. Shimulis, and V. D. Yagodovskii

M. V. Lomonosov Moscow State University

(Presented by Academician M. M. Dubinin, February 4, 1960)

Translated from Doklady Akademii Nauk SSSR, Vol 132, No. 5, pp. 1132-1135, June, 1960

Original article submitted January 30, 1960

The adsorption of various compounds on the surface of a metallic film reduces its electrical conductance in direct proportion to the fraction of still uncovered surface [1-9]; this phenomenon is used for computing the number of conductance electrons in the metal which are tied down by a single adsorbed molecule [5-7].

Such calculations require the appropriate data on the homogeneity of the metallic surface covered by the adsorbate.

In this work we have investigated the effects of benzene vapor at 20° on the electrical conductance of transparent platinum films, which were prepared by subliming the metal at a residual pressure of $1 \cdot 10^{-7}$ mm on the walls of a glass cell. Benzene vapor was introduced into the cell at a constant rate of $(3.8 \pm 0.3) \cdot 10^{14}$ molecules per minute, the rate being slower than the rate at which adsorption equilibrium is established.

The vapor initially adsorbed on a fresh platinum film is very tightly bound, and similar observations have been made on palladium films [10]. Any benzene adsorbed after the initial permanent adsorption is over can be removed by pumping at room temperature, while the strongly adsorbed benzene can not be desorbed below 250°C. Benzene adsorption on glass is fully reversible and constitutes about 50% of the reversible adsorption on an equal visible platinum film surface at the same pressure.

The electrical conductance of all the films we investigated decreases while the permanent adsorption of benzene vapor takes place (see sections AB of the curves in Fig. 1); subsequently, as the surface becomes extensively covered, the conductance may increase or decrease, depending on the amount of metal per unit of visible surface. Figure 1 shows three typical curves representing the change in $(\lambda - \lambda_0)/\lambda_0$, where λ_0 is the electrical conductance of the film prior to the introduction of benzene vapor. Reversible adsorption on a film with an effective thickness of 10 A restored the electrical conductance to its initial value (section BC of curve 1). The electrical conductance of films 10-20 A thick (effective thickness) changes very little during the reversible adsorption of benzene (see section CD, curve 2) but decreases when benzene is pumped off. Though reversible adsorption of films 20-50 A thick does decrease their electrical conductance (section BC, curve 3), it does so to a much lesser extent than does permanent adsorption. When the reversibly adsorbed benzene is pumped off, the electrical conductance in this case does not decrease but increases instead to the level which corresponds to the completion point of permanent adsorption (section CD, curve 3).

* The paper was presented at the Moscow Conference on Organic Catalysis, November, 1959.

The Effect of Permanently Adsorbed Benzene on the Electrical Conductance of Platinum Films of Various Surface Densities

Film No.	Film wt, mg	No. of Pt atoms per 1 cm² N·10⁻¹⁶	Effective film thickness, Å	Electrical conductance before the introduction of benzene λ_0	No. of permanently adsorbed benzene molecules per 1 cm² N·10⁻¹⁴	$\Delta n \cdot 10^{-14}$	$-\frac{\lambda - \lambda_0}{\lambda_0}$, %	β
1	0,21	1,3	20	1,2970	4,3	1,4	0,82	0,4
2	0,46	1,6	24	0,2752	0,6	0,2	0,06	0,4
3	0,53	1,9	29	1,4133	2,7	0,5	1,00	2,2
4	0,60	1,9	29	1,1634	1,0	0,3	0,28	1,8
5	0,82	2,2	34	0,9174	2,2	0,3	0,42	0,4
6	0,36	2,5	38	1,2372	6,6	0,9	0,25	1,5
7	0,83	2,6	39	1,2149	1,4	0,4	0,37	1,2
8	1,01	3,1	50	1,1832	2,6	0,4	0,24	1,2

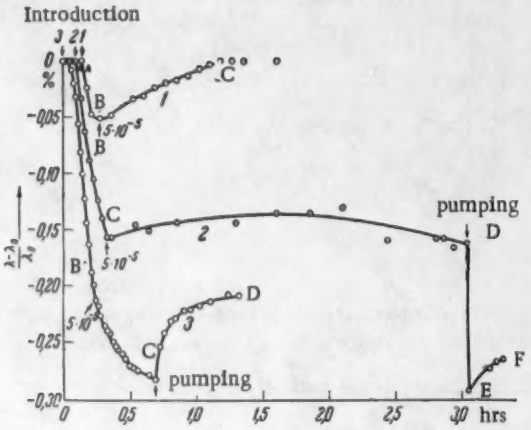

Fig. 1. The relative change in the electrical conductance of platinum films of various surface densities as a function of time from the moment benzene vapor is introduced.

The decreasing electrical conductance of platinum films observed during the permanent adsorption of benzene indicates that the benzene molecules can tie down some of the conductance electrons even when there are great variations in the surface density of the metal. When the reversible adsorption of benzene affects the electrical conductance in just the opposite manner, as was observed on films with an effective thickness of 10 A and 20-50 A, we can assume that the structural differences are extremely great. It is a known fact (see [11]) that if the surface density is low, a great number of the metal granules deposited on the carrier surface still remain unattached to each other. It seems that the electrical conductance of such a system, platinum–glass, may increase when benzene is adsorbed between the metal granules.

In denser films the particles are linked through metallic "bridges". The reversible adsorption of benzene takes place primarily on the metal, decreasing its electrical conductance by tying down some of the conductance electrons, so that the removal of the reversibly adsorbed benzene increases the conductance. For certain film surface densities the effects of reversible benzene adsorption on the metal and on the glass surface between granules may be compared in magnitude, in which case the electrical conductance would not change to any large extent, as is shown by section CD of curve 2 in Fig. 1. But the benzene adsorbed on glass is removed much more readily by pumping than that adsorbed on platinum. That is why at first the pumping results in decreased electrical conductance, but subsequently, as the benzene reversibly adsorbed on platinum is removed, the conductance increases (sections DE and EF of curves 2 in Fig. 1).

To find out how the electrical conductance of platinum films of various surface densities is related to the amount of permanently adsorbed benzene, we carried out a series of experiments, the results of which are presented in the table.

Films Nos. 4 and 6-8 had identical electrical conductances right after the sublimation of platinum was completed, but subsequent heating at 80-100°C affected them variously, with the maximum variation in λ_0 being 6%. Films Nos. 6 and 7, though they had similar surface densities and electrical conductances, differed by a factor of 4 in the amount of benzene permanently adsorbed per cm² of visible surface. Previously investigated platinum films with an effective thickness of 77-85 A also gave λ_0 values which could not be represented as a simple function of surface density [6] and would vary by as much as 4% on various samples with the same surface density.

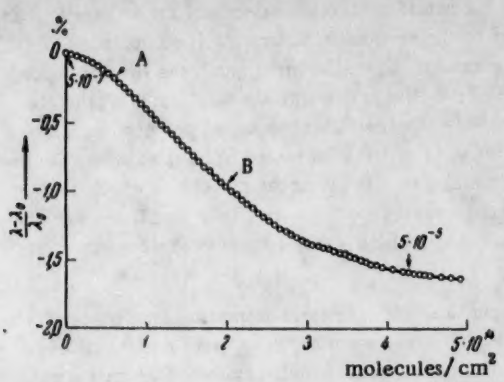

Fig. 2. The relative change in the electrical conductance of platinum film No. 1 as a function of the number of benzene molecules adsorbed per 1 cm² of visible surface.

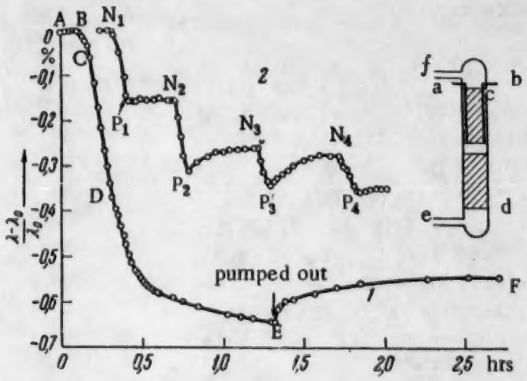

Fig. 3. The effects of conditions prevailing during the introduction of benzene vapor on the relative change in the electrical conductance of platinum films.

These facts indicate that the structure of platinum films depends to a great extent on hard-to-regulate factors in the sublimation and crystallization.

When the electrical conductance is plotted against the number of adsorbed benzene molecules, each one of the films listed in the table gives a curve with a linear segment, despite the variation in properties. Figure 2 shows that the linear portion of the permanent adsorption curve gives $(\lambda-\lambda_0)/\lambda_0$ change of 0.8% for $\Delta n = 1.4 \cdot 10^{14}$ benzene molecules per 1 cm² of film No. 1. The corresponding values $\lambda-\lambda_0/\lambda_0$ and Δn for the other films are listed in the table. The same table gives values of β, the average number of platinum conductance electrons tied down by one benzene molecule. We calculated the values of β with the help of an equation used in [5-7]. β was found to vary from 0.4-2.2 and no simple relationship between it and the surface density could be detected.

When the adsorption of benzene vapor on nickel films was investigated [7], three of the films gave a value of β close to 6 and, hence, it was concluded that 6 covalent bonds are formed between the benzene molecule and the film. Yet, when the electrical conductance of two other nickel films, prepared under similar conditions [7], was plotted against the amount of benzene adsorbed, the slopes of the linear sections differed considerably from the average value for the first three films.

It can be shown that the simplifying approximations used for calculating β do not represent the true phenomena. A linear relationship between the electrical conductance of films and the amount of adsorbed material does not necessarily prove that the centers being filled are homogeneous; such a relationship is also possible on films with centers of various adsorption potentials. The only conditions are that the relative number of these centers be constant on each section of the film, and that the adsorbed molecules should either remain attached to their respective centers or move very slowly from one center to another. Under these conditions the electrical conductance of the film will change, on the average, by a constant amount each time a molecule is adsorbed provided the fraction of surface covered has not been reduced too drastically; however, the change will only represent a certain over-all average limited to a fixed range of actual electronic interactions between the adsorbate molecule and the metal. This range should widen at lower temperatures due to an increased lifetime for the molecules on their adsorption centers. We have discovered that at 20°C, even if a very small fraction of the film surface is covered, benzene vapor is adsorbed simultaneously on centers of varying adsorption potentials. This became particularly apparent in experiments using a cyclindrical cell where the contact wires (a, b, in Fig. 3) used to measure the electrical conductance were placed only under the upper half of a dense platinum film extending from c to d. When benzene vapor was introduced into the cell through tube e the electrical conductance of the upper half of the film remained unchanged as long as benzene was being adsorbed on the lower half of the film (see section AB in Fig. 3). After this, the electrical conductance decreased linearly (section CD) during the permanent adsorption of benzene, then much more slowly (section DE) during the reversible adsorption.

When benzene vapor was introduced through tube f, the electrical conductance declined immediately (point N_1 on curve 2 of Fig. 3). If the flow of benzene is stopped before the permanent adsorption is completed (point P_1 on Fig. 3), the electrical conductance remains practically constant. If, on the other hand, the flow of vapor is stopped after the permanent adsorption on the upper portion of the film is over (points P_2, P_3, and P_4), the electrical conductance increases just as in the case where the reversibly adsorbed benzene is pumped out (see section EF of curve 1). Similar results were obtained when the two film sections were separated from each other (see the design in Fig. 3). It is hard to explain these facts except by assuming that the benzene molecules which at first occupied low adsorption potential centers on the upper film section subsequently moved down to fill the vacant centers on the lower portion of the film (the electrical conductance of which was not measured) where they could be more strongly adsorbed.

The data presented above indicate that both the permanent and the reversible adsorption take place on the film section adjoining the vapor inlet before the permanent adsorption can even begin on more remote film sections. It takes about 10 minutes at 20°C to redistribute adsorbed molecules. It is quite evident that such a redistribution was practically absent in experiments carried out at 90 or 77°K [7], and, consequently, the reported relationship between the electrical conductance of the films and the number of adsorbed molecules was inadequate for any quantitative calculations dealing with the electronic interactions between the benzene and the metal. By studying the effects of adsorption and desorption processes on the electrical conductance of metallic films, we should be able to detect the redistribution of the adsorbate among centers of varying adsorption potentials and compute the average time spent by the molecules on these centers.

LITERATURE CITED

1. R. Suhrman, Catalysis, Electronic Phenomena [Russian translation] (Moscow, 1958) p. 334.
2. W. M. H. Sachtler and G. Dorgelo, Bull. Soc. Chim. Belg. 67, 7-8, 465 (1958).
3. R. Suhrman, B. Hahn, and G. Wedler, Naturwiss. 44, 3, 60 (1957).
4. R. Suhrman and G. Wedler, Z. Phys. Chem. Neue Folge 10, 3-4, 184 (1957).
5. R. Suhrman, G. Wedler and D. Schliephake, Z. Phys. Chem. Neue Folge 12, 1-2, 128 (1957).
6. R. Suhrman, G. Wedler, and H. Gentsch, Z. Phys. Chem. Neue Folge 17, 5-6, 350 (1958).
7. R. Suhrman, G. Wedler, and G. Krüger, Z. Elektrochem. 63, 2, 155 (1959).
8. R. Suhrman and Y. Mizushima, et al., Z. Phys. Chem. Neue Folge. 20, 56, 332 (1959).
9. P. Zwietering, H. L. T. Koks, and C. van Heerden, J. Phys. Chem. Solids 11, 1-2, 18 (1959).
10. V. D. Yagodovskii, Doklady Akad. Nauk SSSR 122, 3, 437 (1958).*
11. G. V. Rosenberg, The Optics of Thin Metallic Films [Russian translation] (Moscow, 1958) p. 18.

* Original Russian pagination. See C. B. Translation.

THE TRANSFER OF EXCITATION ENERGY AND THE SENSITIZATION OF CHEMICAL REACTIONS DURING THE RADIOLYSIS OF SOLUTIONS OF ORGANIC DISULFIDES

V. A. Krongauz and Kh. S. Bagdasar'yan*

The L. Ya. Karpov Physicochemical Institute

(Presented by Academician S. S. Medvedev, February 6, 1960)

Translated from Doklady Akademii Nauk SSSR, Vol. 132, No. 5, pp. 1136-1139, June, 1960

Original article submitted February 6, 1960

In publications [1, 2] a description is given of an investigation of the radiolysis of dilute solutions of organic peroxides and azocompounds in benzene. It has been shown that certain aromatic substances which decompose easily into radicals (benzoyl peroxide, phenylazotriphenylmethane) are then decomposed in the solutions with yields considerably greater than would correspond to the direct effect of the irradiation. This is believed to be connected with a very effective transference of excitation energy from the benzene to the solute.

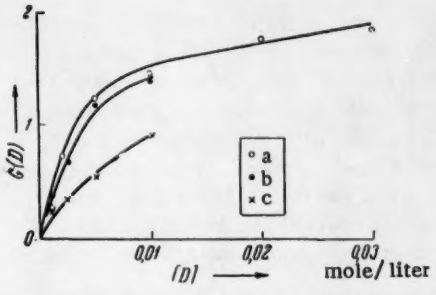

Fig. 1. Relationship of the yield on decomposition of disulfides to their concentration in the solutions. a) Diphenyldisulfide (DFD); b) dibenzyldisulfide (DBD); c) dibenzoyldisulfide (DBOD). The points on the curves represent the mean values from several independent experiments.

In this paper we describe a continuation of this work, in which there is studied the effect of the chemical nature of the acceptor on the effectiveness of the energy transfer, and on the degree to which this energy is utilized in the decomposition of the acceptor. The irradiation of dilute solutions of organic disulfides in benzene has been studied. Disulfides containing aromatic and aliphatic substitutents have been studied.

The thiyl radicals which are formed by the dissociation of disulfides are comparatively inactive, and on recombining with each other form the original molecule. Hence, the rate of radiolytic decomposition of disulfides in benzene solution cannot be directly determined from the reduction in the disulfide concentration, as has been confirmed by specially arranged experiments.

To prevent the reverse reaction from taking place in the disulfide solution, diphenylpicryl hydrazyl (DFPH) was added. The radicals from the DFPH interact with the radicals formed by radiolysis, and thus prevent the recombination of the thiyl radicals with each other.

The solutions were carefully freed from air, and radiolysis conducted by means of the gamma-radiation from Co^{60}. The yield of radicals produced per 100 ev of radiant energy absorbed by the solution was determined by the reduction in the concentration of DFPH. Since the destruction of one molecule of disulfide resulted in formation of two radicals, the yield of products obtained by decomposition of the disulfide is obtained by dividing

* A. N. Silant'eva took some part in the work.

Disulfide	$\frac{k'_3}{k_2}$	$\frac{k_1 k'_5}{k'_4 + k'_5}$
DFD	250±15	0.02±0.002
DBD	200±15	0.02±0.002
DBOD	100±15	0.02±0.002

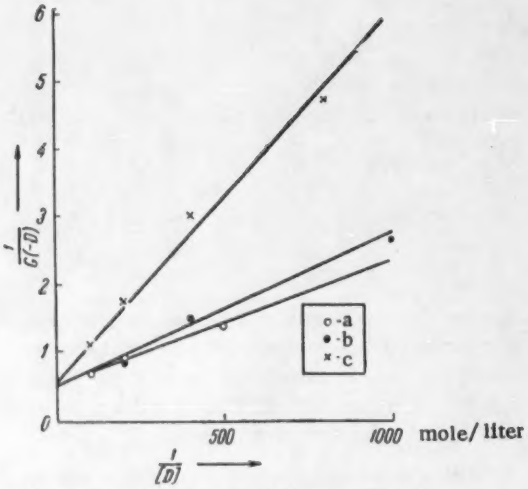

Fig. 2. Relationship of $1/G^0(-D)$ to $1/[D]$. The symbolism is the same as in Fig. 1.

by 2 the difference between the radical yield from the solution and from the pure solvent. The concentration of the DFPH was measured by means of a spectrophotometer of type SF-4 at a wave-length of 520 mμ.

For the determination of the yield of radicals from the solution by means of DFPH, we first of all determined the critical concentration of the latter: that is, the minimum concentration was found for which it could be assumed that all the radicals formed by the radiolysis would react with the DFPH [3]. The concentration of the DFPH was varied between $5 \cdot 10^{-4}$ and $2 \cdot 10^{-3}$ M, which exceeded the critical value in all cases.

Figure 1 depicts the curve of the relationship between the radiation yield of decomposition products from diphenyldisulfide (DFD), dibenzyldisulfide (DBD), and dibenzoyldisulfide (DBOD), and the concentration of these substances in the solution.

The radiation yield calculated from the slope of the initial portions of the curves for the decomposition of various disulfides, based on 100 ev of energy absorbed by the disulfides themselves, were: for DFD and DBD, ~ 1000; and for DBOD, ~400 molecules. The dissociation energies of DFD and DBOD do not, apparently, exceed 30 kcal/mole, while that of DBD is not greater than 70 kcal/mole [4, 5]. This must mean that the yields of the decomposition of these disulfides at low concentrations in the solution exceeds by a least one order of magnitude the maximum yield which could be expected if it were assumed that the energy absorbed by the dissolved substances was completely consumed in their dissociation. It is probable that a transfer of energy takes place in the disulfide solutions from the solvent to the dissolved substances.

Starting from the assumption that such a transfer does occur, and that a stationary state has been attained, we arrive at the following relationship [1] between the yield from the decomposition of the disulfide $G^0(-D)$, and its concentration in the solution [D]:

$$G^0(-D) = \frac{100 k_1 k'_5 k'_3 [D]}{(k_2 + k'_3 [D])(k'_4 + k'_5)}, \qquad (1)$$

where k_1 is the rate constant for the formation of excited benzene molecules under the influence of 1 ev of absorbed energy ; k_2 is the rate constant for the spontaneous deactivation of these molecules; k'_3 is the rate constant for the transfer of energy from the benzene to the disulfide; k'_4 and k'_5 are the rate constants for the deactivation and dissociation of the excited disulfide molecules. When Eq. (1) is applied to concentrations not greater than about 0.01 M, its fall, owing to the exchange of energy is considerably greater than the decomposition due to the direct effect of the irradiation.

Figure 2 gives the relationship between $1/G^0(-D)$ and $1/[D]$, which turns out to be linear, in harmony with Eq. (1). The intersections of these straight lines with the axis of ordinates gives the value of the quantity $(k'_4 + k'_5)/100 k_1 k'_5$ for the relevant disulfide, and the slopes of the lines give the values of k'_3/k_2, as in the table.

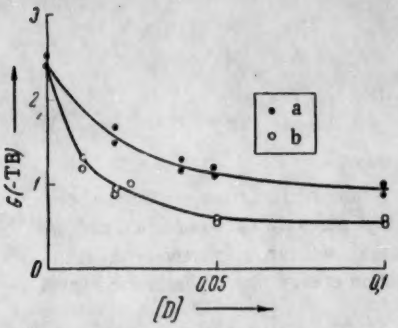

Fig. 3. Relationship between G(−TB) and [D] for DBD and DBOD.

The ratios k'_3/k_2 denote the effectiveness of the transfer of energy from the benzene to the disulfides, and the magnitudes of $k_1 k'_5/(k'_4 + k'_5)$ give the probability of the decomposition of the excited disulfide molecules into radicals multiplied by the constant k_1 which is characteristic for the given solvent.

The table shows that DFD and DBD behave as identical energy acceptors, while DBOD receives the transferred excitation energy with only about half the effectiveness of these. At the same time, the decomposition of the excited molecules takes place with all three molecules with approximately the same probability.

Since $k'_5/(k'_4 + k'_5) \leq 1$, the minimum magnitude of k_1 is 0.02 molecules per 1 ev. Thus, for 100 ev energy provided by irradiation absorbed in the solution, there must be formed not less than two activated benzene molecules capable of effective transfer of their energy to the disulfide.

It may be assumed that in the radiolysis of solutions of aromatic disulfides the excitation energy of the benzene is in the first instance by the phenyl nuclei of the acceptor, and afterwards distributed to other parts of the molecule. If this is so, a comparison of the data for the diphenyl- and the dibenzyl-disulfides suggests that the presence of the aliphatic CH_2 group between the phenyl rings and the disulfide group does not impede the migration of energy from the phenyl nuclei to the S−S group.

We set out below the radiation yields from the decomposition of 0.01 M solutions of all the disulfides which we have investigated.

Diphenyl-disulfide	Dibenzyl-disulfide	Dibenzoyl-disulfide	Methoxy-disulfide	Diallyl-disulfide	Diethyl-disulfide	Dioctyl-disulfide
1.5	1.4	0.9	0.8	0.7	0.3	0.3

The fact that the yields from the decomposition of diethyl- and dioctyl-disulfides are identical suggests the conclusion that the lengthening of the hydrocarbon chain exerts no appreciable effect in reducing the probability of decomposition of the excited disulfide molecule. It may be supposed that the excitation energy can migrate without appreciable loss via the aliphatic chain to the S−S bond. The much lower yield from radiolysis of the aliphatic disulfides as compared with the aromatic may be possibly connected with the considerably lower effectiveness of the intermolecular energy transfer [1]. Since the dissociation energies of DBD and the aliphatic disulfides amount to around 70 kcal/mole, then it is a natural supposition that the quanta of energy transferred from the benzene to the acceptor are not smaller than 3 ev.

It has been shown earlier that addition to a benzoyl peroxide solution in benzene of such energy acceptors as anthracene, phenanthrene, benzoic anhydride, phenylazotriphenylmethane, and diazoaminobenzene, leads to an appreciable reduction in the yield from the radiolytic decomposition of the benzoyl peroxide [1, 2, 6]. This is evidently connected with competition between the acceptors present for the transfer of energy from the activated benzene molecules.

Figure 3 shows the relationship between the yield from the decomposition of 0.005 M benzoyl peroxide and the concentration of DBD and DBOD. (It was established by separate experiments that the effect of DBD and DFD on the radiolysis of benzoyl peroxide was practically the same, while diethyldisulfide at concentrations lower than 0.02 M exercised no detectable protecting influence).

It can be seen from the figure that DBOD exerts a considerably greater protecting influence than DBD. With increase in the disulfide concentration, the yield from the decomposition of the peroxide approaches a limiting value. If we suppose that the energy transfer takes place only from the excited benzene molecule to the competing acceptors, it is easy to obtain the relationship:

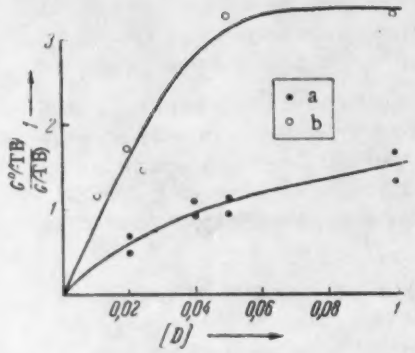

Fig. 4. Relationship between $G^{\circ}(-TB)/G(-TB)-1$ and (D) for DBD (a) and DBID (b).

$$\frac{G^{0}(-TB)}{G(-TB)} - 1 = \frac{\frac{k_3'}{k_2}[D]}{1+\frac{k_3}{k_2}[TB]}, \qquad (2)$$

where $G^{0}(-TB)$ and $G(-TB)$ are the radiation yields from the decomposition of the benzoyl peroxide in the absence and in the presence of the protecting additive, respectively; k_3 is the rate constant of the excitation energy transfer from the benzene to the peroxide.

When (TB) is constant, the magnitude of the left-hand side of Eq. (2) ought to be proportional to [D]. It can be seen from Fig. 4 that for the disulfides which we have investigated this proportionality relationship is not confirmed. As in the earlier work [6], we have supposed that the energy may be transferred also from the excited disulfide molecules to benzoyl peroxide. Again assuming that a stationary state exists, we obtain the relationships:•

$$\frac{G(-TB)}{G^{0}(-TB)} = \left(1+\frac{k_3'}{k_3}\frac{[D]}{[TB]}\alpha\right)\times\left(1+\frac{\frac{k_3'}{k_3}\frac{[D]}{[TB]}}{\frac{k_2}{k_3}\frac{1}{[TB]}+1}\right)^{-1}, \qquad (3)$$

where $\alpha = \varkappa = \frac{k_6[TB]}{k_4'+k_5'+k_6[TB]}$, and k_6 is the rate constant for the transfer of energy from the disulfide to the peroxide. The probability of transfer of energy from the disulfide to the peroxide may be regarded as α.

The decomposition of the benzoyl peroxide in the presence of DBD and DBOD is in agreement with Eq. (3), which, after some rearrangements permits of a graphical determination of the values of α and k'_3/k_2. For DBD and DBOD the values of k'_3/k_2 as determined by their protecting influence are approximately 150 and 400. The correspondence between the values of k'_3/k_2 for DBD obtained from the data on the rate of its decomposition and from its protective effect, is satisfactory. For DBOD such an agreement is not found; measured by its protective effect the DBOD seems to be about four times more effective as an energy acceptor than would be supposed on the basis of its rate of radiolytic decomposition. The reason for this difference is at present uncertain.

The authors wish to express their thanks to V. N. Vasil'eva for providing them with the disulfides.

LITERATURE CITED

1. V. A. Krongauz and Kh. S. Bagdasaryan, Collected Works on the Effect of Ionizing Radiation on Inorganic and Organic Systems [in Russian] (1958) p. 205; Doklady Akad. Nauk SSSR 114, 4, 829 (1957); Zhur. Fiz. Khim. 32, 3, 717 (1958).
2. V. A. Krongauz and Kh. S. Bagdasaryan, Doklady Akad. Nauk SSSR 127, 5, 1047 (1959).••
3. A. Chapiro, J. Chem. Phys. 51, 165 (1954).
4. E. N. Tur'yanova and V. N. Vasil'eva, Works presented at the 5th Congress of the Chemistry of Sulfur and Azo-organic Compounds Contained in Petroleum and Petroleum Products [in Russian] (Bashkirsk AN SSSR, 1960).
5. J. Franklin and H. Lumpkin, J. Am. Chem. Soc. 74, 1023 (1952).
6. V. A. A. Krongauz and Kh. S. Bagdasar'yan, Doklady Akad. Nauk SSSR 116, 5, 817 (1957).••

• The detailed kinetics of the analysis of the results obtained in this and earlier published works will be provided in a later article.

•• Original Russian pagination. See C. B. Translation.

THE ELECTRICAL PROPERTIES OF SYSTEMS COMPOSED OF POLYMERS AND METALS

S. D. Levina, K. P. Lobanova, and N. A. Platé

Institute of Electrochemistry, Academy of Sciences, USSR

(Presented by Academician A. N. Frumkin, February 24, 1960)

Translated from Doklady Akademii Nauk SSSR, Vol. 132, No. 5, pp. 1140-1143, June, 1960

Original article submitted February 24, 1960

A series of studies and monographs devoted to the semiconductor properties of organic compounds has appeared in recent years. In several of these studies it has been shown that the introduction of metal atoms into the molecules of complex aromatic compounds has exerted an influence on the physical properties of the latter. Thus, Vartan'yan [1, 2] and Eley [3, 4] have discovered that copper and magnesium atoms introduced into phthalocyanin molecules have an effect on the electrical conductivity of these compounds. Topchiev, Geiderich, Davydov, Kargin, et al. [5] have shown that polyacrylonitrile acquires semiconducting properties in the range 300 to 900° after heat treatment. At 200° the resistivity of polyacrylonitrile is equal to about 10^{12} ohm·cm. Introduction of copper salts reduces the resistivity to 10^{2} ohm·cm (300°).

The task of the present investigation was the study of the electrical properties of composite materials in which metal particles alternate with extremely thin layers of practically nonconducting polymers. It appeared to be of interest to elucidate whether electron migration was possible in these conditions and in what way the structure of the organic layer affected this process.

In connection with the proposed purpose, use was made of highly dispersed powdered metals. First of all, "semipassive" benzolated iron, obtained by the reduction of the oxide in hydrogen at 450-500°, was employed. Normally, in such conditions of reduction, pyrophoric iron is formed. However, as shown by Burshtein, Pavlova, and Kiperman [6, 7] and also Shurmovskaya and Burshtein [8], if iron of this kind, after reduction in hydrogen and before contact with air, is put into benzene and then dried, it loses its pyrophoric character. The benzene adsorbed on the iron prevents the formation of thick oxide films. A film is formed on the surface of the iron, which is equivalent to a unit cell of Fe_3O_4. The diameter of these iron particles is of the order of tenths of a micron.

The first subject for investigation was a composite material made from the iron described above and polyisoprene (natural rubber) which was added in the form of a 2% benzene solution. Disc-shaped specimens were molded at a pressure of 500-1000 atm. The orientation experiments concerned with the measurement of the electrical resistivity of these samples showed that the introduction of 1% polyisoprene into the composition sharply reduced the conductivity of the iron. At higher rubber concentrations this effect was even more marked. *

The dependence of the logarithm of conductivity (log σ) on temperature (1/T) for a sample containing 20% rubber in the range from 50 to −40° was linear, with increase of conductivity with rise in temperature. In the

* The resistivity of samples molded from pure powdered iron was about 10^{-3} ohm·cm; at about 1% rubber it was 0.125 ohm·cm; with 5% 0.127 ohm·cm; with 10% 3.73 ohm·cm; with 20% 16.18 ohm·cm.

Nos.	Composition	Temperature range, °C		Resistivity change, ohm · cm	
		from	to	from	to
1	Iron + polystyrene	150	−63	0.5	21.8
2	Iron + polyisoprene	150	−52	0.23	1.77
3	Iron + polymethylmethacrylate	150	−45	3.15	87.5
4	Iron + polyacrylonitrile	50	−65	0.38	3.88

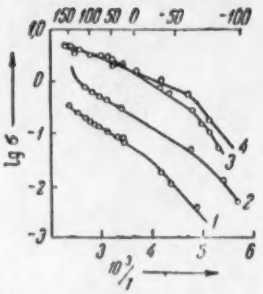

Relationship between the logarithm of conductivity (log σ) and temperature (1/T). Compositions with iron with different polymers: 1) polymethylmethacrylate; 2) polystyrene; 3) polyacrylonitrile; 4) polyisoprene.

temperature range indicated the resistivity of the sample changed from 11.2 ohm · cm to 50 ohm · cm. A resistivity-temperature relationship of this form is typical of semiconductors. The thermoelectric emf and the Hall coefficient had the same sign as type p semiconductors. The thermoelectric emf was equal to about 5 μv/degree. The activation energy ΔE calculated from the equation $\rho = \rho_0 e^{\Delta E/kT}$ was equal to about 0.1 ev. Similar values were also found for the thermoelectric emf and the conductivity of compositions of iron and polystyrene.

It can be seen from what has been stated that the composition obtained acquires a series of new properties differing from the properties of the components of the system. It is also essential to emphasize that it cannot be assumed that conduction in these systems may be attributed to the direct contact of the metal particles with one another. In this case temperature dependence of conductivity, typical of metals, which also occurs in samples pressed from pure iron powder, would be observed.

In order to achieve a more even distribution of the polymer and a stronger adhesion of the polymer to the iron, work was carried out using the method developed by V. A. Kargin and N. A. Platé [9] of vibration milling metal powders in a monomer medium. The essential feature of this method lies in the fact that during the grinding process the metal particles, due to the exposure of fresh, energetically active surfaces, initiate polymerization of the monomer medium in which they are located. At the completion of the run polymers formed in the continuous phase are washed out with appropriate solvents, after which the metallic powder is dried and pressed into the form of discs.

In view of the high degree of dispersion of the iron employed by us, further size reduction during vibration milling could not be expected. In these conditions, however, the exposure of fresh surface must occur as a result of the damaging or removal of the extremely thin oxide film on the surface of the iron particles.

The following monomers were used in these experiments: isoprene, styrene, methylmethacrylate, as compounds with double bonds, and also acrylonitrile.

For compositions of this type, as may be seen from Fig. 1, a linear relationship between log σ and 1/T was also observed in the temperature range from +150 to −55° in which region the resistivity of the samples changed on an average by a factor of 20 (see the table). In the low temperature region, from −55 to −120°, the curves are steeper. The energy of activation, expressed in electron-volts, of different samples ranged from 0.08 to 0.12. It must be emphasized that for all the compositions formed by vibration milling the thermoelectric emf and the Hall effect had the same sign as n-type semiconductors. The thermoelectric emf was equal to 12-14 μv/deg. As regards the Hall effect, it was not possible to measure this in every case. The Hall constant for the iron-polystyrene composition at room temperature is equal to $2.9 \cdot 10^2$ cm³/coulomb. For the sample of iron and acrylonitrile the Hall constant was equal to $4.1 \cdot 10^2$ cm³/coulomb.

From a comparison of the properties of compositions obtained by the addition of ready-made polyisoprene with those which were obtained using the method of polymerizing isoprene during vibration milling it may be

seen that they differ with respect to a whole series of properties. Thus, in the first case, the sign of conductivity is the same as for p-semiconductors; in the second case, it is the same as for n-semiconductors. The thermoelectric emf increased from 5 to 12-14 μv/deg. The specific resistance in the second case was great as in the first. These differences testify to the fact that, when the compositions are made by the second method, the polymer distribution is apparently more even, and also, possibly, a different type of bonding exists between the surface of the metal particles and the organic substance. Analysis of the elements indicated that the total organic content of an iron-polyisoprene composition (made by vibration milling) was equal to 5.1%, in which the proportion of carbon amounted to 4.53% and that of hydrogen 0.56%. In isoprene (C_5H_8) the weight of carbon exceeds the weight of hydrogen by a factor of 7.5 while in the sample under discussion the ratio was equal to 4.55/0.56 = 8. As the ratio of the quantities of carbon and hydrogen is roughly the same as in the monomer, this argues for the fact that the principal reaction during vibration milling was a polymerization reaction.

Inasmuch as the surface area of 1 g of iron in our samples was equal to about 1.5 m^2 while the organic content according to the analysis was 51 mg, it may thence (if it is assumed that an adsorbed molecule occupies 25 A^2 of the surface) be deduced that 51 mg is 75 times greater than the quantity necessary to cover the whole surface with a monolayer. This fact also supports our supposition that polymerization of the isoprene occurred during the vibration milling of the iron. However, polymerization probably does not take place over the whole surface of the iron but only in the neighborhood or on those particles on which the thin oxide film suffers damage during vibration milling. Apparently the formation of grafted polymer occurs at these points, and judging by the fact that the electrical resistivity of the sample (as shown above) increases *, this polymer more or less evenly covers the iron; the structure of these films is interwoven. Analysis of the elements in the case of composition with polymethylmethacrylate and polyacrylonitrile gave more complicated ratios of the elements. It is possible that other reactions also occurred along with the polymerization reaction. These phenomena will be studied in greater detail in the future. At present one may confine oneself to the statement that the quantity of material associated with the metal exceeded a monolayer in the case of methylmethacrylate by a factor of 45 and in the case of acrylonitrile by a factor of 40.

Study of the system under discussion is currently continuing. Work is also being carried out with systems consisting of other metals and other polymers in which electron migration can take place more readily.

We express our gratitude to Academician A. N. Frumkin, Academician V. A. Kargin, and Professor R. Kh. Burshtein for their help and interest in this work.

LITERATURE CITED

1. A. T. Vartan'yan and I. A. Karpovich, Zhur. Fiz. Khim. 32, 178 (1958).
2. A. T. Vartan'yan, Zhur. Fiz. Khim. 22, 769 (1948).
3. D. D. Eley, Nature 162, 819 (1948).
4. D. D. Eley, Res. in Appl. Ind. 12, 293 (1959).
5. A. V. Topchiev, M. A. Geiderich, B. É. Davydov, V. A. Kargin, et al., Doklady Akad. Nauk SSSR 128, 312 (1959).* *
6. R. Kh. Burshtein and M. I. Pavlova, Author's Certificate No. 64304, Class 43-4/01 (December 1, 1944).
7. R. Kh. Burshtein and S. L. Kiperman, Collection of Articles on the Alkaline Elements [in Russian] (1947) p. 93.
8. N. A. Shurmovskaya and R. Kh. Burshtein, Zhur. Priklad. Khim. 30, 1176 (1957).* *
9. V. A. Kargin and N. A. Platé, Vysokomolek. Soed. 1, 330 (1959).

* In comparison to which polyisoprene is added already prepared.

** Original Russian pagination. See C. B. Translation.

RELATION BETWEEN THE DIFFUSION COEFFICIENT AND AMOUNT OF ADSORPTION ON ACTIVE CARBONS

D. P. Timofeev and I. T. Erashko

Institute of Physical Chemistry, Academy of Sciences, USSR

(Presented by Academician M. M. Dubinin, December 25, 1959)

Translated from Doklady Akademii Nauk SSSR, Vol. 132, No. 5, pp. 1144-1147, June, 1960

Original article submitted December 22, 1959

Diffusion coefficients in porous adsorbents change during the sorption process to a different extent, depending on the degree to which the sorption volume is filled, the structure of the adsorbent, the nature of the sorbed substance and some other factors [1-7]. A study of these relationships is of interest in determining rates of sorption processes which take place in the "internal-diffusion" region, and also in explaining the mechanism whereby the substance is transported in the adsorbent pores. There are few investigations in this region, and in some cases the results obtained are of a contradictory nature. Least clear are the reasons for the decrease in diffusion coefficient on filling up of the sorption volume, which has been reported in a series of papers [3, 6, 7].

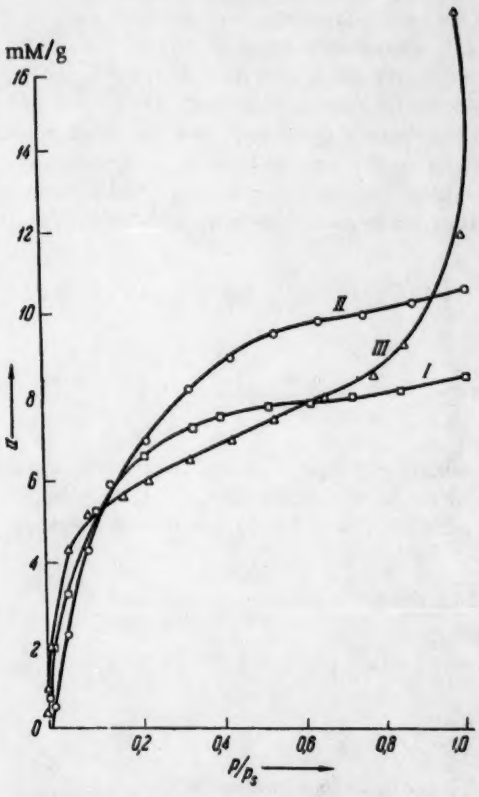

Fig. 1. Adsorption isotherms for methyl alcohol vapor on carbons I, II, and III.

Only in the work of Barrer [8] did we find an attempt to explain this phenomenon. By examining the sorption process on zeolites as diffusion into the crystals, Barrer [8], from the calculated diffusion coefficient, took into account the change in the number of sites available to the diffusing molecules, and obtained a linear decrease of the diffusion coefficient with filling up of the sorption space. However, similar concepts can hardly be applied to such porous adsorbents as activated carbon, silica gel, and so on, in which the transference mechanism differs essentially from diffusion into crystals. In this case the decrease in diffusion coefficient during the sorption process is apparently linked with the nature of the interlinking of different pore types. This question has been partially considered by us [9], and is treated in more detail in this present paper.

The experimental part of the investigation was concerned with the determination of the relation between the diffusion coefficient of methyl alcohol and the

Brief Characteristics of Carbon Investigated

Carbon	Pore volume, cc/g			Particle diameter, mm	Particle length, mm
	micro	intermediate	macro		
I	0.33	0.10	0.25	3	5-6
II	0.38	0.05	0.31	1.6	3-3.5
IIa	0.38	0.05	0.31	1.6	1.6
III	0.28	0.40	0.20	1.4-1.6	2.4

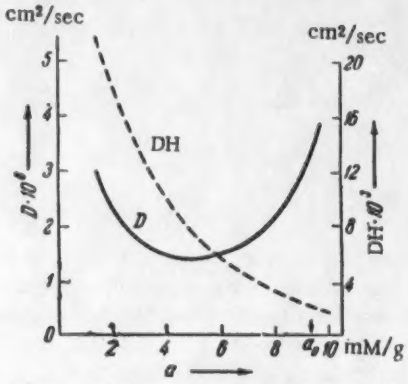

Fig. 2. Relation between diffusion coefficient D and value DH and adsorption on carbon IIa.

amounts of adsorption on active carbons having different pore structures. The granulated activated carbons were obtained under laboratory conditions by a steam-activation method from a mineral carbon and wood tar (carbons I and II) and from a hydrolyzed lignin and tar (carbon III). The essential data concerning pore structure and adsorbent properties of these carbons are shown in Table 1 and Fig. 1.

The measurement of the sorption kinetics was carried out in vacuo at 20° and at a constant pressure of methyl alcohol vapor. The variables of the system, the weighed portion of carbon and the intervals of equilibrium pressures at which measurements were made, were chosen so that during the course of the experiment, in the most unfavorable case, the vapor pressure did not decrease by more than 3-4% of its original value owing to adsorption. Before the experiment the carbon was evacuated with a mercury pump for three hours at 400°. The amount of methyl alcohol adsorbed was determined from the weight increase of the carbon by means of a sorption balance. At another time the working pressure was obtained in the apparatus system and the adsorption tube, containing the carbon connected into the system. Then at determined intervals readings of the adsorption increase were taken until sorption equilibrium was attained.

Diffusion coefficients for carbon IIa were calculated from the diffusion equation for a cylinder of terminal dimensions

$$\gamma = \frac{a - a_i}{a_\infty - a_i} = 1 - \frac{32}{\pi^2} \sum_{n=1}^{\infty} \sum_{m=1}^{\infty} \frac{1}{\mu_n^2 (2m-1)^2} \exp\left[-\left(\frac{\mu_n^2}{R^2} + \frac{(2m-1)\pi^2}{4l^2} \right) Dt \right], \quad (1)$$

where a is the amount of adsorption at time t; a_i is the initial equilibrium amount of adsorption (at $t = 0$); a_∞ is the final equilibrium amount of adsorption ($t \to \infty$); μ_n are roots of the Bessel function $J_0(\mu_n)$; D is the effective diffusion coefficient (calculated for unit cross-section area of a porous medium); R and l are the corresponding radius and length of the cylinder; $n = 1, 2, 3 \ldots$; $m = 1, 2, 3 \ldots$

For $\gamma = 0.5$ the equation has a form which is identical for both adsorption and desorption processes

$$\sum_{n=1}^{\infty} \sum_{m=1}^{\infty} \frac{1}{\mu_n^2 (2m-1)^2} \exp\left[-\left(\frac{\mu_n^2}{\pi^2} + \frac{(2m-1)^2}{16} \right) \frac{\pi^2 D t_{0,5}}{R^2} \right] = \frac{\pi^2}{64}. \quad (2)$$

In Eq. (2) l is replaced by 2R for the given carbon sample (see Table 1).

For calculations involving an accuracy of about 1% the equation can be converted to the form

$$D = 0{,}318 \frac{R^2}{\pi^2 t_{0,5}}, \quad (3)$$

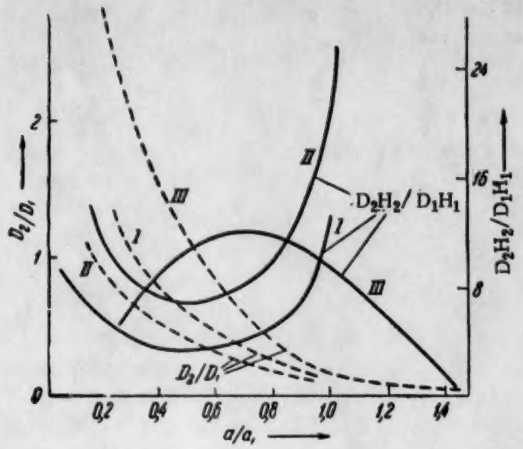

Fig. 3. Relation between the relative diffusion coefficients D_2/D_1 and D_2H_2/D_1H_1 and adsorption a/a_1 on carbons I, II, and III.

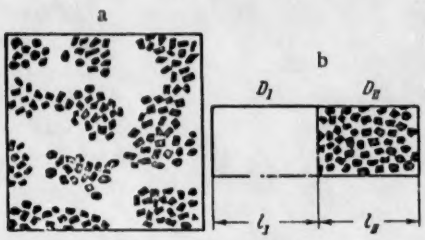

Fig. 4. Schematic representation of the pore structure of active carbon (a), and an element of the pore structure (b).

where $t_{0.5}$ is the time in seconds for the adsorption to reach a value $\gamma = 0.5$; D is the cm^2/sec, and R is in cm.

The dependence of D on the filling up of the sorption volume for carbons I, II, and III was determined from the relation [10].

$$\frac{D_2}{D_1} = \frac{t'_{0.5}}{t''_{0.5}}, \qquad (4)$$

where the quantities with indexes 1 and 2 correspond to two different stages in this filling up process. Each diffusion coefficient is taken for the amount of adsorption a_0 which corresponds to the filled-up micropore volume.

The experimental data satisfy the rule well enough for $\gamma = 0.6$-0.8. Curves showing the relations between the diffusion coefficient D and the value DH (where H is Henry's constant) and the filling up of the sorption volume for the carbon samples investigated are in Figs. 2 and 3.

If it is assumed that the activated carbon consists of aggregations of elemental carbon crystals with more or less close packing, so that free spaces between the crystallites exist as interconnected micropores (see Fig. 4), the simultaneous decrease of D and DH with this filling-up process can be explained in the following way. The path of molecules from the surface to the adsorption centers inside the particle passes through wide and narrow channels, in which the diffusion coefficients differ. The wide channels are open cavities between the crystallite aggregates; the narrow channels are micropores. The over-all diffusion coefficient depends on the individual diffusion coefficients in wide and narrow pores. For an element of the path, as illustrated in Fig. 4b, the over-all diffusion coefficient can be written

$$D = \frac{D_I D_{II}}{\alpha D_I + (1-\alpha) D_{II}}, \qquad (5)$$

where D_I is the diffusion coefficient in a wide pore; D_{II} is the diffusion coefficient in the micropore zone; $\alpha = l_{II}/(l_I + l_{II})$, l_I and l_{II} being the lengths of the paths of the diffusing molecules through the micropores.

During the adsorption process the micropores are filled with the adsorbed substance and the free space between the carbon crystallites decreases; consequently, the diffusion coefficient in the micropore zone decreases. The diffusion coefficient in the wide pores is practically unchanged during this process. From Eq. (5) a decrease in D_{II} leads to a decrease in the over-all diffusion coefficient. A more usual expression for D can be obtained if, in regard to the radial pore distribution, the presence of parallel channels and other more specific conditions are assumed, but qualitatively the picture is unchanged.

LITERATURE CITED

1. R. M. Barrer and D. W. Riley, J. Chem. Soc. 133 (1948).
2. R. M. Barrer and D. W. Brook, Trans. Farad. Soc. 49, 1049 (1953).

3. P. C. Carman and F. A. Raal, Proc. Roy. Soc. A 209, 38 (1951).
4. P. C. Carman and F. A. Raal, Trans. Farad. Soc. 50, 842 (1954).
5. P. C. Carman, Flow of Gases through Porous Media (London, 1956).
6. K. Kammemeyer, Ind. Eng. Chem. 50, 697 (1958).
7. H. W. Habgood, Canad. J. Chem. 36, 1384 (1958).
8. R. M. Barrer, Trans. Farad. Soc. 37, 590 (1941).
9. D. P. Timofeev and I. T. Erashko, Dokl. Akad. Nauk, SSSR 129, 384 (1959).*
10. D. P. Timofeev, Doklady Akad. Nauk SSSR 131, 6 (1960).*

* Original Russian pagination. See CB Translation.

THE KINETICS OF DISTILLATION IN SUPERCOOLED SYSTEMS

K. S. Shifrin and A. Ya. Perel'man

The All-Union Correspondence Institute of Forestry Technology

(Presented by Academician A. N. Frumkin, September 25, 1959)

Translated from Doklady Akademii Nauk SSSR, Vol. 132, No. 5, pp. 1148-1151, June, 1960

Original article submitted September 10, 1959

1. In supercooled systems, in which there may be present at the same time over a considerable temperature range drops of liquid, crystals of solid and vapor, distillation is the fundamental process which determines the change with time of the composition of the system. It may produce continuous growth of the crystals, evaporation of the drop and gradual change in the density of the vapor. This phenomenon is usually complicated by a number of circumstances, but the analysis of the problem carried out in work reported in [1] shows that the rather simple scheme outlined below is the basic one.

The purpose of the present work is to investigate the kinetics of distillation in a simple form and to construct an uncomplicated plan for calculating the phenomena which will occur in any concrete case.

2. We introduce the following symbolism: $a = a(t)$ is the radius of the particle; ρ is the density of the material of which the particle is made up; n is the number of particles in unit volume, for which the index number 1 will be used for drops of liquid, and 2 for crystals; D is the diffusion coefficient of the vapor in air; $c = c(t)$ is the density of the vapor, while c_1 represents the saturated vapor over the liquid drops, and c_2 that over the crystals. Then,

$$\Delta c = c_1 - c_2 > 0. \tag{1}$$

Assuming that at the initial moment, $t = 0$, the system consists of supercooled liquid drops, crystal nuclei of radius $a_1(0)$ which can be taken to be negligibly small, and vapor whose density corresponds to the saturated vapor over the supercooled liquid drops, then the initial conditions of the process will be:

$$a_1(0),\ a_2(0) = 0, \quad c(0) = c_1. \tag{2}$$

The transfer process will be described by a system of differential equations:

$$\frac{dc}{dt} = 4\pi n_1 a_1 D(c_1 - c) + 4\pi n_2 D(c_2 - c)a_2, \tag{3}$$

$$\rho_1 a_1 \frac{da_1}{dt} = D(c - c_1), \tag{4}$$

$$\rho_2 a_2 \frac{da_2}{dt} = D(c - c_2). \tag{5}$$

The system of Eqs. (3) to (5), with the initial conditions given in (2) represents the Cauchy problem. From (3) to (5) taken together we obtain two integrals:

$$c(t) + {}^4/_3\pi\rho_1 n_1 a_1^3(t) + {}^4/_3\pi\rho_2 n_2 a_2^3(t) = M, \tag{6}$$

$$\rho_1 a_1^2(t) - \rho_2 a_2^2(t) = \rho_1 a_1^2(0) - 2D\Delta ct. \tag{7}$$

By means of (6) and substitution of variables we obtain:

$$X = \sqrt[3]{\left(\frac{4}{3}\pi \frac{n_2\rho_2}{M - c_2}\right)^2}\, a_2^2(t), \tag{8}$$

$$Y = \frac{\Delta}{a_1^2(0)}\, a_1^2(t) \tag{9}$$

Equations (4) and (5) may be reduced to a single differential equation (for the detailed process see [2]), giving:

$$\frac{dY}{dX} = \left(\frac{\rho_2}{\rho_1}\right)^{1/3} \nu^{-2/3} \frac{X^{2/3} + Y^{2/3} - \Delta^{2/3}}{X^{2/3} + Y^{2/3} - 1}, \quad Y(0) = \Delta. \tag{10}$$

Here

$$\nu = n_2/n_1, \tag{11}$$

$$\Delta = \frac{q_1(0)}{\Delta c + q_1(0)}, \quad q_1(0) = {}^4/_3\pi\rho_1 n_1 a_1^3(0). \tag{12}$$

We shall denote the time during which the whole process of distillation takes place, by T^*. We determine this from the condition that the process shall be complete when the density of the vapor, c(t) attains the value c_2; that is:

$$c(T^*) = c_2. \tag{13}$$

In view of the uniqueness of the solution of the Kosh problem presented in (2) to (5), (13) gives single-valued determination of the quantities T^*, $a_1(T^*)$, and $a_2(T^*)$.

3. A strict analysis of the problem is given in publication [2]. We note the following conclusions:

1) The process can be divided into two stages. The time of the first stage, T, corresponds to the complete evaporation of the liquid drop; that is, $a_1(T) = 0$. For this,

$$a_2(T) = \sqrt{X_1}\, a_{2\max}, \tag{14}$$

where

$$\Delta < X_1 < 1, \tag{15}$$

$a_{2\max}$ is the maximum possible radius of the crystal,

$$a_{2\max} = \sqrt[3]{\frac{M - c^2}{{}^4/_3\pi\rho_2 n_2}}. \tag{16}$$

The time T is determined by the formula

$$T = \frac{\rho_2 a_{2\max}^2 X_1 + \rho_1 a_1^2(0)}{2D\Delta c}. \tag{17}$$

2) The second stage of the process, during which $a_1 \equiv 0$, consists in the condensation of the excess quantity of vapor on the crystals. It continues indefinitely, since the quantity dc/dt approaches zero asymptotically. We

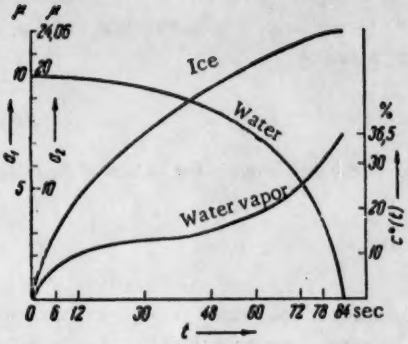

Fig. 1

might take as a practically convenient figure that at which the second stage has acquired not less than 96% of its maximum value, and calculate the corresponding value T' for the time required. Then,

$$T' = \frac{1}{\pi n_2 D a_{2\max}}, \tag{18}$$

and the complete time for the process is given by:

$$T^* \simeq \frac{\rho_2 a_{2\max}^2 X_1 + \rho_1 a_1^2(0)}{2D\Delta c} + \frac{1}{\pi n_2 D a_{2\max}}. \tag{19}$$

3) We now estimate the part played by each stage in the relative increase in the radius of the crystals. The relevant equations are:

$$a_{2I} = \sqrt{X_1}\, a_{2\max}, \quad a_{2II} = (1 - \sqrt{X_1})\, a_{2\max}, \quad \Delta < X_1 < 1, \tag{20}$$

where $a_{2I} = a_2(T)$, and a_{2II} are the growth of the radius at the time of the first and second stages, respectively. We may note that when $X_1 > 0.9$, the second stage may usually be neglected without loss of accuracy worse than 5%.

4) X_1 is determined for the given substance by the values of Δ and ν: its value decreases both with reduction in Δ and with reduction in ν. Reduction in Δ causes increase in the value of Δc^*, that is, the fraction of the substance in the vapor condition which is distilled on to the crystal, relative to the fraction of the substance in the liquid state, $q_1(0) = 4/3\,\pi n_2 \rho_1 a_1^3(0)$. Reduction of the value of ν for fixed values of Δ, Δc, and $a_1(0)$ will take place if the value of n_2 (the amount of crystal nucleus) is reduced.

We may note that if $n_2 \ll n_1$, that is, if $\nu \ll 1$, then the values of a_{2I}, a_{2II}, and $a_{2\max}$ have the order of $\nu^{-1/3}$ irrespective of the value of Δ.

5) The value of X_1 may be determined directly from those of Δ and ν (for a detailed consideration of this see paragraph 4); that is, directly from the initial data, without making a preliminary calculation of the kinetics of the first stage of the process. It is then possible at once to use Eqs. (17), (19), and (20) to determine the time of the first stage, the time of the whole process, and also the growth of the crystal radii A_{2I} and a_{2II}.

4 For the calculation of the kinetics of the first stage, it is necessary to obtain a numerical solution of Eq. (10), which depends on the two parameters Δ and ν**. So as to simplify this massive procedure, we have set up a family of solutions of Eq. (10), corresponding to a wide range of values for Δ and ν: Δ = 0.1 (0.1) 0.9; $\nu = 10^{-3}$; 10^{-2}; 10^{-1}; 0.2; 0.5; 1; 2.5; 10; 10^2; 10^3. These solutions are presented in the form of a table of the special function: $Y = F(X, \Delta, \nu)$ for X in the interval (0.1) with $\Delta X = 0.05$ (or 0.1) ([2], Tables 1-9). This reference contains in addition Table 10, for the determination of X_1 from the values of Δ and ν. With the use of the tables referred to, it is possible to allow for a "substance correction." The reason for this is that the tables are set up with reference to water. Therefore, in the use of Table 1-10 for the analysis of the distillation of other substances, the starting parameter ν in the tables should be taken not as n_2/n_1, but as the quantity ν', given by:

$$\nu' = \sqrt{\frac{1{,}9\sigma_1}{\rho^2}}\,\nu. \tag{21}$$

The calculation is carried out thus: by means of Table 1-9 [2] for the data on the values of Δ and ν', we find the value of X corresponding to each value of Y. With the use of Eqs. (8) and (9) we may obtain values of $a_2(t)$ and $a_1(t)$ from X and Y. Evaluating the equation,

$$M = c_1 + q_1(0), \tag{22}$$

* Δc depends on the temperature at which the distillation is carried out.

** $(\rho_2/\rho_1)^{1/2}$ may be included in ν.

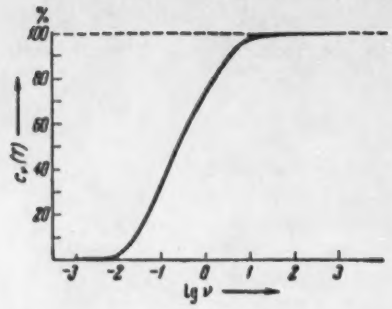

Fig. 2

by means of Eq. (6) we obtain c(t). The time t, corresponding to these values of $a_2(t)$, $a_1(t)$ and c(t), is determined from Eq. (7).

5. In analyzing the second stage it is convenient to bring into discussion a time τ, given by:

$$\tau = t - T, \tag{23}$$

evaluated from the end of the first stage. For values of X_1 satisfying the conditions:

$$0{,}65 \leqslant X_1 < 1, \tag{24}$$

the calculation of the kinetics of the second stage, with errors not greater than 10%, may be carried out according to the approximate relationship:

$$\alpha(\tau) = \alpha_0 e^{-\beta\tau}, \quad 0 \leqslant \tau \leqslant T', \tag{25}$$

where

$$\alpha(\tau) = \frac{a_{2\max} - a_2(\tau)}{a_{2\max}}, \quad \alpha_0 = 1 - \sqrt[3]{X_1}. \tag{26}$$

$$\beta = 4\pi n_2 D a_{2\max}. \tag{27}$$

If the condition proposed in Eq. (24) is not met, the calculation becomes rather more complex (see [2]).

For the second stage, $c(\tau)$ is determined from the relationship:

$$c(\tau) = M - {}^4/_3 \pi \rho_2 n_2 a_2^3(\tau). \tag{28}$$

6. The scheme developed above contains a complete analysis of the problem under consideration, and makes possible the rapid calculation of the kinetics of both stages of the distillation process. We turn now to some physicochemical conclusions.

1) Figure 1 gives curves which describe the first stage of distillation in the system water vapor–water–ice, at a temperature of $-20°$, and with $n_1 = 60$ cm^{-3}, $n_2 = 6$ cm^{-3}, $a_1(0) = 10\ \mu$. Together with the curves for $a_1(t)$ and $a_2(t)$, this figure also gives the curve for $c^*(t)$ as defined by the relationship:

$$c^*(t) = \frac{c_1 - c(t)}{\Delta c}, \tag{29}$$

which characterizes the relative change in density during the first stage of the distillation. It is of interest that, in spite of the fact that the water drop is ten times larger than the crystals, at the end of the first stage of the distillation the density of the vapor is 36.5% higher than c (when measured in fractions of Δc). The time for the first stage is here 83.9 sec, and the value of X_1 is 0.809. The second stage is described by the relationship $\alpha(\tau) = 0.982\exp(-0.040\,\tau)$. Its duration, T' is 10 sec, and the complete distillation time, T* is $\approx$94 sec.

2) The relative change in the density of the vapor at the instant when the drop is completely evaporated is given by:

$$c^*(T) = \frac{M - c_2}{\Delta c}\sqrt[3]{X_1^3} = \frac{q_1(0)}{\Delta c}, \quad \Delta c = M - c_2 - q_1(0). \tag{30}$$

The dependence of $c^*(T)$ on the number of crystalline nuclei, n_2, for the example considered above is depicted in Fig. 2, where the ordinate is given as $c^*v(T)$. We notice in Eq. (30) that it is only the value of K_1 which

depends on n_2. Figure 2 shows if $\nu < 0.01$, so long as the drop exists, the concentration is practically equal to c_1; if $\nu > 10$, at the moment of complete evaporation of the drops it is equal to c_2, and there would be no second stage in the distillation. The almost linear relationship of c^* to $\log \nu$ between the values of 0.01 and 10 for ν is of interest.

LITERATURE CITED

1. K. S. Shifrin, Transactions of the Chief Geophysical Observatory [in Russian] (1951) 31.
2. K. S. Shifrin and A. Ya. Perel'man, Izvest. Akad. Nauk SSSR, Ser. Geofiz. 6 (1950).

THE THERMODYNAMICS OF THE PROTONIZATION OF ISOBUTENE

S. G. Éntelis, K. S. Kazanskii, and N. M. Chirkov

Institute of Chemical Physics, Academy of Sciences, USSR

(Presented by Academician V. N. Kondrat'ev, January 1, 1960)

Translated from Doklady Akademii Nauk SSSR, Vol. 132, No. 5, pp. 1152-1155, June, 1960

Original article submitted January 15th, 1960

The question of the existence of aliphatic carbonium ions and the corresponding π-complexes has been debated in the literature for a long time. On the one hand, a great deal of data obtained in the study of the kinetics of acid-catalyzed reactions leads investigators to mechanisms involving the participation of aliphatic carbonium ions or π-complexes. On the other hand, the lack of any cases where they have been directly identified and the unsatisfactory results of the thermochemical calculations prove, as it were, the instability of these particles and the fact that conditions are unfavorable for their formation, by the same token throws doubt on the postulation of carbonium ions in the interpretation of a series of reactions, for instance olefin conversions.

Regarding the thermochemical calculations, it should be noted that estimates of the heat of reaction for the protonization of olefins in aqueous solution

$$iso\text{-}C_4H_8(aq) + H^{\oplus}(aq) = tert\text{-}C_4H_9^{\oplus}(aq) \qquad (1)$$

available in the literature cannot provide a worthwhile result of the required accuracy. Data on the heats of solvation ΔH_s of carbonium ions which are essential for carrying out such estimates are approximate and very unreliable (for tert-$C_4H_9^{\oplus}$ $\Delta H_s = -40$ to -69 kcal/mole). Even such a basic value as the heat of solvation of a proton, according to the data of different authors, is equal to -225, -257, -259, and -282 kcal/mole. It is therefore not surprising that the results of the calculations of Evans and Halpern [1], who took $\Delta H_s(H^+) = -282$ kcal/mole, indicate for reaction (1) a heat effect $\Delta H_R = 26.1$ kcal/mole while the same calculations carried out using a value of $\Delta H_s(H^+) = -256$ kcal, give $\Delta H_R = \pm 0$ kcal/mole.

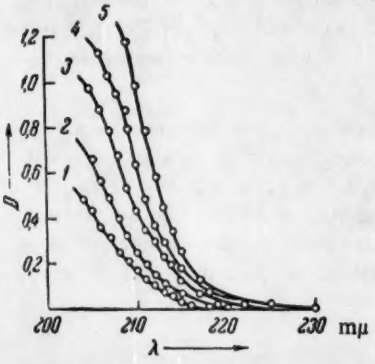

Fig. 1. Absorption spectrum for isobutene in aqueous solution at various concentrations (in mole/liter): 1) $2.2 \cdot 10^{-4}$; 2) $3.3 \cdot 10^{-4}$; 3) $5.7 \cdot 10^{-4}$; 4) $8.1 \cdot 10^{-4}$; 5) $1.27 \cdot 10^{-3}$.

The problem of the direct determination of the equilibrium constant for the protonization of olefins and the heat and entropy of reaction has become an important and fundamental problem, on the solution of which depends our notions of the nature and mechanism of acid catalysis.

An attempt has been made by us to solve this problem by means of direct experiments. Isobutene in the system $H_2SO_4 - H_2O$ was selected as the subject of the investigation. Unlike work described in the literature in which the kinetics and thermodynamics of the absorption of isobutene by acids were investigated, in the present work a spectrophotometer method was adopted for the direct observation of the conversion of

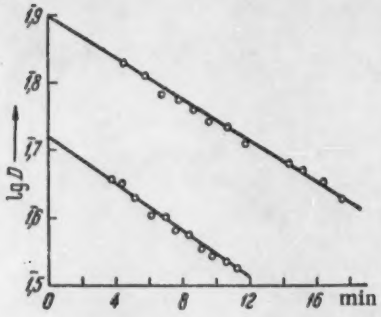

Fig. 2. Extrapolation to t = 0 of kinetic curves showing fall in isobutene concentration.

iso-C_4H_8 in the liquid phase. The use of this method in the present case was possible thanks to the absorption spectrum, which we found, of unprotonized isobutene in aqueous solution (see Fig. 1). This absorption, occurring close to the limit of transparency for quartz (210-220 mμ), is the slope down from the iso-C_4H_8 peak, which has its maximum, according to data in the literature, at 185-190 mμ. We were unable to find spectroscopic effects for ionized particles ($BH^{\oplus}$) and the concentration of these was determined by difference

$$C_{BH^{\oplus}} = C_0 - C_B^0, \qquad (2)$$

where C_0 and C_B^0 are the total concentration of isobutene in solution and the concentration of its un-ionized form, respectively.

Using this method of calculation we cannot, of course, distinguish π-complexes from carbonium ions and we assume provisionally that all the protonized isobutene exists in the form of tert-$C_4H_9^{\oplus}$.

In the system under investigation the hydration of isobutene occurs with the formation of tertiary butyl alcohol. In order to retard this reaction which is too rapid at ordinary temperatures for a reliable extrapolation to zero time to be possible, we worked at reduced temperatures (−15 to −35°). The value of C_B^0, corresponding to equilibrium (1) was determined by extrapolating the kinetic curves to t = 0 on the assumption of monomolecularity (Fig. 2).

EXPERIMENTAL

Solution of gaseous isobutene in sulfuric acid of the required concentration (25-50%) was carried out directly in a seamless quartz cell, connected to a glass apparatus by a smooth section, and placed in a thermostat at −15, −25, or −35°. Mixing in the cell was effected by means of intense agitation with the aid of a special device.*

The total concentration of dissolved isobutene C_0 was determined by the pressure fall in a known volume. When absorption was effected, which took 30-40 sec, the cell was transferred to the cell holder, which was maintained at the same temperature by a thermostat, of a SF-4 spectrophotometer, where the change with time of optical density at 210 mμ (D_{210}), occurring as a result of the fall in C_B due to hydration was recorded (time was measured from the instant of ceasing saturation). By extrapolation on the coordinates $\log D_{210} - \tau$ (see Fig. 2) the optical density was determined which corresponded to $C_B = D_{210}^0/\epsilon l$ where l is the cell length (1.5 cm), ϵ is the molar absorption coefficient for unprotonized isobutene at the temperature of the experiment, expressed in liters/mole·cm.

The absorption coefficients ϵ were obtained from the relationship between D_{210} and the concentration of isobutene in aqueous solution; the concentrations were determined from the pressure over the solution in accordance with Henry's Law, C = hp, and the values of h were measured previously by ourselves [2]. Beer's Law was followed over the whole range of temperatures and concentrations studied. In view of the fact that the measurement of ϵ is theoretically impossible at temperatures below 0°C, the absorption coefficients were measured over a wide temperature range (2-92.5°) and the extrapolation was extended to low temperatures by means of the empirical formula

$$\frac{1}{\varepsilon} = a - bt, \qquad (3)$$

which, as can be seen from Fig. 3, satisfactorily describes the temperature dependence of ϵ ($a = 2.46 \cdot 10^{-3}$ mole·cm/liter; $b = 2.38 \cdot 10^{-5}$ mole·cm/liter·sec).

* Without agitation, transfer between liquid and gas phases was practically nonexistent.

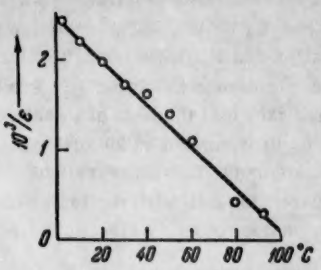

Fig. 3. Temperature dependence of the absorption coefficient of isobutene in aqueous solution at λ 210 mμ.

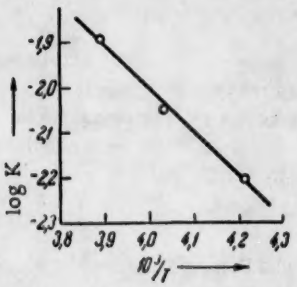

Fig. 4. Relationship between $pK_{iso\text{-}C_4H_8}$ and reciprocal temperature.

Knowing C_0, C_B^0, and from Eq. (2), $C_{BH^\oplus}$, the value of $-\log K$ may be found by means of the well-known formula:

$$pK = H_0 - \lg \frac{C_B^0}{C_0 - C_B^0} = H_0 - \lg \frac{C_B^0}{C_{BH^\oplus}}. \qquad (4)$$

Values of the pH of H_2SO_4 solutions at the temperatures of the experiments were obtained by extrapolation from the data of A. I. Gel'bshtein, G. G. Shcheglova, and M. I. Temkin [3]. The values of the basicity constants (p K) determined by us are presented in the table. The considerable error in the basicity constant determinations and the small observed variation in the values of the latter with acidity are apparently due to the large number of unavoidable extrapolations in the calculations.

The relationship between $-\log K$ and $1/T$, which provides the value of the heat of protonization of iso-C_4H_8, $\Delta H_R = 4.3 \pm 4$ kcal/mole, and the entropy of reaction, $\Delta S = +8.20$ entropy units (for the mean ΔH_R), is presented in Fig. 4. The expression for the constant $K = h_0 C_B / C_{BH^\oplus}$ may be written thus:

$$2{,}3R\, pK = \frac{-4300}{T} + 8{,}20. \qquad (5)$$

ASSESSMENT OF RESULTS

The values of p K obtained indicate the presence of significant concentrations of protonized isobutene at the acid concentrations at which acid-catalyzed conversions normally occur. These concentrations are substantiated in the calculations from kinetic data.

The observed heat of protonization for isobutene equal to $\Delta H_R = 4.3 \pm 4$ kcal, makes it possible to estimate the heat of solvation of the isobutene carbonium ion $\Delta H_s(R^\oplus)$.

The heat of the reaction for the transfer of a proton from $H_3O^\oplus$ to iso-C_4H_8 in the gaseous phase,

$$\text{iso-}C_4H_8 + H_3O^\oplus = \text{tert-}\ C_4H_9^\oplus + H_2O \qquad (6)$$

is equal to difference $(P_{iso\text{-}C_4H_8} - P_{H_2O})$ where P is the affinity of the corresponding molecule with respect to a proton. If $P_{iso\text{-}C_4H_8} = 198$ kcal/mole [4]* and $P_{H_2O} = 169$ kcal/mole [5], then reaction (6) is exothermic, with a heat of reaction $\Delta H_R = -29$ kcal/mole. For the heat of reaction (1), or what amounts to the same thing, the following reaction

$$\text{iso-}C_4H_8\,(aq) + H_3O^\oplus\,(aq) = \text{tert-}\ C_4H_9^\oplus\,(aq) + H_2O_l \qquad (7)$$

to be equal to 4.3 kcal/mole the heats of solvation for the reactants in the left and right sides of Eq. (6) should differ by +33 kcal/mole:

$$\Delta H_s(\text{tert-}C_4H_9^\oplus) + \Delta H_s(H_2O) - \Delta H_s(\text{iso-}C_4H_8) - \Delta H_s(H_3O^\oplus) = 33 \text{ kcal} \qquad (8)$$

Taking $\Delta H_s(H_2O) = -10.3$ kcal/mole [8]; $\Delta H_s(\text{iso-}C_4H_8) = -4.6$ kcal/mole [2] and $\Delta H_s(H_3O^\oplus) = -102$ kcal/mole**, we obtain for the heat of hydration of the tert-$C_4H_9^\oplus$) = -64 kcal/mole (± 4 kcal/mole).

* The heat of formation of iso-C_4H_8 ΔH_f is equal to -4.04 kcal/mole [8].

** $-\Delta H_s(H_3O^\oplus) = \Delta H^0_f(H^\oplus \text{ gas}) + \Delta H^0_f(H_2O \text{ gas}) - P(H_2O) - \Delta H^0_f(H_3O^\oplus aq)$ according to the data of references [4] and [5].

t,°C	pK	±Δ
−15	−1.89	0.10
−25	−2.05	0.15
−35	−2.21	0.16

In an early study, Evans takes a value of $\Delta H_s = -69$ kcal/mole as the most likely for tert-$C_4H_9^{\oplus}$ [6], while according to Franklin [4] and V. N. Kondrat'ev and N. D. Sokolov [7] $\Delta H_s = -40$ kcal. Of the two values, preference should be given to the latter, more accurate one. The fact that the heat of solvation for a carbonium ion observed by us is more than 20 kcal greater than the value calculated by authors [4, 7] is quite natural since calculation by the formula connecting ΔH_s with the ionic radius only takes into account solvation due to purely electrical forces.

As V. N. Kondrat'ev and N. D. Sokolov rightly point out, nonelectrostatic interaction should also be taken into account in these calculations (which clearly plays an important role). However, it is impossible to agree with these authors when they assume, in calculating the affinity of $R^{\oplus}$ for a water molecule CH_2O, that a carbonium ion only exists in water in the alkoxonium form $ROH_2^{\oplus}$. In reality two types of interaction between a carbonium ion and water exist: solvation, which has been discussed above, and the "strong," donor-acceptor interaction with one water molecule to form an alkoxonium ion. These states are separated by a potential barrier.

LITERATURE CITED

1. A. G. Evans and J. Halpern, Trans. Farad. Soc. 48, 1034 (1952).
2. K. S. Kazanskii, S. G. Éntelis, and N. M. Chirkov, Zhur. Fiz. Khim. 33, 1409 (1959).
3. A. I. Gel'bshtein, G. G. Shcheglova, and M. I. Temkin, Doklady Akad. Nauk SSSR 107, 108 (1956).*
4. J. Z. Franklin, Trans. Farad. Soc. 48, 443 (1952).
5. V. L. Tal'roze and E. L. Frankevich, Doklady Akad. Nauk SSSR 111, 376 (1956).*
6. A. G. Evans, Trans. Farad. Soc. 42, 719 (1946).
7. B. N. Kondrat'ev and N. D. Sokolov, Zhur. Fiz. Khim. 29, 1265 (1955).
8. Selected Values of Physical and Thermodynamic Properties of Hydrocarbons and Related Compounds (Pittsburgh, 1953).

* Original Russian pagination. See C.B. Translation.

THE FREE ENERGY OF POTASSIUM IODIDE IN ETHANOL AND ACETONE

V. V. Aleksandrov and Yu. A. Ershov

Chemical Physics Institute of Academy of Sciences of USSR and
The A. M. Gorkii Kharkov State University

(Presented by Academician V. N. Kondrat'ev, February 22, 1960)

Translated from Doklady Akademii Nauk SSSR, Vol. 132, No. 6, pp. 1327-1328, June, 1960

Original article submitted February 19, 1960

The free energy of solvation of potassium iodide (A_X) in ethyl alcohol may be calculated [1] from the value of the emf of a circuit with transference. This method, however, has the disadvantage of suffering from such errors as the difficulty of estimating the diffusion and interphase contribution to the potential. Data as to the magnitude of A_X for potassium iodide in acetone, and, indeed, for other salts in this solvent, are not available. In the present work we have used an apparatus without transference to determine the free energies of potassium iodide in ethanol and in acetone, the cell being: (Hg)K| KI aq.| AgI,Ag. The circuit was arranged experimentally in the form of the cell depicted in Fig. 1. The construction of the cell envisaged control within known limits of the vessel containing the initial amalgam, reliable insulation of the amalgam exhausted in the course of the measurements, and replacement of the capillary. The potassium amalgam and the silver iodide electrode were prepared in the way described in earlier publications [2, 3]. The solvents and the potassium iodide employed were prepared by purification of commercial products of the "chemically pure" brand, and had the physical properties given in the data in the literature. Measurement of the emf was carried out by means of a potentiometer of type R-375 at 25°. During the measurements, dry, carefully purified hydrogen was bubbled continuously through the potassium iodide solution. The results of the measurements of the emf for the cell: (Hg)K| KI aq.| AgI, Ag for various concentrations of KI in water, ethanol and acetone are set out in Table 1.

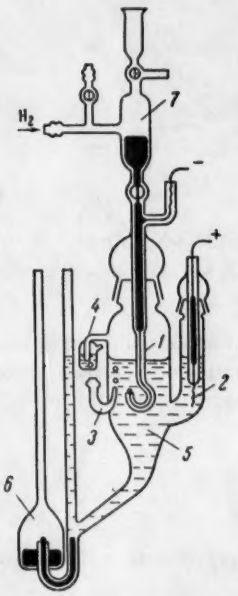

Electrolytic cell for measurement of emf. 1) Capillary for the amalgam electrode; 2) silver iodide electrode; 3) inlet tube for hydrogen into the solution; 4) hydrogen exit tube; 5) vessel containing the solution under investigation (volume of solution 35 ml); 6) vessel for collection of the spent amalgam; 7) vessel containing the initial amalgam

By means of the graphical extrapolation method usually used [4], we have obtained values for the normal potential (E_0) of the cell in the solvents mentioned. (The value of E_0 in water was obtained by calculation from the measured emf and known values of the activity coefficients [5]). The values of E_0 are given in Table 2. From the difference between the normal potentials in the same cell without transference, measured in water and in the nonaqueous solvents, it is easy to calculate the difference between the free energies of solvation of potassium iodide in water

TABLE 1

Emf of the Cell: (Hg)K|KI aq.| AgI, Ag for Various Concentrations of KI

Solvent	m, mole/kg	emf (V)
Water	0.1000	1.8393
	0.0100	1.9497
Ethanol	0.02547	1.660
	0.01274	1.688
	0.00637	1.714
	0.003185	1.736
Acetone	0.02547	1.448
	0.01274	1.465
	0.00637	1.498
	0.003185	1.526
	0.001592	1.552

TABLE 2

Free Energies of Solvation of Potassium Iodide in Water, Acetone and Alcohol

Solvent	E_ϕ, B	A_X, kcal/mole
Water	1.709	137.4 *
Ethanol	1.425	130.9
Acetone	1.208	125.85

* From the data of Izmailov [1].

and these solvents. Taking the free energy of hydration of potassium iodide to be 137.4 kcal/mole [2], we have calculated the free energy of solvation in these solvents from the differences which we have obtained experimentally. The relevant values are also given in Table 2.

The value of A_X for potassium iodide in ethanol, calculated from the emf of a cell with transference [1] is 131.5 kcal/mole. It should be added that the change in the free energy of solvation of potassium iodide in moving from water to ethanol and acetone corresponds to the change in the corresponding magnitudes for hydrogen chloride in the same solvents.

LITERATURE CITED

1. N. A. Izmailov, Electrochemistry of Solutions [in Russian] (Kharkov, 1959).
2. B. P. Nikol'skii, M. Zakhar'evskii, et al., Collected Practical Papers in Physical Chemistry [in Russian] (Leningrad, 1951) 1.
3. B. B. Owen, J. Am. Chem. Soc. 57, 1526 (1946).
4. N. A. Izmailov and V. V. Aleksandrov, Zhur. Fiz. Khim. 31, 2619 (1957).
5. G. Harned and B. Owen, Physical Chemistry of Electrolyte Solutions [Russian translation] (IL, 1952) p. 524.

THE EFFECT OF SOLID SUBSTANCES ON THE DECOMPOSITION OF CARBON TETRACHLORIDE IN AQUEOUS SOLUTION UNDER THE INFLUENCE OF GAMMA IRRADIATION

A. S. Baberkin, N. P. Krushinskaya, and M. A. Proskurnin

The L. Ya. Karpov Physicochemical Institute

(Presented by Academician C. C. Medvedev, February 17, 1960)

Translated from Doklady Akademii Nauk SSSR, Vol. 132, No. 6, pp. 1329-1331, June, 1960

Original article submitted February 10, 1960

In a series of papers [1-5] it has been shown that the radiation yield of inorganic substances on oxidation or reduction in aqueous solution may be increased several fold if solid substances are present in the material being irradiated. The materials used for the solid substances in these investigations have been metals, and the oxides and sulfides of metals. It could be expected that the solid substances would exert a similar effect, when irradiation is carried out, on the processes occurring in aqueous solutions of organic substances. It seems, however, that there is no information on this question in the literature.

In the present communication we describe our experiments on the conditions under which solid substances will accelerate the decomposition of organic compounds in aqueous solution when these are irradiated by gamma rays. For this purpose we have used systems consisting of carbon tetrachloride and water in the ratio 1 : 2, and solid substances whose amount was varied from 1.4 to 20% by weight. The solid substances employed were carbon ("carbolene"), silica gel, alumina, ferric oxide, and cuprous oxide. The source of gamma radiation was Co^{60}, with a dosage power of $4 \cdot 10^{16}$ ev/sec. The mixture was irradiated in a glass vessel, equipped with a bubbler through which the relevant gas (oxygen or nitrogen) could be blown. The irradiation temperature was 8-10°C.

TABLE 1

The System $CCl_4 - H_2O$

Expt. No.	Oxygen blown in			Nitrogen blown in		
	dose $\times 10^{-21}$ ev/36 g	$Cl^- \cdot 10^2$ Conc, g·eq/l.	ions yield Cl^-/100 ev.	dose $\times 10^{-21}$ ev/36 g	$Cl^- \cdot 10^2$ Conc, g·eq/l.	ions yield Cl^-/100 ev.
1	1,38	1,24	10,8	1,26	1,15	11,0
2	2,76	2,08	9,0	2,52	2,32	11,0
3	5,52	4,12	9,0	5,04	4,24	10,0
4	8,28	5,27	7,6	7,56	6,03	9,65

*After irradiation the reaction mixture was separated. The solid substance was washed with a 12% ammonia solution. The concentration of Cl^- ions, obtained as a product of the decomposition of the carbon tetrachloride, was determined by potentiometric titration with silver nitrate solution. The total quantity of Cl^-, obtained on irradiation was taken as the sum of its content in the water and in 2-3 ammonia washings from the solid substance.

TABLE 2

The System $CCl_4 - H_2O$ – 1 gram of Solid Substance

Expt. No.	Oxygen blown in: solid substances	dose $\cdot 10^{21}$ ev/37g	$Cl^- \cdot 10^2$ conc. g. eq/liter	ion yield Cl^-/100 ev	Nitrogen blown in: solid substances	dose $\cdot 10^{21}$ ev/37g	$Cl^- \cdot 10^2$ conc. g. eq/liter	ion yield/100 ev
1	Al_2O_3	1,33	1,62	14,6	Al_2O_3	1,33	1,12	10,2
2		2,66	2,90	13,0		2,66	2,28	10,3
3		5,32	5,33	12,0		5,32	4,18	9,5
4		7,98	6,37	9,6		7,98	7,15	10,7
5	Carbon	1,33	1,95	17,6	Carbon	1,33	1,3	11,7
6		2,66	3,95	17,6		2,66	2,64	11,9
7		5,32	6,66	15,0		5,32	4,52	10,9
8		7,98	9,70	15,0		7,98	6,54	9,9
9	Cu_2O	1,33	3,62	32,7	Cu_2O	1,33	2,6	23,5
10		2,66	4,46	20,1		2,66	4,2	19,0
11		5,32	7,87	18,0		5,32	7,00	15,8
12		7,98	12,00	18,0		7,98	7,85	11,8

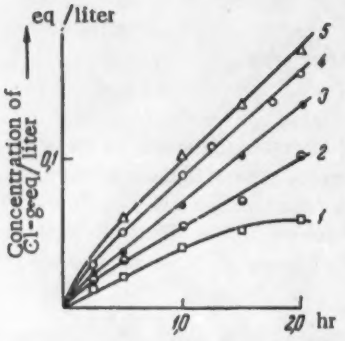

Fig. 1. Relationship of the concentration of chloride ions to the irradiation dosage. The dosage power is $4.0 \cdot 10^{16}$ ev/sec. 1) The system $CCl_4 - H_2O - O_2$. The other curves denote the same mixture in the presence of: 2) 1.4%; 3) 7.7%; 4) 14.2%; 5) 20.0% silica gel by weight.

We have studied the relationship between the quantity of Cl^- produced and the radiation dosage for various contents of the solid substance in the mixture under irradiation. The results of the experiments with silica gel are shown in Fig. 1. Curve 1 of this figure refers to the mixture $CCl_4 - H_2O - O_2$ without solid substance; curves 2, 3, 4, and 5 to mixtures in which the silica gel contents were, respectively, 1.4, 7.7, 14.2 and 20% by weight. It is seen from Fig. 1 that the presence of the silica gel, even in quantities as small as 1.4% leads to a growth in the concentration of chloride ions in the irradiated mixture. All further increases in the silica gel proportions also lead to increase in the concentration of chloride ions, but the increase in the Cl^- is not proportional to the increase in the solid material added. A similar relationship of the concentration of the chloride ions to the irradiation dose is observed for the other solid substances.

The effect of the nature of the solid material on the radiation decomposition of the carbon tetrachloride is well brought out in Fig. 2, whose curves give the relationship between the amount of chloride ion produced and the radiation dose for all the solid substances which we have studied. In all these cases the proportion of solid material was 7.7% by weight.

The solid substances used, according to their capacity to increase the yield of chloride ions, may be arranged in the following order: Al_2O_3, SiO_2, Fe_2O_3, carbon, Cu_2O. None of the solid substances will produce any kind of chemical change in the mixture unless there is simultaneous irradiation, that is, there is no direct catalytic effect. Moreover, there is no catalytic effect if the solid substances themselves are previously irradiated.

In order to solve the question as to how the acceleration of the decomposition of the carbon tetrachloride in the system containing solid phase was concerned with the presence of these solid substances with the presence of the oxygen, a series of experiments were carried out in which nitrogen was blown in. The results in the absence of the solid phase for these systems are set out in Table 1. It is clear that oxygen here plays no part in the decomposition of the carbon tetrachloride, since exchange of oxygen for nitrogen does not affect the yield of chloride ions. The initial yield of hydrogen peroxide in the system $CCl_4 - H_2O - O_2$ is about one third (0.07 mole/100 ev) that obtained in experiments in which nitrogen is blown in. It is typical both of the experiments using nitrogen, and of those using oxygen, that the concentration of hydrogen peroxide diminishes with increase in the irradiation dosage.

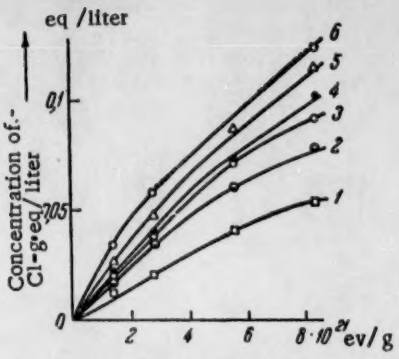

Fig. 2. Relationship of the concentration of chloride ions to the irradiation dosage. 1) The system: $CCl_4-H_2O-O_2$. The other curves denote the same system in the presence of: 2) Al_2O_3; 3) silica gel; 4) Fe_2O_3; 5) carbon; 6) Cu_2O. In each case the proportion is 7.7% by weight.

Table 2 shows that the introduction of solid substances (Al_2O_3, SiO_2, Fe_2O_3, carbon) into the system being irradiated only increases the yield of chloride ions in the presence of oxygen.

The irradiation of the system CCl_4-H_2O—solid substance with the blowing in of nitrogen gives a concentration of chloride ions practically identical with that obtained in the system containing no solid phase. It seems that in this case the solid material simply acts as a ballast, absorbing the gamma radiation, but not transferring the energy from this to the components of the mixture. In all the systems investigated the yield of hydrogen peroxide, both in the presence of nitrogen and in the presence of oxygen, is very low, but, in contrast with the behavior of the system without a solid phase, the concentration of hydrogen peroxide in the solution increases with increase in the radiation dosage. Cuprous oxide differs from the remaining solid additives in that it increases the concentration of chloride ions both in the presence of oxygen and in the presence of nitrogen. The hydrogen peroxide yield reaches the figure of 2 mole/100 ev.

The experimental results which have been obtained show that it is a necessary condition for the majority of the systems investigated, if the radiation yield from the decomposition of the organic substance in aqueous solution is to be increased, that the solid substance and oxygen must be present together in the system, the former as a catalyst. It is possible that adsorption of the oxygen in a more active form takes place on the surface of the solid material, thus making possible a reaction of this with adsorbed molecules of the components of the mixture. The surface reaction is apparently specific for each solid substance, and will no doubt be determined by its electrical and adsorptive properties.

LITERATURE CITED

1. V. I. Veselovskii, N. B. Miller, and D. M. Shub, Collected Works on Radiation Chemistry [in Russian] (Izd. AN SSSR, 1955) p. 49.
2. V. I. Veselovskii and G. S. Tyurikov, Collected Works on Radiation Chemistry [in Russian] (Izd. AN SSSR, 1955) p. 61.
3. A. O. Allen and D. M. Kofrei, Isotopes and Studies in Chemistry [in Russian] (Izd. AN SSSR, 1958) p. 135.
4. M. Haissinsky and A. M. Pujo, Compt.-Rend. 240, 2530 (1955).
5. D. M. Shub, G. S. Tyurikov and V. I. Veselovskii, Works at the First All-Union Congress on Radiation Chemistry [in Russian] (Izd. AN SSSR, 1958) p. 160.

THE PHOTONIZATION OF VAPORS OF COMPOUNDS WHOSE MOLECULES CONTAIN CARBONYL GROUPS

F. I. Vilesov

Physical Institute of the A. A. Zhdanov Leningrad State University

(Presented by Academician A. N. Terenin January 25, 1960)

Translated from Doklady Akademii Nauk SSSR, Vol. 132, No. 6, pp. 1332-1334, June, 1960

Original article submitted January 10, 1960

The most accurate values of the ionization potentials of some simple aldehydes and ketones have been obtained by a spectroscopic method by Price and Walsh [1]. These authors showed, however, that the first ionization potential of aliphatic compounds containing a carbonyl group was determined by the removal of one of the nongeneralized p-electrons of the oxygen of the carbonyl group. Since in these compounds the electron removed by ionization belongs to the electrons localized on the oxygen atom, the magnitude of the ionization potential depends on the density of the electron cloud in the neighborhood of this atom. This fact opens up the possibility of tracing the mutual effect of atoms and radicals forming parts of complex molecules by the aid of their ionization potentials.

TABLE 1

First Ionization Potentials of Aldehydes and Ketones

Compound	Ionization potential, ev	Difference, ev	Compound	Ionization potential, ev
Formaldehyde 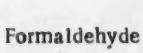	10,90±0,03		Propylbutylketone 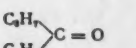	9,10±0,05
		0,7		
Acetaldehyde 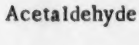	10,20±0,03		Diisobutylketone 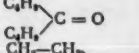	9,04±0,03
		0,51		
Dimethylketone 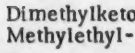	9,71±0,03		Cyclopentanone 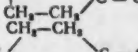	9,42±0,03
		0,17		
Methylethylketone 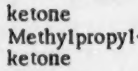	9,54±0,03		Cyclohexanone 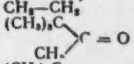	9,14±0,03
		0,07		
Methylpropylketone 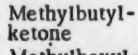	9,47±0,03		Pinacoline 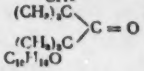	9,18±0,03
		0,03		
Methylbutylketone 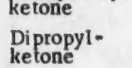	9,44±0,03		Pivalone	8,65±0,03
Methylhexylketone	9,40±0,03		Camphor $C_{10}H_{16}O$	8,76±0,03
Dipropylketone	9,12±0,03			

TABLE 2

Ionization Potentials

Compound	Ionization potential, eV	Compound	Ionization potential, ev
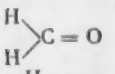	10,90 ± 0,03	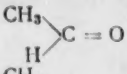	10,20±0,03
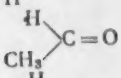	10,20 ± 0,03	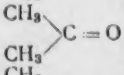	9,71 ± 0,03
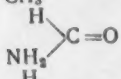	10,16 ±0 ,03	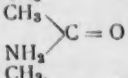	9,65 ± 0,03
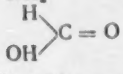	11,05 ± 0,03	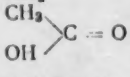	10,38 ± 0,03

In this work, we have determined ionization potentials by using the method described earlier [2]. The values for the ionization potentials which we have obtained are set out in Tables 1 and 2.

In aliphatic compounds, only those types of interaction are possible which have been classified by chemists under the name of the positive inductive effect (+1). In consecutive order the induction effect diminishes in the order:

$$C_4H_9 > C_3H_7 > C_2H_5 > CH_3 > H.$$

The ionization potentials shown in Table 1 are in excellent agreement with this series

If we suppose that the change in the ionization potential in the series under discussion is a linear function of the inductive effect, then, by considering each successive member in the series of the previous one, it is easy to see that the induction interaction diminishes in inverse proportionality to the square of the distance between the methyl and carbonyl groups. Actually, the replacement of the hydrogen atom of formaldehyde by a methyl group leads to a reduction of the ionization potential by 0.7 ev. A second methyl group directly combined to the carbonyl group reduces the ionization potential by a further 0.5 ev. If one of the hydrogen atoms of dimethyl ketone is replaced by a methyl group, then this methyl will be twice as far from the carbonyl group as the methyl of acetaldehyde is, and the reduction in the ionization potential should be only one quarter as great, which is what is observed experimentally.

The ionization potentials of the higher members of the series are also in agreement with this law, and we may express the relationship approximately by the equation:

$$\Delta I_p \simeq \frac{\text{const}}{[l\,(n+1)]^2},$$

where ΔI_p is the difference between the ionization potentials of two neighboring members of the series; $l(n+1)$ is the relative distance between the carbonyl group and the hydrogen atom which is being substituted by a methyl group; the compound then formed being the n + 1nth number of the series.

This relationship is valid not only for linear saturated ketones, but also for more complex branched ketones, whose ionization potentials are given in Table 1. A consideration of the values of the first ionization potentials of these compounds shows that the inverse proportionality of the difference between ionization potentials and the square of the distance between the substituting methyl groups and the carbonyl group describes the actual additivity with good accuracy. Actually, pinacoline may be regarded as acetone in which three hydrogen atoms are substituted by methyl groups. The substitution of one hydrogen atom by a methyl group in acetone leads to a reduction of the ionization potential by 0.17 ev. This means that the ionization potential of pinacoline ought to be found to be 0.51 ev less than the ionization potential of acetone, giving its value as 9.20 ev. The experimental value is 9.18±0.03 ev. A similar consideration of pivalone, which may be thought of as acetone in which six hydrogen atoms have been replaced by methyl groups, leads us to expect an ionization potential of 8.69 ev, compared with the experimental value of 8.65±0.03 ev.

The regularity which we have derived is valid, it seems, not only for ketones in which there exists a positive effect, but also for their halogen derivatives, where a negative inductive effect (-1) occurs. This should

lead to an increase of the ionization potential. We offer as an illustration the ionization potentials of chloroacetone (9.91±0.03 ev) and dichloroacetone (10.12±0.03 ev), which we have measured in the course of this work. The values of the ionization potentials of these compounds are, respectively, 0.20 and 0.41 ev higher than the ionization potential of acetone itself, which is 9.71 ev.

The regularity emerging from these experiments may not only be used to elucidate the mutual interactions of functional groups in molecules, but also for the estimation of the ionization potentials of more complex saturated ketones.

Table 2 gives the ionization potentials of some aldehydes ketones, amides and acids. In the two last cases, in addition to the inductive effect, a conjugation effect enters into the picture. Since the NH_2 and OH groups have larger electron affinities than hydrogen atoms, the direction of the inductive effect ought to be opposite to that found with the aliphatic radicals (−1). The conjugation effect would, in the case under consideration, have opposite sign to the inductive effect, owing to the mobility of the free electron pairs in the atoms of the substituent, which are included in the orbits of the oxygen atom of the carbonyl group, so increasing the electron density concentrated around it.

Both effects in the amide and the acids may be represented schematically thus:

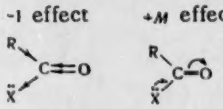

X denotes the NH_2 or the OH group. Since these effects provoke shift of electrons in opposite directions, then the effect on the ionization potential will depend on which of them is the dominant one.

It is seen from Table 2 that the ionization potentials of formamide and acetamide are, respectively, 0.74 and 0.55 ev less than those of formaldehyde and acetaldehyde, and are even somewhat lower than the potentials of acetaldehyde and dimethylketone (by 0.04 and 0.06 ev, respectively). This points to the predominance of the positive conjugation effect, enriching the electron density around the oxygen atom of the carbonyl group. Consideration of the ionization potentials of the acids shows that for these, on the other hand, the negative inductive effect is the predominant one: that is, the shifts of electronic charge is towards the oxygen atom of the hydroxyl group. These conclusions are in harmony with chemical data [3], according to which the positive conjugation effect diminishes in the order

$$N(CH_3)_2 > NH_2 > OH > Cl,$$

while the positve inductive effect diminishes in the order

$$OH > NH_2 > NHCH_3 > N(CH_3)_2 > H.$$

We may note that in the work of Higasi et al. [4] the same compounds were used for measurement of ionization potentials by the method of electron collision, and that the results obtained were appreciably different from our own. The authors, in their analysis of their own results, attribute to the amides a negative inductive effect which exceeds the conjugation effect, which is evidently not in agreement with the reduction of the basicity of the NH_2 group in amides as compared with amines.

This work has been carried out under the direction of Academician A. N. Terenin.

LITERATURE CITED

1. W. C. Price, J. Chem. Phys. 3, 256 (1935); A. D. Walsh, Proc. Roy. Soc. 185A, 176 (1946); T. M. Sugden and A. D. Walsh, Nature 148, 373 (1941).
2. F. I. Vilesov and A. N. Terenin, Doklady Aka. Nauk SSSR 115, 744 (1957) *; F. I. Vilesov, Pribory i Tekhn. Eksp., No. 4, 89 (1958).
3. O. A. Reutov, Theoretical Problems of Organic Chemistry [in Russian] (Moscow, 1956); A Remik, Electronic ideas in Organic Chemistry [Russian translation] (II, 1950).
4. K. Higasi, I. Omira, and H. Baba, Nature 178, 652 (1956).

* Original Russian pagination. See C.B. Translation.

DETERMINATION OF THE RATE CONSTANTS FOR ELEMENTARY REACTIONS OF HYDROGEN ATOMS WITH HYDROCARBONS

H. I. Gorban' and A. B. Nalbandyan

Chemical Physics Institute of the Academy of Sciences of USSR

(Presented by Academician V. N. Kondrat'ev, February 5, 1960)

Translated from Doklady Akademii Nauk SSSR, Vol. 132, No. 6, pp. 1335-1338, June, 1960

Original article submitted February 2, 1960

It is of considerable theoretical and practical interest to know the magnitudes of the rate constants of the elementary reactions, and the activation energies, of atomic hydrogen with the hydrocarbons. These reactions play an essential part in the oxidation and cracking of hydrocarbons.

To determine the constant of the reaction,

$$H + RH = H_2 + R \qquad (I)$$

and its activation energy, N. N. Tikhomiriva and V. V. Voevodskii [1] have made use of the reduction of the second self-ignition limit of hydrogen–oxygen mixtures in the presence of small concentrations of the higher homologs of methane and some unsaturated hydrocarbons. It is a necessary condition of the applicability of this method that the author's fundamental assumption can be taken as correct. This assumption is that the radicals R formed in the course of the reaction, and also any radicals which may arise as a result of the reaction of R with oxygen, should be less reactive than the chain bearers – hydrogen atoms – themselves.

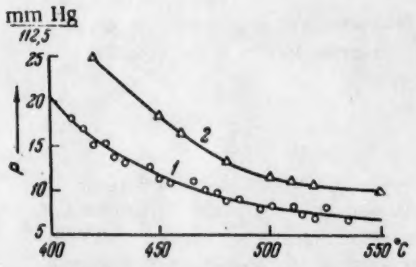

Fig. 1. Relationship of the ignition limit to the temperature. 1) For the mixing $2H_2 + O_2$; 2) for the same mixture containing 0.6% ethane.

The likelihood that this assumption is true has been enhanced by a series of researches by Baldwin and his colleagues [2], the first of which was carried out independently of, and at the same time as, the work referred to in [1].

It appears from the work of Baldwin and his colleagues that, in harmony with the usually accepted idea of the mechanism of the oxidation of hydrogen, mixtures rich in hydrogen exhibit a linear relationship between the difference of pressure at the second ignition limit of the hydrogen–oxygen mixture, when measured in the pure mixture, and at the same limit in the same mixture containing small quantities of saturated hydrocarbons, and the partial pressure of the added hydrocarbon. The weak dependence found by the authors between the quantity of added inhibitor (twice the amount of which is necessary for the lowering of the second limit as compared with the uninhibited limit) and the diameter of the reaction vessel and the composition of the mixture, apparently only takes place in mixtures of low hydrogen content, in which the chief active centers are, apart from the hydrogen atoms themselves, hydroxyl radicals.

The method of inhibition of the second limit for the determination of the rate constants of elementary reactions suffers from certain defects which prevent its being very accurate. Even when working under flow conditions,

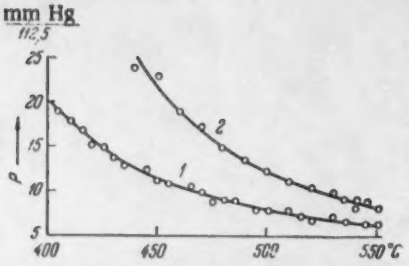

Fig. 2. Relationship of the ignition limit to the temperature. 1) For the mixing $2H_2 + O_2$; 2) for the same mixture containing 0.4% propane.

it is impossible to prevent the formation of water vapor, the molecules of which, as is well known [4], are very active ternary particles in the chain terminating reaction: $H + O_2 + M = HO_2 + M$. At temperatures between 550° and 650°C and comparatively high pressures of the reacting mixture, it is impossible to neglect the reactions of HO_2 with other molecules which may lead to the development of new chain-carriers.

This fact, together with the difficulty associated with work under flow conditions, rather diminishes the value of the method of determining rate constants by the reduction in the upper limit. We therefore suggest a modification of this method which makes possible a more accurate determination of the constants and activation energies of the reaction of atomic hydrogen with various hydrocarbons, and with substances which can act as hydrogen donors. The method is based on the shift (that is, the increase) of the lower limit of self-ignition of mixtures rich in hydrogen in the presence of hydrocarbons. Working in the kinetic region, it is possible to obtain very low values of the lower limit within the temperature range 400-530°C. Under these conditions the influence of water vapor, and also the reaction of HO_2 with other molecules, may be completely disregarded. The condition for the lower limit in the presence of an inhibitor is [3]:

$$2K_2(O_2) = K_4 + K_5(RH), \tag{II}$$

where K_2 is the rate constant for the branching reaction: $H + O_2 = OH + O$; K_4 is the rate constant for the destruction of hydrogen atoms on the walls of the reaction vessel; and K_5 is the rate constant for reaction (I).

Equation (II) may be rewritten in the form:

$$P_{1O_2}^{RH} = \frac{K_4}{2K_2} + \frac{K_5}{2K_2} P_{RH}, \tag{III}$$

where $K_4/2K_2$ is the partial pressure of the oxygen at the first noninhibited limit; $P_{1O_2}^{RH}$ is the partial pressure of oxygen at the first limit in the presence of the inhibitor RH. Hence

$$P_{1O_2}^{RH} = P_{1O_2}^{H_2} + \frac{K_5}{2K_2} P_{RH}.$$

If we denote the difference $P_{1O_2}^{RH} - P_{1O_2}^{H_2}$ by the term ΔP, and take into account the fact that the experiments are conducted on stoichiometric mixtures of hydrogen and oxygen, we arrive finally at the equation:

$$\frac{\Delta P}{P_{RH}} = \frac{3}{2}\frac{K_5}{K_2}. \tag{IV}$$

If we determine the value of ΔP from the experimental data, and knowing the partial pressure of the inhibitor at the first inhibitor limit, together with the value of K_2 determined earlier [5], it is not difficult to calculate the value of K_5 for each temperature. For the determination of its temperature dependence we may employ Eq. (IV), inserting in place of K_5 and K_2 in the equation the expressions: $K_5 = K_5^0 \exp(-E_5/RT)$, and $K_2 = K_2^0 \exp(-E_2/RT)$, where E_5 and E_2 are the activation energies of the destruction of hydrogen atoms in the bulk phase, according to reaction (I), and the branching reaction respectively. Inserting the values of K_5 and K_2 in Eq. (IV) and taking logarithms, we obtain:

$$\lg\frac{\Delta P}{P_{RH}} = \frac{E_2 - E_5}{2{,}3RT} + \lg\frac{3K_5^0}{2K_2^0}. \tag{V}$$

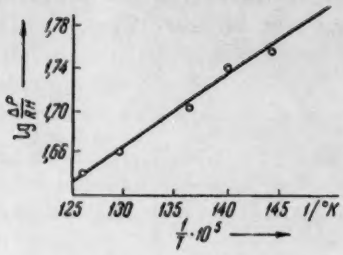

Fig. 3. $H + C_2H_6$. E = 12,000 cal/mole.

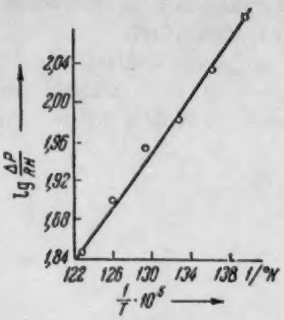

Fig. 4. $H + C_3H_8$. E = 8500 cal/mole

Values of the Rate Constant and Energy of Activation for the Reaction: $H + RH = H_2 + R$.

Hydrocarbon	$K_5 \cdot 10^{13}$ $cm^3/mol \cdot sec$	E_5 cal/mole
Ethane	1.49	12000
Propane	2.67	8500
Butane	2.96	6000

From the slope of the straight line on the coordinate $\log(\Delta P/P_{RH})$ and $1/T$, we may obtain the quantity $\Delta E = E_2 - E_5$, and so $E_5 = E_2 - \Delta E$, where E_2 = 15,100 cal/mole.

The first self-ignition limit of the hydrogen—oxygen mixture has been determined by the ordinary method of passing the gas into an evacuated quartz reactor heated to the required temperature. The reactor was in the form of a tube of diameter 2.8 cm and length 14 cm. So as to obtain reproducible values of the limit when these were low, the vessel was first washed out with hydrofluoric acid and subsequently, after careful washing with distilled water, treated with 2% potassium tetraborate. These precautions in cleaning the reactor, in conjunction with repeatedly exploding in it a mixture rich in oxygen, made it possible to obtain very low values of the limit, extending from $P_1 \simeq 0.18$ mm Hg at 410°C to $P_1 \simeq 0.05$ mm at 550°C. The ignition was recorded by means of a membrane manometer of high sensitivity. The values of the lower limit in a pure mixture of composition $2H_2 + O_2$, and in the same mixture containing 0.6% ethane or 0.4% propane, are depicted in Fig. 1 and Fig. 2. To obtain approximately the same shift in the case of inhibition by butane, as had been obtained in these experiments, experiment showed that only 0.2% butane was needed. The values of K_5 for 480°C, calculated from Eq. (4), are shown in the table.

Equation (V) was used for the determination of E_5. It is clear from this equation that $\log(\Delta P/P_{RH})$ bears a linear relationship to the reciprocal of the temperature. Figures 3 and 4 give the experimental data obtained for ethane and propane; it can be seen that the experimental points lie with good accuracy on their respective straight lines. A similar straight line was obtained for inhibition of the first limit by n-butane. The energies of activation of the appropriate reactions were calculated from the slopes of the lines, and are shown in the table.

The values obtained for the energies of activation of the reaction of atomic hydrogen with ethane molecules, propane molecules and n-butane molecules are somewhat higher than the corresponding values obtained by N. N. Tikhomirova and V. V. Voevodskii [1], and approximate to the values calculated by Steacie [6] and many other investigators on the basis of these methods.

LITERATURE CITED

1. N. N. Tikhomirova and V. V. Voevodskii, Collected Works on Chain Oxidation Reactions of Hydrocarbons in the Gas Phase [in Russian] (Izd. AN SSSR, 1955) p. 172.
2. R. R. Baldwin, Fuel 31, 312 (1952); R. R. Baldwin, N. S. Corney, and R. M. Precions, Nature 169, 201 (1952); R. R. Baldwin and R. F. Simmons, Nature 175, 346 (1955); Trans. Farad. Soc. 53, 955 (1957); Trans. Farad. Soc. 53, 964 (1957); R. R. Baldwin, N. S. Corney, and R. F. Simmons, Fifth Symposium on Combustion (1955) p. 502.

3. A. B. Nalbandyan and V. V. Voevodskii, The Mechanism of Oxidation and Combustion of Hydrogen [in Russian] (Izd. AN SSSR, 1949).
4. N. N. Semenov, Some Problems of Chemical Kinetics and Reactivity [in Russian] (Izd. AN SSSR, 1958).
5. L. V. Karmilova, A. B. Nalbandyan, and N. N. Semenov, Zhur. Fiz. Khim. 32, 1193 (1958).
6. E. W. R. Steacie, Atomic and Free-Radical Reactions (N. Y., 1954).

AN ELECTROMAGNETIC METHOD OF MEASURING THE VELOCITY OF EXPLOSION PRODUCTS

V. M. Zaitsev, P. F. Pokhil, and K. K. Shvedov

Physical Chemistry Institute of Academy of Sciences of USSR

(Presented by Academican V. N. Kondrat'ev, February 20, 1960)

Translated from Doklady Akademii Nauk SSSR, Vol. 132, No. 6, pp. 1339-1340
June, 1960

Original article submitted February 20, 1960

A direct study of the velocity of explosion products would have great value, both from the point of view of developing theory of detonation, and from the point of view of the practical application of explosive substances.

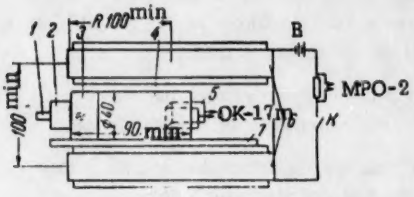

Fig. 1. Schematic presentation of the coil used to create the magnetic field and the charge on the detector. 1) Capsule detonator; 2) supplementary dedonator; 3) explosion lens to create a plane front; 4) basic charge of the explosive substance; 5) detector; 6) half winding of coil; 7) wooden stand for the charge; B) battery; source of constant current. K) switch for closing the electrical circuit.

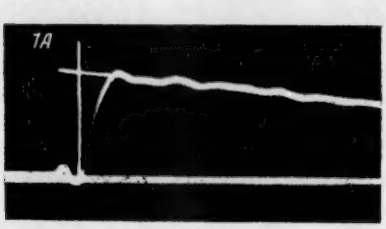

Fig. 2. Photograph depicting the emf induced on the moving detector.

In publications [1, 2] a method is described for determining the velocity of explosion products, which is called by the authors the "cutting off" method. This method is based on the calculation of the Poisson adiabatic index, n, of the explosion products. If use is then made of the equations of the conservation of mass and of momentum, it is possible, from the measured value of the velocity of detonation, D, and the calculated value of the adiabatic index, n, to determine the mechanical parameters of the detonation wave at the Jouget point [3] (the point at which the Chapman and Jouget equation is satisfied, $u + c = D$, where u is the velocity of the detonation products, and c is the velocity of sound in the explosion products); since $u = D/(n + 1)$ = velocity of the explosion products (mass velocity); $\rho = \rho_0(n + 1)/n$ density of explosion products (where ρ_0 = initial density of the explosive substance), and $P = \rho_0 uD = \rho_0 D^2/(n + 1)$ = pressure of the explosion products.

The present paper is devoted to a description of a direct measurement of the velocity of the detonation products by means of an electromagnetic method [4].

This method is founded on the development of an emf in a conductor which is being moved in a magnetic field. It is assumed that the detector in the charge after the passage of the detonation front is moved along with the products of detonation. The likelihood of this assumption is confirmed by the fact that results obtained by this and other methods [5] are close to one another (see Table 1).

Employing the relationship between the velocity of movement of the detector, u, the length of the detector, L, the intensity of the magnetic field, H, and the magnitude of the induced

Explosive substance	ρ_0, g/cm³	D, km/cm	μ_{em}, km/cm	μ_{cal}, km/cm
Compressed trinitrotoluene	1,60	7,00	1,81	1,84
» »	1,55	6,77	1,77	1,80
» »	1,47	6,52	1,71	1,73
» »	1,31	6,05	1,58	1,59
» »	1,00	5,10	1,32	1,30
Cast trinitrotoluene	1,60	7,00	1,81	1,84
TG 50/50 cast	1,68	7,65	2,03	2,07

emf, ϵ, we obtain the relationship: $u = (10^8 \epsilon / HL)$ cm/sec, where ϵ is measured in volts, H in oersteds, and L in centimeters. The emf induced on the detector is determined by means of a cathode oscillograph of type OK-17M.

The detector was made of copper or aluminum foil of thickness 0.3-0.5 mm, bent double into a Π-shape. The detector is made broad enough so as to reduce to a minimum any errors arising from the detonation wave flowing round it. The dimensions of the working part of the detector were 10 × 15 mm.

On the suggestion of B. K. Shembel', we have worked out a nonstationary method of creating the magnetic field. This magnetic field has been created by passing a constant electric current through two coil half-windings, separated by a distance equal to the radius of a coil. In this case the intensity of the magnetic field at the center of the coil may be calculated to a high degree of accuracy from the formula [6]: $H = 0.45\ \omega I / R$, where ω is the total number of turns in the winding, I is the current passing through the coil, and R is the radius of the coil.

The measurement of the current was carried out by determining the drop in potential along a standard resistance of 0.01 ohm included in the feed circuit of the coil.

Figure 1 gives a schematic presentation of the position of the coil creating the magnetic field and the charge on the detector. A typical example of the emf record produced is shown in Fig. 2.

To calculate the mass velocity of the explosion products, the value of the emf is extrapolated to the initial instant when the detector began to move (point A in Fig. 2), and the emf value at this point is obtained. The mean error in the determination of the mass velocity in a series of 3-5 experiments did not exceed 3%. The experiments were performed on both cast and compressed charges of trinitrotoluene and a mixture known as TG 50/50 (that is, a mixture of equal weights of trinitrotoluene and hexogene). The results are given in the table.

It can be seen from the table that the electromagnetic method gives rather lower results than the cutting-off method, which is presumably to be explained by the conductivity of the ionized products of the detonation.

A detailed consideration of the oscillogram shows that in the initial time after the detonation we obtain a linear drop of the mass velocity with time. This points to the fact that the Poisson adiabatic index is not only independent of the initial density [2], but also remains constant for some time (3 to 3.5 μsec) after the detonation front of the wave.

The merits of this method lie in the fact that it permits the direct measurement of the mass velocity not only at the wave front, but also some time behind the wave front of the detonation.

LITERATURE CITED

1. L. V. Al'tshuler, K. K. Krupnikov, et al., Zhur. Éksp. i Teoret. Fiz. 34, 4, 874 (1958).
2. J. M. Walsh and R. H. Christian, J. Phys. Rev. 97, 6 (1955).
3. Ya. B. Zel'dovich and A. S. Kompaneets, The Theory of Detonation [in Russian] (Moscow, 1955).
4. A. A. Brish, M. S. Tarasov, and A. Tsukerman, Zhur. Éksp. i Teoret. Fiz. 37, 6 and 12, 1543 (1959).
5. A. N. Dremin and P. F. Pokhil, Doklady Akad. Nauk SSSR 128, 5 (1959). •
6. E. G. Shramkov, Works Presented at the All-Union Scientific and Research Institute of Metrology [in Russian] (1959) parts 10/70.

• Original Russian pagination. See C. B. Translation.

THE EFFECT OF PRESSURE ON THE RATE OF LAMINAR AND TURBULENT COMBUSTION

V. P. Karpov and A. S. Sokolik

Chemical Physics Institute of the Academy of Sciences of USSR

(Presented by Academician V. N. Kondrat'ev, February 25, 1960).

Translated from Doklady Akademii Nauk SSSR, Vol. 132, No. 6, pp. 1341-1343, June, 1960

Original article submitted February 24, 1960

The difference in mechanism between the spreading of laminar flames and the spreading of turbulent flames ought to be expressed in different relationships between the corresponding rates of combustion and the pressure. This relation for laminar combustion can be arrived at from an approximate heat theory [1], according to which:

$$u_c \sim p_0^{n/2-1}. \qquad (1)$$

where n is the order of the over-all reaction in the flame.

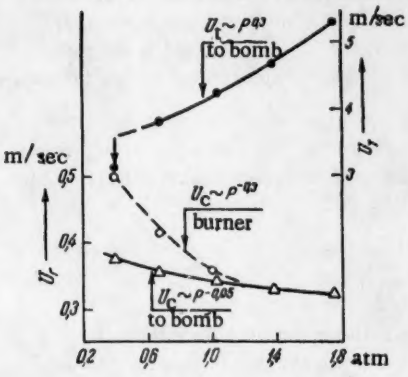

Fig. 1

Measurements which have been made in the cone of the bunsen flame, for a series of air mixtures at pressures lower than atmospheric, have led to values of $k = [n/(2-1)] < 0$. According to publication [2], the value of k for benzene, n-pentane and isooctane is −0.33; according to [3] its value for propane is −0.3; and, finally, a review of the measurements on propane in publication [4] gives values of k from −0.19 to −0.3.

Measurements of the rate of combustion of propane−air mixtures in the initial stages of combustion in a spherical bomb [5], gave k = −0.05. We have also obtained the same relationship with the pressure in our own experiments, which were carried out in the bomb described in [6], for a stoichiometric mixture of propane and air within the pressure limits of 0.4 and 1.76 atm. The rate of spreading of a spherical laminar flame was obtained within limits for the radius of the flame from R ≈ 10 mm (that is, with the exclusion of the stage of ignition) to R ≈ 40 mm (that is, less than 55% of the radius of the bomb), when the increase of pressure from combustion was not more than 3-4% away from the maximum pressure increase.

We shall consider the source of such appreciable difference between the relationship of u_c to the pressure under the conditions found in the flame of a burner, and during spreading in a closed space. The latter case involved a rate of combustion evidently determined by the rate of spreading of the flame, dr/dt, according to the relationship:

$$u_c = (dr/dt)/\varepsilon. \qquad (2)$$

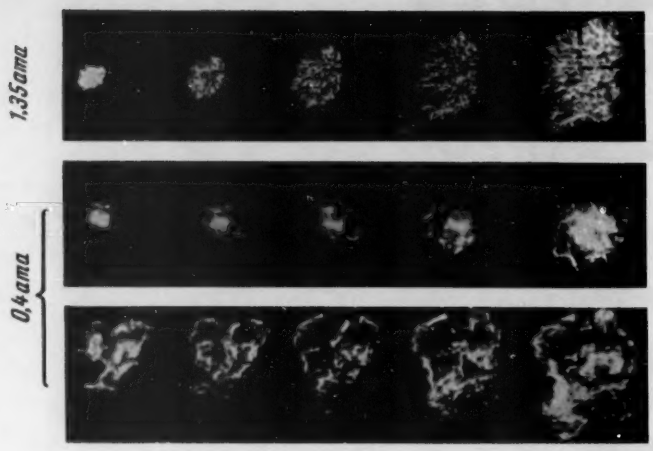

Fig. 2

For determination of ϵ, the degree of spreading due to combustion, the width of the combustion zone is neglected, and taking the mean gas temperature within the sphere of the flame as equal to the adiabatic combustion temperature, we may write:

$$\varepsilon = \frac{T_{ad}}{T_0}\frac{m}{m_0}, \tag{3}$$

where m/m_0 is the change in the number of molecules on combustion. This assumption, however, is valid only for pressures sufficiently close to atmospheric pressure; the more the pressure is lowered, and the wider the zone of combustion, so much the more does the mean temperature of the flame-gas deviate from the adiabatic temperature. The degree of widening calculated from (3) deviates more and more from the actual value, and the rate of combustion calculated from (2) becomes progressively lower in comparison with the true value. The comparison in Fig. 1 of the rate of combustion of a propane–air mixture as measured at a burner in the work mentioned [4], and the results obtained by us in a bomb, shows a considerable divergence between them when p_0 is less than 0.5; this divergence increases still further with further pressure reduction. Since a change in the rate of combustion in the flame of the burner is not bound up with increase in the degree of spreading, the relationship $u_r \sim p^{-(0.2-0.3)}$ must be considered to be the most reliable.

Decrease in pressure is accompanied by decrease in the combustion temperature, T_c, owing to an increase in the degree of dissociation. The growth of this factor in relation to u_c may be represented approximately by the following formula:

$$u_c \sim T_c^{2.7}(T_c - T_0)^{-1.5}\exp(-E_e/2RT_c), \tag{4}$$

which combines in itself all the temperature-dependent quantities in the heat-theory formula for a flame in bimolecular reactions. According to the data of publication [7] for a stoichiometric mixture of propane and air, T_c varied from 2242 to 2277° K within the investigated range of pressure. If we take the value of E_e as 20 kcal per mole from the data of experiments carried out at the time on hydrocarbon–air mixtures, then (4) shows a change in u_c not greater than 1%.

Thus, all the observed change in the laminar rate of combustion within these pressure limits may be completely accounted for by the pressure variation itself. According to Eq. (1), this corresponds to a reaction order of 1.4-1.6 in the flame.

The effect of pressure on the turbulent rate of combustion in the current has been investigated in work reported in publications [4, 8] in an open flame, and in the work of Doroshenko and Nikitskii (see [9], p. 32) and [10] in a chamber under a turbulizing lattice (subatmospheric pressure being used throughout).

In the open flame experiments, which were performed with the Re value kept constant, the turbulent rate of combustion u_t was either unchanged [4], or increased as the pressure was reduced $u_t \sim p^{-0.25}$ [8]. However, the condition that $Re = wd\rho/\mu$ = constant for constant diameter of the burner signifies that reduction in pressure will produce increased current rate, that is, $w \sim p^{-1}$, so that the level of turbulent pulsations will also increase, and exert its own independent effect on the rate of turbulent combustion. Actually, in the experiments reported in [10], it was shown that the relative intensity of turbulence, $u'/w \sim p^{0.34}$. This means that the absolute intensity of turbulence changes according to the relationship: $u' \sim p^{-0.66}$, which ought also to lead to the acceleration of turbulent combustion at reduced pressure, which occurs under the experiments described in [8].

On the other hand, when the rate of flow is maintained constant, a direct relationship is found between u_t and the pressure, such as $u_t \sim p^{0.4}$ which was found for the propane–air mixture in [10], or, with pressure exponents varying from 0.25 to 0.5, in the experiments described in [9]. In an investigation of the effect of pressure on the rate of turbulent combustion in a closed space, a preliminary study showed that the absolute intensity of the turbulence u'_Σ [6] remains constant for a given potential on the electric mixer within a pressure range of 100 to 760 mm Hg. Experimental work gave the value of u'_Σ as 4.2 m/sec, while for the stoichiometric propane: :air mixture the ratio u'_Σ/u_c was greater than 10. The results of these experiments are set out in Fig. 1, within pressure limits of 1.76 and 0.5 atm, and give the relationship: $u_t \sim p^{0.3}$.

The closeness of agreement between the pressure exponents determined in the bomb and under flow conditions is a consequence of the essential similarity in the mechanism of turbulent combustion, irrespective of the process whereby the turbulence is created. On the other hand, the observed increase in u_t with growth in pressure for a constant turbulence intensity cannot be harmonized with a surface-laminar model no matter what form the latter takes, since the laminar and turbulent combustion rates change with pressure in opposite directions.

From the standpoint of the pulsating ignition model [11], and the general relation:

$$u_t \sim u'_\Sigma \frac{t_0}{\tau_i} \tag{5}$$

the observed change of u_t with pressure, under conditions in which u'_Σ is constant, is a combined effect, related to the pressure both by the period of induction of ignition, τ_i, and by the characteristic diffusion time, t_0. According to publication [10] the scale of the turbulence, l_1, does not depend on the pressure, and therefore:

$$t_0 = \frac{l_1}{u'} \sim p^{-0.34}. \tag{6}$$

It follows from this that u_t diminishes with reduction in pressure because of the increase of τ_i and the shortening of t_0.

Under the conditions of experiments in the bomb, however, that is, when μ'_Σ is constant, we must also suppose that t_0 is constant. On this assumption, the observed change with pressure of u_t should be completely determined by the change of the period of induction of the ignition with pressure. That is, $\tau_i \sim p^{-0.3}$. A low value of the pressure exponent would in this case point to the kinetic part of the total induction period as being comparable with the time of mixing of the fresh gas with the combustion products.

When the pressure is reduced to below 0.5 atm, a more abrupt reduction in u_c is observed that would correspond to the value of 0.3 for the pressure exponent. From the cine frames shown in Fig. 2, it can be seen that the reduction within this pressure range of the neutralized rate of propagation of the spherical flame is concerned with the fact that the flame does not occupy the whole volume of the sphere uniformly, but is spread out in separate "tongues," similar to the spreading of a turbulent flame with concentration limits (see Fig. 3 in [11]). This point to the existence of difficulty in turbulent ignition, due to the fact that with reduction of pressure τ_i increases and t_0 is shortened. Under the given experimental conditions turbulent ignition is usually impossible under pressures less than 0.4 atm. The essential basis of the pulsating ignition model would make turbulent ignition impossible when the induction period of ignition exceeds the time of diffusion mixing arising from it, that is, when

$$\tau_i > t_0. \tag{7}$$

This is the general condition for the limits of turbulent ignition, expressed either by pressure or by composition of the mixture. We may note that under this condition the hydrodynamic factor enters in, not only through the quantity t_0, but also through the magnitude of the induction period, depending on the conditions of turbulent mixing.

LITERATURE CITED

1. Ya. B. Zel'dovich and D. A. Frank-Kamenetskii, Zhur. Fiz. Khim. 12, 1, 100 (1938).
2. F. H. Garner, G. K. Ashforth, and K. Long, Fuel 30, 17 (1951);
3. A. Egerton, Fourth Symposium on Combustion (1953) p. 321.
4. B. Fine, Combustion and Flame, 2, 109 (1958).
5. J. Manton and B. B. Milliken, Proceedings of the Gasdynamic Symposium on Aerothermochemistry (Northwest Univers. Evanston, 1956) p. 157.
6. V. P. Karpov, E. S. Semenov and A. S. Sokolik, Doklady Akad. Nauk SSSR 128, 6, 1220 (1959).*
7. D. Simon, F. Bells and A. Spakowskii, Fourth Symposium on Combustion (1953) p. 100.
8. S. A. Gol'denberg and V. S. Pelevin, Seventh Symposium on Combustion (1957) p. 590; Energetics and Automatization, Izv. Akad. Nauk SSSR, OTN 2 (1959).
9. E. S. Shchetinkov, Collected Works on Combustion in a Turbulent Stream [in Russian] (Izd. AN SSSR, 1959) 5.
10. A. V. Khramtsov, Seventh Symposium on Combustion (1957) p. 609.
11. A. S. Sokolik and V. P. Karpov, Doklady Akad. Nauk SSSR 129, 1, 168 (1959).*

* Original Russian pagination. See C. B. Translation.

THE MECHANISM OF HETEROGENEOUS EXCHANGE BETWEEN ACETONE AND WATER IN THE GAS PHASE

B. A. Kuznetsov and I. D. Elkina

The M. V. Lomonosov Moscow State University

(Presented by Academician V. N. Kondrat'ev, February 24, 1960)

Translated from Doklady Akademii Nauk SSSR, Vol. 132, No. 6, pp. 1344-1347, June, 1960

Original article submitted February 19, 1960

It has been shown in an earlier publication [1], that exchange between gaseous hydrogen bromide and acetone takes place by collision of HBr molecules from the gas phase with acetone adsorbed on the walls of the vessel. Owing to the acidic properties of the HBr molecule on the wall, it is presumably possible for protolysis of the acetone to take place in such a way that the whole HBr molecule, rather than one proton, is involved in the combination. By this means a so-called ion pair is formed on the surface, and will be similar to the ion formed in the liquid phase:

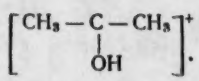

The residual Br is capable of splitting off a hydrogen atom from one of the methyl groups within the complex:

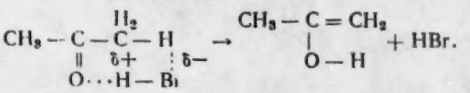

The cycle proceeding in the opposite direction occurs in the volume phase.

In order to put this suggestion to the test, and to elucidate the general rules governing exchange between compounds containing hydrogen and an unshared electron pair, on the one hand, and acetone which contains chemically reactive hydrogen, on the other, we have undertaken a study of the kinetics and mechanism of the isotopic exchange between acetone and water or ammonia.

Experiments carried out on exchange between ammonia and acetone d_6 by the method described earlier [1] in the temperature range 20 to 250°, and at P_{NH_3} = 140 mm and P_{ac} = 70 mm, showed that no exchange took place during a period of 2-3 hours. We drew the conclusion, therefore, that the mechanism analogous to the mechanism of the process in the liquid phase, with ion pairs formed on the wall, and a transitional complex of the form:

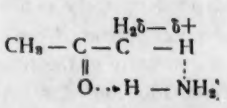

was very improbable, because the H in the methyl group cannot, apparently, be the site of the primary attack by the ammonia.

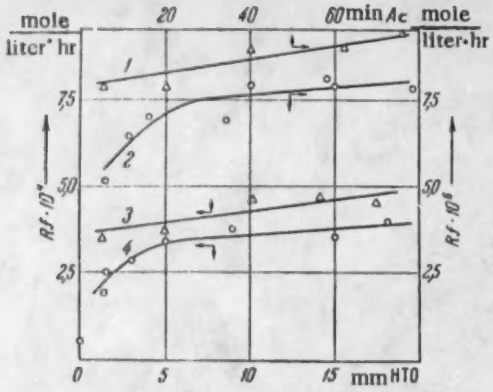

Fig. 1. Relationship between the rate of exchange and the acetone pressure (curves 1 and 3) when P_{H_2O} = 15 mm; and between the rate of exchange and the water pressure (curves 2 and 4) when P_{ac} = 5 mm. Experiments 1 and 2 were carried out in an empty vessel, and 3 and 4 in a vessel with filling.

We have studied the exchange between acetone and water by using tritium as the marker. The method is very sensitive in view of the very high specific activity of the initial tritio–water ($\rho_{HTO}=4.52\cdot10^6$ impulses/min·mm) and we have therefore been able to observe rates of exchange between acetone and water which are very slow (only about 1/1000 of that between acetone and hydrogen bromide), and to determine the kinetics of the process. It will be shown that the exchange between HTO and acetone follows a different law from that set out above. The experiments were done in a vacuum apparatus, using a quartz vessel of volume 1.5 liters which was previously treated with chromic acid mixture and carefully washed with distilled water. The quantity of mixture inserted in the vessel was determined by means of a mercury manometer, using a microcathetometer. After the reaction, the mixture was frozen out and diluted by about 50-100 times its volume of acetone. The mixture of water and acetone so obtained (amounting to about 1.5 ml) was separated in the following way. Dibutyl ether and 2-3 drops of water were added. The mixture was shaken, and separated in a separating funnel, and the solution of acetone in dibutyl ether was dried by means of alumina. The operation of washing out the water was repeated, and then the acetone was distilled away, using a flask fitted with a fractionating column. It was shown by special experiments that no exchange took place during the separation process.

The tritium content of the acetone was determined by means of a counter fitted internally. The pressure of acetone in the counter was determined with an accuracy of 0.01 mm Hg. The tritium content of the water was found from the specific activity of the hydrogen obtained by reducing the water over magnesium in a vacuum apparatus at 470°C. The rate of exchange was calculated according to the formula:

$$Rf_1 = \frac{1}{t}\,\frac{nAmB}{nA+mB}\,\ln\left(1-\frac{\rho_a}{\rho}\right), \qquad (1)$$

$$Rf_1 = \frac{1}{t}\,\frac{\rho_a nA}{\rho_w} \qquad (2)$$

for low percentage of exchange.

These formulas were obtained from the work reported earlier [1] for the conditions $\rho_a, \rho_B, \bar{\rho} \ll 1$, $k = 1|1|$; $\rho_a/\bar{\rho} \ll 1|2|$, where the initial formula, $\rho_a = A^*/nA$ gave the value of the relative isotope composition. That is, $\rho_a = (T)_{ac}/6A$. Since the intensity of the β-radiation is proportional to the tritium content, $I = \lambda[T]$, where λ is the disintegration constant, and only relative values of the quantity I are used in formulas (1) and (2), since it is not necessary in the calculation to know the absolute concentration of the tritium.

Thus, $n\rho_a$ is the specific activity of the acetone at time t; $m\rho_w$ is the initial specific activity of the water; Rf_1 is the rate of exchange; A and B are the concentrations of acetone and water, respectively; n and m are the numbers of atoms of hydrogen in the molecules of acetone and water, respectively; then; $\bar{\rho} = \rho_w Bm/(nA+mB)$, the mean activity of the hydrogen atoms in the system.

A study of the orders of the reaction in an empty quartz vessel at a temperature of 180° has shown (Fig. 1) that the rate of reaction is almost completely independent of the concentration of the reacting substances within certain limits (acetone pressure from 3 to 80, and water pressure from 4 to 20 mm Hg). Increase in temperature does not alter this relationship between rate and the pressure of the reactants. The dependence of the rate on temperature is more complex, as Fig. 2 shows. From 180-250°, E = 1.5 kcal/mole; at t = 350° E has increased to 25 kcal/mole. Measurements were not carried out at higher temperatures in view of the possibility that cracking

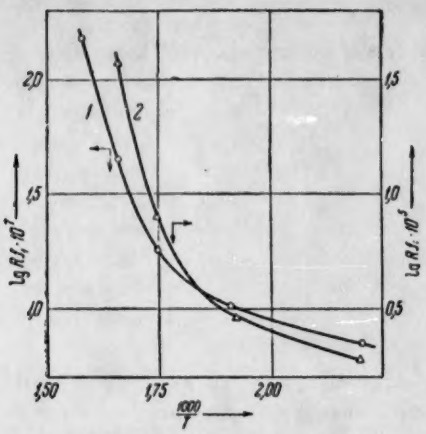

Fig. 2. Relationship between exchange rate and temperature: 1) in an empty vessel; 2) in a vessel with filling.

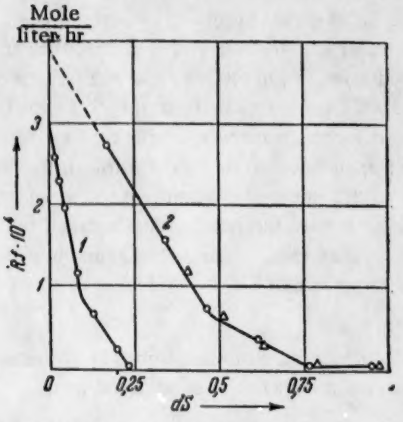

Fig. 3. Relationship between the rate of exchange of acetone and water (1), and acetone and the surface hydroxyl groups (2), and the fraction of exchanged surface.

of the acetone might take place. The relationship between Rf_1 and S/v has also been studied. Changing the size of the vessel caused a proportional increase in S/v. When quartz particles were used as filling material in the vessel, the geometrical magnitude of S/v was increased by a factor of 16. The rate, however, increased by a factor of 100, which may be explained by the difference in properties between fused and powdered quartz [2]. We have proposed the idea that exchange between acetone and water occurs through the action of hydroxyl groups on the surface, which act as an intermediate link in the transfer of the hydrogen isotope. Confirmation of this hypothesis was obtained by investigating the rate of hydrogen exchange between surface hydroxyl groups and water or acetone. The surface of the vessel was treated three times with HTO vapor for some days at a temperature of 300-350°. The experiments were only carried out after careful evacuation of the water from the vessel over a period of 4-5 hours at 300°. Water vapors were admitted at a definite time into the vessel, and after freezing out their specific activity was determined. The operation was repeated several times with an increasing period of extraction of the water vapor in the vessel until the transitory activity on the surface was so small that it could not be detected. The exchange rate was calculated from formula (1), for which the value of mB was taken as 1.5 mm Hg. (This was found from experiments in which the total activity retained on the surface was measured.) From calculations of the rate in each successive experiment the change in the specific activity of the SiOH groups was estimated in such a way that the value Rf_1 for the individual substance would remain constant. The total activity retained on the surface amounted to $3.4 \cdot 10^6$ impulses/min, which corresponded to 30 μmole/m^2 of the geometrical surface (S = = 0.95 m^2). The limiting concentration of SiOH groups on the surface is 11 μmole/m^2. Therefore, the surface studied by us was equal to ≈ 3 m^2. It was found that the SiOH groups had widely varied effects on the rate of exchange. The surface to a large extent entered into the exchange process only slowly. The maximum rate, obtained by extrapolation to $\tau = 0$, was given by $Rf_{1max} = 0.2$ mm Hg/min. The minimum fate was $Rf_{1min} = 0.002$ mm Hg/min at a temperature of 180°. This difference of rate accounts for $\Delta E = 2$ kcal/mole.

Experiments on exchange between acetone and surface hydroxyl groups were carried out in a similar way. Figure 3, curve 1 gives the relationship of the rate of exchange to the proportion of exchanged surface. The latter quantity was defined as the ratio of the activity of the surface at a given time t to the total activity applied. Figure 3 shows that reduction of rate occurs during the experiment, while exchange takes place comparatively rapidly with part of the surface only. Thus, if it is supposed that the water has access to all the SiOH groups [3], then the acetone has access only to a fraction of them. After exchange between acetone and the surface has practically ceased (when $\delta S = 0.24$), exchange was found to continue in the same experiment between the remaining, nonexchanged hydroxyl groups and the water (for which the experimental points are denoted by triangles). In view of the fact that the rate of exchange of water with the surface hydroxyl groups coincides with the previous acetone exchange at the same δS even in the absence of the latter, we conclude that the more reactive SiOH groups behave in the same way both with respect to water and with respect to acetone. In analyzing the curves in Fig. 3 we find that; when $\tau \to 0$, or $\delta S \to 0$, $Rf_{1max} = 3.0 \cdot 10^{-4}$ mole/liter·hour. This is close to the value obtained for exchange between acetone and water when both were present together (Fig. 1). Thus, the exchange rate between

water and hydroxyl groups is greater than that between water and acetone when these are present together, but the rate for acetone and the surface hydroxyl groups is equal to, or less than, this value.

On the basis of the material produced in this paper the whole process of exchange between acetone and water may now be explained in the following way. The acetone forms a chemisorbed compound, which may be obtained by breaking down the Si–O–Si groups, forming the enolate

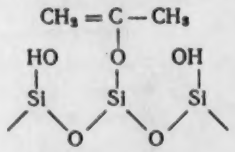

(which is similar to the alcoholate discussed in [4]), followed by removal of the acetone after reaction of SiOH groups of the vessel which have been exchanged with tritium. Since the exchange process between the water and the SiOH is not a limiting process, the observed order with respect to the water should be zero. The increased exchange rate in the presence of water may then be explained by supposing that the adsorbed water takes part in exchange with the chemisorbed acetone in proportion to the fraction of occupied surface (0.01) at the same time increasing the rate of desorption of the chemisorbed acetone. If it is estimated that the adsorbed water reacts with the acetone with a rate $Rf_1 = 3.0 \cdot 10^{-4}$ mole/liter·hour, then the weak dependence of the rate on the water pressure may be supposed to be due to the substitution of the slightly active SiOH groups by the more active hydroxyl groups of water. The temperature dependence of the exchange rate of water and acetone serves to confirm our hypothesis as to the part played by the SiOSi groups. It is found that dehydration of the surface, and increased proportion of SiOSi groups occurs in the same temperature region [5] in which a sudden increase in the exchange rate is found (300°). If preliminary dehydration is carried out at 600°, there is a certain increase in the rate at 180°. For the explanation of the zero order with respect to acetone (or the weak dependence on its concentration), we must suppose that the limiting stage in the pressure range from 5-80 mm Hg of acetone is the desorption of the chemisorbed acetone. This hypothesis is supported by the facts previously adduced as to the relationship between the initial exchange rate between acetone and the groups, and the acetone pressure (zero order at 180°), and between this rate and the temperature (activation energy around 180-200° is the same as that for the exchange between water and acetone when they are present together).

It thus appears that exchange between acetone and water takes place by means of chemisorption of the acetone with hydroxyl groups present on the surface, forming a compound which then reacts with adsorbed water.

LITERATURE CITED

1. B. A. Kuznetsov, Doklady Akad. Nauk SSSR 131, 3 (1960).*
2. S. P. Zhdanov and A. V. Kiselev, Zhur. Fiz. Khim. 31, 2213 (1957).
3. V. A. Nikitin, A. I. Sidorov, and A. V. Karyakin, Zhur. Fiz. Khim. 30, 117 (1956).
4. A. I. Sidorov, Zhur. Fiz. Khim. 30, 996 (1956).
5. S. P. Zhdanov, Doklady Akad. Nauk SSSR, 123, 716 (1956);* W. Stöber, Koll. Z. 145, 17 (1956).

* Original Russian pagination. See C. B. Translation.

THE POSSIBILITY OF INCREASING THE YIELD OF HYDROPEROXIDE IN THE INITIATION OF THE OXIDATION OF CUMOL BY HYDROGEN PEROXIDE

R. V. Kucher, S. D. Kaz'min, and V. D. Enal'ev

The Ivana Franko L'vov State University

(Presented by Academician V. N. Kondrat'ev, February 11, 1960)

Translated from Doklady Akademii Nauk SSSR, Vol. 132, No. 6, pp. 1348-1351, June, 1960

Original article submitted February 9, 1960

In connection with the radical mechanism which governs the oxidation reactions of hydrocarbons, the initiation of this process is a matter of great interest. The short-period initiation of the chain process in the initial stage proposed by N. M. Emanuél' [1] leads to a shortening of the initiation period, and ensures that the rate of the reaction will lie close to the rate of the process with constant initiation, thus making it possible to avoid various secondary processes. The effectiveness of the initiation is determined not only by the experimental conditions, but also by the activity of the radicals introduced into the system. N. N. Semenov [2] has shown that the activity of a radical may be measured on the basis of the so-called relative activity, which defines the reactivity of the radical in question in comparison with that of any other radical. The activity is basically determined by the structure of the radical, which in its turn depends on the nature of the reacting substance. The effectiveness of the initiation produced by any given additive, however, would be expected to vary during the course of a complex process, during which a variety of products are obtained. In actual systems, there may very often be present at the same time both initiator and inhibitor; in such a case the effectiveness of the initiation would be expected to be determined, not only by the rate of origination of new chains, but also by the rate of interaction between the radicals of the initiator and the molecules of the inhibitor.

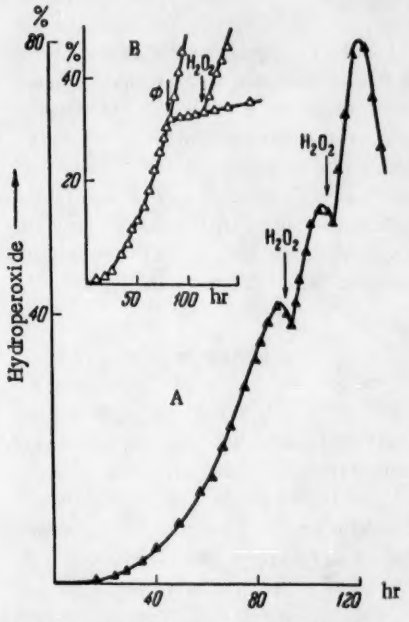

Fig. 1. Kinetic curves for the formation of hydroperoxide during the oxidation of cumol in emulsified form, with phase ratio of 1 : 4, at a temperature of 85°. The arrows denote the points at which there are put into the system H_2O_2 (0.015 mole/liter) and phenol (0.01 mole/liter).

We have used hydrogen peroxide as initiator for the oxidation of isopropylbenzene. The method used has been described in previous communications [3, 4].

It has been shown that the effect of hydrogen peroxide is very specific, and is to a large degree determined by the time at which it is introduced into the reacting system (Fig. 1). The initial short-period initiation produces neither acceleration of the reaction nor a shortening of the induction period.

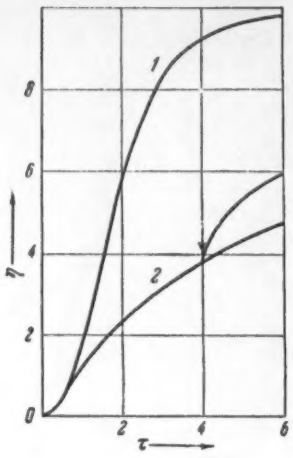

Fig. 2. Theoretical curve of formation of the intermediate product, forming and decomposing by a chain mechanism, calculated from Eq. (6) using the values B = 0 (1) and B = 100 (2). The arrow indicates the moment of disintegration of product C.

The introduction of hydrogen peroxide, however, into the reacting system at a later stage of the process, when the reaction is already slowing down, leads to a quite different effect: it almost seems as though the brake had been taken off the reaction, and the rate of formation of hydroperoxide rapidly rises. The same kind of effect may be obtained repeatedly when new retardation sets in by repeating the operation, until practically complete removal of the hydrocarbon has taken place. The yield of hydroperoxide in this process is increased from 40-80%. It is not possible to explain this picture if the introduction of the initiator is considered only as causing the creation of a large concentration of the active particles in the system, as was formerly supposed. The phenomenon is much more reminiscent of a "de-braking" of the reaction than of its initiation.

With the object of explaining the cause of this phenomenon, we have carried out experiments on the use of hydrogen peroxide as initiator for the oxidation of isopropylbenzene, when this is simultaneously retarded by an inhibitor (phenol). It can be seen from Fig. 1B that after the addition of hydrogen peroxide the reaction is restored to its previous rate. Thus, the introduction of hydrogen peroxide into the system evidently brings about a selective destruction of the inhibitor, according to some such reactions as: $C_6H_5OH + OH^{\cdot} \rightarrow C_6H_5O^{\cdot} + H_2O$. The radicals $C_6H_5O^{\cdot}$, which are only slightly reactive, subsequently recombine.

These facts taken together lead to the idea that the radicals formed during the decomposition of the hydrogen peroxide are only slightly reactive compared with the radicals taking part in the chain, and practically incapable of reacting with the initial hydrocarbon, since if this were not so, there would be observed an abrupt increase in the rate on introducing hydrogen peroxide into the initial system.

The development of the process leads to the increasing formation of molecular intermediate products which, being as one would suspect, more reactive than the initial hydrocarbon, are involved in the over-all chain process, which may therefore in its later stages not be capable of description in terms of kinetic regularities. In consequence of this participation of intermediate products in the chain process – for example, according to the equation $B + R^{\cdot} \rightarrow B^{\bullet\cdot} + RH$ (where $B^{\bullet\cdot}$ is a slightly reactive radical and B is the intermediate product) – the slowing down or cessation of the oxidation reaction long before the initial hydrocarbon has been used up has been recorded by many authors: that is, this stopping or slowing down occurs when the internal resources of the process are by no means exhausted [6]. Hence, the removal of the retarding products from the reaction zone, or their destruction ought to lead to a renewal of the process. This circumstance provides a possibility of raising the final yield of the desired reaction products.

The stopping of the degenerate branching reaction at a point when the rate of initiation is greatest, can only be explained by the presence of an exceedingly effective inhibitor in the system. The initiation of such a system of slightly active radicals, while increasing the over-all concentration of the active centers, ought to lead to a selective increase in the rate of destruction of the reactive products causing the braking reaction, and should do so the more strongly the greater the rate of initiation. Therefore, the short-term but energetic effect of hydrogen peroxide on the retarded reaction in its later stages ought to lead: 1) to the destruction of the reactive intermediate products which retard the reaction; 2) to the cessation of the chain process producing hydroperoxide during the time of its effectiveness; 3) to an increase in the rate of production of hydrogen peroxide to such a value as will be secured for the given hydroperoxide concentration by the rate of destructive branching after its influence has stopped.

We should observe that the effect of the "de-braking" reaction will only be observed under conditions in which the radicals of the initiator are less active than the radicals produced in the chain if the inhibitor is formed in the chain process, but that it will always be produced, if the inhibitor is produced by a molecular process.

Thus, it seems to be possible to promote the yield of products in the reaction involving a destructive-branching chain process, if this yield is limited by the restricting of the fundamental process by the products of the reaction. This method can be illustrated by a model plan for the chain process. Let

$$A \rightarrow B \rightarrow C, \tag{1}$$

where the hydrocarbon A is converted by a chain process into the product B, giving destructive branching, and afterwards into the product C, so breaking the chain. Then a set of differential equations describing the process, on the assumption of a second-order chain-breaking process, may be set out in the form:

$$\begin{aligned} \frac{dn}{dt} &= w_0 + hB - k_3 nC - gn\sqrt{\frac{w_0 + hB}{g}}; \\ \frac{dB}{dt} &= (k_1 A - k_2 B)\, n; \\ \frac{dC}{dt} &= k_2 Bn, \end{aligned} \tag{2}$$

where w_0 is the rate of production of the active centers; k_1, k_2, and k_3 are the rate constants for the reactions of the active centers furthering the chain, corresponding respectively with A, B, and C; h is the rate constant of destructive branching reaction; g is the rate constant of the chain-breaking reaction; and n is the concentration of active centers furthering the chain.

Writing the dimensionless quantities $\frac{B}{A} = \eta$; $\frac{C}{A} = \xi$; $tk_1\sqrt{\frac{h}{g}}\,A = \tau$; $\frac{k_2}{k_1} = \alpha$; $k_3\sqrt{\frac{A}{hg}} = \beta$; $\frac{w_0}{hA} = \omega_0$,

we may rewrite the equational system (2) for the stationary state of the reaction in the form

$$\frac{d\eta}{d\tau} = (1 - \alpha\eta)\frac{\omega_0 + \eta}{\beta\xi + \sqrt{\omega_0 + \eta}}; \tag{3}$$

$$\frac{d\xi}{d\tau} = \alpha\eta\frac{\omega_0 + \eta}{\beta\xi + \sqrt{\omega_0 + \eta}}. \tag{3'}$$

Dividing (3') by (3), and integrating the equation so obtained, with the limiting conditions that $\xi = 0$ when $\eta = 0$, we obtain:

$$\xi = -\eta - \frac{1}{\alpha}\ln(1 - \alpha\eta). \tag{4}$$

If the logarithm is expressed as a series and the first two terms alone retained, Eq. (4) takes the form:

$$\xi \cong \frac{\alpha}{2}\eta^2. \tag{5}$$

After this stage, the integral of (3) is easy to obtain. If we integrate it by means of the result in (5), neglecting w_0 for the condition that $\eta = \eta_0$, when $\tau = \tau_0$, we obtain the relationship:

$$\frac{\beta}{2\sqrt{\alpha}}\left[\alpha(\eta_0 - \eta) + \ln\frac{1 - \alpha\eta_0}{1 - \alpha\eta}\right] + \ln\frac{1 + \sqrt{\alpha\eta_0}}{1 - \sqrt{\alpha\eta}}\,\frac{1 - \sqrt{\alpha\eta_0}}{1 + \sqrt{\alpha\eta_0}} = \sqrt{\alpha}(\tau - \tau_0). \tag{6}$$

If at the point when $\tau = \tau_1$, the substance C which retards the reaction is destroyed, the course of the kinetic curve at this moment will be described by the equation:

$$\begin{aligned} &\frac{\beta}{2\sqrt{\alpha}}\left[\alpha(\eta_1 - \eta) + \ln\frac{1 - \alpha\eta_1}{1 - \alpha\eta}\right] + \ln\frac{1 + \sqrt{\alpha\eta}}{1 - \sqrt{\alpha\eta}}\,\frac{1 - \sqrt{\alpha\eta_1}}{1 + \sqrt{\alpha\eta_1}} + \\ &+ \frac{\alpha^{3/2}\beta}{2}\eta^2\ln\frac{\eta_1}{1 - \alpha\eta_1}\,\frac{1 - \alpha\eta}{\eta} = \sqrt{\alpha}(\tau - \tau_1). \end{aligned} \tag{7}$$

The graph of $\eta = f(\tau)$, calculated for the various values of β is Fig. 2. The moment of destruction of the inhibitor is shown by an arrow. The increase in the reaction rate is clearly seen. It is evident that the initiated system is all the more effective, the later the stage of the reaction at which the effect is introduced. We may note that the patent literature contains an indication of such an increased yield of reaction products when a short-period initiation is employed in the course of the process [5]. It has been found that, in the alkaline oxidation of alkylaromatic hydrocarbons, a short-period ozonization of the oxygen in the course of the reaction leads to an increased yield of hydroperoxide at high rate of reaction. The amount of side products obtained is diminished under this procedure. This method of initiating both liquid phase and emulsion oxidation of hydrocarbons has possible practical applications for the purpose of increasing hydroperoxide yield.

LITERATURE CITED

1. N. M. Émanuél', Doklady Akad. Nauk SSSR 110, 245 (1956).*
2. N. N. Semenov, Some Problems of Chemical Kinetics and Reactivity [in Russian] (Izd. AN SSSR, 1958).
3. R. V. Kucher, A. I. Yurzhenko and M. A. Kovbuz, Doklady Akad. Nauk SSSR 117, 638 (1957).*
4. R. V. Kucher and M. A. Kovbuz, Zhur. Fiz. Khim. 33, 429 (1950).
5. Swedish patents Nos. 140188 and 145741.
6. N. M. Émanuél', Uch. zap. MGU 174, 50 (1954).

* Original Russian pagination. See C. B. Translation.

THE POLAROGRAPHIC CATALYTIC WAVES OF HYDROGEN AND THE ADSORPTION OF A CATALYST

S. G. Mairanovskii

The N. D. Zelinskii Organic Chemistry Institute of the Academy of Sciences USSR

(Presented by Academician A. N. Frumkin, February 5, 1960)

Translated from Doklady Akad. Nauk SSSR, Vol. 132, No. 6, pp. 1352-1355, June, 1960

Original article submitted January 20, 1960

In considering the minetic and catalytic currents occurring in polarography, it is necessary to take into account the effect of the adsorption of substances taking part in chemical reactions in the preelectrode layer, which, generally speaking, leads to an increase in the concentration of the substances in the reaction zone, compared with their concentration in the bulk solution. Because of this, there will be present not only the usual kinetic or catalytic current, but also an additional kinetic current determined by the occurrence of the chemical reaction in that volume of solution lying close to the electrode, and produced by the participation in this reaction of the adsorbed substance. The kinetic current, which is actually observed will evidently be the sum of the current due to the "volume," and that due to the "surface" process. Any calculation of the rate constants of these chemical reactions from experimental data on the basis of equations for volume processes, which fails to take into account the adsorption factor, will lead to appreciable overestimation of their values.

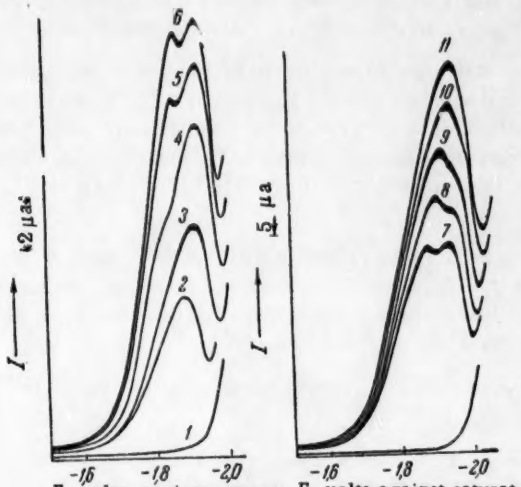

Fig. 1. Catalytic hydrogen waves produced by quinine in 0.1 N borax solution. The concentrations of quinine, C_{quin} (in units of 10^{-4} M) are: 1) 0 (base solution); 2) 0.34; 3) 0.50; 4) 0.79; 5) 0.93; 6) 1.04; 7) 1.2; 8) 1.4; 9) 1.6; 10) 1.8; 11) 2.0.

In this paper we have considered the catalytic waves for hydrogen produced by quinine, and have shown the effect of the adsorption of the catalyst on the value of the catalytic current and on the form of the wave. The experimental data which we produce have been obtained on a polarograph of the type TsLA "Énergochermeta" [1], at 25±0.1°C, using a capillary dropping electrode with a forced drop breakaway [2]. The capillary characteristics were: m = 1.52 mg/sec, t = 0.24 sec.

The catalyst which produces the catalytic waves exists in two forms in the solution: (a) the cationic or acidic, which is electrochemically active; and (b) the basic, which does not take part directly in the electrode process [3]. The two forms exist in protolytic equilibrium, and the ratio between their concentrations is determined by the ionization constant of the catalyst and the pH of the medium.

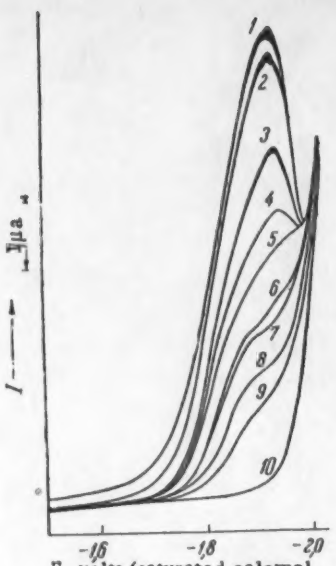

Fig. 2. Change in the catalytic wave for constant C_{quin} of $3.6 \cdot 10^{-5}$ M when the surface-active concentration C_{BSTEA} (in units of 10^{-2} M) is: 1) 0; 2) 0.92; 3) 1.82; 4) 2.16; 5) 3.34; 6) 4.62; 7) 6.72; 8) 7.9; 9) 10.0; 10) represents the base solution only: 0.1 N borax.

The cations of the catalyst in solution, and in the adsorbed state, ought in general to be distinguished from each other according to their depolarizing properties [4], so that for the case of surface-active catalysts one would expect that in certain conditions the waves would show two steps, corresponding to the discharge of the adsorbed and the nonadsorbed particles. Actually, using a base solution of 0.1 N borax solution, a discontinuity arises in the wave at a concentration of quinine, C_{quin}, of about $4 \cdot 10^{-4}$ M,* while increase in C_{quin} leads to the development of separate peaks (Fig. 1).

The bifurcation of the quinine catalytic wave is also observed when a surface-active substance – tetraethylammonium benzosulfonate (BSTEA) – is added to the solution. At comparatively low concentrations of BSTEA in the solution, the lower part of the catalytic wave is shifted somewhat toward a more negative potential, and its steepness increases sharply; increase in the concentration of the BSTEA while the value of C_{quin} is kept constant and the pH of solution maintained unchanged, leads to a reduction in the general level of the curve and to its bifurcation (Fig. 2). The lower, steeper part of the step is somewhat reduced in height with increase in the concentration of the additive, C_{BSTEA}, but its half-wave potential is practically unchanged, while the upper and longer section is abruptly diminished, and shifted considerably towards more negative potentials. The lower wave corresponds to discharge of the cations contained in the bulk solution. This "bulk" wave has an inverse character [3, 5]. The upper, extended wave with its characteristic maximum is due to the irreversible discharge of cations formed from the adsorbed catalyst (the "surface" wave).

For increase in the value of C_{BSTEA} above 0.07N, the bulk wave also begins to diminish because of the retardation of the electrode process [6]. It becomes less steep and is shifted towards more negative potentials. At such high values of C_{BSTEA} the "surface" wave vanishes completely.

It should be noted that the volume wave, in the absence of BSTEA, becomes more negative with increase in C_{quin} (Fig. 1): that is, the reversible discharge seems to be retarded by the adsorbed quinine.** But a comparison of the reversible and irreversible waves which have about the same limiting currents shows that the reversible ("volume") wave, which is distinguished from the usual catalytic curve by the effect of the BSTEA, is situated at less negative potentials than the irreversible one [5].

The bifurcation of the catalytic waves of water is only found rather rarely. Before this can happen, it appears to be essential that the heights of the "surface" and "volume" waves shall be comparable, and that the position of $E_{1/2}$ for the latter shall lie within a definite narrow interval close to the maximum of the "surface" wave. A diagram representing the formation of such "dual" characteristic waves is given in Fig. 3.

As a rule, such division of the catalytic waves is not found, and the observed waves are simply made up of the sum of the volume and surface currents.

For the catalytic currents near to the limiting value – that is, when the reverse chemical reaction hardly occurs at all [3] – which will result in the disappearance of the cationic form of the catalyst, we may write:

$$i_{lim} = i_{vol} + i_{surf} = s F k_1 \mu_1 C [DH^+]_S + s F k_1' \Gamma [DH^+]_S, \quad (1)$$

* Translator's note: Figure 1 does not seem to bear out the quoted figure. The discontinuity seems to arise first in curve 4 at a stated concentration of $0.79 \cdot 10^{-4}$ M, and the maximum concentration used is stated to be $2 \cdot 10^{-4}$ M.

** Translator's note: Again it is hard to see the justification for this statement. In Fig. 1, according to its legend, increased values of C_{quin} are represented by the higher index numbers on the curves, and the higher the number, the less negative is the position of the curve.

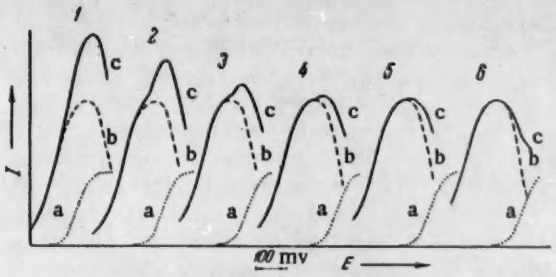

Fig. 3. Diagram of the formation of two peaks in a catalytic wave. a) Reversible ("volume"); b)"adsorption"; c) sum of the two waves. $E_{1/2}^{rev} - E_{max}^{irr}$ for the curves are respectively: 1) +30; 2) −30; 3) −55; 4) −75; 5) −80; 6) −95 mv.

where s is the area of the electrode surface; F is the faraday; $(DH^+)_s$ and C are the concentrations at the surface of the electrode of proton donor and catalyst, respectively (on the assumption that the equilibrium in the bulk is strongly weighted in the direction of the basic or unreactive form of this); μ_1 is the thickness of the reaction layer in which the prior volume reaction takes place [7, 8, 3]; k_1 and k'_1 are the rate constants for the combination of proton and catalyst in the solution and in the adsorbed state, respectively; Γ is the quantity of adsorbed catalyst. The volume catalytic current – the first term in Eq.(1) as given[3] on the basis of the concept of the reaction layer [7, 3] but for the case now under consideration an exact calculation leads to almost exactly the same relationship (Eq.(49) in reference [9]).

For the second catalytic wave of quinine (catalysis by the nitrogen of the quinuclidine nucleus) in 0.1 N borax solution, the experimental data give: $i_{vol}/C_{quin} = 43\ \mu a/mM^*$.

Using the value of $D = 5.4 \cdot 10^{-6}\ cm^2/sec$ as the diffusion coefficient of quinine for the calculation of μ_1, the value being obtained from the diffusion current corresponding to its reduction [10], and as the other values: $S_{mean} = 2.5 \cdot 10^{-3}\ cm^2$, $(OH^-) = 1.7 \cdot 10^{-5}$, and the ionization constant of quinine $K = 1.1 \cdot 10^{-6}$, assuming that $(DH^+) = (H_2O)$, the value of k_1 found from Eq. (1) is $1.6 \cdot 10^3\ sec^{-1}\ (mole/liter)^{-1}$.

If we assume that the rate constants of the reaction of the catalyst present in the body of the solution and in the adsorbed condition with the water molecules are nearly the same, that is, if $k_1 \approx k'_1$, then from the value of the maximum current for the ordinary catalytic wave (6.2 μa) when C_{quin} is $3.6 \cdot 10^{-5}$ M, it is possible to calculate the value of Γ in Eq. (1) as $2.1 \cdot 10^{-13}\ mole/cm^2$. The maximum value of Γ (Γ_∞) corresponding to the saturation of the electrode surface is $4.4 \cdot 10^{-10}$ [11], while the value of Γ_∞ found from the maximum height of the adsorption prewave by Brdicka [12] from the diffusion wave of the reduction of quinine is $1.3 \cdot 10^{-10}\ mole/cm^2$. Taking the value of Γ_∞ as $4.4 \cdot 10^{-10}$, we find that the degree of saturation of the surface under the conditions mentioned (E = 1.91 v relative to the saturated calomel electrode, and $C_{quin} = 3.6 \cdot 10^{-5}$ M) is given by $\theta_{opt} = \Gamma/\Gamma_\infty = 0.0018$. Thus, the degree of saturation of the surface is only about 0.2%. The adsorption process under consideration takes place, evidently, at considerably higher negative potentials than the "desorption peak", and corresponds, as A. N. Frumkin [13] has shown, to the maximum value of $\partial\theta/\partial E$.

It has been shown by means of special experiments that the adsorption of the product of the reduction of quinine (on the basis of the isoquinoline nucleus [10]) – that is, the product which is responsible for the catalytic wave under consideration – obeys the S-shaped adsorption isotherm proposed by A. N. Frumkin [14]. In this case, however, the size of the attractive factor is small, so that the Frumkin adsorption isotherm should be replaced by that of Langmuir:

$$\theta_e = \Gamma_e/\Gamma_\infty = \frac{\beta C}{1 + \beta C}, \qquad (2)$$

where θ_e and Γ_e are equilibrium values; and for the further calculation the results of the work of Delahay and Fike may be used [15].

* Translator's note: The significance of the denominator is not given, but apparently refers to concentration in millimoles per liter.

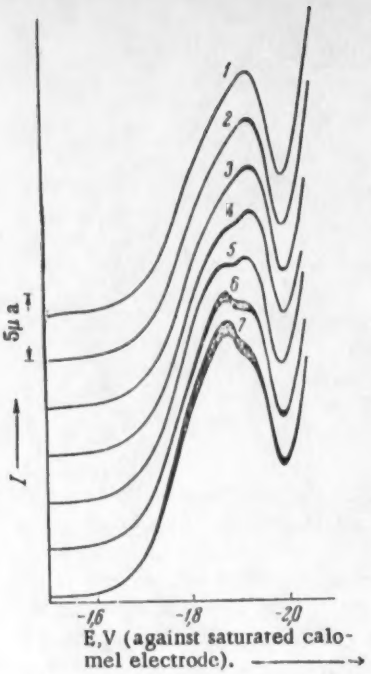

Fig. 4. Catalytic wave when $C_{quin} = 1.4 \cdot 10^{-4}$ M for various heights of the mercury column, h_{Hg} (in cm): 1) 100; 2) 90; 3) 80; 4) 70; 5) 60; 6) 50; 7) 40 (approximate figures).

If we first assume that adsorption equilibrium is attained at the surface of the drop, that is, that $y' = \Gamma/\Gamma_e \approx 1$, Eq. (2) then gives: $\beta' = 0.05$ mmole^{-1}, and β'C (or C^{0}a, according to the notation used in [15]) = 0.0018. Using this value of Fig. 4 of paper [15] we obtain the value: $y''_0 = \Gamma/\Gamma_e = 0.055$, and after introducing into this a correction factor for the fact that the value of D/Γ_∞ is greater than that taken in [15] ($1.25 \cdot 10^4$ cm^4/sec · mole), we obtain as a second approximation: $y'' = 0.069$, and $\theta''_e = \theta_{opt}/y'' = 0.026$. Inserting this value of θ''_e in Eq. (2) we obtain the value of β'', and by going through the whole cycle yet again we obtain finally: $\beta = 0.9$ mmole^{-1}, $y = 0.069$ and $\theta_e = 0.026$. These data show that under the conditions now considered, the adsorption equilibrium only reaches the value of about 7% ($y \approx 0.07$)*. Increase in the time of adsorption t should result in increase in the values of y and, consequently, Γ, in which case Eq. (1) would give an increased value for i_{surf}. In fact, as can be seen from Fig. 4, change in the height of the mercury column has a considerable effect on the adsorption catalytic wave. This phenomenon, and the increase in i_{surf}, may serve to explain also the growth of the wave with increase in the time t during catalysis by pyridine [16, 3] and other substances [17].

The magnitude β, as Frumkin has shown [18], diminishes rapidly with increase in the cathode potential, and therefore for many substances, whose catalytic waves are found at lower cathode potentials than the second wave for quinine, we should expect considerably higher values of β, and therefore [15] of y and Γ, while for the waves of these substances the values of i_{surf} ought to exceed the value of i_{vol} by several orders. If, in such a case $y \approx 1$, the catalytic waves would not depend on the height of the mercury column.

It should be added that the change of β with potential seems to be the cause of the reduction of the current for the kinetic and catalytic waves [5, 19].

The author is grateful to Academician A. N. Frumkin for his help in the work.

LITERATURE CITED

1. S. B. Tsfacman, Zavodskaya Lab. 22, 131 (1956).
2. E. M. Skobets and N. S. Kavetskii, Zavodskaya Lab. 15, 1299 (1949).
3. S. G. Mairanovskii, Doklady Akad. Nauk SSSR 114, 1272 (1957).**
4. N. S. Hush, Z. Elektrochem. 61, 734 (1957).
5. S. G. Mairanovskii, Doklady Akad. Nauk SSSR 120, 1294 (1958).**
6. T. A. Kryukova, S. I. Sinyakova, and T. V. Aref'eva, The Polarographic Method [in Russian] (Moscow, 1959) p. 639.
7. R. Brdicka and K. Wiesner, Coll. 12, 138 (1947).
8. D. Kern, J. Am. Chem. Soc. 75, 2473 (1953).
9. Ya. Koutetskii, V. Ganush and S. G. Mairanovskii, Zhur. Fiz. Khim. 34, 651 (1960).
10. I. Bartek, M. Cernoch, and F. Santavy, Coll. 19, 605 (1954).
11. B. E. Conway, J. O. Bockris, and B. Lovrecek, Proc. VI Met. Intern. Com. Electrochem. (London, 1955) p. 207.
12. R. Brdicka, Coll. 12, 522 (1947).
13. A. N. Frumkin, V. S. Bagotskii, Z. A. Iofa, and B. N. Kabanov, Kinetics of Electrode Processes [in Russian] (Moscow, 1952) p. 41.
14. A. N. Frumkin, Tr. Karpov Inst. 4, 64 (1925).
15. P. Delahay and Fike, J. Am. Chem. Soc. 80, 2628 (1958).

* It should be borne in mind that the calculation here given only gives orders of magnitude, since in general $k_1 \neq k'_1$.

** Original Russian pagination. See C. B. translation.

16. S. G. Mairanovskii, Zhur. Fiz. Khim. 33, 3, 691 (1959).
17. V. Vojîr, Coll. 18, 629 (1953).
18. A. N. Frumkin, Tr. Karpov Inst. 5, 3 (1926).
19. S. G. Mairanovskii, Doklady Akad. Nauk SSSR 133, No. 1 (1960).*

*Original Russian pagination. See C. B. translation.

SYNTHESIS OF SPECIFIC SILICA GELS BY MODIFICATION OF THEIR SURFACE

I. E. Neimark, V. M. Chertov, R. Yu. Sheinfain, and N. S. Kruglikova

L. V. Pisarzhevskii Physical Chemistry Institute, Academy of Sciences, Ukr SSR

(Presented by Academician M. M. Dubinin, February 22, 1960)

Translated from Doklady Akademii Nauk SSSR, Vol. 132, No. 6, p. 1356-1359, June, 1960

Original article submitted February 20, 1960

The chemical modification of the surface of hydrated silica gels and highly dispersed nonporous silica by replacement of the hydroxy groups with various radicals does not give them the property of selectivity. On specimens modified in this way, the adsorption of both polar and nonpolar substances is lower, although to different degrees [1-7]. At the same time the possibility of making the adsorptive properties of silica gel clearly selective to different substances would greatly extend their possible applications.

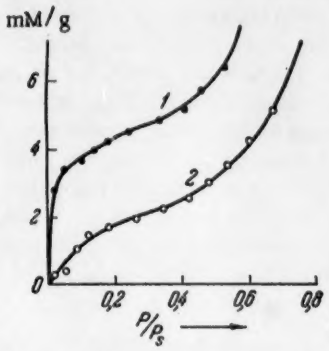

Fig. 1. Adsorption isotherms for CH_3OH vapor on the original silica gel (1) and on silica gel modified with monoethanolamine (2).

The aim of the present study was to carry out chemical modification of silica gel to give it basic properties. Modification in this way should make possible the selective adsorption of acidic substances, which are weakly adsorbed on silica gel. Sorbents with basic properties can also find application as catalysts for dehydrogenation reactions, etc.

In earlier work [8, 9] selective action of silica gel was achieved by saturating the gel with aqueous solutions of ammonia and ethylenediamine. The silica gel treated in this way contained surface amino groups and was able to form coordinate bonds with elements which form ammines (Cu, Zn, Co. etc.). Other work [10-13] and studies in our laboratory showed the possibility of introducing organic residues into silica gel by esterification reactions. We suggested that by carrying out the esterification with alcohols containing amino groups [14], it should be possible to produce silica gels with basic properties. In the present work we have used for this purpose a series of amino alcohols with different degrees of basic character (mono-, di- and triethanolamine). In all cases, according to our assumptions, the reaction between the silica gel and the amino alcohols should take place according to the following equations:

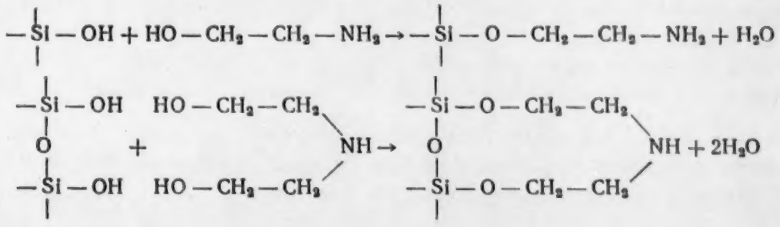

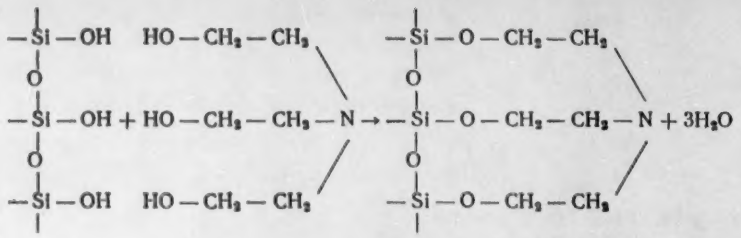

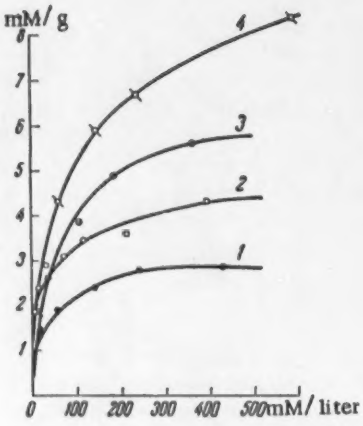

Fig. 2. Adsorption isotherms for acetic acid from CCl_4 solution on the original (1) and modified silica gels: 2) 1.75 meq/g $C_2H_4NH_2$ groups; 3) 1.75 meq/g $(C_2H_4)_3N$ groups; 4) 3.3 meq/g $C_2H_4NH_2$ groups.

It is, however, necessary to take account of the possibility of steric hindrance, so that probably not all hydroxy groups of the di-, and, more particularly, the triethanolamine undergo esterification. The equations given thus merely give a schematic indication of the processes taking place.

The experiments on the chemical modification were carried out with hydrated specimens of coarsely porous silica gel. The introduction of the amino groups was carried out in two ways: in a flask with reflux condenser at a temperature of 100-160°C and in an autoclave at 160-250° for 2-5 hr. The silica gel treated in this way was kept in a vacuum oven at 100-180° and 10^{-3} mm for 2-6 hr.

The modified silica gels were analyzed for their amino alcohol group conent. For this purpose a weighed specimen of the material was treated with excess of a standard solution of hydrochloric acid. The solution was shaken, separated from the specimen, and titrated with alkali using methyl red indicator. The adsorption isotherms for the original specimens and for specimens containing amino groups were recorded for the vapors of methyl alcohol, diethylamine, and carbon dioxide, and for acetic acid from solution in carbon tetrachloride. All the isotherms were recorded at 20°. After the treatment of the silica gel with ethanolamines and prolonged evacuation at 100-180°, the silica surface retained 1.2-13.5 meq/g of ethanolamine. Special experiments on desorption from the silica gels containing amino groups by evacuation at 10^{-5} mm and 200° showed that 1.2-1.75 meq/g of ethanolamine are more firmly bound, and this quantity is undoubtly attached to the silica gel surface by chemical forces. This provides confirmation of the mechanism of the process of amino group introduction suggested by us earlier.

Figure 1 shows the initial sections of the adsorption isotherms for methyl alcohol on the original silica gel specimens and on specimens containing amino groups. The figure shows that, as in the case of modification by other organic radicals [1-7], the introduction of amino alcohol groups into the silica gel leads to a considerable decrease in the magnitude of the adsorption in the initial sections of the isotherms and to a displacement of the relative pressure range corresponding to the sharp rise in the central sections of the isotherms, towards higher negative pressures. This decrease in the adsorption is related to the decrease in the donor–acceptor reaction between the methyl alcohols and the modified silica gel surface.

Figure 2 gives the adsorption isotherms for acetic acid from CCl_4 solutions on the original silica gel and on specimens containing amino groups. The figure shows that the introduction of the organic radical, containing the amino group, into the silica gel increases the adsorption of acetic acid. This difference in the adsorption properties is even more sharply defined for the specimen of high amine content (curves 2 and 4). For the same degree of modification, the adsorption isotherm for acetic acid on the specimen treated with triethanolamine is higher than that for the specimen treated with monoethanolamine (curves 2 and 3). An increase in the adsorption of carbon dioxide is also observed on going from the original to the modified silica gel, as can be seen from Fig. 3.

It was considered of interest to examine how the introduction of amino groups into the silica gel affected the adsorption of basic substances. For this purpose, adsorption isotherms were recorded for diethylamine on the original specimen and for specimens containing amino groups. These isotherms are shown in Fig. 4, from which it can be

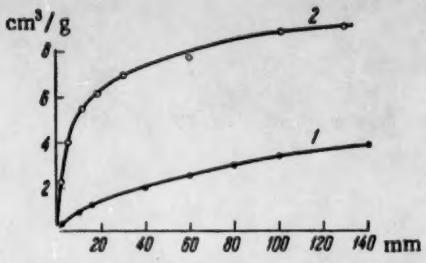

Fig. 3. Adsorption isotherms for carbon dioxide on the original silica gel (1) and on silica gel modified with monoethanolamine (2).

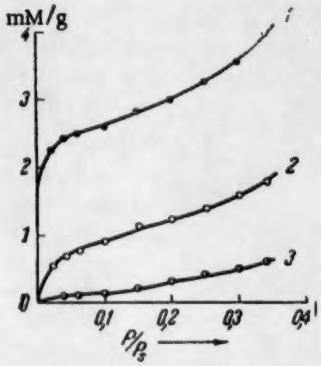

Fig. 4. Adsorption isotherms for diethylamine vapor on the original (1) and modified silica gels: 2) with monoethanolamine; 3) with triethanolamine. Amino alcohol group content 1.75 meq/g.

seen that the adsorption of diethylamine decreases sharply on going from the original silica gel to the silica gel containing amino groups. The decrease in the adsorption is particularly marked for the specimen treated with triethanolamine.

Acetic acid is adsorbed on silica gel with the formation of hydrogen bonds [15]. In the case of silica gel containing amino groups, the adsorption bond formed by acetic acid is much stronger. This also leads to an increase in the adsorption potential of the silica gel containing amino groups with respect to acetic acid and to an increase in its adsorption on going from the initial silica gel to the silica gel containing amino groups. The increased adsorption of carbon dioxide is also related to the basic properties of the specimen containing amino groups. Thus, in both cases, chemisorption takes place on the modified silica gel. The strength of the chemisorption increases with increase in the alkaline properties of the surface. The basic properties increase on going from primary to tertiary aliphatic amines [16]. This explains the fact that the adsorption isotherms for substances of acidic character on silica gel into which amino groups have been introduced with triethanolamine are higher than those for adsorption on specimens modified with monoethanolamine.

Amino groups are not active adsorption centers for diethylamine which also has basic properties, so that there is a decrease in the adsorption of this compound on silica gel containing amino groups. The convex shape of the adsorption isotherms for diethylamine on the specimen treated with triethanolamine indicates the extremely weak interaction between adsorbent and adsorbate. Thus, the data given show that it is possible, by modification of the surface of silica gel with organic radicals containing definite functional groups, to give the material specific adsorptive properties. Replacement of the hydroxy groups of the silica surface by radicals containing acid residues probably gives an adsorbent selective towards basic substances and creates a nonswelling ion exchanger on the silica gel surface. In this way it may also be possible to create selective acid–base catalysts.

LITERATURE CITED

1. I. E. Neimark, R. Yu. Sheinfain, and L. G. Svintsova, Doklady Akad. Nauk SSSR 108, 871 (1956).*
2. I. E. Neimark and R. Yu. Sheinfain, Collection: Methods of Studying the Structure of Highly Dispersed and Porous Solids [in Russian] (Izd. AN SSSR, 1958) p. 128.
3. R. Yu. Sheinfain and I. E. Neimark, Proceedings of the Scientific and Technical Conference on Problems Concerning the Preparation, Structure and Properties of Sorbents [in Russian] (Leningrad, 1959) p. 136.
4. K. H. Ebert, Monatsh. Chem. 88, 275 (1957).
5. A. V. Kiselev, N. V. Kovaleva, A. Ya. Korolev, and K. D. Shcherbakova, Doklady Akad. Nauk SSSR 124, 617 (1959).*
6. I. Yu. Babkin, V. S. Vasil'eva, et al., Doklady Akad. Nauk SSSR 129, 131 (1959).*
7. M. M. Dubinin, E. G. Zhukovskaya, et al., Izvest. Akad. Nauk SSSR, Otd. Khim. Nauk No. 4 (1960).*
8. V. B. Aleskovskii and A. I. Miheeva, Proceedings of the Scientific and Technical Conference on Problems Concerning the Preparation, Structure, and Properties of Sorbants [in Russian] (Leningrad, 1959) p. 80.
9. A. I. Mikheeva and V. B. Aleskovskii, Izvest. Vysh. Uch. Zav., Ser. Khim i Khim. Tekhnol. 1, 69 (1958).
10. O. M. Dzigit, A. V. Kiselev, et al., Doklady Akad. Nauk SSSR 70, 441 (1950).
11. K. V. Topchieva and A. P. Ballod, Doklady Akad. Nauk SSSR 75, 247 (1950).

* Original Russian pagination. See C. B. translation.

12. W. Stöber, G. Bauer, and K. Thomas, Lieb. Ann. 604, 104 (1957).
13. R. K. Iler, The Colloid Chemistry of Silica and Silicates (1957).
14. Berry, Joyce and Kerby, US Patent No. 2757098, 1956; [Ref. Zhur. Khim., 20072] (1959).
15. A. V. Kiselev, I. A. Vorms, et al., Zhur. Fiz. Khim. 19, 83 (1945).
16. T. I. Temnikova, Theoretical Principles of Organic Chemistry [in Russian] (Leningrad, 1959) p. 212.

THE PART PLAYED BY MINORITY CURRENT CARRIERS IN THE ANODIC DISSOLUTION OF ELECTRONIC GERMANIUM

Yu. V. Pleskov

Electrochemistry Institute, Academy of Sciences, USSR

(Presented by Academician A. N. Frumkin, February 12, 1960).

Translated from Doklady Akademii Nauk SSSR, Vol 132, No. 6, pp. 1360-1363, June 1960

Original article submitted February 8, 1960

Studies of the anodic dissolution of germanium have shown that "holes" are involved in the process. At a sufficiently high current density in the anodic dissolution of germanium of the n-type, in which the holes are the minority carriers, the germanium–electrolyte boundary acts as a hole collector, and there takes place a "multiplication of the current" at the collector, related to the fact that the free electrons of the semiconductor also take part in the reaction. In other words, the germanium atom going into solution transfers electrons to the valence zone (for which holes are necessary) and to the free zone simultaneously. The over-all equation for the reaction (in acid medium) is $Ge + x\oplus + 3H_2O \rightarrow H_2GeO_3 + (4-x)\ominus + 4H^+$. Various authors [1-4] have given for the current multiplication factor $\alpha'_0 = 4/x$ (equal to the ratio of the limiting current of the anodic dissolution to the limiting current for the diffusion of holes from the bulk of the semiconductor to its surface) values from 1.3 to 4.4. Attempts have been made to relate the value of α'_0 to various molecular reaction schemes [3, 5]. The aim of the present work was to study the relationship between α'_0 and the conditions for the anodic dissolution of germanium.

EXPERIMENTAL PROCEDURE

Using the method proposed by Brattain and Garrett [1] α' was measured. An electrode of electronic germanium with specific resistance 3 ohm·cm and hole diffusion length 0.7 mm was constructed in the form of a thin (thickness approximately 0.1 mm) disc of 8 mm diameter, on one side of which the p–n-junction was situated, while the other side was immersed in the solution. An annular ohmic contact was fixed in position with tin around the surface of the electrode. The efficiency of contact was checked by recording the volt–ampere characteristic for direct and alternating current. The electrode surface (with the exception of the section immersed in the electrolyte) was insulated by means of pure paraffin. The surface area of the germanium–solution interface amounted to 0.25 cm^2, and the area of the p–n junction amounted to 0.2 cm^2. The anodic dissolution of the germanium was carried out at constant potential corresponding to the limiting dissolution current; a PÉ-312 electronic polarograph was used as potentiostat. By means of the p–n junction, which was connected in the flow-through direction, holes were injected into the n-type region, and these diffused towards the germanium–solution interface and took part in the dissolution reaction. The increase in the anodic dissolution current ΔI_a with change in the injection current I_p was recorded automatically.* The data obtained were used to calculate the value of the current amplification coefficient $\alpha = d(\Delta I_a)/dI_p$ for our system, which can be written in the form $\alpha = \beta\gamma\alpha'$,

* For greater accuracy, the quantity measured experimentally was not ΔI_a, but the quantity $\Delta I_a - I_p$ (using a suitably arranged electrical circuit), i.e., the increase in the electronic current through the electrode surface.

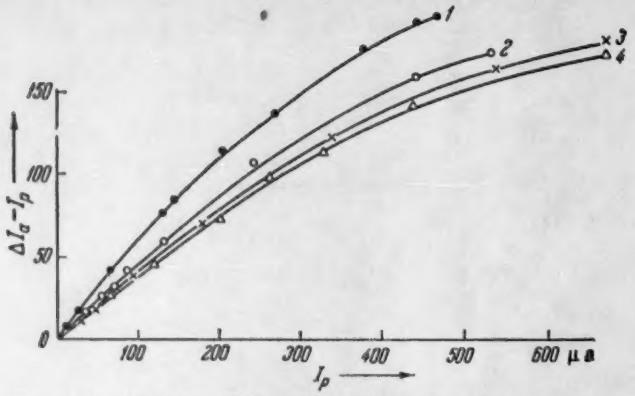

Fig. 1. Acceleration of the anodic dissolution of germanium (μ a) in 1 N H_2SO_4 with change in the injection current via the the p–n junction. Intensity of illumination of the electrode in arbitrary units): 1) 0; 2) 3.5; 3) 5.8; 4) 7.5.

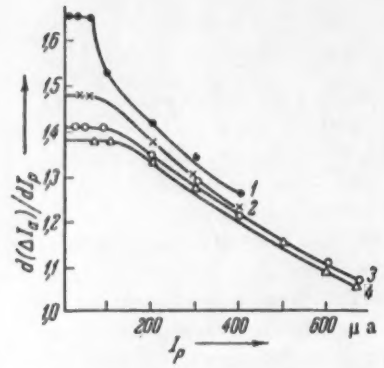

Fig. 2. Relationship between the current multiplication and the current via the p–n junction I_p. Intensity of illumination of electrode: 1) 0; 2) 3.5; 3) 5.8; 4) 7.5.

where γ is the efficiency of the emitter (the proportion of hole current in the p–n junction current); β is the flow-through coefficient (the proportion of holes, injected by the emitter, which reaches the collector without undergoing recombination), and α' is the current multiplication coefficient at the collector (the increase in the reverse current at the collector for unit increase in the hole current). In planar triodes of analogous construction the efficiency of the emitter γ and the flow-through coefficient β· are very close to unity, so that the hole injection current at the germanium–solution interface is equal to the flow-through current of the p–n junction I_p, to within 2-3%. The rate of surface recombination at the germanium–aqueous solution interface is known to be small from literature data [3, 6] and our own indirect data. The experimentally measured quantity $d(\Delta I_a)/dI_p$, thus, practically coincides with the current multiplication coefficient α' for the anodic dissolution reaction.

RESULTS

Figure 1 gives the relationship between $\Delta I_a - I_p$ and I_p for the anodic dissolution of germanium in 1 N H_2SO_4 in the dark and with illumination of different intensities E; Figs. 2 and 3 show the dependence of $d(\Delta I_a)/dI_p$ on I_p and E, calculated from these data. The intensity of illumination was determined from the increase in the reverse current I_s of the p–n junction during illumination (with reverse displacement 3 v) and is given in arbitrary units $\Delta I_s / I_s^{dark}$.

Figure 1 shows that at small values of I_p ($I_p \leq I_a^0$)*, ΔI_a is directly proportional to I_p, as already observed [1], i.e., $d(\Delta I_a)/dI_p$ remains constant. The current multiplication factor $\alpha'_0 = [d(\Delta I_a)/dI_p]_{I_p=0}$ calculated from Curve 1 (Fig. 1) amounts to 1.6-1.7 (Fig. 2), which is in good agreement with the results of direct measurements made by Brattain and Garrett [1] (1.4-1.8) and close to the value 1.4 obtained by Uhlir using a less direct method [4] and the value 1.6-2.5 calculated from the indirect data of Gerischer and Beck [2,8] taking account of our earlier work [7] **. The value of α'o is independent of the germanium potential (in the range 1-3 v) and is the same for dissolution in 1 N H_2SO_4 and in 1 N KOH; in 48% HF solution, α'o=1.3* .

* Without injection, the normal limiting current of the anodic dissolution for the electrodes used I_a^0 amounted to approximately 90 μa.

** In this work [2, 8], the injection of holes into the germanium was achieved not by a p–n junction but by the reduction of $K_3Fe(CN)_6$, which involves the valence electrons. The ratio of ΔI_a to the $K_3Fe(CN)_6$ reduction current amounted to 1.3-1.7. According to our data [7], the fraction of the valence electrons in the reduction of $K_3Fe(CN)_6$ at a germanium electrode is 0.6-0.8 (and not 1, as suggested by the authors in [2, 8]).

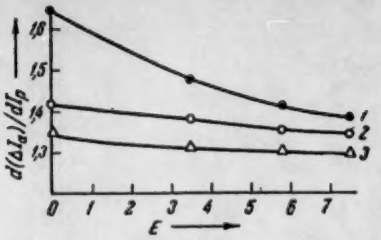

Fig. 3. Relationship between the current multiplication and the intensity of illumination of the electrode E. Current via p–n junction: 1) 0; 2) 200 μa; 3) 300 μa.

the range 1-3 v) and is the same for dissolution in 1 N H_2SO_4 and in 1 N KOH; in 48% HF solution, $\alpha'_0 = 1.3$.*

With increase in I_p relative to I_a^0, $d(\Delta I_a)/dI_p$ decreases and at $I_p \approx 5\ I_a^0$ amounts to 1.15 and at $I_p \approx 10\ I_a^0$ amounts to only 1.03. Illumination of the electrode does not change the relationship between $d(\Delta I_a)/dI_p$ and I_p (Fig. 2), but the absolute value of $d(\Delta I_a)/dI_p$ decreases with increase in the intensity of illumination E (Fig. 3).

Figure 1 shows that as the injection current increases, the qunatity $\Delta I_a - I_p$ tends toward a certain limiting value; extrapolation of curves 1-4 (Fig. 1) to $I_p \to \infty$ (by constructing these curves with coordinates $\frac{1}{\Delta I_a - I_p}$, $\frac{1}{I_p}$) gives a limiting value of approximately 200-250 μa (which is 2-3 times greater than I_a^0).

DISCUSSION OF RESULTS

The observed relationship between the current multiplication coefficient α' for the anodic dissolution of germanium and the hole injection current is confirmed qualitatively by recently published work by Beck and Gerischer [8]. According to the data obtained by these authors, the acceleration of the anodic dissolution of n-type germanium in 0.1 N NaOH in the presence of $K_3Fe(CN)_6$ depends on the concentration of the latter; with increase in this concentration and hence in the rate of reduction I_{red} of the ferricyanide, the value of $\Delta I_a / I_{red}$ decreases. In the work cited, however, no study was made of the proportion γ of valence electrons in the $K_3Fe(CN)_6$ reduction current. If it is assumed that γ changes little with change in the ferricyanide concentration, then the decrease in $\Delta I_a / I_{red} = \alpha'\gamma - 1$ is related chiefly to the decrease in α' with increase in the rate of hole injection by the reduction of $K_3Fe(CN)_6$.

The derivative $d(\Delta I_a)/dI_p$ characterizes the relationship between the electronic component I_n of the total anodic dissolution current $I_a = I'_p + I_n$ and the hole current through the surface; $d(\Delta I_a)/dI_p = 1 + d(\Delta I_n)/dI_p$. Its decrease with increase in I_p indicates that increase in the hole current at the surface of the dissolving germanium leads to an increase chiefly in the hole component of the dissolution current. From the experimentally measured value $\alpha'_0 = 1.65$ it follows that the process of anodic dissolution (without injection) for the transfer of 1 germanium atom from the crystal lattice to the solution requires 2.4 holes, and 1.6 electrons are transferred to the conductivity zone. With increase in the injection (by means of a p–n junction or illumination), the proportion of holes and free electron changes, and at the maximum value of I_p reached in our experiments amounts to 3.9 and 0.1, respectively. The continuous change in the macroscopic value of α' (i.e., the derivative $d(\Delta I_a)/dI_p$) at constant solution composition, potential, and other dissolution conditions (with the exception of the magnitude of the injection), obviously means that we cannot relate this quantity to any definite reaction scheme for the dissolution; we cannot, for example, assume that any intermediate stage takes place exclusively by a process involving holes [3, 5]. The process apparently takes place by two routes simultaneously (with transfer of the charge to the valence zone and free zone of the semiconductor).

On the other hand, the increase in the absolute value of the electronic component of the dissolution current with increase in the hole current provides some support for the views of Dewald [9], who believes that the hole and electronic currents are not related to two independent routes of anodic dissolution, but are related to the elementary stage of the reaction. It may be assumed that the observed decrease in $d(\Delta I_n)/dI_p$ with increase in the rate of dissolution is related to the fact that when high currents pass through the germanium–electrolyte interface, considerable recombination takes place in the three-dimensional charge layer, although the extent of this recombination is usually assumed to be negligible, and the number of holes taking part in the reaction becomes less than the injection current. In this case the microscopic value of the current multiplication coefficient α' (which is determined by the number of holes and free electrons taking part in the elementary stage of the reaction) differs from the experimentally measured values given above.

I wish to express my deep gratitude to Professor B. N. Kabanov for assistance in the discussion of the results.

* According to our data, the limiting current for the anodic dissolution of germanium in HF is 4-5 times greater than that in H_2SO_4 and KOH, which is possibly due to a high rate of recombination at the germanium–HF solution interface.

LITERATURE CITED

1. W. H. Brattain and C. G. Garrett, Bell Syst. Techn. J. 34, 129 (1955).
2. H. Gerischer and F. Beck, Z. Phys. Chem. N. F. 13, 389 (1957).
3. J. B. Flynn, J. Electrochem. Soc. 105, 715 (1958).
4. A. Uhlir, Bell Syst. Techn. J. 35, 333 (1956).
5. D. R. Turner, J. Electrochem. Soc. 103, 252 (1956).
6. W. W. Harvey and H. C. Gatos, J. Appl. Phys. 29, 1267 (1958).
7. Yu. V. Pleskov, Doklady Akad. Nauk SSSR 130, 363 (1960).*
8. F. Beck and H. Gerischer, Z. Elektrochem. 63, 943 (1959).
9. J. F. Dewald, Semiconductors, Am. Chem. Soc. Monograph No. 140 (N. Y., 1959).

* Original Russian pagination. See C. B. translation.

SOME FEATURES OF THE CRYSTALLIZATION OF ALLOYS OF THE EUTECTIC TYPE AT HIGH RATES OF COOLING

I. V. Salli and I. S. Miroshnichenko

Dnepropetrovsk State University

(Presented by Academician G. V. Kudryumov, February 17, 1960).

Translated from Doklady Akademii Nauk SSSR, Vol. 132, No. 6, pp. 1364-1367, June, 1960

Original article submitted February 11, 1960

The few data available in the literature on the solidification of alloys at high cooling rates [1-5] show that in the case of crystallization from a melt, as in the case of the preparation of alloys by electrodeposition or pulverization in vacuo, it is possible to obtain highly supersaturated solid solutions.* Analysis of these works shows

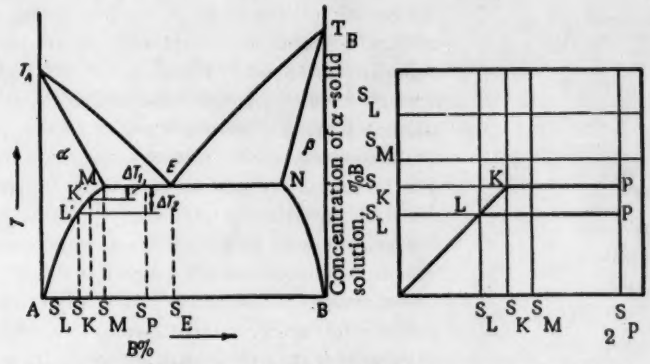

Fig. 1. Phase diagram and relationship between the α-solid solution composition and alloy concentration for two degrees of supercooling ΔT_1 (curve ALKP) and ΔT_2 (curve ALP).

that the tendency to form highly supersaturated primary solid solutions is shown, as a rule, by systems in which there are intermediate phases.

In certain papers [6-8], the possibility of obtaining lightly supersaturated solid solutions is related to crystallization without diffusion, which, in the opinion of the authors concerned, can take place in alloys at high cooling rates.

The present work describes experimental studies of structure formation in alloys cooled at high speeds by the method described in an earlier paper [9]. In this method, drops of melt thrown from the furnace solidify in the form of a thin film between two copper plates moving towards one another. This method makes it possible to

* In the present work highly supersaturated solid solutions are defined as solutions with concentrations greater than the maximum solubility at the eutectic (peritectic) temperature (C_M).

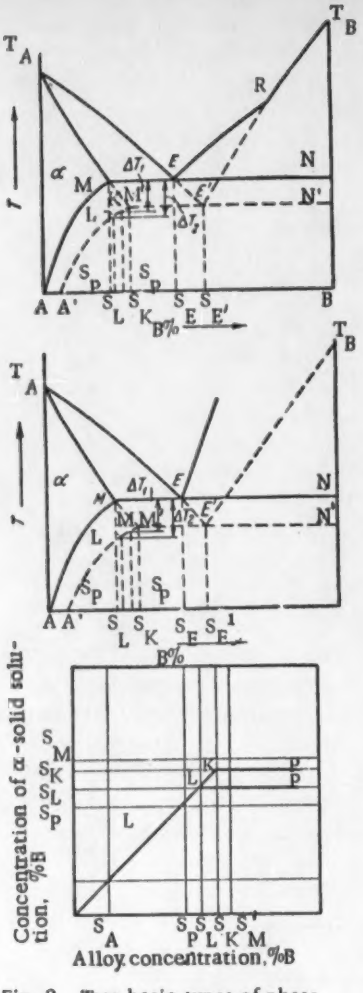

Fig. 2. Two basic types of phase diagram with intermediate phases, and the relationship between the α-solid solution composition and alloy concentration in systems with intermediate phases, for two degrees of supercooling ΔT_1 (curve ALKP) and ΔT_2 (curve ALP).

obtain cooling rates of $\sim 10^5$ deg/sec. Slight supercooling is achieved in the thin layer of melt in direct contact with the interface between the melt and the cooling element. The supercooling decreases slightly in layers further from this interface. This makes it possible to follow the characteristic features of the crystallization at different degrees of supercooling.

The films, of thickness 0.05-0.2 mm, were studied by metallographic and x-ray diffraction methods, and also by quantitative analysis using the Scheele-Saltykov method. The studies were carried out using alloys with concentrations from C_M (Fig. 1) to the eutectic. The composition of the primary solid solution was determined from crystal lattice period data, and the composition of the alloy was found by chemical analysis of the film. The results of the studies can be summarized as follows.

I. In Al–Si, Pb–Sn, and Bi–Sn melts, belonging to the group of binary eutectic systems which do not form intermediate phases, primary solid solutions are formed with concentrations less than C_M. Figure 1 shows the change in composition of the primary solid solution with change in the alloy composition for two degrees of supercooling ΔT_1 and ΔT_2. Thus, increase in the rate of cooling does not lead to an increase in the concentration of the primary solution, as should be expected from the theory of crystallization without diffusion; the concentration in fact decreases.

II. In systems which form intermediate phases, primary solid solutions with concentrations slightly higher than C_M may be produced at high cooling rates. In the Al–Mn and Al–Cr systems studied, substitutional solid solutions are formed, with a maximum solubility of Mn up to 9.8 wt.% and of Cr up to 5.5 wt.%. In Ni–C and Co–C systems, interstitial solid solutions are formed, with maximum solubility of carbon equal to 1.8 and 1.6%, respectively. Melts of this system also show a certain maximum solubility above which the primary solid solution is not supersaturated, and melts with concentrations greater than C_M crystallize to form two phases. The second phase in these cases is metastable: $MnAl_4$ in Al–Mn systems, Cr_2Al_{11} in Al–Cr systems, and Ni_3C and Co_3C in Ni–C and Co–C systems, respectively. Similarly, in Fe–C melts it is not possible, by cooling at high speeds, to achieve a solubility of C in γ-Fe greater than the maximum solubility at the eutectic temperature. On the contrary, the carbon content of rapidly cooled austenite is always less than the maximum solubility at the eutectic temperature.

Change in the rate of cooling over fairly wide limits causes practically no change in the maximum solubility C_M, if we neglect the slight decrease in the maximum solubility with increase in the supercooling, which is similar to that observed in alloys without intermediate phases. It is possible that further increase in the rate of cooling for systems with several intermediate phases may again lead to an increase in the solubility as a result of the crystallization of a less stable intermediate phase.

When the stable and metastable phases crystallize in the alloys simultaneously, two solid solutions are produced: one with concentration C_M and the other with concentration C'_M, showing considerable supersaturation. The x-ray diagrams in these cases show two systems of lines.

On the basis of these data, a larger number of phase diagrams with intermediate phases can be represented in the form of double phase diagrams with continuous (stable equilibrium) and broken (metastable equilibrium)

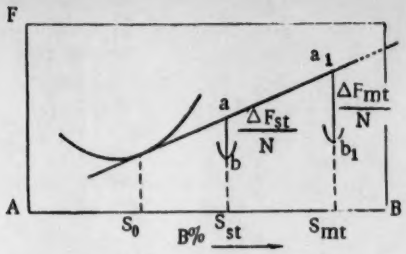

Fig. 3. Diagrammatic arrangement of free energy curves in a system with intermediate phase.

lines. Figure 2 gives diagrammatic representations of two diagrams of this type. The figure also shows the relationship between the composition of the primary solid solution and the concentration for two values of the degree of supersaturation. When the rate of cooling of the melt is insufficient to ensure crystallization according to the metastable diagram, the structure formation in the alloy will take place according to the stable phase diagram, and the change in composition of the primary solid solution with change in the alloy concentration will take place as shown in Fig. 1.

The eutectic point for the primary solution– metastable phase equilibrium is shifted towards the metastable phase, and its melting point decreases to a greater extent the less stable the intermediate phase. Thus, in Co–C melts the eutectic point is displaced to a greater extent than that in the Fe–C system, and that in the Ni–C system to a greater extent than that in the Co–C system. The experimental data given in the present work show that in the alloy studied, the diffusion processes leading to the separation of a component in the liquid are able to take place even at cooling rates of $\sim 10^5$ deg/sec. The results obtained are in agreement with the fundamental assumptions of the diffusion theory of the crystallization of two-component systems. Crystallization of a metastable phase in the system is always associated with an increase in the solubility of the primary solid solution in equilibrium with this metastable phase. The less stable the intermediate phase produced, the greater the solubility of the primary solution.

The separation of metastable phases is usually attributed to more favorable kinetic conditions for their production and to the lower value of the surface tension at the boundary of the original phase and the phase which is separating [10, 11]. In the case where the composition of the metastable phase is further from that of the mother phase than that of the stable phase, however, the change in the free energy of the system per atom of substance undergoing separation ($\Delta F/N$) may be of considerable importance [12, 13]. The value of $\Delta F/N$ for stable and metastable phases is shown in Fig. 3 by the sections ab and a_1b_1. When the difference in the concentrations of stable and metastable phases is high and the mother phase is highly supersaturated, $\Delta F/N$ for the metastable phase may prove to be greater than that for the stable phase ($a_1b_1 > ab$). In this case the conditions for the crystallization of the metastable phase will be thermodynamically more favorable. When the separation process is complete, however, the free energy of the system will be greater than that for the case where the stable phase separates, since the quantity of metastable phase for the system under study is always less than that of the stable phase. Further decrease in the free energy of the system is associated with the formation of stable phase by breakdown of the metastable phase, which will be kinetically unfavorable under conditions of high cooling rates.

LITERATURE CITED

1. I. N. Fridlyander, Doklady Akad. Nauk SSSR 104, 3 (1955).
2. G. Falkenhagen and W. Hotmann, Z. Metallkunde 69, 43, 3 (1952).
3. D. S. Kamenetskaya, Problemy Metallovedeniya i Fiziki Metallov, No. 3 (1952).
4. L. S. Palatnik and B. T. Boiko, Izvest. Vyssh. Uch. Zav., Fizika 112, 3(1958).
5. D. I. Lainer, Collection, The Use of X-rays in the Study of Materials [in Russian] (1940).
6. A. A. Popov, Collection: Problems of Metal Science and Thermal Treatment [in Russian] (1956).
7. I. V. Salli, Zhur. Neorg. Khim. No. 4 (1958).
8. I. V. Salli, Liteinoe Proizvodstvo, No. 7 (1958).
9. I. S. Miroshnichenko and I. V. Salli, Zavodskaya Lab. No. 11 (1959).
10. Ya. S. Umanskii, Trudy Moskovsk. Inst. Stali 28, 160 (1949).
11. L. S. Palatnik, Dissertation (Khar'kov, 1952).
12. A. H. Cottrell, Theoretical Structural Metallurgy (London, 1956).
13. M. Hillert, Acta Metallurgica 1, 6 (1953).

THE MECHANISM OF THE CHANGE IN OXYGEN OVERVOLTAGE WITH TIME AT A NICKEL ANODE AT CONSTANT CURRENT DENSITY

Ya. I. Tur'yan

Lisichansk Section, State Nitric Acid and Synthetic Organic Products Institute

(Presented by Academician A. N. Frumkin, January 28, 1960)

Translated from Doklady Akademii Nauk SSSR, Vol. 132, No. 6, pp. 1368-1371, June, 1960

Original article submitted January 28, 1960

The phenomenon of the increase in oxygen overvoltage η with time t at i = const at a Ni anode has not yet been quantitatively explained. We have suggested [1, 2] that the increase in η, which is produced at high values of i by retardation of the discharge of OH'-ions [1, 3], is due to the fact that η on NiO_2 (Ni_2O_4 [4]),whose

Temp., °C	Current Density, amp/cm²											
	0,01			0,05			0,1			0,3		
	a	b	$\varphi_{t=0}$, mv (n.h.e.)	a	b	$\varphi_{t=0}$, mv (n.h.e.)	a	b	$\varphi_{t=0}$, mv (n.h.e.)	a	b	$\varphi_{t=0}$, mv (n.h.e.)
18	—	$6,94 \cdot 10^{-3}$	632	$2,3 \cdot 10^{-4}$	$7,9 \cdot 10^{-2}$	690	$2,7 \cdot 10^{-4}$	0,158	750			
25										$1,4 \cdot 10^{-4}$	1,37	794
60							$5,0 \cdot 10^{-4}$	$3,6 \cdot 10^{-2}$	660			
80										$1,0 \cdot 10^{-3}$	$7,0 \cdot 10^{-2}$	696

Note. $a = K_2/K_1 + K_4/K_3$, $b\ (hr^{-1}) = K_1 + K_2 \approx K_1$

concentration in the surface solid solution $Ni_2O_3 + Ni_2O_4$ gradually increases, is greater than η on Ni_2O_3 (the anode under consideration is completely covered with Ni_2O_3 even at $t = 0$). The assumption that η on Ni_2O_4 is greater than η on Ni_2O_3 is to some extent confirmed by work [5] which has shown that η on Ni_2O_3 is greater than η on NiO.

In order to check these views quantitatively, we have used experimental data for the relationship between η and t at i = const from [1] and [6] (Fig. 1, 6-7.5 N KOH). The results from [6] for small values of t and 18° gave an $\eta - t$ curve of anomalous shape, possibly due to the nonstationary surface area of the anode [1] or to incomplete covering of the surface with Ni_2O_3. These data were rejected and $(\eta)_{t=0}$ found by extrapolation (Fig. 1).

At high values of i, the evolution of O_2 by the formation and decomposition of Ni_2O_4 should be insignificant compared with the other process taking place in parallel [2], for example

$$2OH \rightarrow H_2O + O. \qquad (1)$$

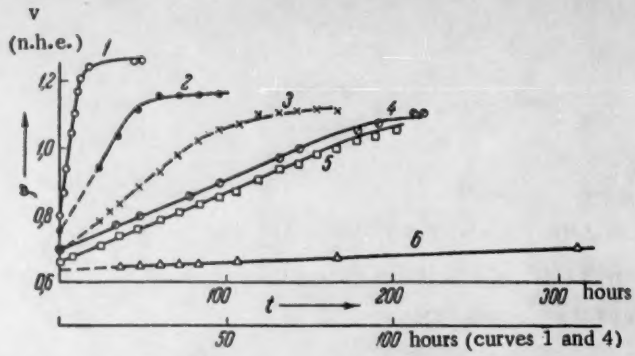

Fig. 1. Relationship between φ and t. The calculated data are given by points and the experimental data by lines. 1) 0.3 amp/cm^2, 25° [1]; 2) 0.1 amp/cm^2, 18° [6]; 3) 0.05 amp/cm^2, 18° [6]; 4) 0.3 amp/cm^2 80° [1]; 5) 0.1 amp/cm^2, 60° [6]; 6) 0.01 amp/cm^2, 18° [6].

Taking account of this, the kinetics of the accumulation of Ni_2O_4

$$Ni_2O_3 + 2OH \rightarrow Ni_2O_4 + H_2O \tag{2}$$

with simultaneous decomposition of Ni_2O_4

$$Ni_2O_4 \rightarrow Ni_2O_3 + O \tag{3}$$

may be given by the expression

$$\frac{dS}{dt} = K_1(1 - S) - K_2S; \tag{4}$$

where S is the fraction of anode surface occupied by Ni_2O_4 (the molar surfaces of Ni_2O_3 and Ni_2O_4 are assumed to be of similar magnitude); $K_1 = K'_1[OH]^2$; and K'_1 and K_2 are the rate constants of processes (2) and (3), respectively.

According to the retarded discharge theory [7], taking account of the discharge of OH'-ions at the surface of the $Ni_2O_3 + Ni_2O_4$ solid solution ([OH'] = const):

$$i = K_3(1 - S)\exp\left(\frac{\eta F}{2RT}\right) + K_4S\exp\left(\frac{\eta F}{2RT}\right). \tag{5}$$

From (4) and (5) (for t = 0, S = 0), assuming $K_3 \gg K_4$, we obtain:

$$\eta = \frac{2RT}{F}\ln i - \frac{2RT}{F}\ln\frac{K_1K_3}{K_1 + K_2} - \frac{2RT}{F}\ln\left[\left(\frac{K_2}{K_1} + \frac{K_4}{K_3}\right) + e^{-(K_1+K_2)t}\right]. \tag{6}$$

Equation (6) shows good agreement with experimental results (Fig. 1) for the values of the constants given in Table 1, and with the condition that

$$(\eta)_{t=0} = \frac{2RT}{F}\ln i - \frac{2RT}{F}\ln\frac{K_1K_3}{K_1 + K_2}. \tag{7}$$

Since $(K_2/K_1 + K_4/K_3) \ll 1$ (the table) and $K_3 \gg K_4$, then $K_1 \gg K_2$. This is confirmed by expression (7), which, when t = 0 and S = 0, should become

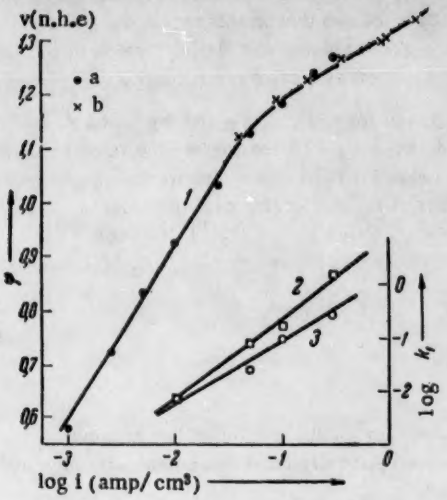

Fig. 2. 1)Relationship between φ_{estab} and log i (a) from data in [2], b) from data in [9];2) relationship between log k_1 and log i; 3) relationship between $\varphi_{t=0}$ and log i.

$$(\eta)_{t=0} = \frac{2RT}{F}\ln i - \frac{2RT}{F}\ln K_3, \qquad (8)$$

which is possible when $K_1 \gg K_2$.

The relationship found between $(\eta)_{t=0}$ and log i is a straight line with gradient $(2RT/F)\cdot 2.3$ (Fig. 2), which shows good agreement with (8).

Thus, Eq. (6) becomes

$$\eta = (\eta)_{t=0} - \frac{2RT}{F}\ln\left[\left(\frac{K_2}{K_1}+\frac{K_4}{K_3}\right)+e^{-K_1 t}\right]. \qquad (9)$$

At low values of t, taking account of the values of K_1 and $(K_2/K_1 + K_4/K_3)$ (the table), we can convert Eq. (9) to a linear relationship between η and t:

$$\eta = (\eta)_{t=0} + \frac{2RT}{F}K_1 t, \qquad (10)$$

which shows good agreement with experiment (Fig. 1).

As t increases, η tends toward its established value (η_{estab}):

$$\eta_{est} = (\eta)_{t=0} - \frac{2RT}{F}\ln\left(\frac{K_2}{K_1}+\frac{K_4}{K_3}\right), \qquad (11)$$

which also agrees with experiment (Fig. 1).

As can be seen from the table, K_1 is dependent on i, which is apparently related to a certain retardation at other stages of the process (change in [OH]), much smaller than that at the stage involving the discharge of OH'-ions. A similar picture has been observed [8] in a study of η at a Pb anode.

Since at constant temperature K_1 increases with increase in i (the table), we can expect that at high values of i, $K_4/K_3 \gg K_2/K_1$, while at small values of i, $K_4/K_3 \ll K_2/K_1$. From this we have, at high values of i, taking account of (8):

$$\eta_{est} = \frac{2RT}{F}\ln i - \frac{2RT}{F}\ln K_4, \qquad (12)$$

and at small values of i

$$\eta_{est} = \frac{2RT}{T}\ln i - \frac{2RT}{F}\ln K_3 - \frac{2RT}{F}\ln\frac{K_2}{K_1}. \qquad (13)$$

If we take account of the fact that $K_1 = K'_1 i^{1.55}$ (Fig. 2) and use (13), we obtain:

$$\eta_{est} = 2{,}55\frac{2RT}{F}\ln i - \frac{2RT}{F}\ln K_3 - \frac{2RT}{F}\ln K_2 + \frac{2RT}{F}\ln K'_1. \qquad (14)$$

Equation (12) agrees with experiment even when $i > 0.1$ amp/cm^2. This is the upper linear region (Fig. 2) of the relationship between η_{estab} and log i, with slope $\sim(2RT/F)\cdot 2.3$ [2, 9, 10]. The presence of this region, which in accordance with (12) corresponds to the complete covering of the anode by Ni_2O_4, was also confirmed in [11].

Equations (13) and (14) are confirmed at smaller values of i ($i < 0.01$-0.02 amp/cm^2, but not below 10^{-3} amp/cm^2, when the mechanism of the production of η changes [2]) in the region of the steep section of the curve

giving the relationship between η_{estab} and $\log i$ [2, 10], which is a straight line with gradient 0.320 (Fig. 2); this is close to the theoretical value 0.303 [Eq. (14)]. From (5) and (13) it follows that in this region the process of OH'-ion discharge takes place chiefly on Ni_2O_3. Each value of η_{estab} corresponds to a definite value of S. As the surface concentration of Ni_2O_4 increases (with increase in i) the process also takes place on Ni_2O_4.

Using (14) and the experimental relationships between η_{estab} and $\log i$ [2], $\eta_{t=0}$ and $\log i$, and K_1 and i, we have calculated that $K_2 = 1 \cdot 10^{-5}$ hr^{-1} at 25°, i.e., as expected, $K_1 \gg K_2$. Approximately the same value for K_2 was obtained from the relationship between η and t. This low value for K_2 does not support the suggestion [4] that the process (3) is the controlling process even at very low values of t, since in this case the calculation gives an unreal, high Ni_2O_4 concentration (for example, at $i = 10^{-5}$ amp/cm^2, $[Ni_2O_4] = 1.1 \cdot 10^{22}$ molecule/cm^2).

The assumption regarding the process

$$2\,Ni_2O_4 \rightarrow 2\,Ni_2O_3 + O_2 \qquad (15)$$

however, is not supported by the relationship between η and t.

Using the relationship between η_{estab} and $\log i$ (for $i > 0.1$ amp/cm^2) and the relationship between $\eta_{t=0}$ and $\log i$, we have calculated that $K_4 / K_3 = 1.7 \cdot 10^{-4}$, which shows exceptionally good agreement with the value of K_4 / K_3 obtained from the relationship between η and t (the table).

The table shows that K_1 decreases with increase in temperature. This is a result of the predominating influence of temperature on the decrease in the surface concentration of OH radicals compared with the simultaneous increase in K'_1.

In conclusion we would point out that Eq. (5), again with the condition that $K_3 \gg K_4$, has already been used [12] to describe the relationship between η and t for a Pt anode. The kinetics of the accumulation of oxide in [12] are not, however, given by the same relationship as in our case, so that a quite different relationship between η and t is obtained in [12].

LITERATURE CITED

1. Ya. I. Tur'yan, Dissertation, Mid-Asian Industrial Institute (1948).
2. V. N. Fiseiskii and Ya. I. Tur'yan, Zhur. Fiz. Khim. 24, 567 (1950).
3. S. A. Gantman and P. D. Lukovtsev, Proceedings of the Third Electrochemistry Conference (Izd. An SSSR, 1953) p. 504.
4. L. M. Elina, T. I. Borisova, and P. I. Zalkind, Zhur. Fiz. Khim. 28, 785 (1954).
5. O. K. Davtyan, The Problem of the Direct Conversion of the Chemical Energy of Fuel to Electrical Energy [in Russian] (Izd. AN SSSR, 1947).
6. G. Grube and A. Vogt, Z. Elektrochem. 44, 353 (1938).
7. A. N. Frumkin, V. S. Bagotskii, Z. A. Iofa, and B. N. Kabanov, The Kinetics of Electrode Processes [in Russian] (Moscow, 1951).
8. B. N. Kabanov, Proceedings of the Fourth Electrochemistry Conference [in Russian] (Izd. AN SSSR, 1959) p. 252.
9. Ya. I. Tur'yan and I. S. Gol'dshtein, Zhur. Prikl. Khim. 28, 379 (1956).*
10. Ya. I. Tur'yan, Zhur. Fiz. Khim. 33, 948 (1959).
11. T. Mine, T. Seiymaa, and W. Sakai, J. Chem. Soc. Japan, Industr. chem. Soc. 58, 725 (1955).
12. J. Bockris and A. Huq, Proc. Roy. Soc. A 237, 277 (1956).

*Original Russian pagination. See C. B. translation.

THE NATURE OF THE HYDROGEN BOND AND ITS INFLUENCE ON THE ELECTRONIC SPECTRA OF MOLECULES

D. N. Shigorin, N. A. Shcheglova, N. S. Dokunikhin, and V. A. Puchkov

L. Ya. Karpov Physicochemical Institute

(Presented by Academician A. N. Terenin, February 11, 1960)

Translated from Doklady Akademii Nauk SSSR, Vol. 132, No. 6, pp. 1372-1375, June 1960

Original article submitted January 10, 1960

A large number of works have been devoted to the influence of the hydrogen bond on the vibrational spectra of molecules. The results obtained in this field characterize the manifestation of the hydrogen bond in the fundamental electronic state. The quantum-mechanical treatment of the triatomic model A–H. . .B without π-electrons, given by N. D. Sokolov [1], shows that the nature of the H-bond in these systems is for the most part determined by the acceptor–donor interaction, and in this case account is taken of the use of the s-orbital of the hydrogen atom by the "unshared" electron pair of the donor atom. The energy of the hydrogen bond (E) in the system A–H. . .B is made up of the energy of the acceptor–donor interaction $E_a(s)$ and the dipole interaction E_d, i.e., $E = E_d + E_a(s)$. In order to explain the characteristic features of the manifestation of the hydrogen bond in the vibrational spectra of molecules with π-electrons (the considerable displacement and blurring of the bands of the X–H. . . groups, the changes in their intensities, the coplanarity effect, etc.), however, it has been necessary to take account of new factors determining the nature of the bond. In earlier works [2-4] it has been shown that the characteristic features of the manifestation of the hydrogen bond (as in the case of a metal–element bond) can be understood only if account is taken of π-electron interaction in the formation of the H-bond. The mechanism by which the electrons of the X–H . . . group (whose electron shell is deformed in the $\sigma \rightarrow \pi$ direction) take part in the π-electron interaction of the molecule is apparently not standard, and depends on the particular features of the structure of the molecular system. The characteristic features of the H-bond in systems with π-electrons was explained in earlier works [2-4] by the fact that its formation involves the direct participation of a modified p-orbital of the hydrogen atom (in the case of a metal–element bond, a p- or d-orbital of the metal atom), which is used by the π-electrons of the C=O group (Fig. 1). In the case under consideration, an additional (quasiaromatic) ring is produced with π-electron interaction involving 6 electrons of the system. Thus, the H-bond (and the metal–element bond), in the general case, is made up of three types of interaction: E_d, $E_a(s)$ and the π-electron interaction $E\pi(p)$ involving a p-orbital of the hydrogen atom, i.e., $E = E_d + E_a(s) + E_\pi(p)$. The model of the H-bond which takes account of the participation of the modified p-orbital of the hydrogen atom explains (albeit quantitatively) all the features of its manifestation in the vibrational and electronic spectra of the molecules. In compounds of the type exemplified by the enol form of acetylacetone, tropolone, α-hydroxyanthraquinone, etc., the

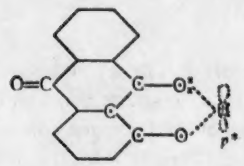

Fig. 1. Electronic model of the ring with H-bond in α-hydroxyanthraquinone. The points denote the electrons taking part in the formation of the ring with π-electron interaction, in which the p*-orbital of the H atom is used.

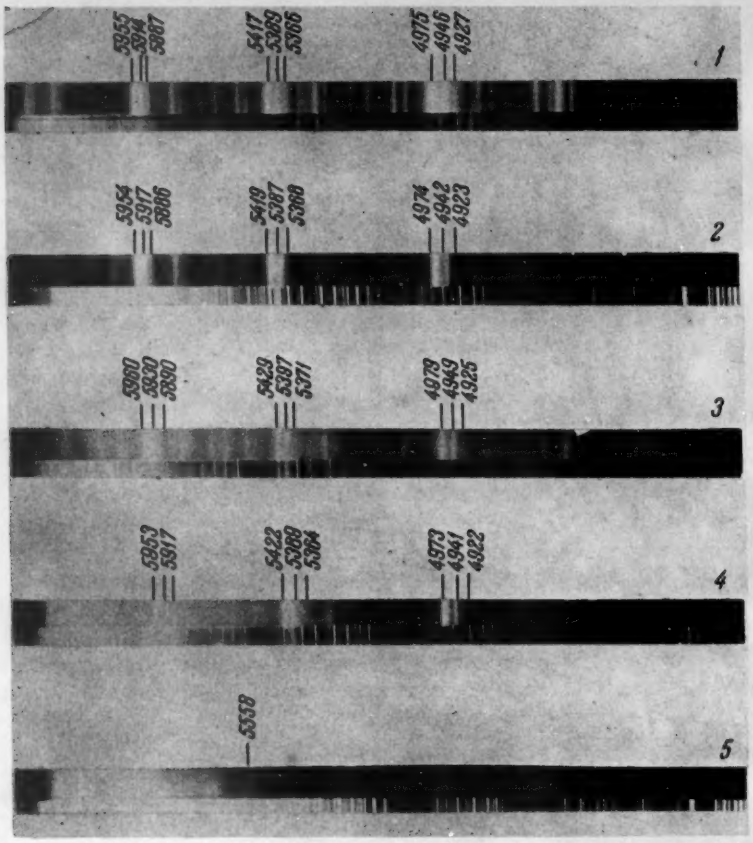

Fig. 2. Spectra of luminescence of anthraquinone and its α-derivatives at 77°K with heptane: 1) anthraquinone; 2) α-methyl anthraquinone; 3) α-phenylanthraquinone; 4) α-methoxyanthraquinone; 5) α-hydroxyquinone.

fraction of the total energy of the H-bond due to the π-electron interaction reaches almost 90% [3, 4]. Without this foundation, it is apparently impossible to study the influence of the hydrogen and metal–element bonds on the electronic absorption and emission spectra of molecules with π-electrons. The influence of the hydrogen and metal–element bonds on the electronic spectra of molecules has been considered by A. N. Terenin [5]. The hydrogen bond produces a considerable displacement of the absorption bands of the electronic spectra towards the red range. For example, the absorption band for α-hydroxyanthraquinone is displaced by 45 mμ into the long-wave region compared with the corresponding band for α-methoxyanthraquinone (the table). As a result of the formation of intermolecular hydrogen bonds, the absorption bands for indigo in the crystalline state are displaced into the red range by 100 mμ, compared with those in the spectra of the vapor [6]. The reason for the displacement of an absorption band in the electronic spectrum towards longer wavelengths is that the H-bond, when part of a conjugated system of bonds, brings about a significant change in the π-electron interaction throughout the whole molecule and leads to a change in the position of the energy levels of the system. As a result of the fact that π-electrons take part in the formation of the H-bond, an additional ring is produced, with π-electron interaction, which is equivalent to a lengthening of the chain of conjugated bonds or to an increase in the breadth of the "potential box," so that we should observe a shift in the absorption band in the electronic spectra towards the red range, according to the equation $\nu_{N\to N+1} = \frac{h}{8mcL^2}(2N+1)$, where L is the breadth of the potential box and N is the number of atoms in the conjugated chain [7]. To make a more complete study of the influence of the

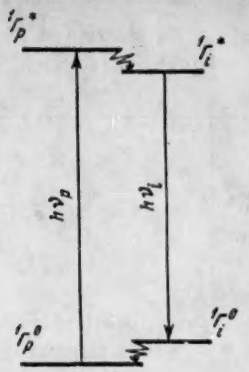

Fig. 3. Diagram showing possible electron levels.

H-bond on the absorption and emission spectra of molecules with π-electrons, however, it is necessary to find out what takes place when the hydrogen bond is excited. For this purpose we shall examine the most typical case of a coplanar system with π-electron interaction in which a C=O group takes part in the formation of an H-bond and "is responsible" for the electronic excitation. An example of such a system is α-hydroxyanthraquinone (Fig. 1). The study of the electronic–vibrational spectra of anthraquinone and some of its derivatives in frozen solutions at T = 77°K has in fact shown that the corresponding components of the intense bands lie at an average distance of 1664 cm^{-1} from one another, which characterizes the valence vibration of the C=O group in the fundamental electronic state [8]. From these data it follows that the C=O group is largely responsible for the position of the electron level of the molecules of anthraquinone and its derivatives in the excited state. When the molecule is excited as a result of $n \rightarrow \pi^*$ transition (with subsequent transfer of the molecule to the triplet state), the π-bond of the C=O groups is weakened considerably. This is shown by an analysis of the electronic–vibrational spectra for anthraquinone and some of its derivatives. The distribution of the band intensities in the spectrum can be explained, in accordance with the Frank–Condon principle, by the increase in the equilibrium internuclear distance (in the C=O group) for the excited electron level. On the other hand, in α-hydroxyanthraquinone, the probability that the electron pair of the hydroxyl group O–H. . . will take part in the π-electron interaction in the system also increases. Thus, at the moment when the molecule absorbs a light quantum, a change takes place in its structure (the electron density distribution, internuclear distance and angles), which may lead to an increase in the stability of the ring with the H-bond (Fig. 1). In the excited state of the molecule, the participation of the p-orbital of the hydrogen atom in (O–H. . .O=C) in the π-electron interaction in the system apparently becomes even more probable, and much more efficient [8]. In this connection the proportion of electronic energy and the rate of its conversion to vibrational energy, together with the probability of redistribution of the latter throughout the vibrational sublevels will be increased. The lifetime of each excited vibration will therefore be reduced, and this may lead to blurring of the fine vibrational structure in the luminescence spectra of the compounds containing the H-bond (since $\tau \Delta E \simeq \simeq h$).

The luminescence spectra of α-hydroxy derivatives of anthraquinone (1-hydroxy, and 1,4- and 1,5-dihydroxy) do not in fact have a fine vibrational structure [8]. These spectra (Fig. 2) are displaced considerably toward the red range and appear as rather indistinct bands. The blurring of these bands is directly related to the state of the carbonyl group, which is directly involved in the formation of the H-bond, whereas the luminescence spectra of α-derivatives of anthraquinone (α-methyl-, α-methoxy- and α-phenylanthraquinone) which do not contain H-bonds have a fine vibrational structure (Fig. 2 and the table). The formation of the H-bond in the α-hydroxyanthraquinone molecule has such an marked effect on the whole system that the manifestation of the fine vibrational structure as a result of the second carbonyl group becomes impossible.

In the infrared absorption spectra, the valence vibration bands of the O–H. . . and C=O groups are displaced into the long-wave region and are indistinct. There thus exists a parallelism in the manifestations of the H-bond in the electronic and vibrational spectra (the table).

Comparison of the absorption and emission spectra of compounds with and without an H-bond shows that the extent of the displacement of corresponding bands in the absorption spectra is much less than that in the emission spectra. For example, the displacement Δλ for α-hydroxyanthraquinone compared with α-methoxyanthraquinone is 34 mμ in the absorption spectra and 97 mμ in the emission (the table). The electronic emission spectra for the vapor of anthraquinone derivatives were first studied in A. N. Terenin's laboratory [9]. The value of the "Stokes" displacement for compounds with an H-bond is much greater than that for compounds without an H-bond [10]. The emission bands are less distinct than the absorption bands. These features which have been observed in the absorption and emission spectra are most characteristic of molecules in which the ring with the H-bond is coplanar with the π-electron system of the molecule. These facts can obviously only be explained by the fact that the change in the structure of the molecule and in its electronic state, which starts at the moment when the energy quantum $h\nu_p$ is absorbed, is complete in the system only when it has emitted a light quantum $h\nu_i$.

It may be assumed that in systems with a hydrogen bond (or metal–element bond), the excited electron level of the system ($^1\Gamma^*_p$) produced at the moment of absorption of the energy quantum, and the electron level

Compound	Absorption		Emission at T = 77°K		Vibrational structure at T = 77°K	I.R. spectrum of of vapor, ν cm^{-1}
	$\lambda m\mu$	$\Delta\lambda m\mu$	$\lambda m\mu$	$\Delta\lambda m\mu$		
Anthraquinone	312/v*				Fine vibrational structure	
	330/s*		457/s			
α-Methylanthraquinone	331/s		455/s		Fine vibrational structure	
α-Phenylanthraquinone	322/s		455/s		Fine vibrational structure	
α-Methoxyanthraquinone	340/v	0/v				
	368/s	0/s	455/s	0/s	Fine vibrational structure	
α-Hydroxyanthraquinone	385/v	45	550/v		Very indistinct band	Very indistinct band with maximum 3050-3100 cm^{-1}.
	402/s	34	552/s	97		

* v—vapor; s—solution.

at which the molecule starts to emit energy ($^1\Gamma^*_i$), are not identical. An increase in the stability of the ring with the hydrogen bond (or metal—element bond) in the excited molecule leads to a lowering of its electron level, and this is illustrated diagrammatically in Fig. 3. A characteristic photochemical process takes place, with a change in the structure of the molecule, and the possibility that the proton is transferred from one oxygen atom to another is not excluded. In molecules with a symmetrical structure (the enol form of acetylacetone, tropolone, etc.), in the excited state, movement of the hydrogen atom from one potential valley to another is possible. The potential barrier which the hydrogen atom has, classically, to overcome on going from one valley to another should be lowered as a result of the similarity and equivalence of the potential valleys [11]. This problem requires special study, however. In the case under consideration, the movement of electrons is not independent of the movement of the nuclei, and changes not involving emission take place with conversion of part of the electronic energy to vibrational energy of the nuclei. Under these conditions, Levshin's law of mirror symmetry should not be strictly obeyed [12]. This is confirmed by experiment. In molecules analogous to those under consideration, the law of mirror symmetry is not in fact obeyed [10]. The problem of the relationship between the luminescence and absorption spectra has been dealt with in a number of works [14, 15].

All that has been said for an intramolecular bond applies with the condition that the coplanarity factor is fulfilled. In the case of the H—N—H. . .O=C— or H—N—H. . .N=N—, etc., groups, for which the coplanarity condition is not completely fulfilled, therefore, these phenomena may not be observed. In these systems it is possible that the H-bond does not become stronger on excitation but is weakened or even broken, as a result of the breakdown of the acceptor—donor interaction and the impossibility of participation of the N—H group in the π-electron interaction.

Intensification of the interaction on excitation is also possible in bridges with an H-bond, formed between molecules with π-electrons, as in the case of β-hydroxyanthraquinone, for example [8]. This type of phenomenon was detected from the fluorescence spectra by A. N. Terenin and A. V. Shablya using 9-(p-hydroxy)-phenylacridine[13]. When the bridge $\overset{\diagup}{\underset{\diagdown}{C}}-\overset{-\delta_1+\delta_2}{O}-H\ \ldots\ \overset{-\delta_2}{N}\overset{\diagup}{\underset{\diagdown}{}}$ is excited, the hydrogen atom proves to be more strongly bound to the nitrogen atom $\overset{\diagup}{\underset{\diagdown}{C}}-\overset{-\delta_1}{O}\ldots H\ldots\overset{+\delta_2}{N}\overset{\diagup}{\underset{\diagdown}{}}$ as a result of the intensification of the acceptor—donor interaction and, more particularly, of the π-electron interaction. Here again account must be taken of the increase in the stability of the molecule giving up the proton, as a result of the delocalization of the electron (the negative charge) in the system. In other words, the dissociation constant of the system $Ar-OH \leftrightarrows [Ar-O]^- + H^+$ should increase on excitation, but this limiting process is possible only under definite conditions.

The phenomenon of intensification of the interaction in H-bond bridges on excitation evidently plays an important part in processes of energy migration, which is of considerable interest in high-molecular compounds (polyamides, proteins, etc.), and also in the study of problems related to the removal and transfer of a proton in excited systems.

Thus, the study of the hydrogen bond in the excited state is of considerable importance for the examination of the nature of the hydrogen bond and the study of a number of other phenomena.

LITERATURE CITED

1. N. D. Sokolov, Doklady Akad. Nauk SSSR 82, 369 (1952); Uspekhi Fiz. Nauk 57,205 (1955).
2. D. N.Shigorin, Izvest. Akad. Nauk SSSR, Ser. Fiz. 14, 395 (1953); Zhur. Fiz. Khim. 27, 554; Spectrochim. Acta 14, 198 (1959); Problemy Fiz. Khim. No. 1, 173 (1958).
3. D. N. Shigorin and N. S. Dokunikhin, Zhur. Fiz. Khim. 29, 1958 (1955).
4. D. N. Shigorin, M. M. Shemyakin, et al., Doklady Akad. Nauk SSSR 108, 672 (1956).*
5. A. N. Terenin, The Photochemistry of Dyes [in Russian] (Izd. AN SSSR, 1947) p. 158.
6. D. N. Shigorin, N. S. Dokunikhin, and E. A. Gribova, Zhur. Fiz. Khim. 29, 867 (1955).
7. M. V. Vol'kenshtein, The Structure and Physical Properties of Molecules [in Russian] (Izd. AN SSSR, 1955) p. 539.
8. D. N. Shigorin, N. A. Shcheglova, and R. N. Nurmukhametov, Doklady Akad. Nauk SSSR 120,1242 (1959).*
9. A. V. Karyakin, Zhur. Fiz. Khim. 23, 1332 (1949).
10. Yu. V. Naboikin, B. A. Zadorozhnyi, and E. N. Pavlova, Izvest. Akad. Nauk SSSR, Ser. Fiz. 23, 9 (1959).
11. D. N. Shigorin, Zhur. Fiz. Khim. 23, 505 (1949).
12. B. I. Stepanov, The Luminescence of Complex Molecules [in Russian] (Minsk, 1955) p. 172.
13. A. N. Terenin and A. V. Shablya, Disc. Farad. Soc. No. 27, 83 (1959).
14. B. I. Stepanov, Izvest. Akad. Nauk SSSR, Ser. Fiz. 22, 1367 (1958).
15. B. S. Neporent, Izvest. Akad. Nauk SSSR, Ser. Fiz. 22, 1372 (1958).

* Original Russian pagination. See C. B. translation.

THE DIPOLE MOMENTS OF SOME HALOPOLYNITROPARAFFINS

A. N. Shidolovskii, Ya. K. Syrkin, Corresponding Member of the Academy of Sciences USSR, S. S. Novikov, A. A. Fainzil'berg, V. V. Sevost'yanova and V. I. Gulevskaya

The M. V. Lomonosov Institute of Fine Chemical Technology and N. D. Zelinskii Institute of Organic Chemistry, Academy of Sciences, USSR

Translated from Doklady Akademii Nauk SSSR, Vol. 132, No. 6, pp. 1376-1377, June, 1960

Original article submitted February 14, 1960

The dipole moments of aliphatic polynitro compounds incorporating carbon-halogen bonds are of interest in elucidating the problem of how the repetition of nitro groups affects polarity and how this effect is reflected in the chemical properties.

To this end we measured the dipole moments of eight compounds at 25° in benzene by the heterodyne method. All these compounds were synthesized by ourselves and obtained in a chemically pure form. Electron polarization in some cases was obtained by experiment while in others it was calculated from bond refractivities. From experimental data for the refraction of the $C-NO_2$ group a value of 7.65 cm^3 has been obtained for the cases where three nitro groups are located on one carbon atom and 7.5 cm^3 where one carbon is linked with two nitro groups. The atomic polarization of each nitro group was estimated as 2 cm^3. The Hedestrand formulas were used to calculate dipole moments.

The chemical formulas, the range of measured concentrations in mole fraction, the total polarization, the sum of electronic and atomic polarizations and the dipole moments in debye units are presented in that order in the table.

Let us compare the dipole moments of C–Cl, C–Br, and C–I bonds in compounds of the CH_3Hal and $CHal(NO_2)_3$ types.

If the value of 0.31, as suggested recently for the case of sp^3 hybridization (with a positive charge directed toward the hydrogen) [1], is taken provisionally for the moment of the C–H bond, then from the dipole moment for CH_3Cl in benzene solution of 1.86; for CH_3Br of 1.82 and for CH_3I of 1.48 debye units, we obtain the value of 1.55 for the moment of the C–Cl bond 1.55; for C–Br, 1.51; C–I, 1.17 debye units.

Increase in the number of halogen atoms on a carbon causes a decrease in the bond moment. Using the same assumption regarding the C–H bond, from experimental value 1.2 for the moment for $CHCl_3$; for $CHBr_3$, 1.06 and for CHI_3, 0.95 debye units, we obtain for the C–Cl, C–Br, and C–I bonds the values 0.89, 0.75, and 0.64 debye units, respectively.

From the dipole moment of nitromethane in benzene of 3.15 we obtain for the $C-NO_2$ moment the value 2.84 debye units. The moment of nitroform, known from published data, and also from our own measurements, is equal to 2.71, giving 2.4 for the $C-NO_2$ bond. Using this value and the following moments determined by us: $CCl(NO_2)_3$ 2.17, $CBr(NO_2)_3$ 2.56 and $CI(NO_2)_3$ 3.79, we find that in these compounds the moments of the carbon-halogen bond are equal to: C–Cl 0.23 (with the negative charge towards the chlorine), C–Br 0.15 (with the positive charge towards bromine) and C–I 1.39 debye units (with the positive charge on the iodine). In comparison

Formula	l	P_∞	$P_{el}+P_{at}$	$\mu \times 10^{18}$
$CCl(NO_2)_3$	0,003—0,006	133,5	35,7	2,17
$CBr(NO_2)_3$	0,005—0,012	174,1	38,1	2,56
$CJ(NO_2)_3$	0,002—0,004	341	43,5	3,79
$CH_3C(NO_2)_3$	0,002—0,007	243,8	35,3	3,17
$CH_3CH(NO_2)_2$	0,005—0,01	276,8	27	3,47
$CH_3CBr(NO_2)_2$	0,003—0,015	254,6	34,7	3,26
$CH_3CCl(NO_2)_2$	0,004—0,008	226,1	31,85	3,06
$CH_3CHBr(NO_2)$	0,006—0,014	206	26,9	2,94

with compounds of the CH_3Hal type the moment of the C—Cl bond has changed by 1.32, of the C—Br bond by 1.66 and of the C—I bond by 2.56.

Consequently, in the halotrinitromethanes there exists a slight negative charge in the case of chlorine, a weak positive charge in the case of bromine, while iodine has an appreciable positive charge. The theoretical side of the matter lies, of course, not in the absolute quantitative values but in the fact that the increase in the dipole moment of the molecule from $CCl(NO_2)_3$ to $CBr(NO_2)_3$ and to $CI(NO_2)_3$ (the moment of which is 1.08 debye units greater than that of nitroform) indicates that in the C—I bond iodine is the positive end of the dipole. Independently of the accuracy of the quantitative equations (one value for the C—H bond was taken as a provisional value for all the halogen derivatives of methane) it is apparent that electropositivity increases rapidly in the halotrinitromethane series from chlorine to iodine. This is associated with the fact that in the presence of three nitro groups on one carbon the interaction between iodine and carbon does not end with the formation of the usual two-electron linkage in a partially ionized state $\overset{\oplus}{C}-\overset{\ominus}{I}$. Apparently, the iodine acts here partly as a donor on account of its unshared pair of p-electrons, the displacement of electrons from iodine to carbon causing a further electron shift and a partial transition from a nitro group $-\overset{+}{N}\begin{matrix}\overset{\ominus}{O}\\ O\end{matrix}$ to a nitrite group $N\begin{matrix}O\\ \overset{\ominus}{O}\end{matrix}$.

The characteristic polarization of the carbon—halogen bond in halotrinitromethanes is the cause of the specific chemical properties of these compounds, for example, the readiness with which they hydrolyze to form hypohalous acids [2], oxidize hydrazine [3] or potassium iodide [4], and are rapidly reduced at a mercury electrode [5]. The ease of these reactions increases with the transition from chlorotrinitromethane to bromotrinitromethane, and, especially, to iodotrinitromethane (for example, the hydrolysis constants of the stated compounds are $8 \cdot 10^{-12}$, $3 \cdot 10^{-11}$, and $4 \cdot 10^{-7}$ [2], respectively]. The electropositivity of the halogen in halotrinitromethanes increases in the same order, as indicated by their dipole moments.

If the value of 2.4 debye units is taken for the dipole moment of the $C(NO_2)_3$ group and this value is applied to the $CH_3C(NO_2)_3$ molecule (3.17 debye units), then a value of 0.77 debye units is obtained for the moment of the CH_3 - C group. Consequently with the three adjoining nitro groups the electropositivity of the methyl group is increased and the acidic properties of its hydrogen atoms are enhanced, a fact which is in good agreement with the chemical behavior of 1,1,1,-trinitroethane, which readily loses the elements of nitrous acid to form 1,1-dinitroethylene [6].

Taking the stated values for the moments of $C-CH_3$, C—H, and $C-NO_2$, it is possible to calculate the resultant dipole moments of a series of gem-dinitro compounds. Thus, for $CH_3CH(NO_2)_2$ calculation gives 3.38 debye units instead of the experimental value of 3.47 debye units; for $CH_3CCl(NO_2)_2$ the calculated value is 3.15, while the experimental value is 3.06 debye units; for the $CH_3CBr(NO_2)_2$ molecule we obtain by calculation 3.29, in satisfactory agreement with 3.26 debye units by experiment. It follows from the above that in the case of dinitro compounds also, experiment accords with the fact of a considerable decrease in the dipole moment for the carbon—halogen bond.

LITERATURE CITED

1. A. Petro, J. Am. Chem. Soc. 80, 4230 (1958).
2. L. Birkenbach, K. Huttner and W. Stein, Ber. 62, 2065 (1929).
3. A. Macbeth and D. Pratt, J. Chem. Soc. 119, 1356 (1921).
4. S. S. Novikov, A. A. Fainzil'berg, V. I. Gulevskaya, and V. V. Sevost'yanova, Izvest. Akad. Nauk SSSR, Otdel. Khim. Nauk [in press].*
5. S. G. Mairanovskii, A. A. Fainzil'berg, S. S. Novikov, and V. A. Klimova, Doklady Akad. Nauk SSSR 125, 351 (1959).*
6. L. Zeldin and H. Shechter, J. Am. Chem. Soc. 79, 4708 (1957).

* Original Russian pagination. See C. B. translation.

SIGNIFICANCE OF ABBREVIATIONS MOST FREQUENTLY ENCOUNTERED IN SOVIET PERIODICALS

FIAN	Phys. Inst. Acad. Sci. USSR.
GDI	Water Power Inst.
GITI	State Sci.-Tech. Press
GITTL	State Tech. and Theor. Lit. Press
GONTI	State United Sci.-Tech. Press
Gosenergoizdat	State Power Press
Goskhimizdat	State Chem. Press
GOST	All-Union State Standard
GTTI	State Tech. and Theor. Lit. Press
IL	Foreign Lit. Press
ISN (Izd. Sov. Nauk)	Soviet Science Press
Izd. AN SSSR	Acad. Sci. USSR Press
Izd. MGU	Moscow State Univ. Press
LEIIZhT	Leningrad Power Inst. of Railroad Engineering
LET	Leningrad Elec. Engr. School
LETI	Leningrad Electrotechnical Inst.
LETIIZhT	Leningrad Electrical Engineering Research Inst. of Railroad Engr.
Mashgiz	State Sci.-Tech. Press for Machine Construction Lit.
MEP	Ministry of Electrical Industry
MES	Ministry of Electrical Power Plants
MESEP	Ministry of Electrical Power Plants and the Electrical Industry
MGU	Moscow State Univ.
MKhTI	Moscow Inst. Chem. Tech.
MOPI	Moscow Regional Pedagogical Inst.
MSP	Ministry of Industrial Construction
NII ZVUKSZAPIOI	Scientific Research Inst. of Sound Recording
NIKFI	Sci. Inst. of Modern Motion Picture Photography
ONTI	United Sci.-Tech. Press
OTI	Division of Technical Information
OTN	Div. Tech. Sci.
Stroiizdat	Construction Press
TOE	Association of Power Engineers
TsKTI	Central Research Inst. for Boilers and Turbines
TsNIEL	Central Scientific Research Elec. Engr. Lab.
TsNIEL-MES	Central Scientific Research Elec. Engr. Lab.–Ministry of Electric Power Plants
TsVTI	Central Office of Economic Information
UF	Ural Branch
VIESKh	All-Union Inst. of Rural Elec. Power Stations
VNIIM	All-Union Scientific Research Inst. of Metrology
VNIIZhDT	All-Union Scientific Research Inst. of Railroad Engineering
VTI	All-Union Thermotech. Inst.
VZEI	All-Union Power Correspondence Inst.

Note: Abbreviations not on this list and not explained in the translation have been transliterated, no further information about their significance being available to us. – Publisher.